LUT UNIVERSITY
LUT School of Energy Systems
LUT Mechanical Engineering

Rasmus Karlsson

UTILIZATION POSSIBILITIES OF HIGH-PRESSURE GAS INJECTION FOR 4-STROKE DIESEL COMBUSTION

Examiner(s): Mika Lohtander
Teemu Turunen-Saaresti

TIIVISTELMÄ

LUT-Yliopisto
LUT School of Energy Systems
LUT Kone

Rasmus Karlsson

Utilization possibilities of high-pressure gas injection for 4-stroke diesel combustion

Diplomityö

2021

128 sivua, 90 kuvaa, 34 taulukkoa ja 11 liitettä

Tarkastajat: TkT Mika Lohtander
Professori Teemu Turunen-Saaresti

Hakusanat: monipolttoainemoottorit, polttoaineen syöttöjärjestelmät

Tämän työn tavoitteena oli tarkastella korkeapaineisen kaasunsyötön käyttömahdollisuuksia puristussytytteisellä, IMO Tier III päästörajoitukset täyttävällä 4-tahti monipolttoainemoottorilla. Työssä käydään läpi monipolttoainemoottorille mahdollisesti soveltuvia vaihtoehtoisia polttoaineita, jonka jälkeen tarkastellaan moottorin tarvitsemaa kaasunsyöttöjärjestelmää. Kaasunsyöttöjärjestelmän tarkastelu tehdään nesteytetylle maakaasulle. Työssä käydään läpi kaasunsyöttöjärjestelmän tarvitsemia komponentteja, kuten pumppuja, kompressoreita, lämmönvaihtimia sekä mahdollisia pakokaasun puhdistusjärjestelmiä nesteytetyn maakaasun käytön kannalta.

Työ pohjautuu teoreettisiin tutkimusmenetelmiin. Polttoaineet ja korkeapaineisen kaasunsyöttöjärjestelmän tarvitsemat laitteet sekä moottorin päästöjen arviointi pohjautuvat kirjallisuustutkimukseen. Lisäksi työssä on suoritettu markkinoilla olevien suuritehoisten 2- ja 4-tahti monipolttoainemoottoreiden vertailuanalyysi. Kirjallisuustutkimuksen sekä vertailuanalyysin lisäksi kaasunsyöttöjärjestelmien polttoaineen paineistamiseen tarvitsema teho sekä kaasunsyöttöjärjestelmän mahdollinen lämmitys- tai jäähdytystarve on arvioitu HYSYS simulointiohjelmistolla. Lopulta järjestelmien komponenttien hintoja on vertailtu toimittajien- ja kirjallisuudesta löydettyjen hintavertailujen pohjalta.

Työn tuloksena on arvio korkeapaineisen kaasunsyöttöjärjestelmän toteutettavuudesta. Korkeapaineinen kaasunsyöttöjärjestelmä voidaan toteuttaa ainakin pumppujen tai kompressoreiden avulla. Verrattuna matalapaineiseen järjestelmään, hinta, huollon tarve sekä järjestelmän monimutkaisuus ja tehon tarve kasvavat. Korkeapaineisen järjestelmän etuna on metaani päästöjen eliminointi sekä mahdollisuus heikompi laatuisen maakaasun käyttöön. Toisin kuin matalapaineisella kaasunsyöttöjärjestelmällä, korkeapaineinen järjestelmä vaatii kuitenkin pakokaasujen jälkikäsittelyä tai muita toimenpiteitä moottorilla täyttääkseen IMO Tier III NOx päästörajoitukset. Suurimmat ongelmat korkeapaineisen kaasunsyötön toteutuksessa 4-tahtimoottorilla liittyvät ruiskutussuuttimen tai -suuttimien sijoittamiseen moottorin sylinterikannella, missä tila on vähissä.

ABSTRACT

LUT University
LUT School of Energy Systems
LUT Mechanical Engineering

Rasmus Karlsson

Utilization possibilities of high-pressure gas injection for 4-stroke diesel combustion

Master's thesis

2021

128 pages, 90 figures, 34 tables and 11 appendices

Examiners: D. Sc. (Tech) Mika Lohtander
Professor Teemu Turunen-Saaresti

Keywords: dual fuel engines, fuel supply systems

The aim of this thesis was to evaluate the utilization possibilities of high-pressure gas injection in a compression ignited 4-stroke dual fuel engine operating in IMO Tier III emission limits. In this thesis the applicable fuels as well as the fuel gas supply systems of such an engine are investigated. The fuel gas supply system evaluation is done with the assumption that liquefied natural gas will be used as the fuel. The various components of the fuel gas supply system, such as pumps, compressors, heat exchangers as well as possibly needed exhaust aftertreatment systems are investigated.

The research methods used in this thesis are primarily theoretical. A literature review was conducted for the alternative fuels and for the fuel gas supply system components as well as for the emission level of the engine. A market benchmarking of high output 2- and 4-stroke dual-fuel engines was also made. Additionally, a simulation model made in HYSYS was used to estimate the power – and heating as well as cooling consumptions required for the different fuel gas supply systems. Finally, the rough prices of the components constituting the systems was made with the help of price comparisons found from suppliers and literature.

The results serve as a feasibility study to utilizing high-pressure gas injection in a 4-stroke engine. High-pressure gas injection can be used by pressurizing the fuel with pumps or compressors. The high-pressure gas supply system has a higher price, needs more maintenance and the fuel pressurization consumes more power than a low-pressure gas supply system. The high-pressure system is also more complex. The advantage of using high-pressure gas injection is that the engine methane slip can be eliminated, and lower quality natural gas can be used. But unlike low-pressure systems, a high-pressure system will need exhaust aftertreatment or other on-engine methods to comply with IMO Tier III NOx limits. Biggest on-engine obstacles for high-pressure injection are related to the placement of the injector on the cylinder head, as the space is limited on a 4-stroke engine.

ACKNOWLEDGEMENTS

First of all, big thanks to both the examiners Mika Lohtander and Teemu Turunen-Saaresti for their guidance and valuable comments throughout the writing of this thesis. From Wärtsilä side a big thank you goes to Petri Aaltonen and Christer Hattar for helping me throughout the thesis. Also, invaluable help has been received from Stefan Fältén for the simulation side of this work. Additionally, a big thank you to all the people, such as Giacomo Sciuto, Jan Sjögren, Luca Zuanigh, Markus Laaksonen, Toni Stojcevski and anybody potentially missing from the list, who have had the time to discuss and provide valuable information from the varying subjects covered in this thesis.

Lastly and most importantly, a big thank you also to my family for their support.

Rasmus Karlsson

Rasmus Karlsson

Turku 23.12.2020

TABLE OF CONTENTS

TIIVISTELMÄ **1**
ABSTRACT **2**
ACKNOWLEDGEMENTS **3**
TABLE OF CONTENTS **5**
LIST OF SYMBOLS AND ABBREVIATIONS **8**
1 INTRODUCTION **11**
1.1 Research problem 12
1.2 Research question 12
1.3 Research scope 13
1.4 Research methods 14
2 LITERATURE REVIEW **15**
2.1 Overview of possible fuels for "Gas diesel" concept 16
2.1.1 Fuel storage and energy content 18
2.1.2 Fuel properties for handling and injection equipment 20
2.1.3 Fuel combustion properties 23
2.1.4 Methanol (CH_3-OH) 25
2.1.5 Ethanol (C_2H_5-OH) 27
2.1.6 Ethane (C_2H_6) 27
2.1.7 Liquefied petroleum gas, LPG 28
2.1.8 Biomethane (CH_4) 29
2.1.9 Dimethyl ether (C_2H_6O), DME 30
2.1.10 Fatty acid methyl ester, FAME 31
2.1.11 Ammonia (NH_3) 32
2.1.12 Hydrogen (H_2) 34
2.2 Overview of fuel combustibility from GD perspective 36
2.3 Overview of fuel emissions 38
2.3.1 NOx emissions 39
2.3.2 SOx emissions 42
2.3.3 GHG emissions 43
2.3.4 Well-to-wake and tank-to-wake emissions 45

2.3.5 Emission reduction for HP-DF process 50
2.4 LNG details 51
2.5 Overview of the systems needed to utilize the HP gas in a 4-stroke engine 54
2.5.1 LNG Storage 54
2.5.2 HP compression of LNG 57
2.5.3 HP pumping of LNG 63
2.5.4 HP Feed system on engine 67
2.6 LNG in a combustion process 69
2.6.1 Basics of conventional CI and SI combustion 70
2.6.2 Low pressure injection, diesel process 71
2.6.3 High pressure injection, diesel process 74
2.7 Calculation model for the fuel gas supply system of 46TS-GD 75
2.7.1 Aspen HYSYS model of fuel gas supply system 77
2.8 Market benchmarking of LP-DF and HP-DF engines 80
2.8.1 4-Stroke DF market 83
2.8.2 2-Stroke DF market 85
3 RESULTS 91
3.1 Cryogenic HP compressor and HP Compressor gas feed systems 91
3.2 Cryogenic HP pump gas feed system 95
3.3 LP-DF gas feed system 98
4 ANALYSIS 100
4.1 Analysis of calculation results 100
4.2 “HP-DF” vs “LP-DF” 102
4.3 HP Compressor vs HP pumping 108
4.4 Equipment and layout possibilities 112
4.4.1 Cryogenic HP Compressors 112
4.4.2 Cryogenic HP Pumps and HP vaporizers 114
4.4.3 HP Compressors 116
4.5 Sensitivity analysis 118
5 CONCLUSION 120
5.1 Future research 126
LIST OF REFERENCES 128
APPENDICES

Appendix I: Fuel prices

Appendix II: Basic properties of hydrocarbons

Appendix III: LNG production

Appendix IV: LNG fuel tanks in marine applications

Appendix V: Additional information about the LNG compositions

Appendix VI: MAN 2-stroke portfolio products

Appendix VII: Results, HP Compressor

Appendix VIII: Results, HP Pump

Appendix IX: Results, LP Pump

Appendix X: Averaged mass –, heating – and cooling flows

Appendix XI: FGSS CAPEX Price comparison data

LIST OF SYMBOLS AND ABBREVIATIONS

ACQ	Annual contract quantity
BOG	Boil-off gas
BSEC	Brake specific energy consumption
BTU	British thermal unit
CAPEX	Capital expenditure
CCS	Carbon capture and storage
CI	Compression ignition
DF	Dual fuel
ECA	Emission control area
EPA	Environmental Protection Agency
DME	Dimethyl ether
DOC	Diesel oxidation catalyst
EEDI	Energy efficiency design index
EGCS	Exhaust gas cleaning system
EOS	Equations of state
FAME	Fatty acid methyl ester
FGSS	Fuel gas supply system
GD	Gas diesel
GHG	Greenhouse gases
GVU	Gas valve unit
HC	Hydrocarbon
HCCI	Homogenous charge compression ignition
HFO	Heavy fuel oil
HP	High-pressure
HP-DF	High-pressure dual fuel
HRR	Heat release rate
ICCT	International Council on Clean Transportation
ICE	Internal combustion engine
IEA	International Energy Agency

IGC	International Code for the Construction and Equipment of Ships Carrying Liquefied Gases in Bulk
IGF	International Code of Safety for Ships using Gases or other Low-Flashpoint fuels
IMO	International Maritime Organization
IPCC	Intergovernmental Panel on Climate Change
LBSI	Lean-burn spark ignition
LCA	Life cycle assessment
LHV	Lower heating value
LNG	Liquefied natural gas
LOHC	Liquid organic hydrogen carriers
LP	Low-pressure
LP-DF	Low-pressure dual fuel
LPG	Liquefied petroleum gas
LTC	Low temperature combustion
MDO	Marine diesel oil
MEPC	Marine Environment Protection Committee
MGO	Marine gas oil
MTPA	Million tonnes per annum
NPV	Net present value
NG	Natural gas
NOx	Nitrogen oxides
NPSH	Net positive suction head
OPEX	Operational expenditures
PM	Particulate matter
ppmv	Parts per million by volume
PVU	Pump vaporizer unit
RCCI	Reactivity controlled compression ignition
SCR	Selective catalytic reducer
SEC	Specific energy consumption
SI	Spark ignition
SOx	Sulphur oxides
THC	Total hydrocarbon

TTW	Tank-to-wake
UNFCCC	United Nations Framework Convention on Climate Change
VFD	Variable-frequency drive
VOC	Volatile organic compound
VLGC	Very large gas carrier
WTT	Well-to-tank
WTW	Well-to-wake

1 INTRODUCTION

Emissions from internal combustion engines (ICE´s) have for a long time been a subject of discussion, while numerous emission regulations have been put into place both on land and sea. Usually the regulations have been local, but recently more global regulations have also come into force. For example, in 2020, the International Maritime Organization (IMO), a specialized agency working under the United Nations, brought into effect the amendments made to MARPOL Annex VI in 2008, which limit the sulphur emissions of ships globally. The gradual adjustment towards more global regulations, not only in the marine industry, has resulted in the positive issue of sustainability being discussed within a wider panel. During the last couple of years, for example the International Council on Clean Transportation (ICCT) has published a couple of papers related to emissions of marine shipping. The same subject has also been discussed by research organizations such as for example SINTEF and companies such as Thinkstep. Also, classification societies, such as DNV-GL, have published papers assessing the choices of fuels and engines in the marine environment, with a strong focus on future sustainability.

The IMO is “responsible for safe, secure and efficient shipping and the prevention of pollution from ships”. In addition to the global sulphur emission limit, MARPOL Annex VI also regulates emission limits in certain regions, known as emission control areas (ECA´s). There exists four ECA´s globally, in which the nitrogen oxide (NOx) and volatile organic compound (VOC) emissions are limited. In 2018 the IMO has set an objective of reducing the total annual greenhouse gas (GHG) emissions from international shipping by at least 50% by the year 2050, with the reference year being 2008. As GHG emission levels are still currently rising, IMO has an objective to have the GHG emissions peak as quickly as possible, and in the long run to phase out the GHG emissions created by international shipping altogether. (IMO 2018, p.4-6)

For ships to comply with the current emission regulation, the traditionally most widely used shipping fuel, heavy fuel oil (HFO), cannot be used anymore globally, unless significant amounts of sulphur is removed from it. The tightening emission regulations along with the raise of public awareness has created an interest in using more environmentally friendly fuels and combustion technologies. Of the new wave of alternative fuels, liquefied natural gas

(LNG) has been the most popular to-date, with other gaseous fuels, such as methanol and liquefied petroleum gas (LPG) also gaining some usage.

LNG has become a popular fuel duel to its relatively low emissions as well as well as being attractively priced and quite easily available. Using LNG in a low-pressure dual fuel (LP-DF) engine enables the operator to comply with the currently most stringent IMO tier III emission legislation, without additional exhaust aftertreatment. There are however several different fuel injection strategies available for DF engines using LNG, with the fuel injection strategy having an effect amongst others on the needed fuel feeding equipment, the final emission levels achievable and the exhaust aftertreatment needed.

1.1 Research problem

The target of this thesis was to look at the ways in which DF engines can efficiently comply with the current emission regulations, while considering the possible future legislation. One problem associated with future legislation is that it is uncertain. IMO has predicted in 2018, when the IMO GHG strategy was unveiled, that the mid-term measures to reduce the carbon intensity of shipping would be active somewhere between 2023-2030 (IMO. 2018, p.2). The predicted lifetime of a ship can be in the range of 25 to 30 years, with the average merchant ship age being 20.5 years in 2018 (European Commission 2020, p.4,28). This means, that a vessel built now could still be in operation in 2050, when the GHG reductions are wanted to be at half the level. As such the importance of selecting fuel systems and engine technologies, that can be used throughout the entire lifecycle of the vessel or plant is large. In this regard DF engines provide good value, as they are flexible.

1.2 Research question

The research question of this thesis was to evaluate the technical and economical consequences related to the utilization of high-pressure (HP) gas injection instead of low-pressure (LP) gas injection, in a compression ignited 4-stroke DF engine. For this thesis an engine with a bore size of 46 cm was chosen for closer evaluation. In addition to the engine, the other necessary fuel gas supply system (FGSS) components, such as pumps, compressors and heat exchangers as well as the possibly needed exhaust aftertreatment equipment were at the focus of this thesis. For comparability, the power generation systems compared were chosen so that the final exhaust emission levels would be IMO Tier III compliant.

1.3 Research scope

The target of this research was to analyze alternative gas feed systems for DF engines, so that the engines could efficiently comply with the current – and possible future emission legislation. Therefore, the research scope was focused on subjects directly relating to the engine and its emissions. This includes components such as the fuel storage system, the FGSS and the possible exhaust aftertreatment system. In this work the fuels are analyzed from the engine and engine related system perspective, meaning that less detail is given for the upstream fuel processing and the challenges related to the fuel supply.

During the writing process of this thesis it became clear that there is a lot of discussion happening at the moment on the fuel side, both about the extraction and processing as well as about the supply. This might in some degree be a cause of 2020 being the first year when the new sulphur emission limits have been in use, causing changes to both the fuel suppliers as well as the end-users. Nevertheless, the most frequent themes related to the fuel discussion seemed to be the lifecycle emissions related to fuels. Some of the findings are discussed on a quite general level in chapter 2.3 when fuel emissions are touched upon. A deeper look into the emissions related to the fuel extraction, processing and transportation are not included in the scope of this thesis, because of the complexity of the subject.

On the emissions, most of the effort is put into currently regulated marine emissions, which are NOx and sulphur oxide (SOx) emissions. Also, the currently indirectly regulated GHG emissions are discussed in this work, especially as the current objectives are to reduce the carbon intensity of shipping. It is therefore quite safe to assume some work to happen on the GHG emission side in the future. There are also other emissions related to engines that are not discussed in this thesis, mainly due to their irrelevance for marine legislation, at least for the time being. An example of such emissions are the formaldehyde emissions, which can be carcinogenic and as such are dangerous to human health. Formaldehyde emissions are limited for example in the German TA luft regulations for stationary, gaseous fueled engines, but no plans to limit them from the IMO side has been communicated.

For the FGSS, various compositions of LNG along with LNG boil-off-gas were considered. Although there are alternative fuels available already also for shipping, LNG is by far the most common of the “non-traditional” fuels. As the FGSS efficiency was evaluated using

LNG, the fuel injection pressures inspected in this thesis range from 300 bar to 600 bar. 300 bar is estimated, based on past experience from GD engines at Wärtsilä, to be a little under the minimum required gas feed pressure, and as such is a good baseline. For higher pressures the amount of suitable equipment starts to diminish.

Another subject, which was tried to keep simple, was the LNG storage on board the ship. Several alternative storage systems are shortly touched upon in the literature review, with the main difference being in the possibilities of storing LNG under pressure or at ambient pressures. The storage solution and the fuel tank pressure level influence the FGSS system. However, to limit the number of simulation variants, only the storage at ambient pressures was considered finally.

1.4 Research methods

The research methods employed in this thesis were mostly theoretical, with no field testing or similar methods used. The used methods consisted of a literature review around the subject, a steady-state simulation to compare the efficiencies of the FGSS alternatives and a rough evaluation of the FGSS equipment suppliers, availability and prices. For the prices various equipment manufacturers were contacted, but understandably there is a reluctance to disclose concrete prices. Therefore, the price results rely partly on data provided by engine manufacturers, such as MAN and WinGD, on their price estimations of the differing FGSS for differing ship types and sizes. Price comparisons of differing LNG FGSS were also available from SEA-LNG, a multi-sector industry coalition formed to promote the usage of LNG. With the inspection of several different price comparisons, a general trend can be observed at least, even though an exact price comparison cannot be made.

For the FGSS performance simulation HYSYS software from Aspen Technologies was utilized. HYSYS is a chemical process simulation software specially developed for the oil – and gas industry for simulating process containing hydrocarbon as well as other gases and liquids. In this thesis only the steady-state simulation was used, as the focus on the FGSS performance side was on the full load efficiencies. As such part-load performance nor dynamic system changes were not thoroughly investigated in the scope of this work.

2 LITERATURE REVIEW

The intention of this literature review is to try to inspect at a quick glance the whole process related to the combustion of a gaseous fuel in a DF engine using the diesel process, known as a gas diesel (GD) engine in the Wärtsilä portfolio. The literature review starts from the fuel and ends in the exhaust stack. The literature review was conducted during the course of 2020. The main sources of information have been the various studies around the subject made by organizations such as the International Council on Clean Transportation (ICCT) and SINTEF and companies such as Sphera (formerly Thinkstep), along with the references from these studies. Also, the database search, LUT Primo, provided by Lappeenranta University of Technology, has been a valuable source for finding information, especially for the comparison of fuels and fuel pressurizing equipment. DieselNet, an independent online information portal, with editorial reviewed technical papers on diesel engines, was utilized to some extent also. For the market benchmarking the thesis has had to rely on project guides and white papers provided by the various engine manufacturers as well as by the classification societies.

The literature review starts by inspecting the physical properties affecting storage, transportation and combustion of several fuels that could be used on a GD engine. After this each fuels pros and cons are analyzed. A more detailed look at natural gas and LNG is also provided in the appendices. The emissions related to the combustion and the production of the fuels is also quickly discussed.

After the fuels, the GD process usage for LNG is evaluated, starting from the LNG storage and ending in the combustion and the emissions. Different means of pressurizing the fuel are discussed as well as quickly glancing over the equipment that is needed on-engine. The fuel pressurization strategies considered here are compression and pumping.

To get a better understanding of the fuel pressurization differences and especially the power consumptions and efficiencies related to each choice, the setup of a calculation model utilizing Aspen HYSYS is discussed through. Finally, a market benchmarking of 2-stroke and 4-stroke DF engines is made, the focus being on the gas injection side of the engines.

2.1 Overview of possible fuels for “Gas diesel” concept

This chapter intends to give a short overview firstly on the traditional marine fuels for a baseline, but more importantly on some of the alternative fuels for diesel engines that are available or quite close to being on the market. The market availability and prices of the fuels is compared first. After this the physical properties affecting the storage, handling and combustion of the fuels are analyzed collectively. Lastly the emissions from combustion and production as well as the pros and cons and possible market data of each fuel are quickly viewed fuel-by-fuel.

There have been changes recently on the marine fuel market, as the global sulphur cap for fuels came into force at the beginning of 2020. The traditional marine fuels can be classified into residual – and distillate fuels. Residual fuels contain the heavier hydrocarbons and other components that remain after fuel oil has been distilled away from crude oil in refinery operations. Distillate fuels, on the other hand, have gone through a distillation process of at least some sort. The residual fuel, called heavy fuel oil (HFO), can contain a substantial amount of harmful substances such as sulphur, heavy metals (vanadium, nickel) and asphaltenes. In marine distillate fuels most of these harmful substances are not present, at least in as large amounts. HFO has had until 2020 a global average sulphur content of roughly 2.5 mass % (Thinkstep 2019, p.24-25). As the sulphur regulation has come into force in 2020, the amount has significantly decreased, with sulphur content typically being between 0.1% to 0.5%. As HFO is viscous at ambient conditions, it must be heated before the flow properties are such, that it can be used in an engine (Kass et al. 2018. p.8). The closer fuel properties are specified in ISO 8217. (Aakko-Saksa & Lehtoranta 2019, p.12-13)

For alternative fuels to be used, the price and availability has to be competitive compared to the traditional fuels. In figure 1 are shown the estimated annual production volumes of the fuels for which data was found. The annual volumes are not all for the same year, with the oldest data being from 2017, but it gives an overview of the situation, nevertheless. As can be seen, HFO and LNG constitute a large share of the marine fuels. It is worth noting, that for example ammonia, hydrogen, liquid propane gas and ethane are produced for other than fuel usage also.

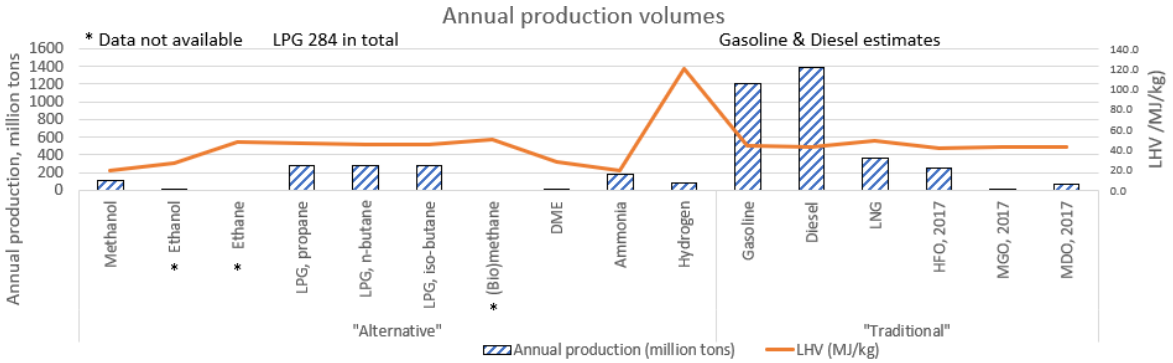

Figure 1. *Annual production volumes and the lower heating value of the fuels considered. (Bae & Kim 2017, p.3404, DNV-GL 2019b, p.50, Kass et al. 2018, p.8, Meriteollisuus ry, 2020, p.7,10-14, McAllister, Chen & Fernandez-Pello 2011, p.244, Heywood 1988, p.915)*

In figure 2 below are shown fuel prices from 2019, with the baseline being Brent crude oil. As can be seen, HFO and LNG were the most price competitive, with MGO and different biofuels having a higher price.

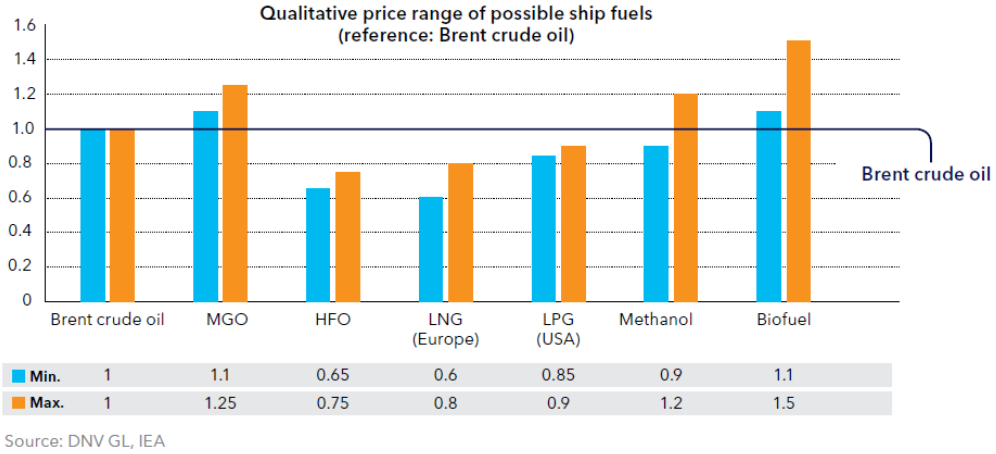

Figure 2. *Fuel prices compared to Brent crude oil price. (DNV-GL 2019a, p.11)*

There are many studies being conducted on alternative fuels at the moment. To name a couple, the International Energy Agency (IEA) has published a paper named "Advanced Biofuels – Potential for cost reduction" in 2020 while also ICCT has published a working paper in September 2020 titled "The potential of liquid biofuels in reducing ship emissions". Also, in Finland a paper titled the "Ways to decarbonize shipping" has been published in 2020, by Meriteollisuus ry. In these studies, the costs associated to alternative fuel production, with at least some functioning pilot plants, are assessed, amongst other things. A closer look at the alternative fuel prices is presented in appendix 1.

2.1.1 Fuel storage and energy content

In addition to price and availability, important properties of fuels are that they are easy and safe to handle and transport. This has been the strength of the traditional fuels. Marine fuels have needed separation and residual fuels have needed some additional pre-treatment, such as heating, before injection into the engine, but these have been relatively easy to do. The physical properties of fuel that influence the handling are at least the temperature at which the fuel is liquid and the flash point. Liquid state is preferred to the gaseous, to get a bigger energy density. Also, from an energy efficiency point-of-view pumping incompressible liquids would be preferable to compressing compressible gases. Naturally, liquefication at ambient pressure would be preferable for easier and cheaper storage. For a gas to be liquefied, its temperature must be lowered below its critical temperature (Eastop, Thomas & McConkey 1993, p.520). In figure 3 below the liquefication temperatures of the fuels can be observed between the solid lines. Some of the liquefication values have been obtained with REFPROP v10 software. LNG and hydrogen are the fuels with the lowest liquefication temperatures. For the more complex hydrocarbon fuels, the pouring point has been selected as the lower storage temperature, while the actual values will depend on the composition.

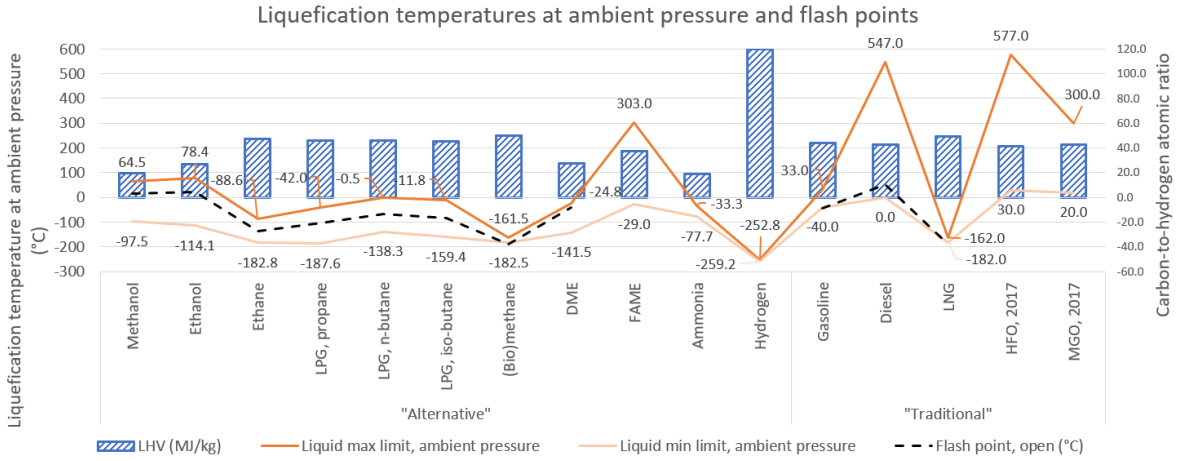

Figure 3. *Liquefication temperatures at ambient pressures and the flash points of the fuels. (McAllister et al 2011, p.12, 293, Martins & Brito 2020, p.6, REFPROP v10 2018, Sarvi et al. 2011, p.26, Stojcevski, Jay & Vicenzi 2016, p.4)*

In addition to the liquid state, fuels with a high energy content are desirable to reduce the needed storage volume. The lower heating value (LHV) is the typical SI unit which expresses the amount of heat generated by the combustion of the fuel, typically informed in MJ/kg units (McAllister et al. 2011. p.23). In figure 4 below the volumetric and gravimetric energy contents of several fuels are illustrated.

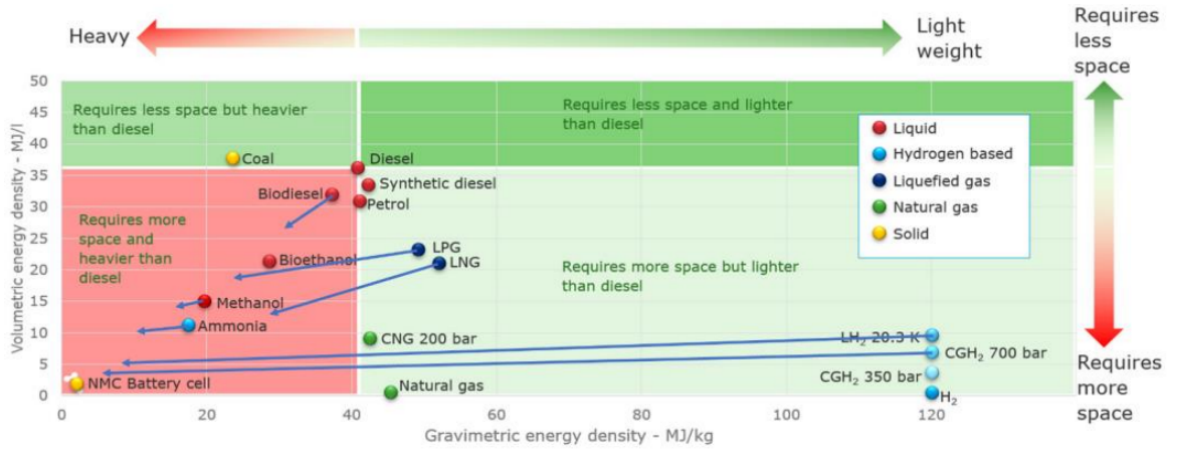

Figure 4. *Specific energies of several fuels plotted against the volumetric energy density. The blue arrows indicate the energy density, when the storage system is considered. (DNV-GL, 2019b, p.29)*

In figure 5 below are shown estimates of the volumetric tank needs to contain the same energy content as MGO with and without considering the insulation needs. Without insulation values have been calculated for liquid storage at ambient pressure with REFPROP software. In addition to insulation, cold storage conditions might need additional equipment and tank room space. In a study complied by Wik and Niemi, the LNG fuel tank volumes doubled compared to MDO, when the insulations, tank room and the cryogenic tank were considered (2016, p.13).

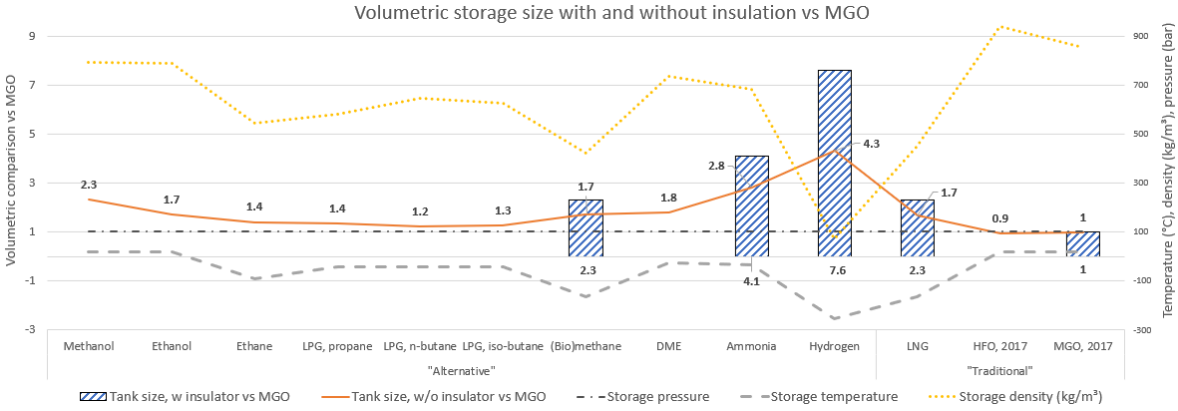

Figure 5. *The comparative fuel tank size with and without insulation vs MGO (Korean Register 2020, p.12, REFPROP v10 2018)*

Fuel storage of alternative fuels may also present other challenges in addition to the energy content and volume challenge. The fuels must remain stable under storage and in use. Fuels are stored for months in tanks and must interact to varying degrees with water and dioxygen. Over time some biofuels might degrade, with the degradation products potentially causing corrosion. In general, fossil fuels are less likely to degrade due to branching of hydrocarbons and the aromatic compounds present in fossil fuels. (Lee et al. 2014, p. 145-146)

The physical properties that have an effect on the safety are at least the flammability limits of the fuel-air vapor, the flash point and the vapor density The flash point is the temperature to which a substance must be heated, for it to from sufficient amounts of vapor, so that the resulting vapor-air mixture can be ignited. The flashpoint and the flammability limits are illustrated in figure 6. (McAllister et al. 2011, p. 99-100)

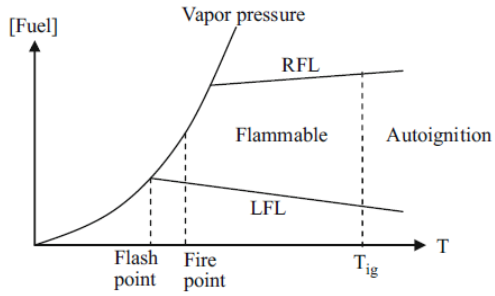

***Figure 6**. Flammability and the flash point of a vapor. (McAllister et al. 2011, p. 100)*

The storage, transportation and usage conditions have to be set-up so, that no ignition sources can affect the gas/substance at temperatures lower than the flash point. Typically for fuels with flash points under 40°C extra precautions are necessary. In figure 7 the flammability limits and minimum ignition energies of the fuels are shown. (Speight 2007, p.75-76)

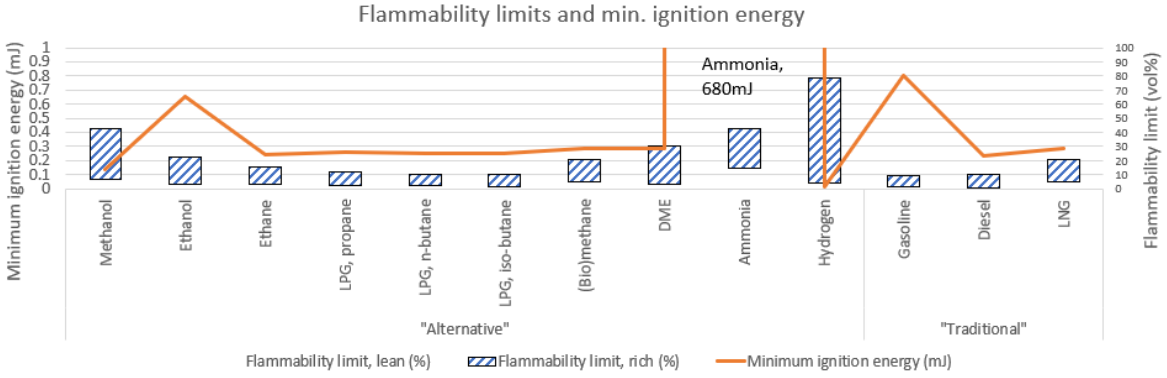

***Figure 7.** Flammability limits and minimum ignition energy of the fuels. (Kutz & Reed 2015, p.679, McAllister et al. 2011, p.126,281,287-288,293, Valera & Agarwal 2019, p.12)*

Another safety related property is the vapor density ratio, which describes the density of the vapor or gas versus the density of air (Nolan 2014, p. 62). Denser gases will sink while lighter gases will dissipate into the atmosphere (Speight 2007, p. 70). Some fuels are also toxic, such as methanol to some - and ammonia to a larger degree (DNV-GL, 2019b, p. 30).

2.1.2 Fuel properties for handling and injection equipment

Properties affecting the handling of fuels are at least the bulk modulus. viscosity, and density. They all vary by temperature and pressure. The bulk modulus defines the compressibility of

the substance. Pumping of fluids with higher bulk modulus requires less power (Bae 2016, p. 3404). It also has an influence on the fuel delivery and pumping characteristics (Mollenhauer & Tschöke 2010, p.90-91). On hydraulically controlled systems, such as jerk pump systems, the bulk modulus can even influence the fuel injection timing, while on common rail systems it has an effect amongst others on the pressure fluctuations of the system (Lapuerta et al. 2012, p.1336, Mollenhauer et al. 2010, p.153). In figure 8 below are shown the found bulk modulus values for the fuels inspected.

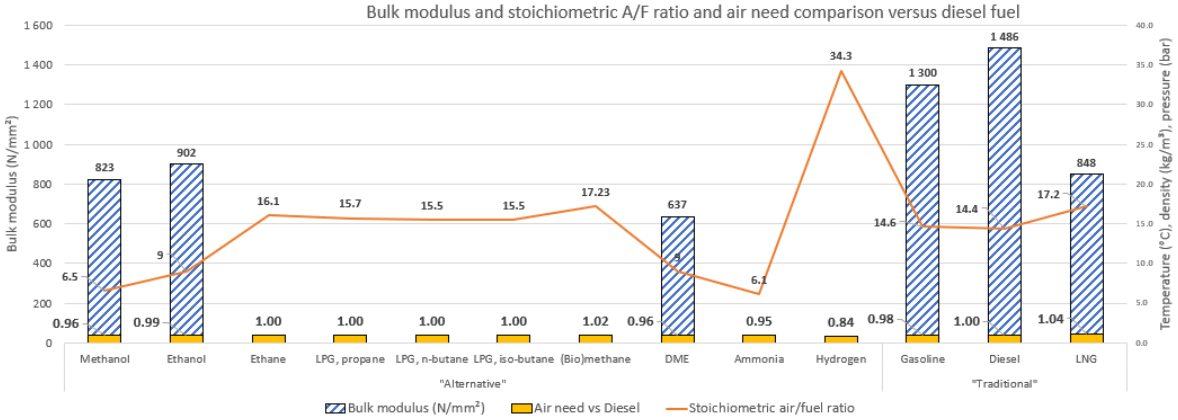

Figure 8. *Bulk modulus, stoichiometric air fuel ratios and relative air needs in comparison to diesel fuel at the stoichiometric air-fuel ratio for the fuels. (Valera et al. 2019, p.12, Mollenhauer et al. 2010, p.96, Arcoumanis et al. 2008, p. 1016, Stojcevski et al. 2016, p.4, Heywood 1988, p.915, McAllister et al. 2011, p.244)*

The fuel composition also has an effect on the needed air amount. The stoichiometric air-fuel ratio informs the amount of oxidizer, such as air, needed to burn the fuel. The air-fuel ratios of the fuels are shown in figure 8. Diesel engines operate on excess air, but the air-fuel ratios can be used to predict if significantly more air is needed for a fuel at the same output. The air need for a given output has been calculated as in equation 1 below. As can be seen, there are no large differences on the needed air amounts. (McAllister et al. 2011, p.17)

$$\dot{m}_{air} = \frac{\lambda}{\dot{m}_{fuel}} = \frac{\lambda \times P}{Q_{\mathrm{LHV}}} \qquad \textit{(Eq. 1)}$$

Where, λ = Air-fuel ratio

P = Power output

The viscosity, which is temperature and pressure dependent, affects the pump characteristics of the fuel system, with high viscosity preventing pumping while low viscosity causes pumping power losses and pump wear. Viscosity also has an effect on the injector equipment, with low viscosity usually causing sealing problems, while an excessively high

viscosity will disurpt the injection. Typical diesel fuel kinematic viscosity is between 2 and 4.5 mm²/s at 40°C. (Mollenhauer et al. 2010, p.91, 587)

The handling properties of fuels can to a certain extent be predicted from phase diagrams and envelopes, which show the phase of a substance at a certain temperature and pressure. An example of a phase diagram is shown in figure 9 below. In the case of fuels, the main interest lies around the liquid and gaseous states, which are separated by the vaporization curve. The vaporization curve ends at the critical point, at which the substance is indistinguishable between liquid and gaseous states. As the pressure is raised further, the substance becomes a supercritical fluid. (Mokhatab 2019, p.41)

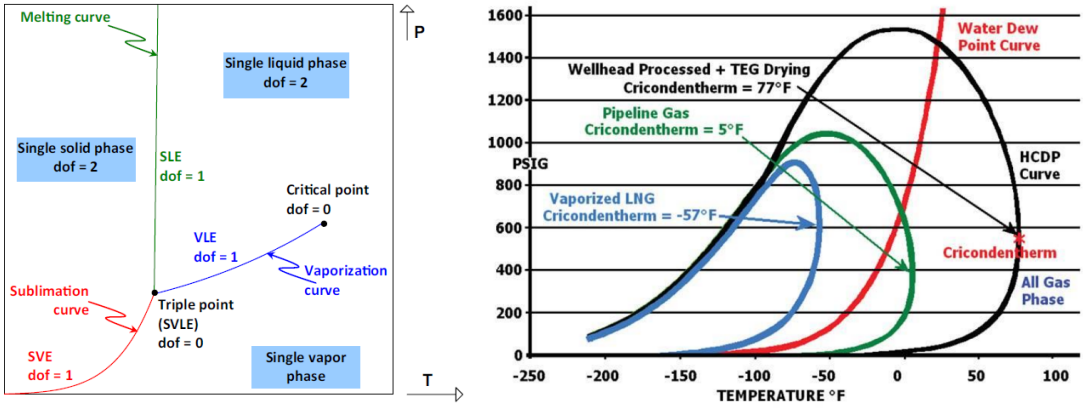

Figure 9. *A generic phase diagram of a single component on the left and a phase envelope of several components on the right. (Mokhatab 2019, p.38, Michell Instruments. p.2)*

When inspecting multi-component systems, the various components of the system would have differing phase diagrams. A phase envelope, such as in figure 9, can be used to inspect the phases at differing states. The dew-point line forms the bottom part of the envelope, while the top is formed by the bubble-point line. Inside the phase envelope the multi-component system is in both gaseous and liquid state, according to a ratio. The highest pressure point of the envelope is called the cricondenbar, above which gas phases cannot exist. Alternatively, the highest temperature of the envelope is called the cricondentherm, and it is the temperature beyond which the liquid phase cannot exist. In figure 9 is shown a typical phase envelope for natural gas at the composition of extraction, as pipeline gas and as vaporized LNG. As can be observed, the composition changes have a big effect on the phase envelope, and especially on the dew line. (Speight 2017, p. 171-172)

2.1.3 Fuel combustion properties

The basic fuel properties affecting the combustion are examined to be able to compare the different fuels. The GD combustion is still covered in more detail later. The properties that affect the combustibility of a fuel in a CI-engine are related to the ignition properties. The most important property for CI-engines is the experimentally determined cetane number (CN). A high CN means that the fuel is easier and faster to ignite. The normal diesel fuel CN range is from 40 to 55. (Heywood 1988. p.550). A lower CN will cause a longer ignition delay, resulting in a higher rate of pressure rise once combustion eventually starts (Valera et al. 2019, p.25). For SI-engines a high octane number (ON) is important, to avoid uncontrolled auto-ignition. The ON describes the ignition resistance of the fuel. (Mollenhauer et al. 2010, p. 66,12).

Properties that affect the ignitability of the fuel are at least the auto-ignition temperature, the flame speed, the required ignition energy and the flammability limits. Of these the ignition energy and flammability limits were already covered in figure 6. In figure 10 are shown the cetane and octane numbers, where applicable, in addition to the laminar flame speeds. It is worth noting that especially the flame speeds are estimations, with the actual flame speed depending on the mixture temperatures and the air-fuel ratios in addition to the fuel properties (Mollenhauer et al. 2010, p. 61).

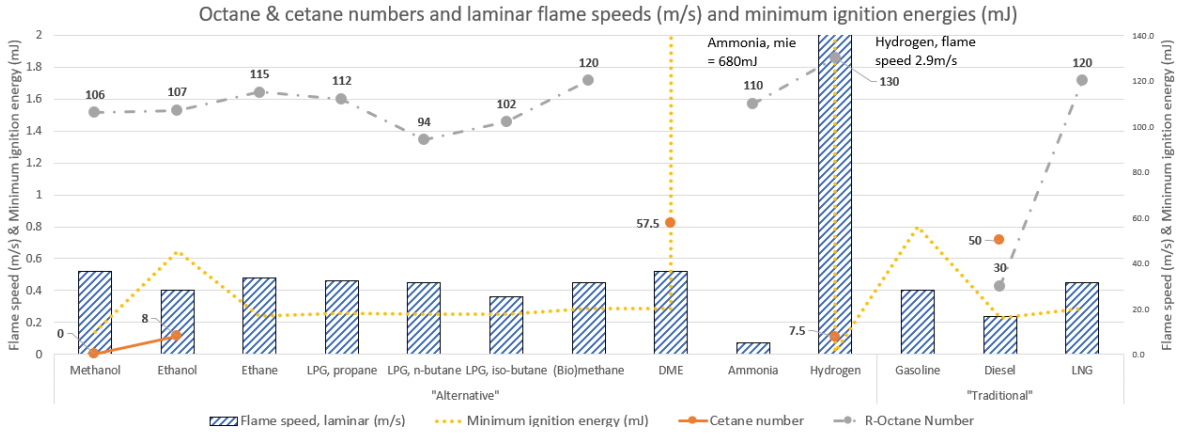

Figure 10. *Cetane – and octane numbers of fuels as well as the flame speeds and minimum ignition energies. (Mollenhauer et al. 2010, p.102, Valera et al. 2019, p.12, Bureika et al. 2020, p.24, McAllister et al. 2011, p.244, Glassman & Yetter 2014, p.869, Kutz et al. 2015, p.679, Flekiewicz et al. 2020, p.100)*

Combustion temperature has an effect on many things, such as NOx formation, and as such the properties affecting that are also of interest. The properties related to combustion temperatures, such as auto-ignition temperature, flame temperature and latent heat of

evaporation are shown in figure 11 below. The fuel properties have an effect on the combustion temperature, with high LHV´s, low heat of vaporization and a high oxygen content raising the flame temperature and thus also the in-cylinder temperature (Heywood 1988, p.575, 591, 814). The heat of vaporization tells the amount of energy required to vaporize the fuel. This heat amount is considered to cool the charge, as the energy is used into the phase transformation (McAllister et al. 2011, p.23). As such high heat values of vaporization are desirable to limit the combustion temperature and increase the thermal efficiency of the engine (Valera et al. 2019, p.13).

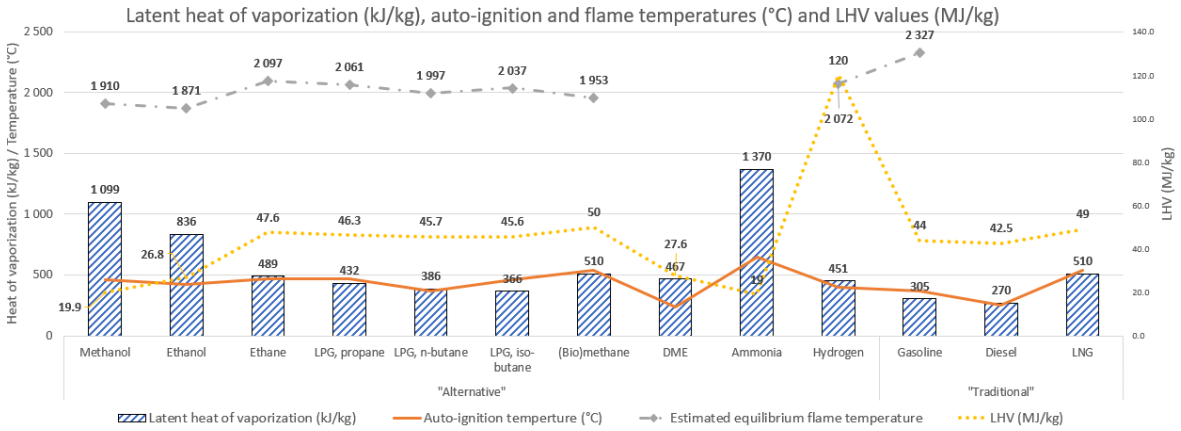

Figure 11. *Latent heat of vaporization, auto-ignition – and flame temperatures along with the heating values of the fuels. (McAllister et al. 2011, p.93, 244, Arcoumanis. et al. 2008, p. 1016, Heywood 1988, p.915, Martins et al. 2020, p.6, Bureika et al. 2020, p.24)*

In addition to the combustion temperature the emissions depend on the fuel composition. Most of the fuels contain hydrocarbons to some extent. Hydrocarbons provide the heating value of natural gas, and as such also LNG (Speight 2018, p.259). Hydrocarbons range from methane to heavier and longer carbon compositions ending in fuels such as gasoline and diesel. The basic properties of light hydrocarbons are presented in closer detail in appendix 2. The hydrocarbon composition also has an effect on the emissions that are formed during combustion. In figure 12 below are shown the hydrogen to carbon ratios of some of the fuels discussed in this paper. For more complex hydrocarbon compounds the ratio will vary. The H-C ratio has an effect on the amount of CO_2 that is produced, with a larger H-C ratio resulting in smaller CO_2 emissions. (Kutz et al. 2015, p.674)

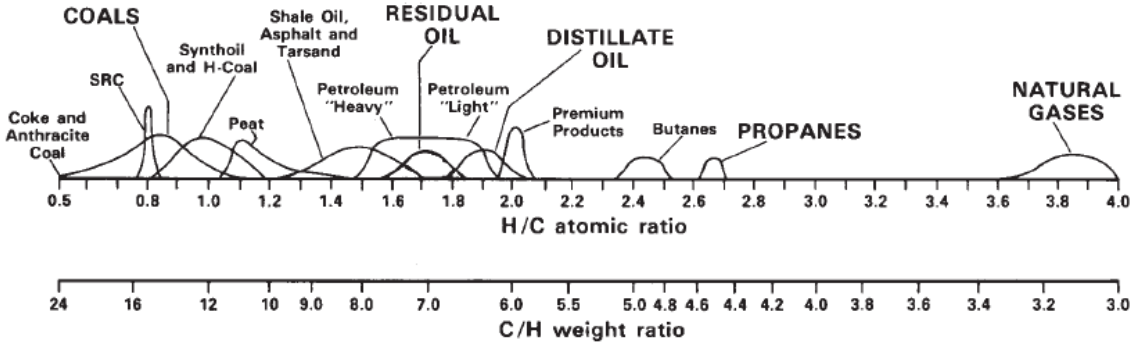

Figure 12. *Hydrogen/carbon ratios of fossil and synthetic fuels (Kutz et al. 2015, p.674)*

In the combustion process hydrocarbons are converted mainly into carbon dioxide and water, as illustrated in equation 2 below. In addition to carbon, hydrocarbon fuels also contain small quantities of organic compounds, such as sulphur, nitrogen and oxygen, which are also involved in the combustion process. As combustion is imperfect, incomplete products of combustion can also be found in the emissions. The C-H ratio of the fuel has a significant effect on the GHG emissions, as on a mass basis the CO_2 carbon emissions constitute for the largest percentage of the emissions. For example, if 16 kg of methane is completely combusted, the amount of CO_2 created is 44 kg (Winterbone 2015, p.211). (Aakko-Saksa et al 2019, p.4)

$$\text{FUEL (CH)} + O_2 \rightarrow CO_2 + H_2O + \text{heat} \qquad \textit{(Eq. 2)}$$

2.1.4 Methanol (CH_3-OH)

Methanol is a colorless and flammable liquid alcohol at room temperature. Methanol has been used as a fuel in spark ignited (SI) and compression ignited (CI) engines. Methanol is an attractive fuel mainly due to its low carbon content and its good storage and transportation properties, resulting in lower infrastructure expenditures compared to other fuels. As methanol is liquid at ambient conditions, the storage of methanol is less complicated than for most of the other fuels. Thus, also the costs related to the infrastructure needed for methanol use are projected to be significantly lower. Additionally, methanol bunkering could be done with same types of barges that are used for HFO and MGO (Andersson & Salazar 2015, p.30). Methanol is already produced and transported globally so the fuel infrastructure technology is existing (Andresson et al. 2015. p.23). Basic properties of methanol are shown in table 1.

Table 1. *Basic properties of methanol (McAllister et al. 2011, p.244, 293)*

Fuel	Combusitibility	Energy content	Phase at NTP	Tank size vs MGO	Low-flashpoint fuel
Methanol	Bad, CN ≤ 5	19.9MJ/kg	Liquid	2.3	Yes, 16°C

The disadvantages related to methanol are that it is toxic, corrosive and has a low viscosity as well as bad lubrication properties. These cause challenges especially on the fuel injection and - storage equipment. The combustion properties are also bad, but not a large problem if pilot ignition is used. Due to the low ignitability, the ignition delay is longer, so the eventual rate of pressure rise will be large once combustion occurs (Valera et al. 2019, p.25). In table 2 are the top-3 pros and cons of methanol as a fuel. (DNV-GL 2019a, p.25)

Table 2. *Top 3 pros and cons of methanol (DNV-GL 2019a, p.25-26, MAN 2020e, p.29, Andersson et al. 2015, p.30, Meriteollisuus ry 2020, p.16)*

Advantages	Disadvantages
Favorable storage properties, resulting in low costs (similar to HFO, 1/3 of LNG)	If production is based on usage of natural gas, no well-to-wake (WTW) advantage
Infrastructure technology existing, resulting in low costs	Low energy content (LHV≈19.9 MJ/kg), larger tanks needed
Production -, transportation - and bunkering technology existing	Price is currently (2019) more expensive than for marine distillate fuels

Emissions from burning of methanol are less than that of diesel fuel. A summary of emissions is shown in table 3. Methanol HP-DF operation on the passenger ferry Stena Germanica has proven that tier III emissions levels cannot be reached by pure methanol use, but the NOx levels are anyhow decreased compared to LFO operation (Stojcevski et al. 2016, p.10). DNV-GL has also estimated that an EGR or SCR system is needed to comply with IMO Tier III NOx regulations (DNV-GL 2019a, p.26)

Table 3. *Emission properties of methanol. (DNV-GL 2019a, p.9, 25-26)*

Fuel	NOx emission, LP-DF	NOx emission, HP-DF	Well-to-tank	Tank-to-wake	Well-to-wake
Methanol	-70% vs MGO, SCR/EGR/H_2O mix for Tier III	-30% vs MGO, SCR/EGR/H_2O mix for Tier III		-10%	≈ + 0-5 %

The environmental impact of using methanol significantly depends on the manufacturing method of methanol. The annual production of methanol is about 100 million tonnes, of which the majority uses natural gas as a feedstock (Meriteollisuus ry 2020, p.16). When the well-to tank emissions are also accounted for, methanol produced from fossil feedstocks does not reduce the total emissions compared to oil-based fuels. To reduce the environmental impact, methanol could be produced from various biomasses or be synthetically manufactured from renewable hydrogen (Meriteollisuus ry 2020, p.16). According to some

studies, renewable methanol could reduce the carbon emissions in the range of 65 to 95% compared to fossil fuels (Methanol institute 2018, p.7). (DNV-GL 2019a, p.26)

2.1.5 Ethanol (C_2H_5-OH)

Ethanol is a colorless, water soluble liquid alcohol at ambient conditions. The boiling point of ethanol is 78°C at ambient pressure. In some sources it is estimated that ethanol, in its liquid form, could be easily supplied with the current fuel infrastructure with relatively minor modification (Bae et al. 2017, p.3399). The combustion of ethanol provides relatively low emissions compared to traditional fuels, due to the C-H ratio and the high latent heat value. Bioethanol is a globally used and produced fuel. The bioethanol production process is considered carbon neutral, meaning that the bio-organic raw materials act as a carbon sink. The basic properties of ethanol are shown in table 4. (Florentinus et al. 2012, p.9)

Table 4. *Basic properties of ethanol. (McAllister et al. 2011, p.244, 293)*

Fuel	Combusitibility	Energy content	Phase at NTP	Tank size vs MGO	Low-flashpoint fuel
Ethanol	Bad, CN ≈ 8, ON ≈ 109	26.8 MJ/kg	Liquid	1.7	Yes, 22°C

The disadvantages of ethanol are the bad ignition properties and the low energy content. The combustion is nevertheless possible with the utilization of a pilot ignition. Ethanol also attracts water, and as such tends to be dissolved if it is in the presence of water, which could cause problems on the storage side. (Florentinus et al. 2012, p.10).

The well-to-wake emissions can be greatly reduced with the application of biofuels. Of the roughly 100 million oil equivalent tonnes of biofuels produced in 2019, bioethanol accounted for 63% (Meriteollisuus ry 2020, p.7). The bioethanol production volumes are significantly higher than for example biodiesel production. Ethanol is for example blended into automotive fuels, for use in spark ignited engines (Bae et al. 2017, p.3390). 1st generation ethanol has been produced from e.g. sugar cane, corn and sugar beets, while 2nd generation ethanol, which has come onto the market during the last couple of years, is produced from cellulosic, non-edible biomass, such as woody biomass or agricultural residues. (IEA. 2017, p.53)

2.1.6 Ethane (C_2H_6)

Ethane is a colorless and odorless gaseous hydrocarbon. It is a constituent of natural gas, normally found in small amounts. Ethane is normally separated from natural gas by

liquefying it, as it is of more value as a feedstock in petrochemical production (Speight 2018. p.277). Ethane is in a gaseous state at ambient conditions, but can be liquified at higher pressures, at relatively low temperatures around 32°C (Speight 2018, p.273). Main usage of ethane is in the chemical industry, so it is already transported with purpose-built ethane carriers in some amounts globally (Speight 2018. p.275). The increased shale gas production has led to an increase in ethane production, resulting in a price drop (Yang 2015, p.3263). This has made ethane a slightly more attractive option for fuel usage. MAN has to date sold 21 ME-GIE ethane engines, all to ethane carriers (Gingell 2019, p.40). The basic properties of ethane are shown in table 5.

Table 5. *Basic properties of ethane. (McAllister et al. 2011, p.244, Duan et al 2019, p.4)*

Fuel	Combusitibility	Energy content	Phase at NTP	Tank size vs MGO	Low-flashpoint fuel
Ethane	Bad, ON ≈ 118	47.5 MJ/kg	Gas	1.4	Yes, -135°C

The disadvantages of ethane are the price and the fact that the fuel storage costs would be comparably high, between the high price of LNG and the lower LPG and methanol prices. Not a significant amount of data was found about the emission levels achievable with the combustion of ethane, but MAN has estimated the emission levels to be quite similar to LNG (Gingell 2019, p.21). Ethane is a GHG, with a global warming potential of 5.5 on a 100-year scale, so ethane slip should also be avoided (Yang 2015, p.3263).

2.1.7 Liquefied petroleum gas, LPG

Liquefied petroleum gas (LPG) is a mixture of propane (C_3H_8) and butane (C_4H_{10}) in liquid form, with propane being the major component. Propane, which is the constituent that dictates the liquefication limits of LPG, can be liquefied at around the temperature of -42°C (Speight 2018, p.279). It is a commonly used fuel that is a by-product from oil and gas production as well as oil refining. In 2017 the LPG production was 309 million tonnes (DNV-GL 2019b, p.49). LPG price has fallen in the last 10 years, as it is a byproduct of shale oil and – gas production. LPG is currently still however more expensive than for example LNG. Advantages of LPG are that the production technology and infrastructure are available, and that the storage in liquified form is reasonably cheap. The basic properties of LPG are shown in table 6. (DNV-GL, 2019a, p.23-24)

Table 6. *Basic properties of LPG. (McAllister et al. 2011, p.12, 244, 293)*

Fuel	Combusitibility	Energy content	Phase at NTP	Tank size vs MGO	Low-flashpoint fuel
LPG	Bad, MN 34 & 10 - ON≈96	≈46 MJ/kg	Gas	≈1.3	Yes, -68°C

The disadvantages of LPG are mainly related to the combustion properties. The methane number (MN) of propane is 34, while the corresponding value for n-butane is 10 (Mollenhauer et al. 2010, p.114). LPG can not be directly used in a LP-DF engine due to the low MN, resulting in knocking, but with a pilot ignited HP-DF engine LPG can be utilized. On the LP-DF side, LPG can be used as a fuel by generating methane from LPG and steam in a gas reformer. This is a technology developed by Wärtsilä, which allows the generated mixture to be directly used in a LP-DF engine. Finally, as propane is denser than air, LPG storage is also a safety risk. (DNV-GL 2019a, p.24)

The well-to-wake CO_2 emissions can be reduced by approximately 17% compared to HFO. The LPG slip should be minimized, as the global warming potential of propane and butane is 3 to 4 times that of CO_2. NOx emissions for a HP-DF engine will require EGR´s or SCR´s to satisfy IMO Tier III limits. (DNV-GL 2019a, p.24)

Table 7. *Emission properties of LPG. (DNV-GL 2019a, p.9, 24)*

Fuel	NOx emission, LP-DF	NOx emission, HP-DF	Well-to-tank	Tank-to-wake	Well-to-wake
LPG	-70% vs MGO, SCR/EGR maybe for Tier III	-15% vs MGO, SCR/EGR for Tier III	≈ ±0	-16%	-17%

In 2020 at least three LPG tankers have been ordered with MAN ME-LGIP engines, with propane to be used as the main fuel (The Motorship, 2020). In the LGIP engines the LGP is brought into the injector at relatively low pressures and the final pressure rise is done in the injector. The required injection pressures for the 2-stroke DF diesel process are relatively high, around 600 to 700 bar (Jeppesen, M. 2020, p.20). It is estimated that the price for an LPG system, when using pressurized IMO-type C fuel tanks, for a vessel is roughly 50% of a similar LNG system, when using same types of fuel tanks (DNV-GL 2019a, p.24).

2.1.8 Biomethane (CH_4)

Methane is the main constituent of natural gas, and as such methane is not covered in this section in particular detail. Methane can however also be produced from varying feedstocks, such as for example forest biomass or crop residues. The production method naturally has no effect on the end product. The production and use of biomethane is relatively small in scale but growing rapidly in Europe and North America. Currently used production processes can be separated into anaerobic digestion and gasification. The basic properties of methane are shown in table 8. (Meriteollisuus ry 2020, p.19)

Table 8. *Basic properties of methane. (McAllister et al. 2011, p.244, Duan. et al. 2019, p.4)*

Fuel	Combusitibility	Energy content	Phase at NTP	Tank size vs MGO	Low-flashpoint fuel
Methane	Bad, MN = 100, ON ≈ 120	50 MJ/kg	Gas	1.7	Yes,-188°C

Producing and liquefying biomethane is a costly process, at least currently. Biomethane could be used directly in place or as a mixture with LNG, to reduce the GHG emissions of LNG. Biofuels are generally considered CO_2 neutral fuels, as the emissions from burning are considered to be compensated by growing the renewable feedstock. The emissions of biomethane are the same as of "normal" methane, but the CO_2 emissions are captured by the feedstock. If biomethane is used, the methane emissions from fuel production and combustion would make up the well-to-wake emissions. (DNV-GL 2019a, p.27-28)

Table 9. *Emission properties of methane (DNV-GL 2019a, p.9)*

Fuel	NOx emission, LP-DF	NOx emission, HP-DF	Well-to-tank	Tank-to-wake	Well-to-wake
Methane	Tier III	-25% vs MGO, SCR/EGR for Tier III	If bio, 0	No CO_2, CH_4 slip only	

2.1.9 Dimethyl ether (C_2H_6O), DME

Dimethyl ether (DME) is a non-toxic gaseous fuel, mainly produced from methanol. As the physical properties of DME are very similar to LPG, also the transportation and storage requirements are quite similar. As such the storage and infrastructure costs are seen as an advantage. From the diesel fuel system point-of-view DME has been proven to be a suitable fuel with excellent combustion properties (Mollenhauer et al. 2010, p.98). If DME were to be injected in the liquid phase, the low boiling point would lead to quicker evaporation of the fuel, and possibly lower the needed injection pressures (Arcoumanis et al. 2008, p.1016,1018). The basic properties of DME are shown in table 10.

Table 10. *Basic properties of DME. (Martins 2020, p.6, Arcoumanis et al. 2008, p. 1016)*

Fuel	Combusitibility	Energy content	Phase at NTP	Tank size vs MGO	Low-flashpoint fuel
DME	Good, CN ≈ 57.5	27.6 MJ/kg	Gas	1.8	Yes, -41°C

The disadvantages of DME are low availability, low energy content, low viscosity and bad lubrication properties (Majewski 2017, p.6, Mollenhauer et al. 2010, p.98). DME is not currently a mature enough technology for shipping usage, with the main problems being in the production capacity and the non-existing distribution infrastructure (Aakko-Saksa et al. 2019, p.15-16). The low LHV combined with the relatively low liquid density means that the mass flow of DME that needs to be injected is relatively large. Other potential problems with DME are the low bulk modulus, with the compressibility of DME being 4 to 6 times higher than diesel and the fact that DME is quite close to its critical pressure when injected

into a diesel engine. This can result in cavitation in the fuel injection nozzle, if the pressure drops too much. (Arcoumanis et al. 2008, p.1017)

Not a lot of data about the combustion emissions was found, as DME has mainly been used as a blend with other fuels. On the WTT side, emissions differ for the two production methods suitable for large volumes. DME can be produced from methanol or synthesizing DME from synthesis gas (H_2, CO). The WTW efficiency of DME produced from methanol is comparable to LPG. For DME produced from bio-feedstock the WTW CO_2 emissions are 20% of diesels emissions. The amount of DME produced from bio-feedstock is however, at least to date, insignificant. Overview of the emissions is in table 11. (Bae et al. 2017, p.3404)

Table 11. *Emission properties of DME. (Bae et al. 2017, p.3404)*

Fuel	NOx emission, LP-DF	NOx emission, HP-DF	Well-to-tank	Tank-to-wake	Well-to-wake
DME				-16%	Methanol, -17%

DME has attracted some interest as an alternative marine fuel. For example, Maersk, the Technical University of Denmark and China have announced plans to investigate DME as a marine fuel (Fredriksen 2019). DME has been tested in marine engines by blending into conventional fuels, with some modifications needed to the fuel system. MAN has projected that DME could be used as a fuel in the ME-LGI engine (Gingell 2019. p.10). (Bae et al. 2017, p. 3392, 3404-3405)

2.1.10 Fatty acid methyl ester, FAME

FAME is a biodiesel produced from fats, oils and greases through a transesterification process. FAME can be produced from various feedstocks, and as such it is an umbrella term for many different fuels. Typical feedstocks are rape seed -, sunflower - and palm oil, but it can also be produced from animal-based fats and waste oils. (Neste 2016, p.28). The amounts of FAME produced are relatively large, with the EU annual production in 2018 being 11 650 million liters, roughly 4,4% of the annual EU diesel consumption, with the majority of this consumed in automotive applications (Flach, Lieberz & Bolla 2019, p.15,28). To date FAME has been used as a blend with traditional diesel fuels (Mollenhauer et al. 2010, p.80). The properties of FAME are quite similar to diesel, and blends with conventional fuels containing up to 20% are not expected to need any modification on the engine side (Zhou et al. 2020, p.13). Basic properties of FAME are shown in table 12.

Table 12. *Basic properties of FAME. (Neste 2016, p.15, Mollenhauer et al. 2010, p.102)*

Fuel	Combusitibility	Energy content	Phase at NTP	Tank size vs MGO	Low-flashpoint fuel
FAME	Good, CN ≈ 51	37 MJ/kg	Liquid	Blended fuel	No

The disadvantages of FAME are related to the storage and the low LHV. As FAME degrades relatively quickly, storage of over 5 months is not recommended. Other possible problems are that FAME, being a stronger dissolvent than traditional marine fuels, can "clean" the fuel storage system and dislodge oil fuel deposits from the tanks and lines, possibly causing problems on the pipes, filters and pumps. (Zhou et al. 2020. p.13)

As FAME is used as blends, not a lot of emission data was found about pure FAME. The aim with FAME blending into diesel fuel is to reduce the CO_2 emissions though the CO_2 captivation associated to FAME production (Mollenhauer et al. 2010, p.93). Combustion of FAME biodiesel blends in marine slow-speed diesel engines have in various studies reduced SOx - and PM emissions compared to traditional marine fuels. The NOx emissions have not been reduced with blending of FAME, with some studies reporting no changes and some even reporting NOx emission increases (Zhou et al. 2020, p.27).

2.1.11 Ammonia (NH_3)

Ammonia is a carbonless gas, and as such the CO_2 emissions of ammonia combustion are zero. Ammonia storage is also easier compared to most other alternative fuels. Ammonia can be liquidized at ambient pressure at temperatures lower than -34°C. As ammonia has been widely used and globally distributed as a fertilizer, there is already significant experience about the transportation of ammonia. Reasonable storage properties combined with existing production and handling infrastructure, expect for bunkering infrastructure, and the lack of CO_2 emissions from combustion make ammonia usage attractive. The basic properties of ammonia are shown in table 13. (Korean Register 2020, p.12)

Table 13. *Basic properties of ammonia. (Reiter & Kong 2010, p.88, Kobayashi 2019, p.111)*

Fuel	Combusitibility	Energy content	Phase at NTP	Tank size vs MGO	Low-flashpoint fuel
Ammonia	Very bad, ON ≈ 110	19 MJ/kg	Gas	2.8	No, ≈130°C

The major disadvantages of ammonia are the very bad combustion properties, the toxicity, the low LHV and the lack of sustainably produced ammonia coupled with a relatively high price. As the flammability range of ammonia-air mixtures is low along with a high autoignition temperature and minimum ignition energy, the ignition of ammonia-air

mixtures is difficult. A pilot fuel or mixing of ammonia is the sensible way for ammonia combustion, as for example the Korean Register has estimated that a compression ratio of 35:1 is required to achieve sufficient temperatures for pure ammonia combustion in a CI engine (Korean Register 2020, p.31). Ammonia might require a larger share of pilot fuel a to compensate the combustion properties (Reiter et al. 2010. p.88). Other disadvantages include a low viscosity value, being roughly 10% of the value of diesel and a low density. The low density and low LHV mean that the fuel injection mass flowrates would be relatively high. Ammonias corrosivity mean that brass, copper and rubber-based materials cannot be used (Reiter et al. 2010, p.88). Ammonia also has a tendency to cause stress corrosion, especially in a pressured tank, and as such special coating of the inner surfaces of the fuel tank might be needed, with effects on the cost of the tank (Abdullah et al. 2011, p.3). Ammonia is also very toxic. The vapors are lighter than air and invisible, and an exposure to a high concentration of ammonia vapor can be fatal within minutes. (Meriteollisuus ry, 2020, p.15).

The CO_2-emissions from ammonia combustion are zero. The WTW CO_2 emission are however very dependent on the production of ammonia. Majority of ammonia is produced from fossil feedstocks. The WTT emissions of ammonia produced from fossil feedstocks is high, as ammonia production accounts for 1% of global CO_2 emissions (Meriteollisuus 2020, p.15). Methods exist for sustainable ammonia production by combining hydrogen and nitrogen, but there is no adequate capacity currently. Sustainable production has been done by combining electrolysis and Haber-Bosch processes, but currently there are no operational plants (Meriteollisuus 2020, p.15). The production method is electricity intensive, which is why previous plants have been next to hydroelectric dams. For ammonia generated by renewable electricity the WTT emissions would be zero. The WTW emissions could be lowered without having the ignition problems by mixing ammonia into hydrogen or natural gas (Meriteollisuus 2020, p.15). Regarding other emissions, ammonia combustion produces significant amounts of NOx, mainly due to the nitrogen content of the fuel. To satisfy IMO NOx limits SCR´S will be needed. The emission properties are shown in table 14. (McKinlay, Turnock & Hudson 2020, p.4-5)

Table 14. *Emission properties of ammonia. (McKinlay et al.2020, p.4-5)*

Fuel	NOx emission, LP-DF	NOx emission, HP-DF	Well-to-tank	Tank-to-wake	Well-to-wake
Ammonia	Not applicable	SCR needed for Tier II			

Ammonia usage as a fuel on ships is a problem, as the International Code for the Construction and Equipment of Ships Carrying Liquefied Gases in Bulk (IGC) code nor the International Code of Safety for Ships using Gases or other Low-Flashpoint Fuels (IGF) code do not allow toxic substances as a fuel, at least yet. The consequence of this is that ammonia fueled ships could be built, but every ship would need to individually demonstrate that the design meets the IGF Codes general requirements. (DNV-GL 2019b, p.32-33)

There is a lot of interest around the usage of ammonia as a marine fuel at the moment. MAN will use the ME-LGIP 2-stroke engines, with some modifications, to run on ammonia with injection pressures projected to be around 600 bar, with a low-pressure feed where the final pressurization is done in the injector. The 1st engine tests are scheduled to be in 2021 while engine delivery to yard would be in 2024.The first ammonia engines will be used on LPG carriers, that are transporting ammonia and thus can utilize the cargo as a fuel (Riviera MM 2019). Ammonia is seen as a one of the most potential carbon-neutral fuels, as the production methods are existing, the production price is forecasted to be favorable and storage as well as transportation are relatively easy (Korean Register 2020, p.11-14). The overall ambition in relation to ammonia usage is to produce the ammonia by renewable electricity and use it as a fuel, thus allowing the use of a carbon-free fuel for shipping. (MAN ES, 2020j, p.7,10).

2.1.12 Hydrogen (H_2)

Hydrogen is the most abundant element on earth. At NTP conditions hydrogen is a non-toxic, colorless gas. It is however not found in a pure form from nature, instead it must be produced or extracted from an existing raw material, such as water. Hydrogen can be extracted from fossil - or renewable resources. There were 80 million tonnes of hydrogen produced in 2019, of which the majority (96%) was produced from fossil based raw materials, such as natural gas and coal. Hydrogen production amounted for 6% of the global natural gas use (IEA 2019, p.17). Producing hydrogen is also energy intensive. At the moment hydrogen is mainly produced for chemical - and refinery production. Basic properties of hydrogen are shown in table 15. (Meriteollisuus ry 2020, p.10-14)

Table 15. *Basic properties of hydrogen. (McAllister et al. 2011, p.244, Bureika et al. 2020, p.24)*

Fuel	Combusitibility	Energy content	Phase at NTP	Tank size vs MGO	Low-flashpoint fuel
Hydrogen	Too good, MN=0, ON=130	120 MJ/kg	Gas	4.3	Yes

The advantages of hydrogen are that it is carbon free and has a very high energy content per mass. If the production of hydrogen can be done using energy from renewable resources, the burning of hydrogen would be carbon neutral. The combustion properties of hydrogen are too good, due to amongst others a very low minimum ignition energy, a wide flammability range and a high flame speed. As a result, hydrogen catches fire very easily. Due to the high auto-ignition temperature of hydrogen, about 585°C, high compression ratios would be needed for pure hydrogen (Flekiewicz et al. 2020, p.100). The primary way to utilize hydrogen in CI-engines could be to use it as a blend with for example methane and utilize a pilot fuel. Hydrogen has also been successfully blended for example to ammonia in 4-stroke SI engines and to diesel in 4-stroke CI-engines (Deb 2015, p.8591, Commotti 2015, p. 10673). (Meriteollisuus ry 2020, p.11-12)

The disadvantages of hydrogen are related to the storage as well as the combustion control. The high energy content of hydrogen can translate to knock problems, high in-cylinder peak pressures and high in-cylinder temperatures (Deb 2015, p.8587). Also, the mass flows needed are large due to the very small density. The combustibility and very low energy density of hydrogen means that the storage of hydrogen is problematic. To improve the energy density hydrogen can be stored as a compressed gas or a liquid. When stored as a compressed gas, the pressures are between 200 – and 700 bar. Pressurizing hydrogen requires a lot of energy, 3-5 kWh/kg of H_2, equivalent to 9-15% of the energy content of the fuel, with the storage efficiency remaining relatively poor (Meriteollisuus ry 2020, p.11). Hydrogen can be liquefied at atmospheric pressure at -253°C, which is extremely cold and hence also expensive. Even in the liquid state, the energy density of hydrogen is 5 times less than that of HFO. Problems with liquefication are the large boil-off gas (BOG) amounts, high liquefication energy (6 to 13.6 kWh/kg of H_2) and challenges related to the temperature, such as handling and the tendency of hydrogen to degrade high-strength steel (Korean Register 2020, p.11, Berstad 2010, p.4513-4514, Kramer et al, 2015, p.14). As neither compressing nor liquefication of hydrogen seems to be particularly attractive, alternative storage methods, such as metal hydrides, liquid organic hydrogen carriers (LOHC) and transformation of hydrogen to ammonia have been tested (IRENA, 2019, p.31).

Hydrogen does not cause CO_2 emissions when burned. If the production of hydrogen can be done using energy from renewable resources, hydrogen would be a carbon neutral fuel. The

other emissions are also low. According to Schlapbach and Züttel, burning of hydrogen with rich air-fuel mixtures could cause some NOx formation (2001, p.354). Some of the emission properties are shown in table 16.

Table 16. *Estimates of the emission properties of hydrogen. (DNV-GL. 2019b. p.9)*

Fuel	NOx emission, LP-DF	NOx emission, HP-DF	Well-to-tank	Tank-to-wake	Well-to-wake
Hydrogen	Tier III	-30% vs MGO, SCR/EGR for Tier III	Production	≈0	

For lowering GHG emissions of shipping, hydrogen should be produced from a renewable source and with electricity created by renewable resources. Of the currently established production methods, electrolyzed hydrogen produced from water would be suitable. The problem is that at the moment electrolyzed hydrogen represents under 0.1% of the global dedicated hydrogen production, while only 0.7% of the production is from renewable sources (IEA. 2019, p.30-31,42). Needed production amounts are also large. If the anticipated amount of fossil-free-diesel needed for global shipping in 2050, estimated to be 185 to 419 million tonnes, was satisfied with hydrogen produced by electrolysis, the electricity need would correspond to 1 to 2 times the annual electricity production of Europe (Meriteollisuus ry 2020, p.13). If renewable electricity prices continue to get lower along with the equipment and production costs of hydrogen, hydrogen production could become cost competitive. At the moment hydrogen prices vary significantly by the production method as well as the production region. (Aakko-Saksa et al. 2018, p.804).

2.2 Overview of fuel combustibility from GD perspective

The intention of this chapter is to give a quick look at the properties of fuel that have an effect on the injection in a GD engine. The properties as such are not discussed at length, as they have already been covered in chapter 2.1.3. In traditional compression ignition engines, the fuel is injected during the compression stroke and ignited with the aid of the high temperature and pressure prevalent in the cylinder. For pure CI-engines the auto-ignitability of the fuel is critical from the functionality point-of-view (Bae et al. 2017. p.3401). With the GD concept auto-ignitability of the fuel is not as crucial, as the air-fuel mixture is ignited with the help of a pilot fuel. Nevertheless, the auto-ignition temperature of the fuel has to be in such regions, that the pilot fuel can ignite it. From a combustion point-of-view lower auto-ignition temperatures are not problematic in the GD process either, as the fuel is injected at the end of the compression stroke with a view to burn it immediately, thus eliminating knock problems. (Woodyard & Latarche 2009, p.51)

The fuel density and the lower heating value determine the fuel mass flow needed for a given output. Injection duration can be used to control the mass flow to some extent, but it can not be extended endlessly, with a typical max value for CI-engines being around 70° crank-angle (McAllister et al. 2011, p.231). The massflow through the injector can be raised by at least using higher injection pressures. The fuel properties that have significant effects on the injetor and fuel pressurization equipment are at least the density -, the bulk modulus -, the viscosity - and the lubricity of the fuel. From a injector functionality and lifetime point-of view lubricity of the fuel is important. Viscosity also has an effect on the injector equipment, with low viscosity usually causing sealing problems, while an excessively high viscosity will disurpt the injection (Mollenhauer et al. 2010, p.91, 587). An simplified overview of the liquid fuel combustion process and the affecting factors is displayed in figure 13 below.

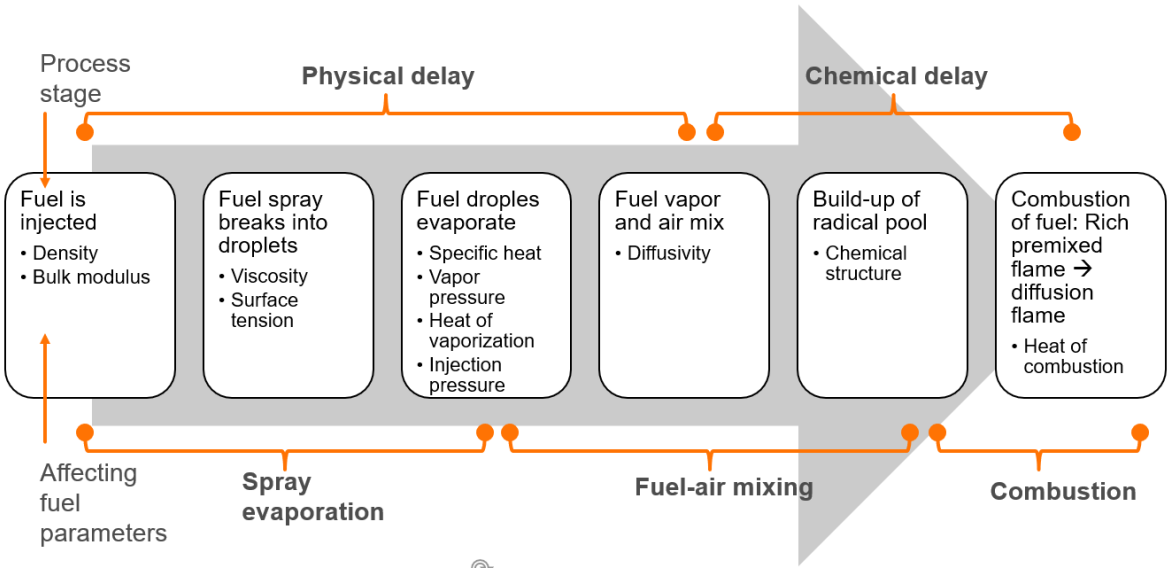

Figure 13. *A simplified overview of liquid fuel CI-process and the affecting fuel parameters. (Modified from McAllister et al. 2011, p.230)*

After the fuel is injected into the combustion chamber, it atomizes into small drops. These drops start to vaporize and mix with the charge-air in the cylinder. In a traditional CI-engine spontaneous ignition occurs when the mixture reaches its ignition point. In the GD process the mixture is ignited with the pilot fuel injection. The easier the fuel vaporizes and the better the air and fuel mix in the cylinder, the more complete the combustion will be. Some of the properties that influence the mixing rate are for example the viscosity, surface tension, vapor pressure and diffusion rate (McAllister et al. 2011, p.231-232). Generally smaller viscosity, surface tension and vapor pressure values are beneficial for evaporation. with lighter molecular weight normally translating into lower diffusion rates (Valera et al. 2019, p.12-

13). Higher injection pressures, which result in higher fuel droplet velocities, also speed up the evaporation process. (Mollenhauer et al. 2010, p.66). Sources causing incomplete combustion, an undesirable phenomenon, are for example insufficient air-fuel mixing, insufficient amount of air, insufficient amount of time for the combustion reactions and quenching of the flame (ASHRAE 2009, p.28.1). (Heywood 1988, p.491-492)

2.3 Overview of fuel emissions

As the engine emissions are a very important point both from legislation and customer point-of-view, the very basic theory is examined here. This chapter is structured to first inspect the commonly regulated emissions related to the burning of the fuel, known as the tank-to-wake (TWT) emissions, along with the related marine emission regulations After this, the emissions related to the production of the fuel, known as well-to-tank (WTT), are shortly discussed. The whole chain is referred to as well-to-wake (WTW) emissions. Lastly, a quick look on emission reduction methods for HP-DF engines is made.

Emissions related to the combustion of fuel in compression ignition engines are a complicated matter. In this work a general look into the emissions and their formation methods is made. On a very general level, the causes of emissions can be thought to be incomplete combustion of the fuel, reactions between components of the air-gas mixture in high temperatures and - pressures along with the combustion of engine lubrication oil. The typical composition of diesel exhaust gas is shown in figure 14. As can be seen, the actual emissions constitute a small amount of the total exhaust gas formation. If the emission formation is looked at in more detail, the emissions are dependent amongst others on the charge air and the fuel. The formation is dependent on the charge-air temperature, - pressure and -motion along with the fuel composition,- injection, - atomization, and - evaporation as well as the interaction between the air and the fuel, which causes local concentrations of oxygen or fuel (Abdul Karim & Sulaiman 2018. p. 2).

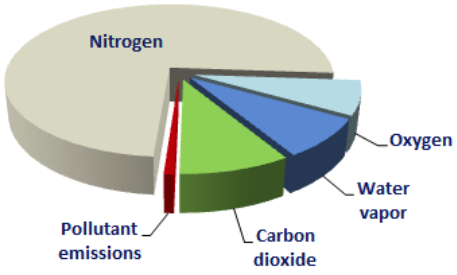

Figure 14. *Relative composition of diesel exhaust gas. (Majewski 2012, p.2)*

As emissions are a problem both locally and globally, there is legislation to try to reduce the emissions. Some of the environmental concerns related to emissions are shown in figure 15. GHG emissions, such as CO_2 and CH_4 are global issues while particulate matter emissions and smog for example are more local problems that directly affect the health and the quality of life of the people. Main emissions related to compression ignition engines are hydrocarbon - (HC), carbon monoxide - (CO), particulate matter - (PM) and NOx emissions. (Abdul Karim et al. 2018, p. 2-3)

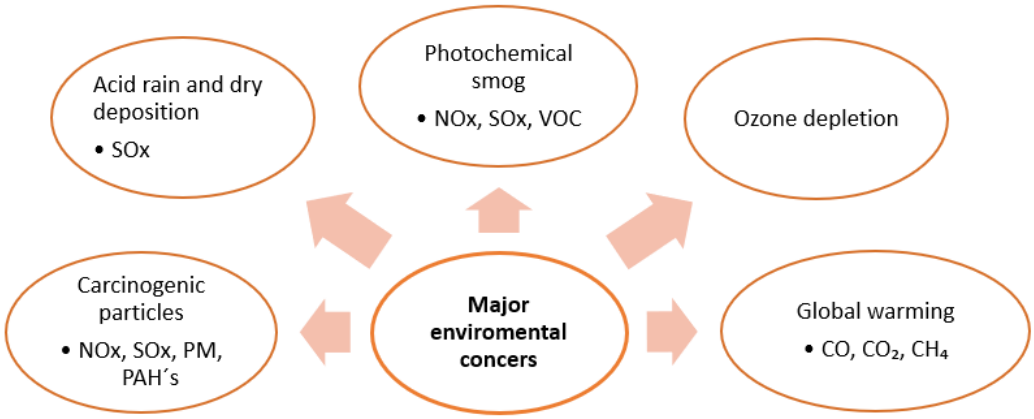

Figure 15. *Environmental concerns related to internal combustion engines (Modified from, Maurya 2018, p.3)*

Marine emissions are regulated globally by the IMO. The marine emission rules can be found from the "International Convention on the Prevention of Pollution from Ships", also known as MARPOL 73/78. The regulated emissions, stated in MARPOL Annex VI, are NOx and SOx emissions along with the indirectly regulated GHG emissions, which are limited through an energy efficiency design index (EEDI). The emission limits have been applied in differing tiers, to gradually implement stricter emission regulations while giving time to adapt for the changes. The NO_x emission limits are applied to ship engines over a certain power amount while the SO_x limit guides the choice of fuel. The PM emissions, that are the result of the pyrolysis of the fuel, are not regulated. (DieselNet 2020)

2.3.1 NOx emissions

The NOx limit applies for internal combustion engines when an output of over 130kW is installed on the ship. NO_x emission limits are defined by the maximum operating speed of the engine, as shown in figure 16 below. The allowable NOx emission limit is based on the rated speed of the engine. The measured NOx emissions are measured on predefined engine load cycles according to ISO 8178 using distillate diesel fuels. With the application of a HP-

DF process the NOx emissions will be in the IMO Tier II levels, meaning that additional measures are needed if Tier III levels are needed (DNV-GL 2019b, p.9). (DieselNet 2020)

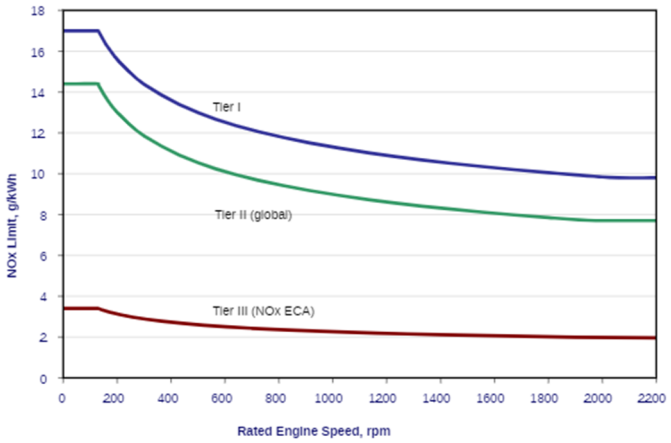

Figure 16. *MARPOL Annex VI NOx emission limits (DieselNet 2020)*

Currently Tier II limits are in use globally, and in addition stricter Tier III limits have been in use since 2016 in two specific ECA´s, the North American - and the US Caribbean ECA. Additionally, the stricter Tier III limits will be taken into use on the 1st of January 2021 in two ECA´s, the Baltic Sea - and the North Sea ECA. The typical NOx emissions from marine diesel engines, that use residual and distillate fuels vary between 50…10 g/kg of fuel when no NOx reduction technologies are applied, meaning that the Tier levels need exhaust aftertreatment or other measures (Aakko-Saksa et al. 2019, p.21). (DieselNet 2020)

NOx emissions are formed mainly from two sources: fuel NO and thermal NO (Okubo & Kuwahara 2019, p.62). Of these the thermal NO is the primary source of NOx emissions. (Okubo et al. 2019, p.63). Thermal NO is produced, when nitrogen, N_2, and oxygen, O_2, react with each other during the combustion process at temperatures roughly over 1500°C (Okubo et al. 2019, p.63). These are components that come into the combustion process mainly with the charge air, as air is roughly 78% N_2 and 21% O_2 , but also fuels can contain some amounts, with HFO N content being about 0.05 to 0.4 mass% (Okubo et al. 2019, p.63). NOx emissions are mainly NO, but also a minor amount of NO_2 is created. The amount of NO can be thought to be in the regions of 90 to 95%, with the amount increasing as the load is lowered (Okubo et al. 2019, p.67, Heywood 1988, p.577). In addition to NO and NO_2, NOx emissions also contain minor amount of other nitrogen oxides. Exhaust gas can contain very small amounts of for example, N_2O, which is a GHG emission with a global warming potential of 298 on the 100-year GWP scale. (Aakko-Saksa et al. 2019, p.21)

The relation between the NOx formation rate and the in-cylinder temperature is shown below in figure 17. The fuel influences the combustion temperature, with high LHV´s, low heats of vaporization and high oxygen content raising the flame temperature and thus also the in-cylinder temperature (Heywood 1988, p. 575, 814, 591). LNG and methanol for example reduce the NOx emissions, as the combustion peak temperature is not as high as for residual – or distillate fuels, while also the N content of these fuels is non-existent. The NOx emissions will rise for a HP-DF engine compared to a LP-DF engine, because the combustion temperature rises due to the utilization of diesel- instead of otto-process. On the other hand, the raising of the combustion temperature typically results in the lowering of HC, CO and PM emissions, known as the NOx-PM trade-off. (Abdul Karim et al. 2018. p.2-3

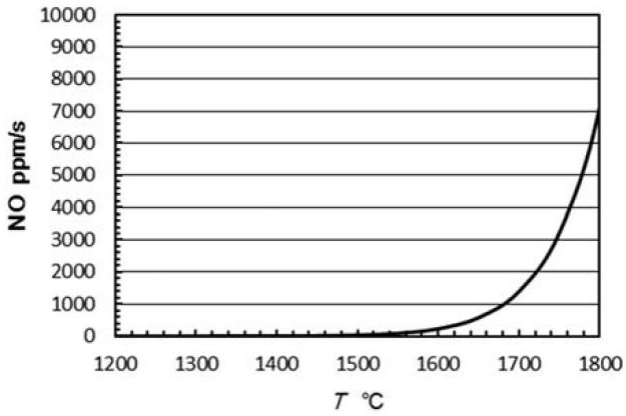

Figure 17. *The relation between thermal NO formation and the in-cylinder temperature. (Okubo et al. 2019, p.67)*

The on-engine ways to control NOx emissions are mostly related to cooling of the combustion temperature. Such methods are for example the charge air cooling and the usage of Miller timing or water injection to cool the charge air. Also, an exhaust gas recirculation (EGR) system can be used to reduce NOx emissions. EGR reduces NOx emissions by lowering both the charge air oxygen content as well as the charge air temperature, due to the increase of water and CO_2 in the charge air. (Aakko-Saksa et al. 2019, p.21)

NOx emissions can also be reduced after the engine, with the application of exhaust treatment, such as a SCR unit. In a SCR unit ammonia (NH_3) is used to react with nitrogen monoxide (NO) and oxygen (O). The result turns the nitrogen monoxide present in the emissions into nitrogen and water. An SCR unit can reduce the NOx emissions by 80 to

90%. In figure 16 below are shown the effects of some technologies and fuel choices on the NOx emissions of a marine diesel engine. (Aakko-Saksa et al. 2019, p.21)

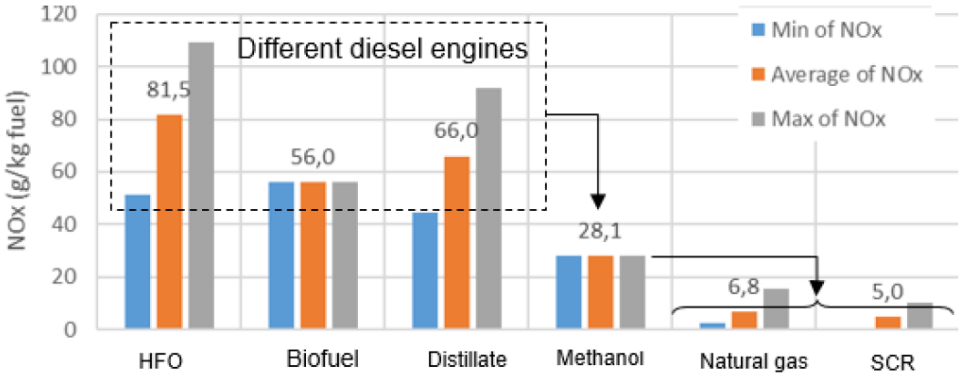

Figure 18. *NOx emissions from a marine engine using different fuels, and finally a SCR exhaust aftertreatment system. (Aakko-Saksa et al. 2019, p.23)*

2.3.2 SOx emissions

SOx emissions are a product of the combustion of the fuel sulfur components (Okubo et al. 2019, p.86). The sulfur content of the marine fuels, which has a direct effect on the sulfur emissions, is regulated. The fuel sulfur limits are currently 0.5% of the fuel globally with a stricter limit in specific SOx ECA´s, as shown in figure 19 below. As a comparison to the marine environment, the European road diesel sulphur limit is in most regions around 0.001% (Aakko-Saksa et al. 2019, p.12). Alternatively, sulfur rich fuel can be used if adequate emission aftertreatment, such as exhaust gas cleaning systems are used to ensure the exhaust emissions contain less than 6 g/kWh of SO_2. (DieselNet 2020)

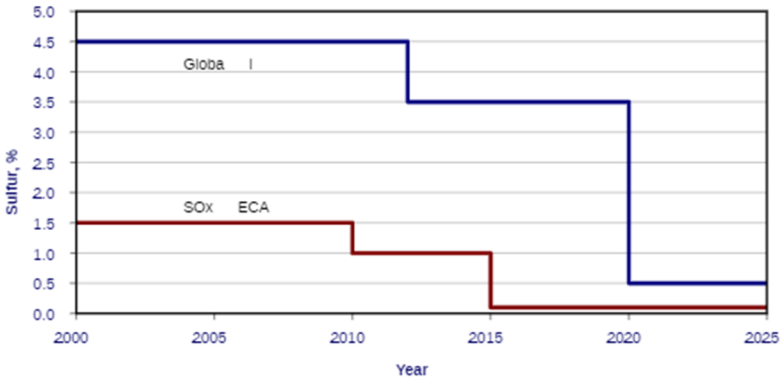

Figure 19. *MARPOL Annex VI fuel sulfur limits (DieselNet 2020)*

Sulphur in the combustion processes creates mainly SO_2, but also small amounts of SO_3. These sulphur oxides are classified under the term SOx, even though exhaust gas emission measurement normally only detects and accounts for SO_2. Fuel composition practically defines the SOx emissions. Residual fuels have the largest amount sulphur content while

distillate fuels and LNG barely contain any sulphur. For example, the distillate fuels for SOx ECA tier III regions contain less than 0.1% of sulphur, resulting in SO_2 emission of 1g of SO_2/kg of fuel burned. (Aakko-Saksa et al. 2019, p.18)

Fuels with a high sulphur content can be used if exhaust gas aftertreatment methods are used. SOx can be removed with SOx scrubbers. There are several different types of scrubbers available on the market, mainly depending on the water used, with fresh water used in a closed loop circulation and sea water in an open loop scrubber.

2.3.3 GHG emissions

One of the biggest motivations for HP-DF usage are the reduced GHG emissions, and as such they are covered here in a bit more detail. IMO has indirectly regulated greenhouse gases with the EEDI requirements for new ships, which has been in force in principle since 2013. In practice there has been a six-year flexibility period, where depending on when the keel of the ship has been laid, the EEDI requirements have not been compulsory. The EEDI requires a certain minimum energy efficiency for new build ships. The methods on how to achieve the required rating are left for the ship designers and constructors to decide.

In the future the focus on greenhouse gas emissions will almost certainly rise. IMO communicated in 2018 a target of reducing total annual GHG emissions by at least 50% by 2050, compared to the GHG emissions of 2008. The strategy is at this early stage based upon improving the EEDI requirements and perhaps creating new emission limiting tools. Some possible tools discussed include operational efficiency measures, ship speed reductions, measures to control or regulate emissions of CH_4 and VOC´s, the usage of alternative low - and zero carbon fuels and market-based measures, such as emission taxation. (DieselNet 2020)

The engine GHG emissions consist primarily of CO_2 and unburnt HC, such as CH_4, and potentially a minor part of N_2O. Traditionally in the fossil fuels the main GHG emissions have been CO_2 based emissions. CO_2 emissions are almost directly related to the selection of fuel and the fuels carbon-to-hydrogen ratio, as CO_2 is formed always when a fuel containing carbon is burned with air (McAllister et al. 2011, p.178). For comparison, the

global anthropogenic GHG emissions in 2010 were estimated to be 52 billion CO_2-equivalent tons, of which CO_2 from fossil fuels and industrial processes accounted for 62% on a 100 year basis, as shown in figure 20 (Lindstad & Rialland 2020, p.2). (Abdul Karim 2018, p. 2-3)

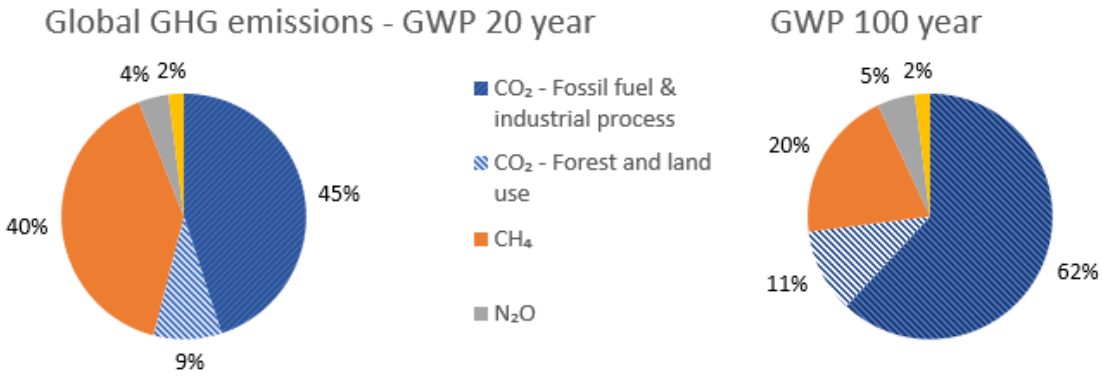

Figure 20. *Global GHG emissions as CO_2 equivalents in 2010. (Modified, from Lindstad et al. 2020, p.2)*

With the widening portfolio of fuels, also the fuels main source of GHG emissions has expanded. For example, the main GHG emissions related to the life cycle assessment (LCA) of DME, FT-diesel and methanol produced from forest residues have been N_2O and CH_4 emissions. In figure 21 below are shown some of the GHG emissions along with their global warming potential on a 100-year and a 20-year basis. These values are evolving with time and have been updated several times during the last decades, with the 2014 IPCC Assessment Report 5 values shown. The 100-year measure is commonly used, by for example the United Nations Framework Convention on Climate Change (UNFCCC) and the Environmental Protection Agency (EPA). The 20-year basis will prioritize the pollutants with a shorter lifetime when compared to CO_2, such as methane (IPCC 2014, p.87). (Zhou et al. 2020, p.5)

	Lifetime (yr)	GWP 20-Year	GWP 100-year
CO_2		1	1
CH_4 - Fossil source	12.4	85	30
CH_4 - Biogenic source	12.4	84	28
N_2O	121	264	265

Figure 21. *The global warming potential and lifetime of some GHG emissions on a 100 - and 20-year basis. (Modified from, IPCC. 2014, p.87, Myhre et al. 2013, p.714)*

On the engine side the unburnt HC emissions can be roughly classified to methane and non-methane hydrocarbons. The methane emissions are known as methane slip and it is typically the result of too lean or too rich air-fuel mixtures. In both cases the ignition or continued burning of the mixture is prevented resulting in unburned HC emissions. HC emissions

depend a lot on the fuel composition as well as on the combustion process. Fuels containing significant amounts of aromatics and/or olefins create emissions with a relatively higher amount of reactive HC emissions compared to fuels that don't contain as much these components (Heywood 1988, p. 597).

CO emissions are the results of incomplete burning; thus, they occur in combustion regions where there is a lack of oxygen, meaning that the air-fuel ratio is below or close to the stochiometric ratio. The CO emissions are dependent on the availability of unburnt fuel and the air-fuel mixture temperature, two properties which dictate the rate of fuel decomposition and oxidation. Typically, CI-combustion engines are operated on a lean mixture, thus CO emissions are not a significant problem for diesel CI-combustion (Heywood, 1988, p.592).

Of the GHG emissions, methane as well as carbon dioxide emissions are very relevant for gas fueled engines. For LP-DF engines the power specific methane slip formation is typically larger at lower loads than at high loads. The main formation method of methane slip is the quenching of the fuel inside the cylinder (Ushakov, Stenersen & Einang 2019, p.1311). Quenching is mainly the problem at lower loads and lean mixtures, and happens, when the gas mixture touches colder parts, such as the cylinder liner, and cools down. With the application of HP gas injection, the quenching problem disappears. Another source of methane emissions is the unburnt fuel. Unburnt fuel can be found from combustion chamber crevices, which the combustion flame has not reached during the combustion process. The crevice problem is well known and should have been minimized. Previously also exhaust and inlet valve opening overlap could contribute to methane emissions as well, but this should also be fixed in modern engines. (Stenersen & Thonstad 2017, p.13-14)

2.3.4 Well-to-wake and tank-to-wake emissions

Emissions related to the burning of a fuel can be thought from a lifecycle or an engine process point-of-view. When the lifecycle view is adopted, the emissions related to the extraction of the fuel as well as its processing and transportation to the end user are noted in addition to the emissions resulting from the combustion of the fuel. The lifecycle view of the fuel usage in the marine environment is called the "well-to-wake" (WTW) emission. If the on-ship emissions are only considered, as is often the case due to difficulties in measuring

emissions related to fuel extraction, preparation and transportation, then in the marine environment this is considered as “tank-to-wake” (TTW).

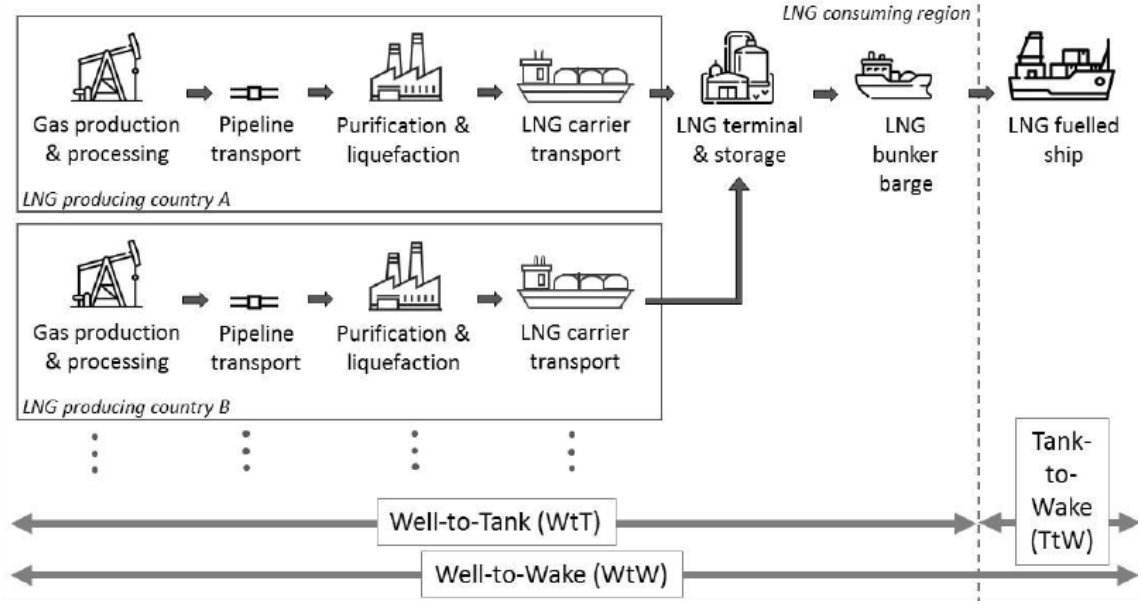

Figure 22. *Overview of WTT, TTW and WTW chain. (Thinkstep, 2019, p.35)*

The determination of the WTW emissions is difficult, due to a long process chain, where the measurement of emissions is not practically possible at all stages while the processes and equipment vary significantly. In figure 23 is a collection of estimations of the upstream emissions related to LNG production, as gathered by Tagliaferri et al (2017). As can be seen, the estimations of upstream emissions can vary significantly. They depend amongst others on the NG source, the transportation distance and - method, LNG processing and process efficiency, possible storage and bunkering as well as on the final usage location.

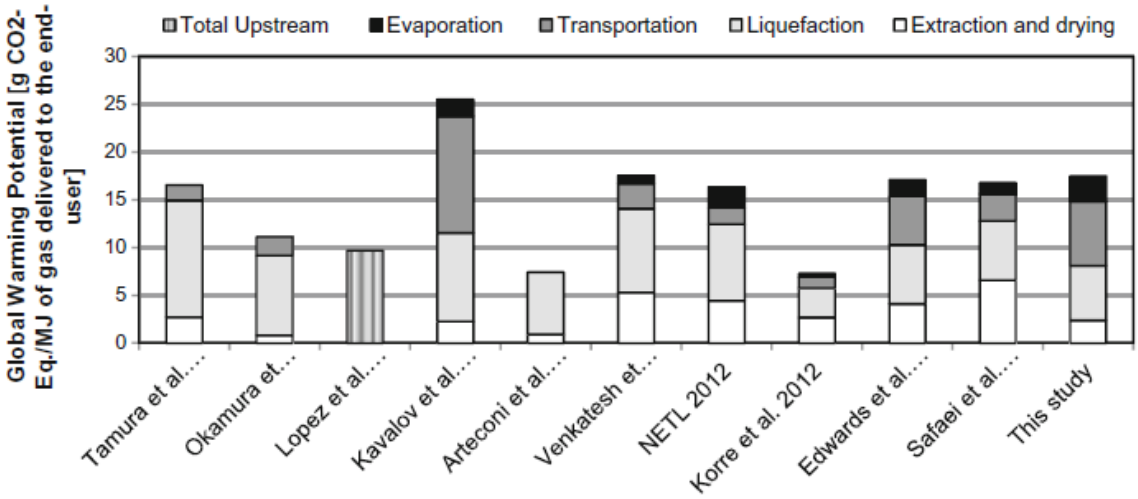

Figure 23. *GWP comparison of LNG upstream emissions, according to different studies. Values are reported per functional unit (1MJ of NG delivered to the end-user). (Tagliaferri et al. 2017, p.1954)*

To minimize the upstream emissions the processes should naturally be as efficient as possible while methane should not be allowed to slip out of the process. For example, fuel BOG should be re-liquefied or used directly as fuel, whenever possible. The liquefication process is generally the largest contributor to the upstream emissions, for example in studies by Verbeek et al (2011, p.18) and Lowell et al (2013, p.18,36). Liquefication consumes energy between 275-400 kWh/LNG ton produced (UNECE, 2013a, p.5). Lower liquefication emissions come from larger base load LNG plants, while smaller peak shaver plants have higher levels of emissions. Parts of the process with smaller impact on the overall emissions are for example the transportation, storage and handling, such as the bunkering activities, of the fuel. (Lowell et al. 2013, p.13-14). A similar comparison was made on the well-to-tank figures of some of the papers published on alternative fuels for shipping, as shown below in figure 24.

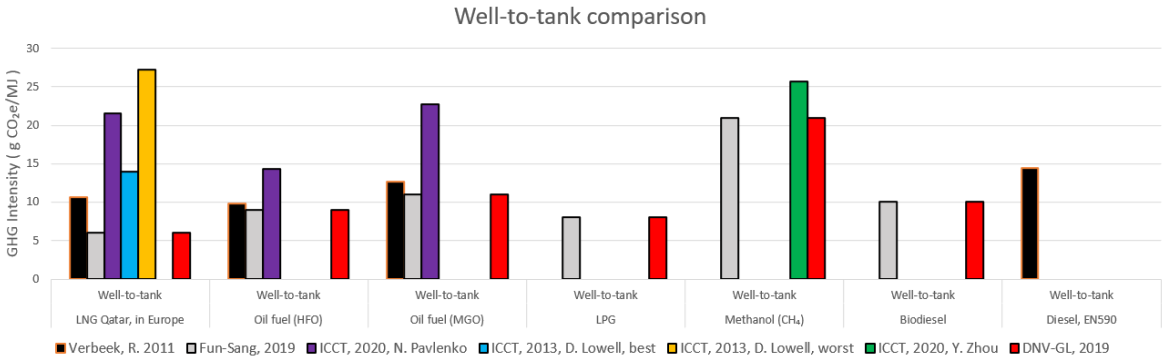

Figure 24. *A rough well-to-tank emission comparison of several fuels picked out from several papers. (Verbeek et al. 2011, p.4,23; Fun-sang et al. 2019, p.78; Pavlenko et al. 2020, p.7,12; Lowell et al. 2012, p.27; Zhou et al. 2020, p.7-8; DNV-GL 2019a, p.8)*

In addition to upstream emissions, the emissions related to the combustion of the fuel also vary in the estimations of GHG emissions. Factors affecting the GHG emissions are the assumed specific fuel consumptions of the engines, the heating value of the fuel, the global warming potential (GWP) factor used and the emission levels or factors used. As CH_4 emissions are multiplied by a figure in the range of 30 to get the CO equivalent emission, the CH_4 emission estimation is important. Some values that have been used for LP-DF engines include slip percentages of 2.6% (Verbeek et al. 2011, p.22), 1.5% (DNV-GL 2019a, p.55) and 1.7% (Thinkstep 2019, p.69) of the fuel input and specific emissions of 4 g/kWh for (Lowell et al. 2013, p.36-43) and 5.5 g/kWh (Pavlenko et al. 2020, p.6). A comparison of the TTW emissions from the same studies is shown below in figure 26.

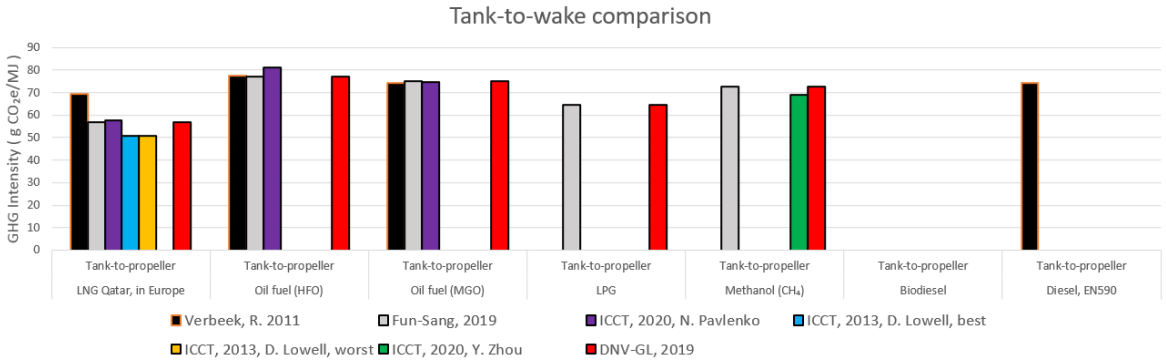

Figure 25. *A rough tank-to-wake emission comparison of several fuels picked out from several papers. (Verbeek et al. 2011, p.4,23; Fun-sang et al. 2019, p.78; Pavlenko et al. 2020, p.7,12; Lowell et al. 2012, p.27; Zhou et al. 2020, p.7-8; DNV-GL 2019a, p.9)*

As can be predicted based on the variations in the WTW and TTW, also the WTW emission estimations vary significantly. In most of the studies the WTW GHG emissions of LNG are estimated to be around 8 to 20% less than with the usage of distillate marine fuels (Balcombe et al. 2019, p.76). In figure 26 are shown the WTW emission estimations by DNV-GL for some fuels and technology pathways, into which the 4-stroke HP-DF CO_2equivalent emissions have been estimated to be similar to 2-stroke HP-DF. The 4-stroke HP-DF engine values are very similar to the 2-stroke values, with the change being in the engine efficiency. For 4-stroke HP-DF engines running on natural gas instead of LNG, the liquefication energy associated to LNG production, estimated to be about 4 to 5 g CO_2e/MJ, could still be removed, if pipeline gas was used (Verbeek et al. 2011, p.18-19). The CO_2equivalent emissions can be lowered roughly by 14 to 24% with the HP-DF process in comparison to LP-DF. (DNV-GL, 2019b. p.40)

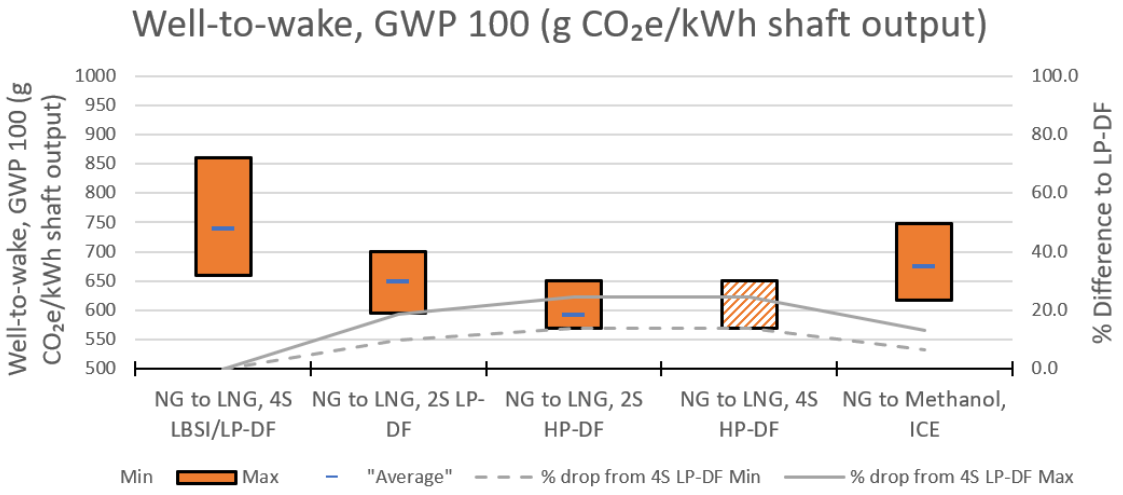

Figure 26. *The well-to-wake emissions for various fuels and technology pathways according to DNV-GL, when taking into account the energy content of the fuel and the system efficiency. (Modified from DNV-GL, 2019b. p.40)*

The estimation of the lifecycle emissions becomes even more difficult when alternative fuels are added into the equation. Alternative fuel emissions can be thought to consist at least of emissions related to cultivating feedstock and producing the fuel. In some studies, indirect land-use change for feedstock cultivation is also accounted in the life-cycle assessment. For example, the lifecycle emissions of FAME biodiesel varied from 22 grams of CO_2 equivalent per megajoule to more than 110 g of CO_2 equivalent/MJ (Zhou et al. 2020, p.4). For biofuels the main GHG emissions usually come from NOx and methane emissions, which differs to the traditional fossil fuels, whose main GHG emissions consist typically of CO_2 (Zhou et al. 2020, p.5). In figure 27 are shown GHG emission reduction estimations of some alternative fuels relative to HFO and MDO according to Balcombe et al.

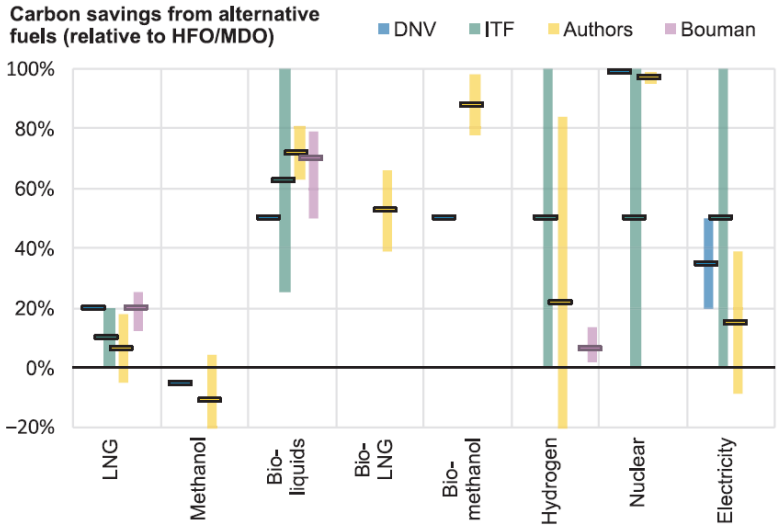

Figure 27. *Possible GHG emission reductions with the usage of alternative fuels. (Balcombe et al. 2019, p.82)*

Consequently, there are also many results about the emission levels associated with LNG use. Generally, the HP-DF engines have a smaller GHG emission footprint than the LP-DF engines, mostly due to the significantly lower methane slip. The GHG emissions from LNG usage will depend a lot on the amount of methane slip. For example, Ushakov et al have estimated, that with methane emissions at a level of 3.0-4.0 g/kWh, the net GHG reduction from LP-DF engines would be in the range of 12-18% when compared to operation on conventional distillate fuel (2019, p.1312), while Balcombe et al have offered a general estimation of 10% total GHG reduction with the use of LNG, and a 50% reduction if bio-LNG is used, when compared to HFO (2019, p. 81-82).

2.3.5 Emission reduction for HP-DF process

The engine emissions can be reduced by properly selecting the fuel, utilizing a suitable combustion technology along with controlling the combustion, and/or reducing the emissions from the exhaust stack after the engine. The intention in this chapter is to highlight the different emissions reduction methods needed for HP-DF engines, and not to go into detail about the functionality. In figure 28 are stated some of the pre-engine, on-engine and after-engine emission producers as well as control methods.

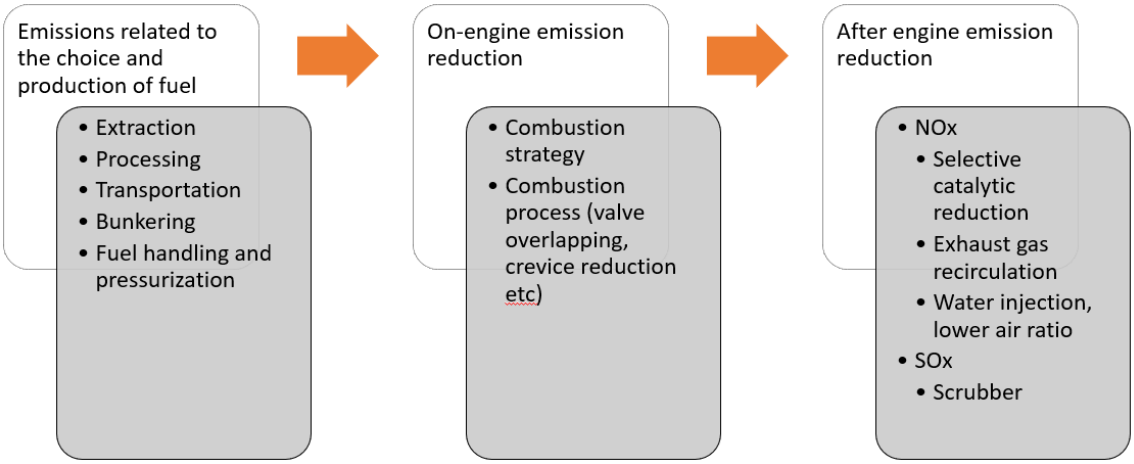

Figure 28. *Emissions related to the production of the fuel and some means of reducing the emissions with on- or off-engine choices.*

In figure 29 are shown the main fuels currently used in the marine environment, along with the possible exhaust aftertreatment solutions needed to comply with the currently existing IMO emission legislation. LNG use in a diesel process will need aftertreatment for IMO Tier III NOx levels, meaning EGR or SCR is needed. The NOx emissions are primarily a consequence of the higher combustion temperature associated and needed for the diesel process (Mollenhauer et al. 2010. p.445-446).

		HFO	LSHFO/MGO	LNG
Diesel	SO_x	Scrubber	Compliance	Future-proof
	NO_x	Tier III: EGR/SCR	Tier III: EGR/SCR	Tier III: EGR/SCR
	CO_2	High carbon	High carbon	Reduced CO_2*
Otto	SO_x			Future-proof
	NO_x			Future-proof
	CO_2			Reduced CO_2 (CH_4 slip)*

Figure 29. *Overview of HFO, MGO and LNG fuels with differing combustion processes, showing the possible exhaust aftertreatment systems needed to comply with emission legislation. (Modified, from DNV-GL, 2019a, p.10)*

After-engine emission reduction methods applicable to compression ignition (CI) engines are based on thermal oxidation, catalytic oxidation and various traps or filters. The applicable methods for the marine environment are the thermal – and catalytic oxidation methods. Oxidizing catalysts are used for reducing HC and CO emissions, while reducing catalysts are for NOx. The CI-engine exhaust gases are typically at temperatures of roughly 200 to 550°C, while the exhaust contains excess oxygen from combustion. This is important for the oxidizing catalysts, as the exhaust must contain sufficient amounts of oxygen, for the oxidation to be possible. An oxidizing catalyst functions by oxidizing CO and CO_2. Different emissions require different minimum oxidation temperatures. For example, thermal oxidation of HC emissions requires an oxidation temperature of over 600°C, while CO emissions require over 700°C. Catalytic oxidation can be done at lower temperatures than thermal oxidation. For example, for NOx reduction temperatures around 400°C are needed while 250°C can be enough for HC and CO emissions. (Heywood 1988, p.648-649)

In addition to NOx and SOx, also methane slip from the combustion process could be eliminated by using a methane oxidation catalyzer. Currently no system is commercially available, but there are development projects on-going, which aim to develop a functioning methane oxidation catalyzer. Examples of such projects are for example the German MethQuest and Shells "Methane Abatement Catalyst" projects. The challenge in the oxidation of methane is that methane is very stable, so the temperature required to oxidize the methane molecules is high. The oxidation of methane is difficult, due to the high stability of C-H bond, which results in a higher light-off temperature when compared to longer chains of hydrocarbons (Srinivasan et al. 2019, p.369-370). The temperatures required are so high, that the oxidation must be done downstream of the turbine of the turbocharger. Amongst other things, this presents space utilization problems. It is projected that the oxidation catalysts could reduce the methane slip amount by 60-80%. (Thinkstep, 2019, p.89).

2.4 LNG details

LNG is an odorless, noncorrosive cryogenic liquid that is liquified to increase the energy density of it and thus allow a cost sensible way to transport the fuel. The energy density of LNG is roughly 600 times more than that of natural gas (Speight 2007, p.79). The properties of LNG depend primarily on the composition of the natural gas to be liquified. Also, the processing and fractionation history of the fuel have some effect on the composition. As

natural gas consists mostly of methane, about 87 to 99 %mole, so does also LNG. LNG also composes of heavier hydrocarbons, such as ethane and propane, along with nitrogen and very small amounts of sulfur, under 4 parts per million by volume (ppmv), and CO_2, 50 ppmv. According to the commercial specification of LNG, the nitrogen content should be less than 1 mole%. Some typical LNG compositions from varying liquefication plants are shown in table 17. (Mokhatab et al. 2014, p.9, 499)

Table 17. *Average LNG compositions from various liquefication plants. (Modified, from Mokhatab et al. 2014, p.4)*

	Nigeria	Arun	Brunei	Oman	Atlantic	Kenai	Average	Standard deviation
CH_4 - Methane	87.9	88.48	89.4	90	95	99.8	91.76	4.27
C_2H_6 - Ethane	5.5	8.36	6.3	6.35	4.6	0.1	5.20	2.55
C_3H_8 - Propane	4	1.56	2.8	0.15	0.38	0	1.48	1.49
C_4H_{10} - Butane	2.5	1.56	1.3	2.5	0	0	1.31	1.03
O_2 - Nitrogen	0.1	0.04	0.2	1	0.02	0.1	0.24	0.34
LHV, MJ/kg	49.1				49.8		49.3	
Methane number	64				87		73	

The components that raise the energy content of the gas are methane, ethane, propane and butane, while non-combustible components, such as nitrogen and carbon dioxide, naturally lower the energy content of the gas. (Speight 2007, p.72). LNG is typically in a liquid state at ambient pressures at a temperature of -around 160 °C (Speight 2007, p.79). The phase changes of LNG can be inspected from phase envelopes, as shown in figure 30. As can be seen, generally at higher pressures and temperatures, such as when fed into the combustion process, LNG will be in the gaseous phase. (Mokhatab et al. 2014, p.4)

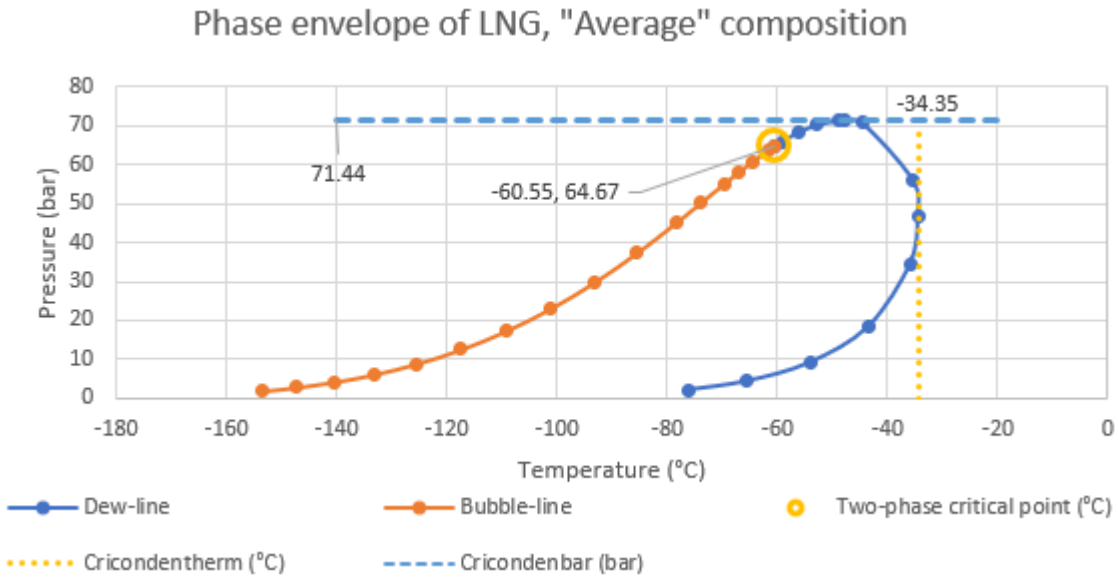

Figure 30. *The phase diagram for LNG according to the average composition used in this work, for composition see table 17.*

The combustion properties of LNG are generally good. The low C-H ratio of LNG translates to lower CO_2 emissions compared to other hydrocarbon fuels, while the LHV of LNG is high, typically in the regions of 49 MJ/kg, which is 115% of diesels value. In the liquid phase the density is about 450 ±20 kg/m³, meaning that the volumetric energy density is roughly 22MJ/l, about 61% of the value of diesel (Martins et al. 2020, p.4). LNG will not ignite by itself, but the vapors from LNG can be ignited, with the flammability limits being from 5 to 15 % by volume in air. The auto-ignition temperature of LNG is comparably high, being about 550 °C. The laminar flame velocity of vaporized LNG is low, with the value for methane being 0.38 m/s (Agarwal et al. 2019, p.189). LNG burns however "cleanly", as the simple chemical composition of methane reduces soot formation compared to other fossil fuels (Srinivasan et al. 2019, p.7). (Mokhatab 2019, p.8)

LNG is primarily produced in large base load liquefaction plants located near large gas reservoirs is Asia, Australia, the Middle East and West Africa. From the liquefaction plants LNG is shipped to customers, typically quite far away. LNG transportation via ships is typically commercially viable if the transportation distance is over the range of 1 000 km, while shorter distances are pipelined. More information about the LNG production details can be found in appendix 3. (Mokhatab et al. 2014, p.10-11)

The majority of LNG is transported by specially designed LNG carriers. They are designed to contain the cargo at a cryogenic temperature with the pressure typically being slightly above the atmospheric pressure. Normally the storage tanks of LNG carriers operate at roughly 0.3 barg while having a design pressure of 0.7 barg. The LNG is kept at the cryogenic temperature by having the storage tanks insulated well enough, so that the cargo remains in a liquid state during the whole voyage. The storage of LNG is addressed in more detail in chapter 2.5.1. (Mokhatab et al. 2014, p. 13)

As LNG is produced around the world, from varying natural gas compositions, to guarantee interchangeability the Wobbe Index (WI) has been developed. It is an internationally used measure of gas quality, which ensures that gas quality is sufficient for the end user equipment. The WI value correlates the heat release from combustion with the heating value and the density of the gas. The WI can be calculated by dividing the higher heating value with the square root of the gas density - or the molecular weight of the gas relative to air.

During LNG transportation, the WI will gradually increase, due to the boil-off off nitrogen. This phenomenon is known as weathering. As the weathering may change the WI of the gas out of specification limits, nitrogen or LPG can be used to mix the composition to a correct WI value in regasification terminals. (Mokhatab et al. 2014, p.47,49)

The advantages of LNG include a comparably high availability of gas combined with a competitive price. The “natural emissions”, which are based on the composition of the fuel, are also favorable when comparing to traditional marine fuels. The NOx, SOx and PM emissions of LNG are significantly lower than for traditional fuels. In addition, LNG does not cause sludge deposits in storage tanks while it is also noncorrosive. The disadvantages related to LNG are related to the fuel system as well as to the unburned HC emissions, specifically methane emissions. As LNG needs to be liquefied to have a decent volumetric energy content, the FGSS as well as the storage tanks are relatively complicated and expensive. According to a study performed by the classification society Germanischer Lloyd in 2013, the utilization of LNG as marine fuel introduces an additional investment cost of 25% over the cost for constructing a typical new container ship. (Srinivasan et al. 2019, p.177). Liquefication also consumes energy, with the production and supply chain estimated to consume 10 to 20% of the delivered gas (Mokhatab et al. 2014, p.500). To realize the GHG emission advantages, the methane emission level should be minimized when LNG is burnt.

2.5 Overview of the systems needed to utilize the HP gas in a 4-stroke engine

This chapter will give information about basic theory on LNG storage, compression, and pumping, and finally the gas injection system will be shortly discussed. Before being fed to the engine, LNG is vaporized to a gaseous state. An ICE LNG fuel system consists at its simplest of an LNG fuel tank, a method of transferring the fuel to the engine and some method to regulate that the fuel gas pressures and temperatures at the engine inlet are satisfactory.

2.5.1 LNG Storage

LNG is stored as a cooled liquid in insulated tanks. The tanks are well enough insulated so that additional cooling energy is not needed on the ship. As the amount of insulation is basically a trade-off on insulation thickness and insulating cost, a certain amount of external

heat will affect the LNG. This gradual heating of the cargo causes boil-off of the LNG, known as boil-off gas (BOG). The components with lower boiling points, such as nitrogen and methane, are naturally the first to evaporate. Therefore, the BOG consists also primarily of methane and nitrogen. The consequence of this phenomenon is that the BOG composition as well as the composition of the LNG in the storage tank will change over the transportation time. The LNG in the tank will start to contain more heavy hydrocarbons as the lighter hydrocarbons are evaporated, while at the end also the BOG will contain more heavier hydrocarbons. In figure 31 are shown the boiling points of LNG components. (Mokhatab et al. 2014, p.13)

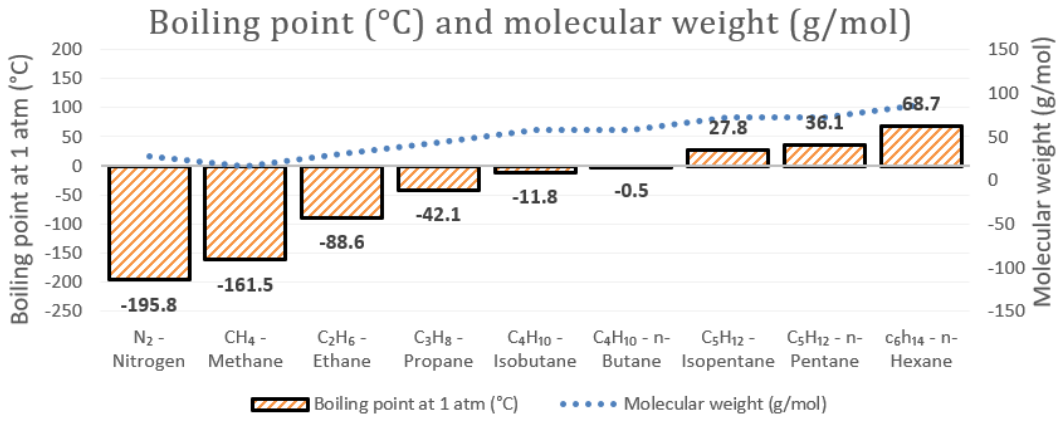

Figure 31. *The boiling points of the various components of LNG. (Modified from, Mokhatab et al. 2019, p.)*

The BOG is an unwanted problem on vessels, which must be handled in some way, to prevent the fuel tank pressure from raising too much. The amount of BOG depends on the boil-off rate, which is typically 0.10 to 0.15% of the tank volume. The boil-off-rate is dependent on several parameters, including the tank insulation system, the fuel tanks cooling system and the fuel tanks pressure (Thiagarajan & Seah 2016, p.969, 972). The amount of boil-off created is proportional to the volume of LNG stored, and can be calculated as: (Mokhatab et al. 2014, p.13)

$$BOG = V_{LNG} \times BOR \qquad (Eq.\ 3)$$

On the marine side the IGF code dictates the methods to handle BOG. The IGF Code 6.9.1.1 states that a liquified gas fuel tanks pressure and temperature must be maintained within the design range by one of the following four methods (IGF 2013, p.61):

- Reliquefication of the BOG.
- Storage under pressure or pressure accumulation to some other device.
- Thermal oxidation, meaning the burning of the BOG.

- (continued) Cooling the gas fuel by some means.

The suitable BOG handling solution must be determined case-by-case and is largely affected by the LNG containment system used. LNG containment systems can be divided into three separate categories according to IGC Code. “Type A” tanks are built according to standard oil tank type, while “type C” tanks are designed as pressure vessels. “Type A” tanks are designed using classical ship-structural analysis and require a full secondary barrier that is able to collect a possible fuel leak (Chorowski et al. 2015, p.3). Typically, “Type A” storage tanks operate at 0.3barg (Mokhatab et al. 2014, p.13). “Type C” tanks can be designed to pressures around 8 or 9 barg, so BOG can be handled at least partially by allowing a pressure rise inside the tank, if wanted (Mokhatab et al. 2014, p.19). The third type, “Type B” tanks, are similar to A-type tanks, but only need a partial secondary barrier due to use of more sophisticated design methods, such as model tests and analytical tools (Chorowski et al. 2015, p.3). Type A tanks are common in LNG carriers, but for smaller fuel amounts the independent “type C” tanks are often used. In figure 32 some type-A and type C tank FGSS solutions are illustrated. For simplicity, the closer inspection of these solutions is not carried out in this work, despite the containment system having a large effect on the fuel system. Details about some exemplary tank sizes is provided in appendix 4. (Mokhatab et al. 2014, p.13-15)

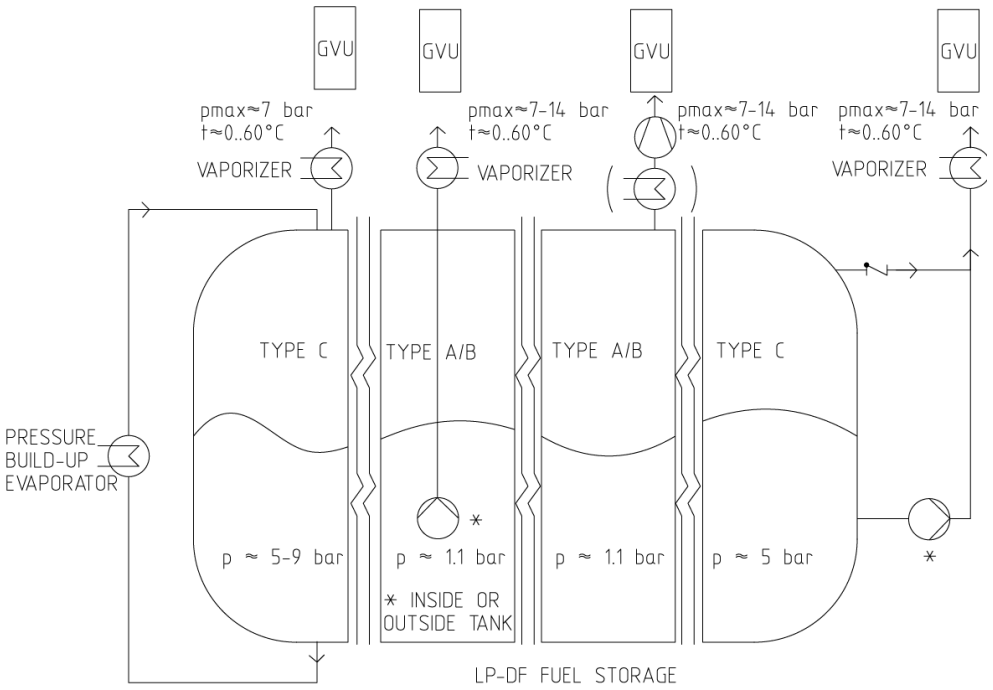

Figure 32. *Examples of FGSS solutions for different types of LNG tanks.*

2.5.2 HP compression of LNG

In this chapter the compression of LNG is covered. First an overview about centrifugal and reciprocating compressors is made. The focus being on the reciprocating compressors, as they are the most likely choice in the marine environment, due to their ability to operate on a wider pressure ratio and flow output while having a smaller footprint (Lyons, Plisga & Lorenz 2015, p.3-58). After this the specialties of a cryogenic compressor are quickly looked at along with the demands on compression caused by the FGSS. In general, a compressor is a mechanical device designed to increase the pressure of a gas or a vapor. Generally, compressors can be classified into either positive displacement - or dynamic compressors (Giampaolo 2010, p.1).

For an LNG FGSS compressor solution there are two different fuel conditions to be compared. The gas can be taken directly as the extremely cold BOG, which requires a cryogenic compressor. The alternative, in case of LNG, is to use a traditional compressor, for which the BOG gas is preheated. For non-cryogenic compressors the BOG must be heated to manufacturer specific temperatures, in the regions of -40°C and higher. On applications where natural gas is used in non-liquefied form, compressors can naturally be used to pressurize gas from supply grids.

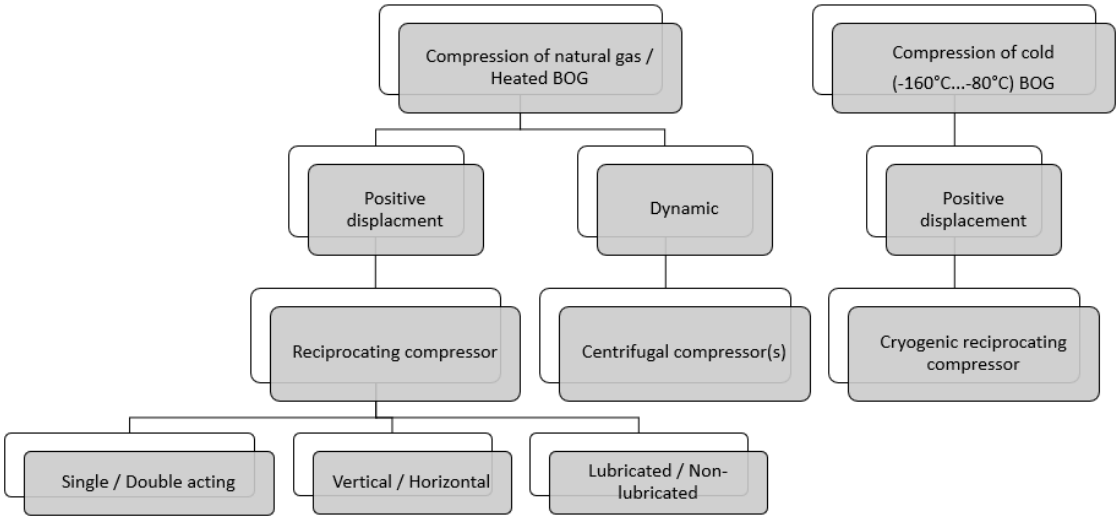

Figure 33. *The different types of compressors considered in this work (Modified, from Giampaolo 2010, p.1).*

For compression of natural gas there are basically two types of compressors available, reciprocating - and centrifugal compressors. Centrifugal compressors are commonly not suited for high pressures, due to a limited pressure ratio. However, when adding stages to a

compressor and/or using compressors in a series, very high pressures can be reached. Typical application ranges of compressors are illustrated in figure 34, where a 1 000 acfm flow is roughly 1 700 m³/h while a 10 000 acfm flow is already 17 000 m³/h. (Mokhatab, Poe & Mak 2019, p.435-439)

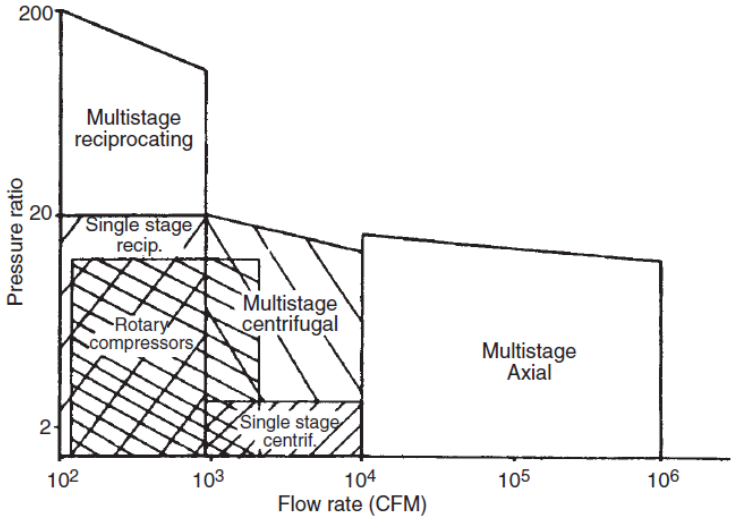

Figure 34. *Comparison between reciprocating and centrifugal compressor flows and discharge pressures (Lyons et al. 2015, p.3-58)*

Reciprocating compressors consists of several cylinder assemblies, called stages. The amount of stages is dependent on the total pressure ratio needed. Each cylinder assembly contains a piston for compressing the medium, the cylinder, cylinder head, and suction – and discharge valves. A reciprocating compressor can be single – or double acting. The difference being that single-acting pistons only compress the gas when the cylinder is moving in one direction, while double acting pistons compress the gas when moving in both directions (Giampaolo 2010, p.37). Components of a single acting piston are shown in figure 35. The amount of cylinder assemblies, called stages, defines the end pressure of compression. The pressure ratio of compressor or a stage states the ratio between the inlet – and the outlet pressures. Typically, the pressure ratio of a single stage for natural gas compression does not exceed 4, although it can be up to 6 (Mokhatab 2014, p.447). Each stage of the compressor is sized according to optimal need, resulting in different piston sizes for the stages. Theoretically the amount of stages for a certain pressure ratio can be calculated as (Mokhatab et al. 2019, p.445): (Guo & Ghalambor 2010, p.179-180)

$$CR = \left(\frac{p_{out}}{p_{in}}\right)^{\frac{1}{n_s}} \qquad \textit{(Eq. 4)}$$

Where, CR = Compression ratio

p_{out} = pressure at outlet

p_{in} = pressure at inlet

n_s = number of stages

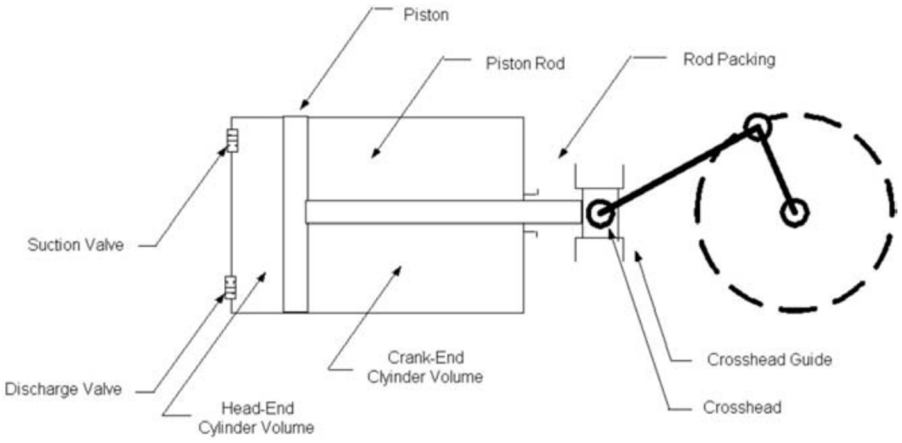

Figure 35. *A single acting reciprocating compressor. (Giampaolo 2010, p.38)*

Reciprocating compressors, with lower rotational speeds, for larger flows have been traditionally driven with steam – or gas turbines. Reciprocating compressors can also be driven with electric motors with gearing between the electric motor and the compressor, or alternatively the motor can be controlled with a variable frequency drive (VFD).

The internal power losses related to friction in the bearings, seals and possible gears differ between compressor types. For reciprocating compressors, the mechanical and internal friction losses can be estimated to be in the range of 3 to 8% of the compressor break power (Mokhatab et al. 2019, p.448). There are also non-mechanical losses involved in the compression process. The intercooler pressure loss depends on the method of intercooling, namely gas-to-air or gas-to-liquid. An initial rough estimation for intercooler pressure loss can be made at roughly 0.7 bar (Mokhatab et al. 2019, p.446). The reciprocating compressor interstage losses can be estimated to be 3% of the pressure produced (Mokhatab et al. 2019, p.446). The pressures losses are created in the intercooling, scrubbers, connecting piping and possibly other equipment (Mokhatab et al. 2019, p.446). (Guo et al. 2012, p.176-177).

The compression ratio is especially of interest when inspecting reciprocating compressors. A reciprocating compressor is designed for use with a range of piston displacement and clearance volumes within the cylinder, which results in the compressor having a certain compression ratio range. High compression ratio values are typically limited by mechanical loads and gas temperatures. In the case of the natural gas compression, the rising temperatures are often the limiting value, while rod-loads are typically a problem for heavier gases. Therefore, multi-stage compressors are often intercooled between stages. Intercooling decreases the required compressor power while keeping the process gas in a temperature range, where the thermal loads are not too high. Typically, the discharge temperature of a reciprocating compressor should be lower than 150°C. The temperature limit is to extend the lifetime of components and the lubricating oil, which is normally directly involved in the compression process, except in oil-free reciprocating compressors. (Mokhatab et al. 2019, p.445-447, 450).

Caution must be taken when cooling the gas to avoid cooling the gas to a low enough temperature for condensation formation. Typically, in the case of natural gas, the first components to condensate are the heavier hydrocarbons. If liquids are formed during cooling, they must be removed typically with a separator or coalescer before the gas if fed into the next compressor stage. The biggest reason to avoid the formation of liquids, is to avoid a “water lock”, which will happen once the amount of liquid exceeds the piston clearance volume, resulting in rod or piston failure. Smaller amounts of liquid can also cause problems in the form of corrosion. (Giampaolo 2010, p. 70-71)

For the compression of very cold gases also cryogenic compressors are an alternative. For a cryogenic compressor, the gas feed temperatures can vary significantly. For example, Burckhardt cryogenic compressors can have a suction side temperature of -160°C to -80°C, with transient temperatures of even +45°C allowable. If very cold gases are compressed with cryogenic compressors, usually the heat exchanger after the 1st compressor stage is by-passed, if the suction gas temperature goes low enough (Duebi 2015, p.9).

A cryogenic compressor can be thought to consist of two parts, firstly the cold side or the low-pressure side – secondly the high-pressure side. In cryogenic compressors the low-pressure side consisting of the first couple of stages are labyrinth sealed, because lubricating

oil would solidify at the temperatures of the cylinders, which can be in the region of -160°C in case of LNG. The high-pressure side of the compressor is normally oil lubricated and sealed with piston rings (Riviera MM 2013). A trend related to cryogenic compressors is the rising of the allowable temperatures, for example on the Laby GI compressor compression end temperatures can be in the regions of 160°C. (Ernst 2015, p.4)

Reciprocating compressors are commonly used in the gas-processing industry, especially in smaller power ranges. A reciprocating compressor is better suited for low volume flows while having a high-pressure ratio. Some of the pros and cons of reciprocating compressors versus centrifugal compressors are shown in table 18 below.

Table 18. *Comparison of reciprocating compressors versus centrifugal compressors (Mokhatab et al. 2019, p.437-438, Giampaolo 2010, p.70, Guo et al. 2012, p. 174).*

Advantages	Disadvantages
Suitable for high pressure ratios (max 10 per stage, for total machine as required)	Requires more maintenance
Higher efficiency at high pressure ratios	Higher operational expenditure
Less sensitive to gas composition, meaning molecular weight, specific heat ratio, compressibility and density	Pressure pulsations in the pressure line, pulsation dampers needed in suction inlet of the compressor and at the discharge of each stage
Less sensitive to suction conditions, meaning pressure and temperature	Lower availability
Smaller capital costs (for power range ≤ 2 000 kW	Normally oil lubricated, meaning that oil blow-through is present in fuel, must be allowed or filtered before engine
Smaller footprint at high pressure ratios	

Centrifugal compressors are also an option for FGSS use. Common parts of a centrifugal compressor are the housing of the compressor, a rotating shaft onto which the impeller is mounted and seals and bearings for sealing the pressure chamber. The centrifugal compressors compress gas by utilizing the centrifugal force, so the impeller exerts work on the gas, resulting in a velocity raise. The gas is discharged into a diffuser, where the velocity of the gas is reduced, resulting in an increase of the pressure. (Guo et al. 2012, p.175-177)

Centrifugal compressors are large and expensive pieces of equipment. Typically, the mechanical efficiency is good, as the only rotating parts are the impeller and the shaft (Guo et al. 2012, p.175-177). They are normally driven with either electric motors or steam- or gas turbines (Watterson 2018, p.63). The power losses related to friction in the bearings, seals and possible gears differ between compressor types but for centrifugal compressors, an estimation of 1 to 2% of the break power can be used. (Mokhatab et al. 2019, p.448).

To achieve higher pressures the compressors can consist of more stages. For centrifugal compressors the pressure ratio per stage for natural gas compression is typically about 2 (Mokhatab et al. 2019, p.445). So, when higher pressures are needed, consequently more compressor stages are needed. The pressure ratio is kept moderate, because as the pressure ratio increases the volumetric efficiency decreases while also the mechanical stress on the components increase. When stages are added, normally the target is to have an as similar pressure ratio over all the stages as possible, to keep the power requirement to drive the compressor at a minimum. (Guo et al. 2010, p.179-180)

Centrifugal compressors are well suited for high flows and low-pressure ratios. They are used in the oil and gas industry especially when high availability and low maintenance is desired. Some of the advantages and disadvantages of centrifugal compressors in comparison to reciprocating compressors are shown in table 19 below.

Table 19. *Comparison of centrifugal compressors versus reciprocating compressors (Mokhatab et al. 2019, p.437-438, Giampaolo 2010, p.70, Guo et al. 2012, p. 174, Lieberman 2009, p.25).*

Advantages	Disadvantages
Suitable for high flows	High capital costs
Smaller footprint at low pressure ratios	Larger footprint at high pressure ratios
High energy efficiency at low pressure ratios	Lower energy efficiency at high pressure ratios
Low maintenance, high availability	Sensitive to gas composition, meaning molecular weight, specific heat ratio, compressibility and density
Good mechanical efficiency	Sensitive to suction conditions, meaning pressure and temperature

Table 19 continues. *Comparison of centrifugal compressors versus reciprocating compressors (Mokhatab et al. 2019, p.437-438, Giampaolo 2010, p.70, Guo et al. 2012, p. 174, Lieberman 2009, p.25).*

Advantages	Disadvantages
No vibrations or pulsations are generated while the gas is compressed.	Low compression ratio per stage (2 to 4.5)

2.5.3 HP pumping of LNG

Cryogenic pumps can be used to increase the pressure of a cryogenic liquid. Typically, cryogenic pumps are reciprocating pumps. Usually the pumps are powered by an electric motor, either directly or with a gearing or a belt, but also the usage of hydraulics, either directly or via a hydraulic motor with a gearbox, is quite common. Typically, the pump can be divided into two separate sections, the warm – and the cold end, as shown in figure 36. In modern pumps the cold end, including the piston, suction – and discharge valve assemblies are enclosed in a vacuum jacket, to minimize the heat transfer into the liquid. The cold end cylinder can also be enveloped by the cryogenic liquid, to reduce heat ingress (Krytem 2018b, p.3). The warm end contains the crank drive mechanism of the pump. Typically, the pumps have a crosshead design, with low-duty crank drives running dry while higher duty crank drives are oil lubricated. (EIGA 2014, p.4-7)

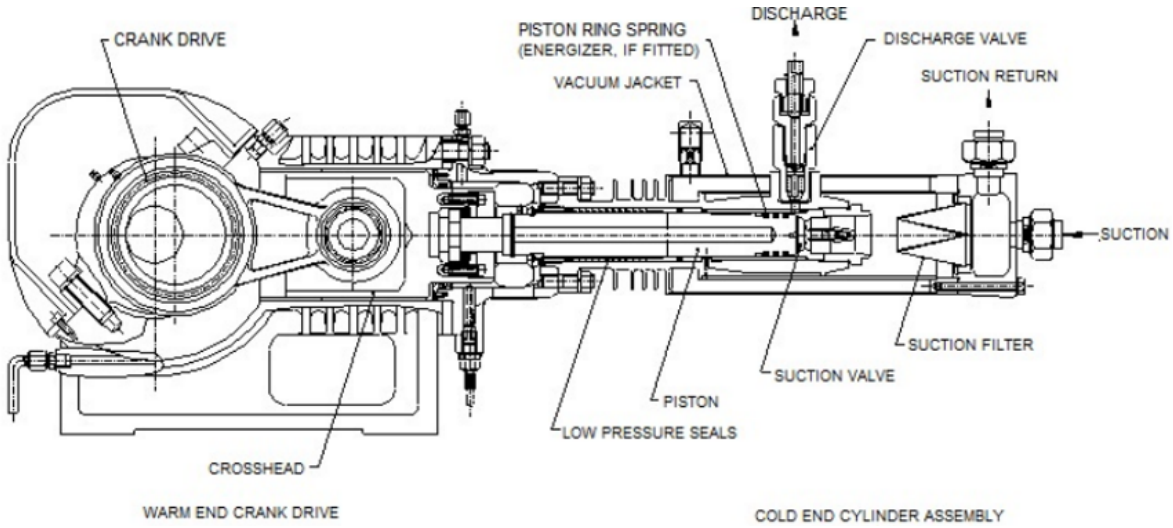

Figure 36. *An example of a reciprocating, cryogenic pumps construction. (EIGA 2014, p.6)*

A single warm end can drive several cold ends, as shown in figure 37. The warm – and cold end can be mechanically connected or - with for example flexible couplings (EIGA 2014, p.4-7). For the expected lifetime of the warm end, it is better to try to insulate the warm end

from the cold end. Contrary to compression, pumping does not significantly affect the temperature of the medium to be pumped. If the medium to be pumped is needed in a gaseous state, it has to be passed through a separate vaporizer after pumping, where it is heated sufficiently to become gaseous. The pumps can be provided with pulsation dampeners, but for a FGSS a buffer volume of sorts is mostly likely needed after the pumps to dampen the pressure pulsations created during the pressurization (Krytem 2018b, p.7).

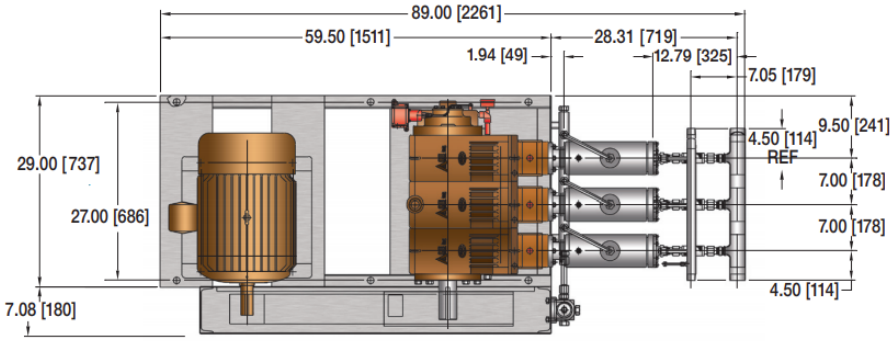

Figure 37. *A cryogenic HP pump, with a single warm end driving three cold ends. (ADC. 2017, p.2)*

The biggest challenges related to cryogenic pumping are naturally the very cold temperatures and the limitations that this causes on the materials and lubricants. Other challenges are that the fluids pumped are often not very good lubricants at cryogenic temperatures along with the fact that the fluid to be pumped is normally close to its boiling point. If the fluid temperature and pressure would reach its boiling point, it would "flash" to vapor causing cavitation. The phase envelope of LNG, such as in figure 30, can be inspected to check at what conditions the liquid starts to turn into gas. With high pressure injection, the end pressures are well above the cricondenbar. (Cox 2000, p.50-51)

The LNG storage tank forms an integral part of a functioning pump. If the liquid to be pumped is at its boiling point, any pressure drop, which will inevitably happen at the pump suction side, will cause the liquid to boil in the pump. To avoid this, some net positive suction head (NPSH) needs to be provided for the pump. For example, the SGV 1.625x1.38 cryogenic pump has a net positive suction pressure requirement (NPSPR) of 0.35bar (ACD 2017, p.1). The NPSH can be created by for example having the pump lower than the liquid feed or by pressurizing the feed to the pump with a "booster pump". Minimizing the feed piping pressure losses before the pump is naturally beneficial. (Cox 2000, p.50-51)

Sufficient NPSH is needed for a couple of reasons. The pressure coming into the pump has to be high enough to overcome the suction pipe flow pressure losses, to move the liquid into the compression chamber of the pump and still have enough pressure versus the boiling conditions, to avoid boiling of the fluid. If the liquid to be pumped reaches its saturation curve, it will start to boil, usually at the suction port of the pump, where the pressure tends to be the lowest. This will cause cavitation on the pump. Another problem is that the bubbles cannot be pumped, and as such the pump will stop creating flow after sufficient amount of gaseous state is present. (Cox 2000, p.51)

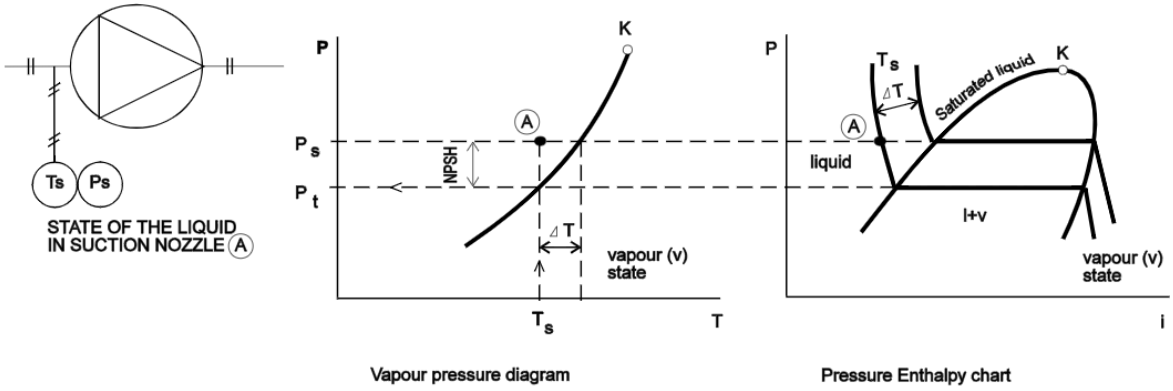

Figure 38. *The NPSH illustrated on the phase diagram and the pressure-enthalpy-diagram of the pumped medium. (Cryostar 2009, p.45)*

Mostly due to the cold temperatures, the materials create a limitation on cryogenic pumps. This can be seen especially on the cold end maintenance requirements. Typically, for LNG operation, the cold end must be changed, roughly after 2 000 to 6 000 hours of operation. The cold temperatures prevent the usage of lubricating oils in the cold end, which is a factor for the relatively short lifetimes of components. Cold end sealing can be done with for example different mixtures of PTFE and high nickel/copper alloys (EIGA 2014, p.11). The parts under the harshest treatment are the seals and the piston rings. (Cox 2000, p.54)

For fuel injection systems that are continuously used for long times, the pump rotating speed is most probably wise to be kept reasonably low. As the footprint and power consumption of cryogenic pumps seems to be very attractive, the lifetime of components and the resulting maintenance needs certainly seem to be the least attractive part. Differences compared to “traditional” pumping are the large temperature gradients. This must be taken into account, when a “warm” pump is started. From a component lifetime point-of-view, flushing of the pump system with the cool process liquid before starting the pump is important. At least

some pump manufacturers have HC measuring systems available for the cold end, for measuring when the cold end has come to its end. When such systems are used, the replacement is not done after a certain number of hours, but after a certain amount of leakage is detected.

In addition to the possibility of constant operation, the part load operation is also important when considering fuel injection systems. There are different possibilities of handling part load operation depending on the source of power. For electrical motors, VFD is the most straightforward option. Gearbox drives via belts or gears is also an option (Krytem 2018b, p.4). For hydraulic systems driven by a hydraulic motor the part load control can be done by controlling the hydraulic motor. Advantage with hydraulics is, that each pump can be separately controlled (MAN 2019e, p.2). HP LNG pump flow, ranging typically from 5-15 to 100 %, is controlled mainly by the pump speed (ACD 2017, p.1, Krytem 2018a, p.2). An alternative to VFD control could be to feed a single high-pressure tank, which would act as the means to balance the input required to the engine and the output from the pumps.

Before feeding the pressurized fuel to the engine, it must be heated to ambient temperatures. This is accomplished with HP vaporizers. HP vaporizers are heat exchangers designed for high pressures and large temperature differences. The fuel must be heated in the ranges of ΔT 160 °C. HP vaporizers normally utilize an intermediate fluid. HP vaporizers utilizing intermediate fluids are often operated on air, a water/glycol mixture, seawater, steam or propane, with propane being a solution mostly for LNG plants. The principle of an intermediate fluid vaporizer is illustrated in figure 39. (Mokhatab 2014, p.460)

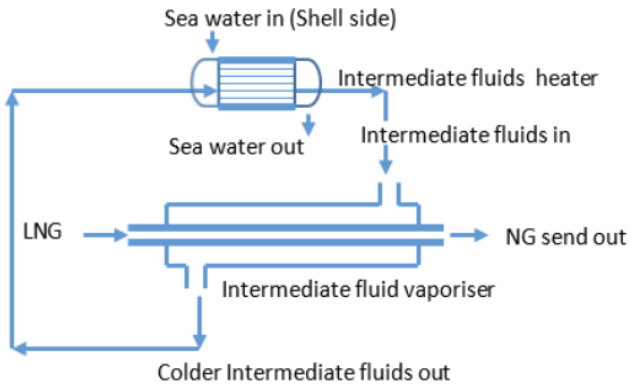

Figure 39. *The working principle of a HP vaporizer. (Agarwal et al 2017, p.7)*

Vaporizer constructions are available at least as shell-and-tube -, spiral – and printed heat exchangers. The printed circuit heat exchangers (PCHE) are especially interesting for marine environments, as they are claimed to have a weight reduction of 85% compared to the traditional shell-and-tube heat exchangers, while allowing a temperature range between -196°C to 800°C and pressures from vacuum to a 1 000 bar. (Alfa Laval 2020, p.3)

2.5.4 HP Feed system on engine

The "gas-diesel" process is a compression ignition process, in which the fuel gas is injected at a high pressure during the compression stroke, after which the charge is ignited with a liquid pilot fuel. The on-engine gas feed system is at its simplest comprised of a gas valve, which controls when and for how long gas is injected into the cylinder. For the liquid pilot fuel injection, a means of controlling the injection duration and quantity is also needed. For safe operation also other equipment is needed. A shut-off valve is needed before the gas admission valve, in order to ensure that the gas fuel feed can be stopped even if the gas admission valve were to malfunction.

For marine usage of engines, the IGF and IGC codes state the safety rules. Rules affecting the LP- and HP- feed systems on the engine include rules such as the gas safe machinery space. This means that for the installation of gas engine(s) in a normal engine room, the engine gas feed piping has to be double-walled and the volume between the inner and outer pipes has to be vented a certain amount and be equipped with a gas detection system. Alternatively, the intermittent volume can be pressurized with nitrogen, from which a gas leakage must be detected. The rules are the same for all DF engines, so no new problems come from them. (CIMAC 2013, p.6)

The main problems with 4-stroke engines and the GD process are related to the lack of space on the cylinder head, which results in difficulties in injector placement and injector size. The alternatives are to use the same injection needle for both fuels, or to have two separate injectors fitted onto the cylinder head.

Traditionally 4-stroke GD engines, such as for example Wärtsilä 32GD, - 46GD and MAN 28/32 GI have combined both the gas – and the liquid pilot injection needles into the same injector. For example, in the 46GD engine the liquid fuel has been brought through the

cylinder head into the bottom of the injector, with the gas feed coming from the top of the injector. The gas injection has been controlled with an electronic rail valve (ERV), which has actuated the gas injection needles with the help of high-pressure hydraulic oil. To prevent the gas from escaping from the injector, the gas volume has been sealed from the rest of the system by applying a control oil, with a higher pressure than the fuel gas, in between the injectors sealing surfaces. In case of GD engines, the load control has been done by adjusting the gas injection duration. In theory the GD gas piping has been a common rail system, where the compressor has kept the fuel inside the piping at a constant high pressure. A similar system has been used on the MAN 28/32GI engines, where the gas has been introduced though the cylinder head into the bottom of the injection valve, as shown in figure 40. (Wärtsilä 2011, p.2-2, 2-3)

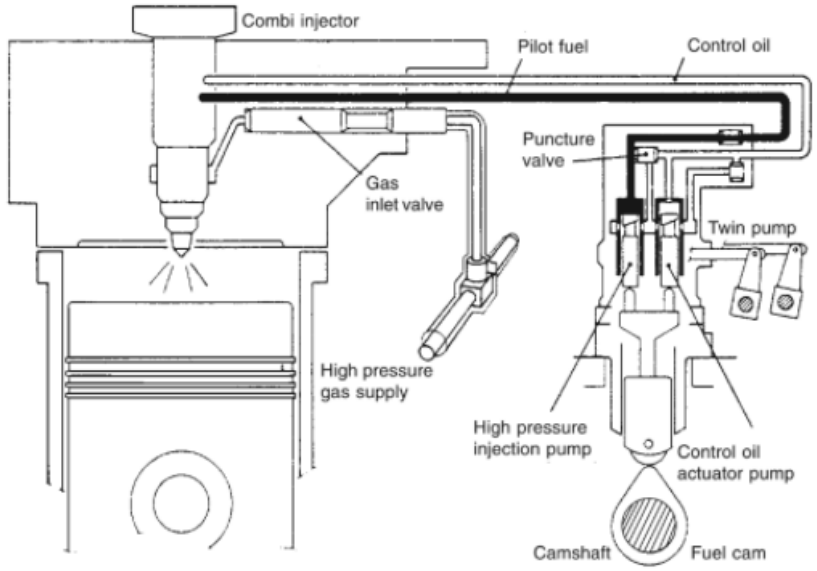

Figure 40. *The fuel injection system of MAN B&W Diesel 28/32GI HP-DF engine. (Woodyard et al. 2009, p.53)*

For the functionality of the injection system, an accumulator volume must be placed somewhere in the system, to dampen gas pressure fluctuations (Woodyard et al. 2009, p.263,266). It would be beneficial to have the accumulator gas volume as close to the injector as possible (Woodyard et al. p.263,266). The same problem is also on the liquid fuel injection side if a common-rail system is used. Sufficient gas pressure is necessary to achieve a sufficient gas feed amount (Woodyard et al. 2011, p.147). Other factors that have been traditionally thought to affect the injection rate are the discharge coefficient C_D, which is dependent on the flow restrictions, along with the nozzle minimum area A_n, as illustrated in equation 5 (Heywood, J. 1988, p.520-521).

$$\dot{m}_f = C_D \times A_n \times \sqrt{2 \times \rho_f \times \Delta p} \qquad \textit{(Eq. 5)}$$

Where, C_D = Discharge coefficient

A_n = Nozzle minimum area

ρ_f = Fuel density

Δp = Pressure drop across the nozzle

As the energy flow through the injector also depends on the density of the fuel gas, a cooler gas fuel is beneficial. With methane, a temperature drop from 45° to 5° at a pressure of 310 bar, results in the gas density increasing from 198kg/m to 239 kg/m³, roughly 20% (REFPROP v10 2018). It must be remembered however that the fuel gas composition includes other components in addition to methane also.

On modern 4-stroke engines a common-rail fuel system is available for the liquid operation mode. Such a system should be well suited for use also for the pilot injection, as the common-rail injection system is electronically controlled. The important things to consider in the gas feeding system are an overall suitable system pressure along with the dimensioning of the rail volume with regards to the injector volume, with feed happening from larger volumes to smaller volumes to minimize pressure fluctuations. In addition to the overall pressure, the amount of gas in the very near proximity of the injection nozzle influences the gas feed amount possible through the nozzle. If the pressurized volume of gas at the injection nozzle is not large enough, the pressure at the needle will drop resulting in a smaller amount being injected. Other properties of the fuel that might have a large effect on the injector design, but are not covered here in more detail, include the fuel bulk modulus, - density and – viscosity. (Woodyard et al. 2011, p,149-150,153)

2.6 LNG in a combustion process

LNG can be used as a fuel in the traditional combustion processes of compression ignition (CI) as well as spark ignition (SI). The CI-process, which can be separated to contain two variations based on the gas injection pressures, the low-pressure gas injection and the high-pressure gas injection, is looked at closer here. Along to these traditional combustion processes, LNG could also be used as a fuel for example lean burn spark ignited (LBSI) -, homogenous charge compression ignition (HCCI) -, low temperature combustion (LTC) -

and reactivity-controlled compression ignition (RCCI) engines. The differences between these processes is large and will not be gone into in detail here. (Srinivasan et al. 2019, p.3)

2.6.1 Basics of conventional CI and SI combustion

CI-engines are widely used, especially in medium – and heavy-duty applications, where efficiency benefits compared to SI-engines can be realized. In the CI-engine, the fuel is injected directly into the cylinder at the end of the compression stroke, usually some crank-angles before top-dead-center (TDC), at pressures around 2000 bar. When a liquid fuel is injected, the fuel vaporizes and mixes with the charge air. As the temperature and the pressure of the air-fuel mixture is typically high enough at the end of the compression stroke, the fuel will auto-ignite once the air-fuel mixture reaches combustible proportions. In this chapter the CI-combustion process basics are quickly looked at, at the level necessary for understanding the effects on the gas-diesel concept. (Heywood, J. 1988, p.27, 491)

The heat release rate (HRR) of a typical diesel engine is shown below in figure 41. As can be seen, it consists of four different phases. After the injection is started, the first phase is the ignition delay phase. At this stage the fuel is evaporating, and the fuel-air mixture is mixing inside the combustion chamber. Typically, the in-cylinder temperatures and pressures are high, resulting in a spontaneous auto-ignition process of the air-fuel mixture when the mixture reaches combustible air-fuel proportions. The phase after auto-ignition is called the premixed combustion phase. It is notable in the heat release rate as the heat release is at its largest. The next phase is the mixing-controlled combustion phase. At this stage the HRR is defined by the rate at which the air-fuel mixture becomes available for burning. The last phase is the late combustion phase, which can continue long into the expansion stroke. At this phase the HRR is already significantly lower. (Srinivasan et al. 2019, p.252-253)

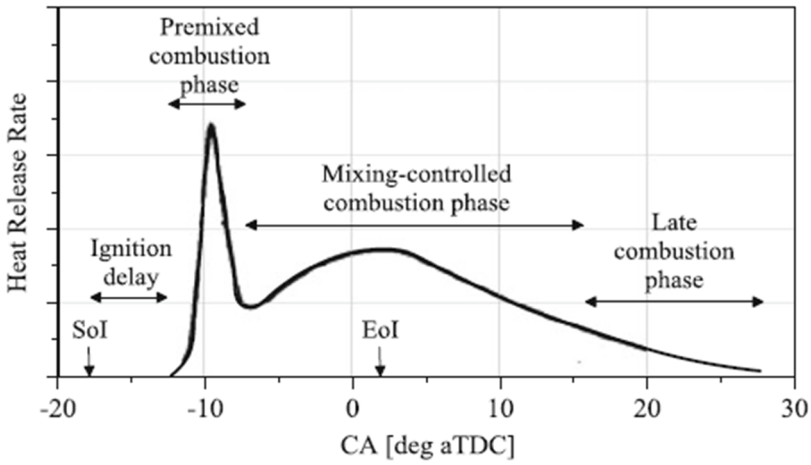

Figure 41. *"Typical heat release rate identifying different conventional diesel combustion phases" (Heywood 1988, p.506)*

In SI-engines the air and fuel are mixed already in the charge air intake system. Thus, a high-pressure fuel injection system is not needed. Combustion is initiated at the end of the compression stroke typically with a spark plug. Combustion causes a turbulent flame that spreads across the cylinder and burns the premixed fuel and air (Heywood 1988, p.371-372)

The main difference of the SI-engine with regards to the CI-process is that the air fuel mixture cannot be compressed too much, otherwise it would prematurely ignite as a cause of the temperature rise. Premature ignition of the charge is known as knocking. The energy release in knocking can happen at a rate of 20 to 25 times higher than when compared to normal combustion. As such it can cause damage to the components and is an undesirable phenomenon. In addition to the knocking limitation, the air-fuel mixture ratio must be controlled so that the air-fuel mixture is in ignitable proportions. (Heywood 1988, p.375)

2.6.2 Low pressure injection, diesel process

LP-DF engines function as SI engines from a fuel feeding point-of-view. In LP-DF engines the gaseous fuel is mixed into the charge air, normally outside the cylinder, at the start of compression stroke. Typically, the gas is injected into the charge air at the air intake manifold of the cylinder. After gas admission, the lean fuel-air mixture is compressed in the cylinder, until it is combusted with a pilot fuel, that is injected into the cylinder before TDC. Normally the pilot fuel will be a liquid diesel fuel, that can also be used as a backup fuel. LP-DF engines are a combination of the SI- and the CI-process. Fuel is mixed into the charge air prior to ignition as in the SI-process, while the combustion, controlled by the injection of the

pilot fuel, is reminiscent of the compression ignition of the diesel-process. (Ushakov 2019, p.1312)

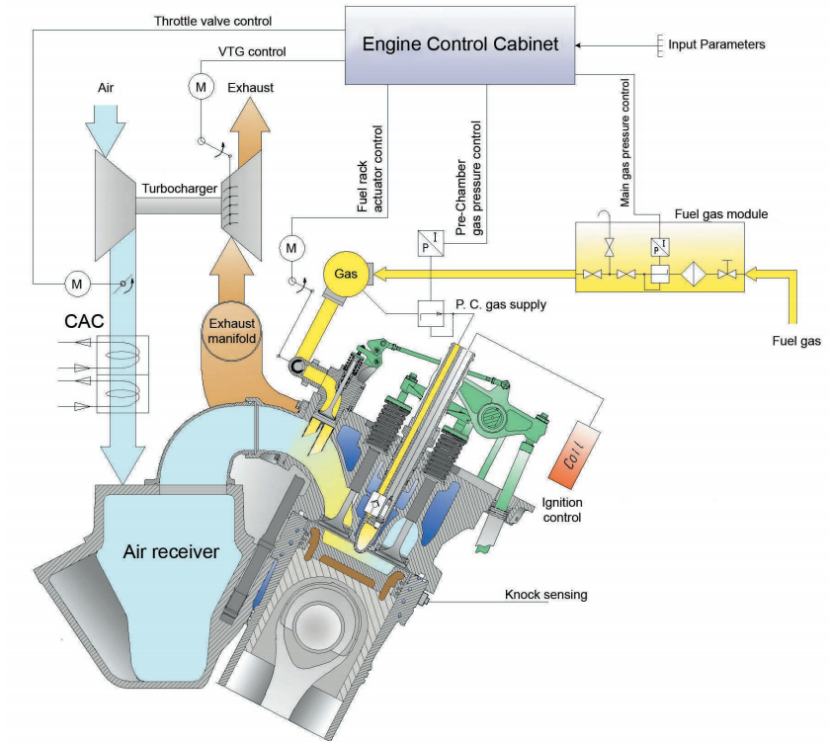

Figure 42. *The principle of gas injection into the charge air. (Rolls-Royce. 2018, p.11)*

One big advantage of the LP-DF process is the simplicity of the gas injection. As the fuel is injected into the charge air before compression of the charge air is begun, the needed injection pressures are significantly smaller than for a HP-DF engine. For proper gas admission, the gas "only" has to be at a higher pressure than the charge air. This greatly reduces the complexity and power consumption of the FGSS. An example of gas feed into the charge air is shown in figure 42. (Woodyard et al. 2009, p.59-60)

Another advantage of the LP-DF process is the lower amount of NOx emissions when comparing to HP-DF. The amount of NOx is lower, because the in-cylinder temperatures are lower. The reason for the in-cylinder temperatures being lower than in the HP-DF engines is the high excess air ratio along with the relatively low compression ratio, which must be used with the LP-DF process to avoid knocking. LP-DF engines using LNG as a fuel are IMO Tier III compliant without exhaust aftertreatment (DNV-GL 2019b, p.9). (Woodyard et al. 2009, p.59-60,)

The negatives of the LP-DF process are mainly related to operating window of the engine. The ideal operating window of a LP-DF is illustrated in figure 43. Break mean effective pressure (BMEP), which can be calculated as work done per cycle divided by the cylinder displacement volume, is an engine size independent measure of the performance (Heywood 1988, p.50). High BMEP values are desirable, but as the BMEP raises, the margin to knocking and misfiring starts to decrease. This means that for example compression ratio, which increase has a positive effect on the efficiency and BMEP, cannot be as high as for example for the HD-DF engine (Heywood 1988, p.842). Reason being that if the air-fuel mixture is exposed to high enough temperatures during the compression in a LP-DF engine, it will cause knocking. A LP-DF process also requires good controllability of the air-fuel ratio, for example with a charge-air wastegate (Woodyard et al. 2009, p.43). Another disadvantage of the LP-DF process is that the gas composition and quality have a big effect on the knocking margin. Heavier hydrocarbons, resulting in lower methane numbers, decrease the margin to knocking, meaning that fuel mixtures under a certain methane number cannot be used. (Stenersen et al. 2017, p.37-38)

Efficiency and NOx emissions are linked to each other. To achieve a high efficiency along with low NOx emissions, the air-fuel ratio must be adjusted between the knocking and misfiring limitations, as illustrated in figure 43. High enough air-fuel ratios will cause the compression ignition of the pilot fuel to not function anymore, resulting in misfiring. On the other hand, low enough air-fuel mixtures, combined with a high enough compression ratio, will cause knocking (Heywood 1988, p.450). (Stenersen et al. 2017, p.15-16)

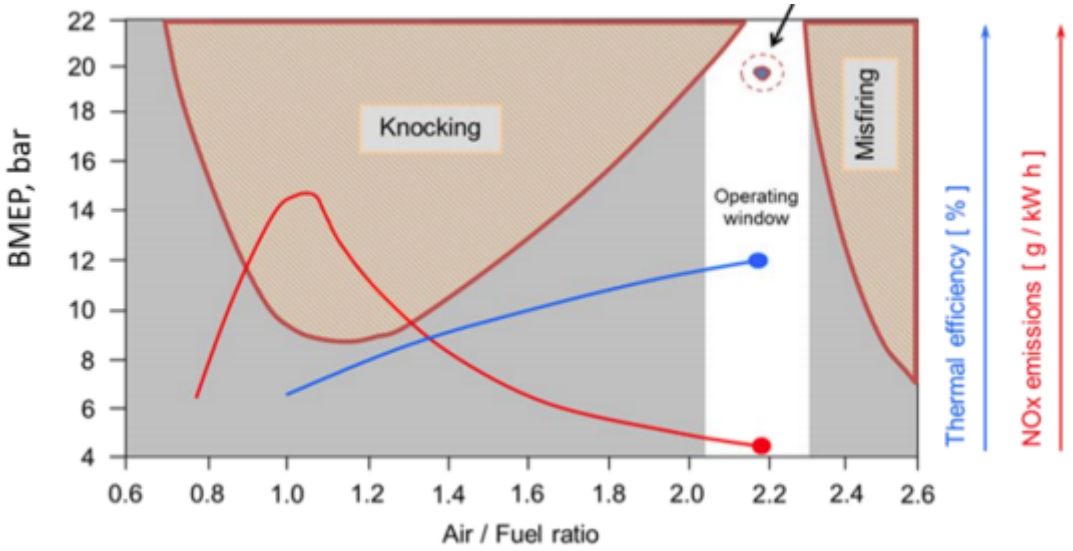

Figure 43. *The ideal operating window of a LP-DF engine. (Stenersen et al. 2017, p.38)*

2.6.3 High pressure injection, diesel process

Unlike in LP-DF engines, in HP-DF engines only air is compressed inside the cylinder. Both the pilot fuel and the gaseous fuel are injected into the combustion chamber, at the end of the compression stroke. The function of the pilot fuel, typically in the range of 1 to 5% of the fuel energy, is to auto-ignite under the compression and provide the ignition source for the burning of the gaseous fuel. The aim is to inject pilot fuel into multiple points inside the cylinder, in order to create multiple ignition points inside the chamber. When the pilot fuel ignites in multiple points, flame propagation throughout the cylinder is more even, resulting in a relatively fast burning rate. (Srinivasan et al. 2019, p.371-373)

When a HP-DF process is used, the engine parameter limitations related to knocking are removed, as the fuel is injected with the view to be burned straight away. This means that the process is not very sensitive to the gas composition that is injected. In addition to providing the option to use lower quality gas, also higher compression ratios are achievable, as there is no risk of knocking when compressing only air. The higher compression ratio translates to higher efficiency, especially at lower loads. The fact that there is no air-fuel mixture compressed eliminates the majority of the methane slip emissions (Ushakov et al. 2019, p.1312). HP-DF engines also have a higher thermal efficiency when comparing to LP-DF engines, even at lower loads. (Stenersen et al. 2017, p.16-17,19)

The main disadvantages are in the complexity of the fuel injection equipment. To inject the gas at the end of the compression stroke, the gas pressure must naturally be higher than the prevalent pressure in the cylinder. As injection pressures in excess of 300 bar are needed, the injection equipment is much more complex. Also, the parasitic losses associated to the pressurizing of the fuel are larger. The NOx emissions of a HPDF engine are larger than the emissions from a LPDF engine, mostly due to the higher combustion temperatures. HP-DF engines can satisfy IMO Tier II NOx emission limits, but for the tighter Tier III limits exhaust aftertreatment is needed. To minimize the NOx emissions, the amount of pilot fuel should be minimized, as this lowers the combustion temperature due to the combustion temperature of diesel fuel being higher than that of LNG. (Ushakov et al. 2019, p.1313)

2.7 Calculation model for the fuel gas supply system of 46TS-GD

A calculation model was made, first with excel and then with Aspen HYSYS, to estimate the FGSS power – and cooling power requirements for a 9L engine using a couple of different LNG compositions. The considered FGSS systems were the HP compressors and the HP pumps. In all the cases the fuel tank pressure was assumed to be 1.1 bar. For compressors, which utilize the BOG or vaporized LNG, the BOG temperatures were inspected between -40 and -160°C. The inlet temperatures for pumps were not varied, as the medium must be in liquid phase for pumping. For comparison purposes, also a similar LP-DF model was made, in which the fuel pressure is raised by pumping from 1.1 bar to 11.5 bar. A constant brake specific energy consumption (BSEC) value was used for all cases. The basic parameters of the engine to be calculated are given in table 4. below

Table 20. *Basic input parameters of the engine, for which gas feed values are calculated*

Gas pressure at engine inlet	300…600 bar
Gas temperature at engine inlet	0…60°C
Needed gas mass / volume flow	1815 to 2167 kg/h, see table 21 below.
Mean effective pressure	27 bar
Power output / cylinder	1300 kW
Brake specific energy consumption, BSEC	7760 kJ/kWh

For gas engines the specific fuel consumption is often stated using the BSEC value, which tells how many Joules are needed for producing a kWh. By using the BSEC value, the heating value of the fuel is considered in the efficiency. Compared to the traditional way of expressing brake specific fuel consumption (BSFC) as g/kWh, the BSEC comparison can be done for engines using different fuels. For DF engines the BSEC value can be divided into the gaseous – and the liquid pilot fuel, as in equation 6 below. The total specific energy consumption of the engine is:

$$bsec_{total} = bsec_{gas} + bsec_{pilot} \qquad \textit{(Eq. 6)}$$

In this work the pilot injection quantity was assumed negligible, as a well-controlled pilot injection represents 3 to 5% of the total fuel input. As such the gas consumption was calculated for the whole cylinder output, meaning that the previous equation is simplified to:

$$bsec_{total} = bsec_{gas} \qquad \textit{(Eq. 7)}$$

The power produced in the cylinder depends on the efficiency at which energy is converted, the amount of fuel injected and the heating value of the fuel that is fed into the cylinder, as shown in the equation below (Heywood 1988, p.51-52):

$$P_{cylinder} = \frac{Q_{LHV} \times \dot{m}_{gas/cylinder}}{bsec} \qquad \textit{(Eq. 8)}$$

When inspecting the fuel mass flow, to get a given power out of a cylinder, the amount of energy that has to be fed into the system can be calculated as:

$$\dot{m}_{gas/cylinder} = \frac{bsec \times P_{cylinder}}{Q_{LHV}} \qquad \textit{(Eq. 9)}$$

As our cylinder output was defined to be 1 300 kW with an BSEC value of 7760 kJ/kWh, the amount of gas needed per cylinder with an LHV of Q_{LHV} = 35.8MJ/kg for example, can be calculated with equation 9 to be:

$$\dot{m}_{gas/cylinder} = \frac{7760\,\frac{\text{kJ}}{\text{kWh}} \times 1300\ \text{kW}}{35{,}8\,\frac{\text{MJ}}{\text{kg}}} = 281.8\,\frac{\text{kg}}{\text{h}}$$

For a constant power output, the fuel consumption will have to be adjusted according to the lower heating value of the gaseous fuel that is used. This means that the fuel mass flow rate will be a function of the lower heating value. In the scope of this work we estimated the usage of three different LNG compositions. The LNG compositions considered in these results had LHV values as shown in table 21.

Table 21. *Considered fuels, LHV´s and the mass flows needed for a 9L engine output and the methane number according to EN 16726.*

LNG Composition	Lower heating value	Mass flow for 9L engine at an output of 11 700 kW	Methane number (acc. to EN 16726)
"Atlantic"	49.8 MJ/kg	1824 kg/h	87
"Nigeria"	49.1 MJ/kg	1850 kg/h	64
"Average"	49.3 MJ/kg	1842 kg/h	73
"100% CH_4"	50.0 MJ/kg	1815 kg/h	100
"90% CH_4 - 10% N_2"	41.9 MJ/kg	2167 kg/h	100

The first composition being according to the composition from the LNG liquefication plant "Atlantic", in Trinidad & Tobago. The second LNG composition chosen was according to the composition from LNG liquefication plants in Nigeria. The third composition was an average composition calculated based on the compositions in table 17. With these choices, the effects of using methane rich and – poor LNG compositions could be inspected. Also, worth noting, that the compositions chosen are not "niche products", even though they represented good opposite extremes with regards to the methane content. The Nigerian liquefication terminals annual contract quantity (ACQ) in 2019 was 21 million metric tonnes per year (MTPA), accounting for roughly 6% of the global share, while Trinidad & Tobago had an export of 12.5 MTPA, which accounted for 3.5% of the global share in 2019 (GIIGNL, 2020, p30). More specific details of the three fuels can be found in appendix 5.

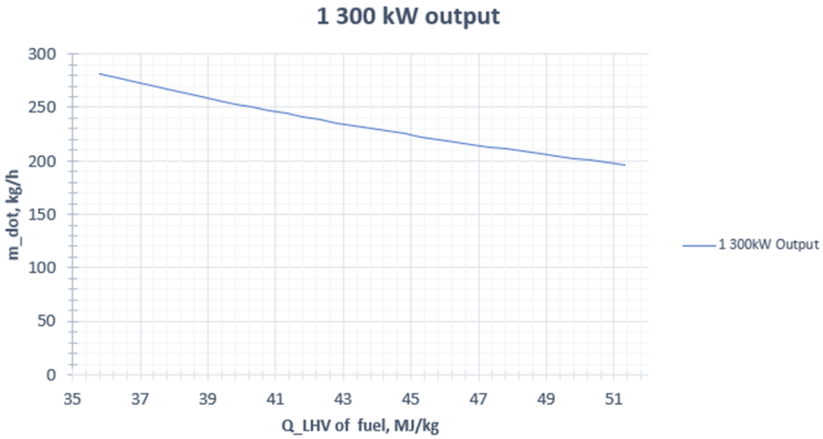

Figure 44. *Fuel gas mass flow rate dependency on the lower heating value of the fuel gas.*

The fuel LHV can vary significantly more than in our example cases. Especially nitrogen content reduces the LHV value. When the fuel contains less energy, more fuel will have to be fed to get the same output. In figure 44 is shown the needed mass flow as the LHV varies from a minimum value of 35.8 MJ/kg to a maximum value of roughly 51 MJ/kg.

2.7.1 Aspen HYSYS model of fuel gas supply system

To estimate the power consumptions Aspen HYSYS was used. It is a process modelling software developed by Aspen Technology Inc. It is intended for use in primarily oil and gas production, gas processing, petroleum refining and air separation industries, and as such is suitable for the GD fuel feed system evaluation. HYSYS has the capability of calculating also dynamic simulations, but in the scope of this work only static calculation was done. The aim of the modeling was to get an overview of the differing phenomena and major energy

flows related to the fuel feed system, and not to go into exact values. (Aspen HYSYS V11 2019c)

Aspen HYSYS V11 was used in this work. HYSYS has numerous property packages available for selection, which can be selected according to the components or mixtures of interest within the simulation. Property packages can be chosen based on for example the temperatures, pressures and mixtures that will be calculated. As we were dealing with hydrocarbon mixtures in the scope of this work, the Peng-Robinson fluid package was selected. The Peng-Robinson model is ideal for vapor-liquid equilibrium calculations of hydrocarbon systems. It is recommended amongst others for LNG process - and methanol injection calculation. The concrete effect of the fluid package selection is, that it determines the equations of state (EOS) that are used to calculate the reactions between components in the mixture. Closer inspection of the EOS calculation is not discussed here. Results should be always carefully reviewed, as an unsuitable property package for the pressures and temperatures related to the process or faulty input data can cause big offset's in the results. (Aspen HYSYS V11 2019a)

Both the reciprocating compressor and pump cases were calculated with HYSYS with the compositions and final injection pressures of interest. The calculation models can be found in figures 45 to 47. In the following chapters the values inside the model are gone through.

The reciprocating compressor model was built with a separator before every compressor stage and intercooling between every compressor stage. The separators are present in some form or the other in real compressors as well, but in the simulation model they are useful for checking on the phase of the mixture to be compressed. From the separators it can be quickly checked that the gas is not cooled into a state where some component possibly starts to condense. No pressure drop was specified for the separators in this model. In the model, the inlet flow composition, temperature and pressure along with the end pressure were user defined. For the simulation of the compressor the pressure ratio of the whole compressor was equally divided between the stages. The resulting pressure ratios are shown in table 23, in chapter 3.

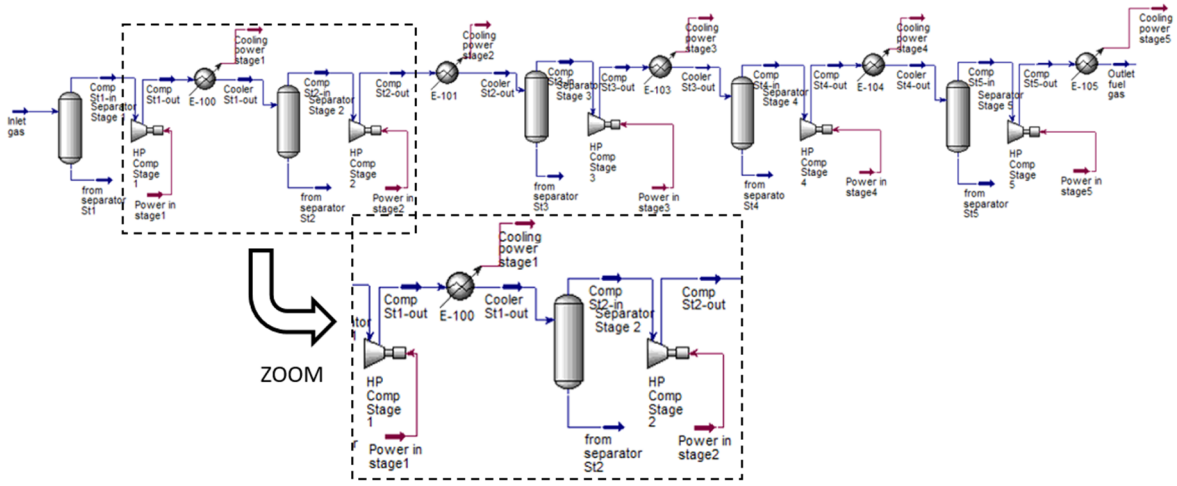

Figure 45. *The HP-DF FGSS simulation model with a compressor.*

The compressor stages were modeled using the centrifugal operating mode with the adiabatic efficiency estimated to be 80%. The adiabatic compression efficiency depicts the percentage of the actual work performed by the compressor versus the ideal work amount. In adiabatic compression the heat exchange to the surrounding environment during the compression is considered to be zero (Eastop et al. 1993, p.59). The adiabatic efficiency of 80% was chosen to take into account that the compressor in reality is a reciprocating compressor. In the HYSYS manual the adiabatic efficiency of reciprocating compressors is estimated to be in the range of 85 to 95%, which is higher than the values recommended for centrifugal compressors (Aspen HYSYS V11 2019b.) The pressure ratio will influence the efficiency. Mokhtab et al have estimated parasitic efficiencies of low speed reciprocating compressors to be around values of 72 to 85% with a compression efficiency of 100%, while large centrifugal compressors can be assumed to have a parasitic efficiency of 99% and a compression efficiency of 80 to 87% (Mokhatab et al. 2019, p.448).

Alternatively, the compressor stages could have been modeled using the reciprocating compressor mode provided in HYSYS, but the centrifugal operating mode was chosen to keep the model simple. For the reciprocating compressor mode, the compressor geometry data must be filled into the model, with data such as the bore, piston rod diameter, stroke length and constant volumetric efficiency to be filled. Most of these could be estimated also, but the centrifugal operating mode, which only requires the efficiency for calculation, gave an easier method of taking into account the compressor efficiency. If exact results are needed for a certain application, then the reciprocating operating mode might be more accurate.

For the HP pump a calculation model, as shown in figure 46 below was constructed. As with the compressor cases, the inlet temperatures and pressures as well as the final pressure and temperature after the heat exchanger were defined. The model consists of a pump and a heat exchanger. The pump adiabatic efficiency was defined to be 75%. A relatively low value was wanted due to the lack of information on cryogenic pumps. The heat exchanger is included in the model so that the needed heating power can be estimated, as the fuel must be heated for it to be at a temperature between 0°C and 60°C at the engine inlet.

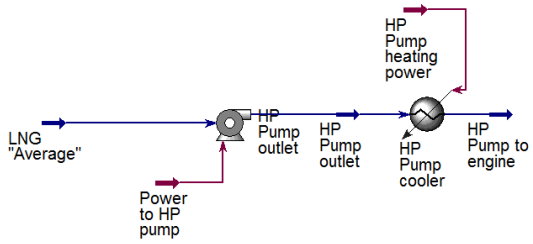

Figure 46. *The HP-DF FGSS simulation model with pumps.*

Finally, a LP-DF system, as shown in figure 47 below, was constructed to allow comparison between HP- and LP-DF systems. Here also an adiabatic efficiency of 75% was assumed for the pump. In this case the pump power consumption is not really of interest, as the values will be relatively low, but the heating power is significant.

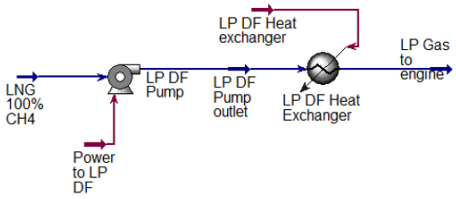

Figure 47. *The LP gas feed system simulation model.*

2.8 Market benchmarking of LP-DF and HP-DF engines

A market benchmarking of both 4-stroke and 2-stroke DF engines was carried out as a part of this work. The structure of this section is to first take an overall look at the market, after which the 4-stroke and 2-stroke products that are foreseen to directly compete are briefly looked at. The market benchmarking contained engines with outputs varying roughly from 3 000 kW to 63 000 kW. Most of the attention naturally given to the power range of the Wärtsilä 46 engines, ranging from roughly 8 000 kW to 23 000 kW. In the list are also LBSI medium-speed pure gas engines manufactured by Rolls-Royce such as Bergen B33:45 and Bergen C25:33. The DF engines manufactured by Himsen are also included in this power output inspection, but as not in the other inspections as enough data was not found. All the

market benchmarking values are from product guides and whitepapers provided by the engine manufacturers. The engine outputs of the engines compared are presented below in figure 48 along with the stated SEC values in gas operation.

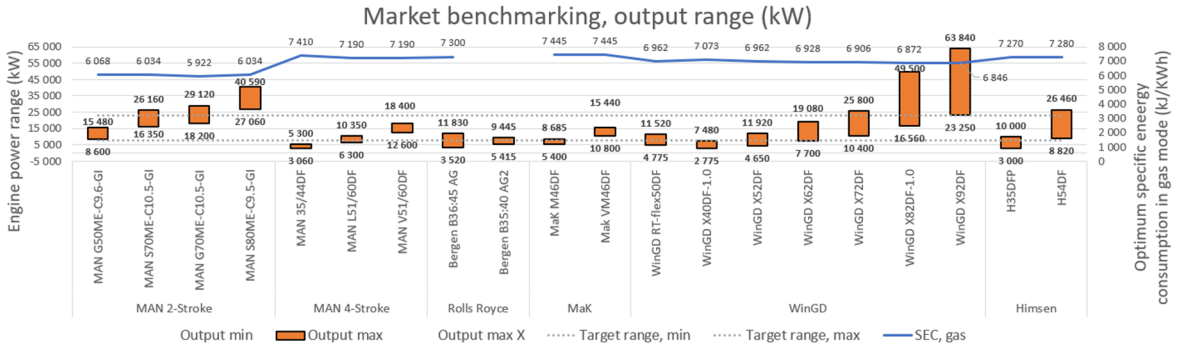

Figure 48. *2- & 4-Stroke dual-fuel engines and their output ranges in available cylinder configurations. (Himsen 2020, p.13,34, MaK 2015a, p.5, MaK 2016, p.1, MAN ES 2020b, p.38, MAN ES 2018b, p.38, MAN ES 2020k. p.20, MAN ES 2020l, p.20, MAN ES 2020h. p.20, MAN ES 2020m, p.20, Rolls-Royce 2020, p.8,12, WinGD 2019. p.21-45)*

All the DF engines compared here are able to use LNG as a fuel. LNG is the baseline "dual-fuel". In addition to LNG DF engines can be capable of combusting various other fuels. In figure 49 below are shown the fuels utilized by different engine manufacturers in 2020. This might be a quickly outdated list, as some of the fuels are quite similar and as such the roll-out to market might only be depending on a suitable customer. The fuels are arranged by the carbon number from the lighter to the heavier, with biofuels having its own column. As can be seen, MAN has many engines available for differing fuels. The engines marked with design are directly available for customers. The engines marked with the conversion note mean that a fuel conversion package can be delivered to an existing engine, thus allowing the conversion to a specific fuel.

		Amount sold	NH_3 /Ammonia	CH_3-OH / Methanol	CH_4 / LNG	C_2H6 / Ethane	C_2H_5-OH / Ethanol	C_3H_8 C_4H_{10} / LPG	0-0.5% S Fuel	HFO	Biofuels
MAN 2-stroke	ME-GI	233	Conv.	Conv.	Design	Design		Design	Design	Design	Design
	ME-GIE	32	Conv.			Design	Design		Design	Design	Design
	ME-LGIM	26	Conv.	Design					Design	Design	Design
	ME-LGIP	46	Conv.					Design	Design	Design	Design
	ME-GA	0			2022				Design	Design	Design
WinGD	X-DF	265			65				Design	Design	
MaK	M46DF				80				Design	Design	
MAN 4-stroke	35/44DF				70				Design	Design	
	51/60DF				70				Design	Design	

Figure 49. *Comparison of DF engine fuel options and natural gas methane numbers allowable before engine de-rating. (MAN ES 2020h, p.171, WinGD 2019d, p.3, MAN ES 2018b, p.42, MaK 2015b, p.64, Gingell 2019, p.7)*

In figure 49 in the LNG column are also collected some of the methane numbers, over which LP-DF engine de-rating is not needed at ISO conditions. The numbers range from 80 to 65.

On the HP-DF ME-GI engines the MN is not relevant as such, instead de-rating is needed if the N_2 content of the fuel gas exceeds 15% (MAN ES 2020h, p.171).

In figure 50 the reported gas injection pressures are shown. Notable points from the figure include 2-stroke MAN-GI engines, which utilize a gas injection pressure of roughly 300 bar. The other 2-stroke manufacturer in the list, Winterthur Gas & Diesel (WinGD) utilize a low-pressure gas injection strategy, with the gas injection pressure varying between 6 and 14 bar, depending on the engine load (WinGD 2020b, p.129). The 4-stroke products are all low-pressure dual-fuel engines. MaK DF-engines use a gas injection pressure varying from 6.5 to 9 bar, while MAN 4-stroke DF-engines have a maximum gas injection pressure of 6.5 bar (MaK 2015b, p64) (MAN ES 2018b, p.151). The pilot injection amount for MaK DF engines is calculated based on a pilot fuel consumption of 1.8 g/kWh (MaK 2015a, p.1)

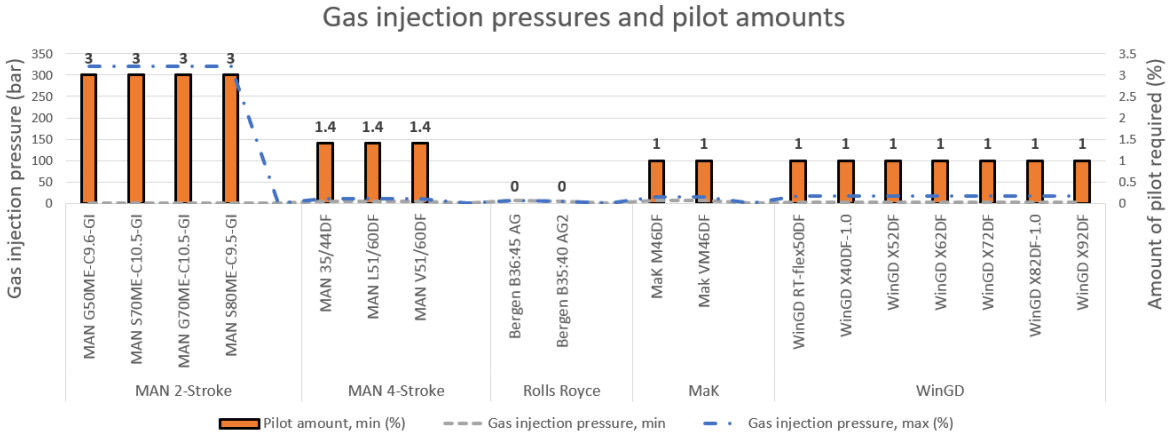

Figure 50. *Gas injection pressures and the minimum used liquid pilot fuel amounts. (WinGD 2020b, p.129, MaK 2015b, p64, MaK 2015a, p.1, MAN ES 2018b, p.151)*

Some of the methane slip values along with the gas injection pressures are collected into figure 51. The minimum values typically represent values given at 85 to 100% engine loads, while maximum values, where data was found, are for low loads. As there is a lot of discussion around methane slip at the moment, some values outside the figure are highlighted here. MAN has announced that it is prepared to guarantee a maximum methane slip value in the range of 0.2 to 0.3 g/kWh for the 2-stroke ME-GI portfolio (MAN 2020c, p.11). MAN 4-stroke methane slip values were not found for comparison in this work, but MAN has indicated that the GI high-pressure direct gas injection is under a feasibility study for application onto the 4-stroke DF portfolio, with methane slip reductions estimated to be 90% (MAN, 2020c, p.14-15). WinGD has reported total hydrocarbon (THC) emission values for the X-DF 2-stroke engines with cylinder sizes between 50 to 72 to be in the range of 2 to

3 g/kWh, with the methane slip constituting 80% of this resulting in slip values of 1.6 to 2.4 g/kWh (WinGD 2019, p.5). For the larger bores, a value of 3 to 4 g/kWh is assumed in the figure, based on estimations presented by Stenersen et al (Stenersen et al. 2017, p.22). Other estimations in the figure are for B35/40 engines, where a value of 4.2 g/kWh is used as presented by Stenersen et al (Stenersen et al. 2017, p.21).

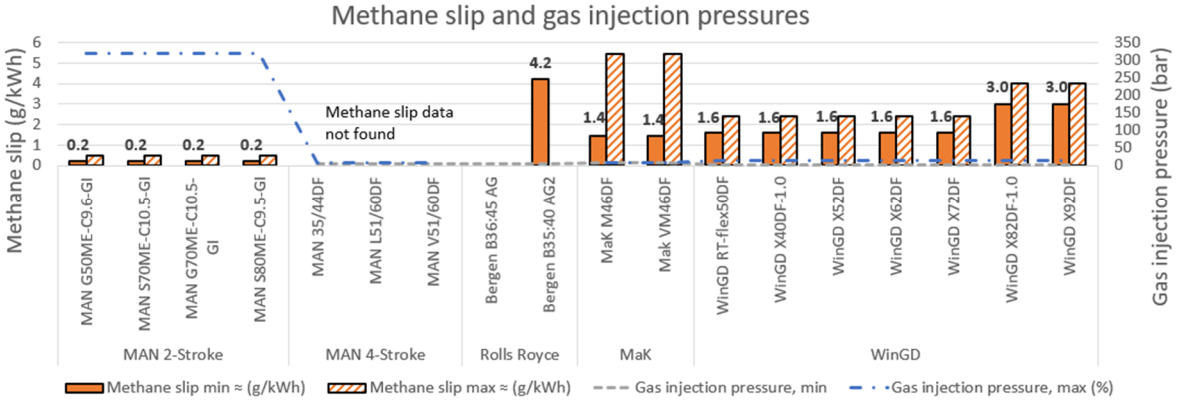

Figure 51. *Methane slip estimations and gas injection pressures of DF-engines. (MaK 2015a, p.23, 26, MAN ES 2020c, p.1, Stenersen et al. 2017. p.21, WinGD 2019, p.3)*

As a general trend, the reported methane slip values have come down from the values for example reported in the 2016 CIMAC conference report. In the report for example WinGD two-stroke LP-DF X-DF engines had methane slip values of 3 to 4 g/kWh while the two-stroke HP-DF MAN ME-GI engines had values of 0.4 to 0.5 g/kWh (CIMAC 2016, p.4). Typically, the methane slip values are given as energy specific values, such as g/kWh or kJ/kWh. For example, the MaK M46DF project guide states the methane slip values for L M46DF engines at an output of 900 and 965 kW/cylinder to be 72kJ/kWh, 96kJ/kWh and 272kJ/kWh at 100%, 50% and 15% loads respectively (MaK 2015a, p.23, 26). These values have been transferred to g/kWh by dividing with the LHV of methane, assumed to be 50 MJ/kg in this context. To express the methane slip emission values as specific emission values in g/kWh´s, the following calculations are made:

$$\dot{m}_{CH_4} = \frac{72\,{}^{\mathrm{kJ}}/_{\mathrm{kWh}}}{50\,{}^{\mathrm{MJ}}/_{\mathrm{kg}}} = 1.44\,{}^{\mathrm{g}}/_{\mathrm{kWh}}$$

2.8.1 4-Stroke DF market

In this section only 4-stroke DF engines with relatively high cylinder outputs, in the order of 500 and more kW/cylinder are considered. This means that manufacturers such as Mitsubishi and Niigata are not inspected more closely here. The 4-stroke DF market can be divided into the LBSI engines and the LP-DF engines. LP-DF engine manufacturers in this

output range are Himsen, MaK and MAN, of which MaK and MAN are inspected closer. Both manufacturers engines are IMO Tier III NOx compliant when operated in gas mode.

MaK LP-DF engines, such as the M46DF and the VM46DF, can be run on gas at loads from 10-15 to 100% (MaK 2015a, p.19). The switchover time from gas to diesel operation is 300s, with emergency switching happening in 1s. When switching the fuel from diesel to gas, the changeover takes approximately 2 minutes. As an additional option, MaK DF engines can be started on gas, in addition to the common diesel mode start (MaK 2015a. p.19). For the pilot injection MaK has a separate electronically controlled pilot injector with a common rail system feeding it (MaK 2015a, p.70). MDO is used as the pilot fuel, with a single HP pump providing the required flow for L-engines (MaK 2015a, p.68). The minimum amount of pilot fuel is roughly 1% of fuel consumption at rated load, with a value of 1.8 g/kWh of liquid fuel consumption reported (MaK 2015b, p.1) The pilot fuel is circulated through the pilot injector also on liquid fuel operation, for cooling purposes. For diesel operation, meaning that MGO, MDO or HFO is used, the fuel pressure is provided with cylinder specific injection pumps. (MaK 2015a, p.20)

MAN LP-DF engines, such as the 35/44DF and 51/60DF, can be run on gas at loads between 10 to 100% (MAN ES 2018b, p.46). The engines have a pilot fuel oil common rail system (MAN ES 2018b, p.13). The pilot fuel amounts are in the regions of 1.4% of the engine fuel consumption at the minimum, with pilot fuel values reported to be 2.3 g/kWh (MAN ES 2018b, p.76). The liquid fuel mode has its own main injector, which is not used under gas-mode operation, but liquid fuel is nevertheless circulated in the system even when gas mode operation is performed (MAN ES 2018b, p.354-355). In liquid mode, meaning MGO, MDO or HFO, fuel pressure is created in the case of the 51/60DF engines with the same plunger pumps that are used in the MAN48/60B diesel engines, (MAN ES 2018b, p.354). In the 35/44DF engines there is no plunger pumps, as a common rail injection system, similar to the one used in 32/44CR engines, is used for the liquid mode fuel pressure (MAN ES 2020b, p.301). For the MAN 51/60DF engines the pilot fuel can be MGO or MDO, but for the MAN L35/44DF only MGO can be used as the pilot fuel (MAN ES 2018b, p.253).

2.8.2 2-Stroke DF market

The DF engines on the 2-stroke market can be separated to LP-DF engines, manufactured by WinGD and HP-DF engines manufactured by MAN. The output powers are generally more than the Wärtsilä 46 output range, but at the lower range there are some overlaps. Here special focus is given on the LNG powered DF engines and especially the HP-DF engines and their equipment. As MAN provide many engines using other fuels also, some additional information on these is given in appendix 6 also.

WinGD has a wide portfolio of LP-DF 2-stroke engines, with the DF bore sizes ranging from 40 to 92mm. At the moment the engines are for LNG, but also at least ethanol has been laboratory tested (WinGD 2020e, p.4). WinGD DF engines have three operating modes: gas mode, diesel mode and fuel sharing mode. The gas mode is IMO Tier III compliant without exhaust aftertreatment. In the gas mode an electro-hydraulic pilot injection of MDO or MGO is used. The pilot injection amount is very low, in the range of 0.5-1.5% of the overall fuel consumption for the larger bores and a little bit more, roughly 1 to 2%, for the bore sizes under 62mm (WIN GD 2020c, p.20, WinGD 2020b, p.21). The gas operation mode is available at loads upwards from 5-10% and ending at 100% (WinGD 2020b, 28). (WinGD 2020b, p.21)

Fuel gas is fed to the engine at pressures between 6 and 16 bar(g) (WinGD 2020b, p.128-129). A gas admission valve is used to feed the gas into the cylinder, where it is immediately mixed with the charge air. (WinGD 2020b, p.132) The FGSS gas storage can be at ambient pressures or at higher pressures, depending on the application. (WinGD 2020b, p.135)

The diesel mode is IMO Tier II compliant with the use of HFO, MDO or MGO. The liquid pilot fuel nozzles stay in operation even with diesel mode operation, with an injection rate corresponding to 0.5% of the engine fuel feed, to avoid clogging of the nozzles (WinGD 2020b, p.21). Diesel operation mode is available throughout the whole load range, from 0 to 110%. The main liquid fuel is injected with WinGD´s “Flex system” common rail fuel injection system. For the pilot fuel injection, a separate common rail system with a single

HP pump and two electronically controlled pilot fuel injectors per cylinder are used. The pilot injectors are used in a pre-chamber. (WinGD 2020b, p.122-123)

In addition to gas – and diesel mode, a fuel sharing mode is also available, for extra cost, between 50% and 100% loads. In the fuel sharing mode, the ratio between liquid fuels such as HFO, MDO and MGO, and the gas fuel can be adjusted. Fuel sharing mode is specifically for LNG carriers. It is meant to be used to decouple the ships speed from the BOG amount that is available. So, if the BOG amount available is not enough for the speed wanted, the fuel sharing mode allows additional input of liquid fuel to reach the desired voyage speed. The minimum amount of liquid fuel is 5% of the total fuel energy input and the maximum is 50% of the total fuel energy input. (WinGD 2020b, p. 28-33)

Transfer from gas mode to liquid mode happens instantaneously, within one engine revolution, and it can be done at any load. The engine cannot be switched to gas mode directly from HFO operation, instead it has to be run on MGO or MDO first to flush the system and to ensure that the liquid backup fuel system is ready if a gas trip happens due to any abnormality in the gas or the gas feed system. (WinGD 2020b, p.33-34)

For NOx emission control WinGD has both LP- and HP-SCR units available, with both having the capability to reach IMO Tier III emission levels. If sulphur rich fuels are used, scrubbers can be used to manage the SOx emissions. For the GHG emission side WinGD has announced a X-DF2.0 technology program, which is already in laboratory trial phase, with targets amongst others to reduce the gas energy consumption by 3% and the methane slip by 50%. One method talked about is an EGR method utilizing inert gas, branded as iCER (WinGD 2020c, p.1). The idea with iCER use is to expand the operating window of the X-DF engines, as illustrated in figure 52. If simplified, the methane emissions are lowered, as the unburnt methane is circulated into the combustion with the exhaust gas recycling (WinGD 2020d, p10). (WinGD 2020b, p.213)

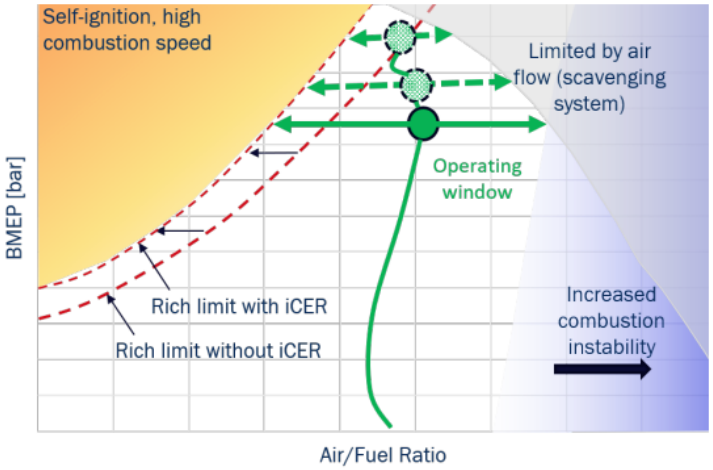

Figure 52. *Projected X-DF2.0 operating window with iCER. (WinGD 2020d, p.5)*

In the 2-stroke DF market MAN uses HP gas injection. The most known and sold engine is the ME-GI engine designed for natural gas, or methane, combustion, which has been on the market since 2012 (MAN ES 2011, p.1). The ME-GI engine is built upon the ME-B and ME-C two-stroke diesel engines. Today the HP-DF portfolio of MAN includes also engines such as ME-LGI and ME-LGIM. The ME-LGI engine is intended for use with low-flashpoint fuels such as methanol, ethanol, DME and LPG (MAN ES 2020f, p.5). The ME-LGIM on the other hand is intended for using methanol as the gaseous fuel. For different fuels the injection pressures - and in some cases also the gas injection equipment differs. The basic idea behind ME-GI, ME-LGIP and ME-LGIM is to utilize mostly the same hardware, but then according to fuel needs change gas control blocks, fuel injection piping and accumulators according to the needs of the fuel to be used. Here is provided a closer look at the engines utilizing natural gas, the ME-GI and ME-GA. In appendix 6 can be found some additional information regarding the ME-LGI, ME-LGIP and ME-LGIM engines.

The MAN ME-GI HP-DF engines can be operated in three different operation modes: fuel-oil-only -, minimum-fuel – and mixed gas mode. The minimum fuel mode can be run at loads from 10-15% to 100% and in the mixed mode from 50% to 100%. In the gas mode operations, the ME-GI engines can use HFO, MGO and MDO as the pilot fuel (MAN ES 2020e, p.13). The preset minimum amount of pilot used is 5% at 100% load, with the amount of pilot reducing towards lower loads. In tests 1.5% pilot amount is achievable, but this has caused load limitations on the liquid fuel mode. For the DF engines MAN uses electronically controlled and hydraulically actuated exhaust valves. (MAN. 2020e, p.11-13)

The ME-GI engines have alternative FGSS setups, which provide the fuel to the engine at a pressure of roughly 300 bar. For the fuel injection the gas is fed through a gas control block, with an integrated accumulator volume, to two or three gas injection valves depending on engine size. The gas control block contains two electronically controlled hydraulically actuated valves that are connected in series. The other one is the electronic gas injection valve (ELGI), used for gas admission, while the other valve, the electronic window/shut-down valve (ELWI) is used for timing of the gas injection. For the pilot injection the number of valves is similarly two or three depending on engine size. The ME-GI cylinder gas feed system is illustrated in figure 53. (MAN ES 2020e, p.6-7)

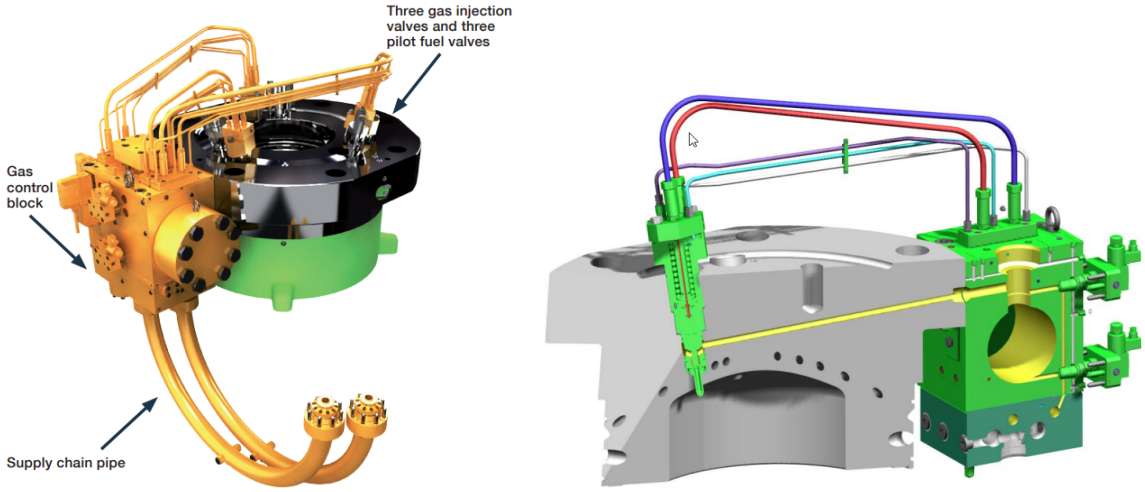

Figure 53. *The cylinder cover and the gas fuel injection equipment of a ME-GI engine. (MAN ES 2020e, p.7, Christensen 2017, p.10)*

The gas injection valves are electronically controlled, with the actuating medium being high pressure hydraulic control oil. A schematic of the ME-GI gas injection valve is shown in figure 54. Sealing of the gas is done with a control oil in a higher pressure. The liquid pilot fuel injection valves are standard “ME” diesel liquid fuel valves, with some changes made to the nozzles. Operation on liquid fuel for full load is allowed, but for prolonged operation the injector nozzles are recommended to be changed for fuel efficiency reasons. (MAN. 2020e, p.9-10)

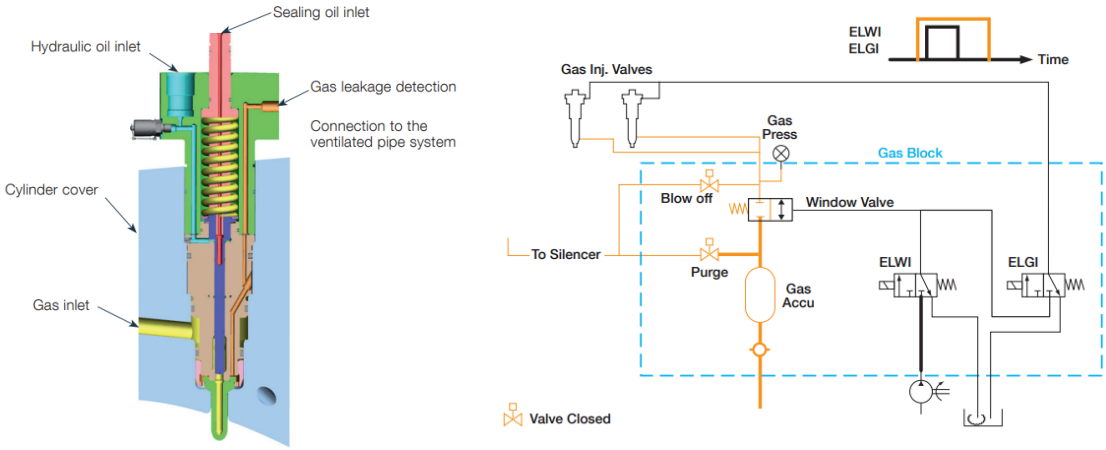

Figure 54. *The gas injection valve on the ME-GI engine. (MAN ES 2020e, p.9-10)*

MAN 2-stroke products have various strategies to cope with the IMO tier III NOx emission regulation. For the 2-stroke engines the options are either the application of EGR or an SCR, available in both SCR-HP and -LP. In the future applying a LP-DF process will also be an alternative, as most probably due to lower capex and easier compliance with NOx regulation, MAN is also developing an LP-DF engine. The LP-DF process is known as the ME-GA engine in the MAN two-stroke engine portfolio, with MAN estimating to have the first ME-GA engine installed on an LNGC vessel during the 1st half of 2022 (MAN ES 2019b, p.1). (MAN ES 2020d, p.10-11)

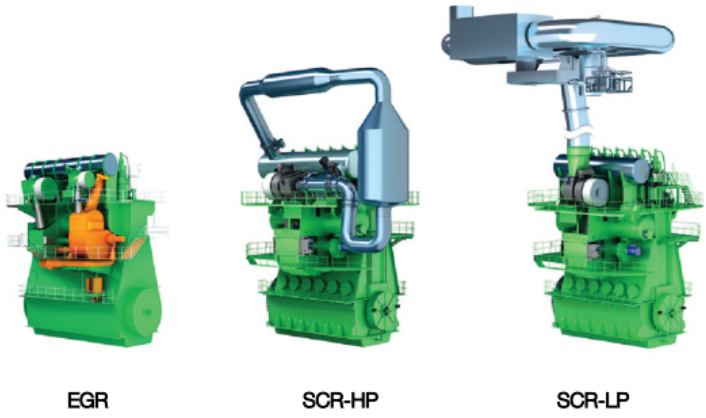

Figure 55. *Solutions for complying with Tier III NOx emission regulations with ME-GI engines. (MAN ES 2020d, p.10)*

To comply with sulphur limitations, when using sulphur rich fuel, SOx scrubbers are available. SOx scrubbers are available as open –, closed and hybrid loop systems. They are also available with a “dry -” or a “wet agent”, with the wet agent, usually sea water or fresh water, being the normal marine solution. (MAN ES 2020d, p.87-88)

On the HP-DF gaseous fuel injection side MAN has used pumps and compressors for the fuel pressurizing equipment from a variety of suppliers. At least Cryostar has provided HP pumps and BOG reliquefication solutions to MAN engines (MAN ES 2020e, p.15-16). At the moment MAN is starting to provide an own portfolio of pump vaporizer units (PVU), designed for fuel feeding of ME-GI engines (MAN ES 2019a, p.4-6). For cryogenic HP compressors, the suppliers have been at least Burckhardt along with Daewoo Shipbuilding and Marine engineering, Hyundai Heavy Industries and Mitsubishi Heavy Industries (MAN ES 2020e, p.21,29).

The MAN PVU is a skid type unit, available in various sizes ranging from LNG mass flows of 1000 kg/h to 8000 kg/h. The PVU units contain three hydraulic powered HP pumps along with a printed circuit glycol water HP vaporizer. The footprint of these units is comparably small, with most of the skids 3.7m in length and 2.2m in width. Hydraulic power supply for the pumps can be taken from the ME-GI engine hydraulic power supply system or alternatively via an external supply unit (MAN ES 2017b, p.2). The advantage with hydraulic powered units is that each pump can be individually controlled. As each of the three pumps is sized for 50 % capacity, the PVU unit provides redundancy. This also means that one pump can be overhauled while the PVU is in full operation. Compared to other HP pumps, the maintenance intervals reported are somewhat better than with traditional cryogenic HP pumps, with a reported overhaul interval of 6 000 hours (The Motorship, 2019). The PVU is designed so that it can be fed from the LNG tank with a feed pump, and it will feed the pressurized and filtered gas directly into the gas valve train of the engine, thus the process scheme is quite simple. (MAN ES 2019a, p.4-6)

3 RESULTS

In this section the calculation results from two different HP fuel injection cases are shown as well as from the LP-DF base case. The results are calculated for an engine output of 11 700 kW, corresponding roughly to a 9L46TS engine. The amount of fuel feed is adjusted by the fuel composition to match the required engine output. The pressurization methods considered are the usage of compressors, either cryogenic or non-cryogenic, and HP pumps.

The main results taken from the calculations are the power consumption to pressurize the fuel and the amount of cooling or alternatively heating needed to satisfy the engine fuel inlet temperature requirements. The common variables were the gas injection pressures and the gas compositions. For the compressor calculations differing BOG temperatures were also considered. The considered gas and LNG compositions are shown in table 22.

Table 22. *The gas and LNG compositions used in the calculation.*

Gas compositions	100% CH_4	90% CH_4 - 10% N_2	
LNG compositions	LNG-1 = "Methane poor" composition, composition acc. to "Nigeria", table 17	LNG-2 = "Methane rich" composition, composition acc. to "Atlantic", table 17	LNG-3 = Average composition, table 17

3.1 Cryogenic HP compressor and HP Compressor gas feed systems

Compressors and cryogenic compressor can be used to pressurize the fuel in a gaseous state. In these results two gas compositions, 100% methane and 90% methane -10% nitrogen mix, are considered, as the amount of heavier hydrocarbons is normally low in the BOG. The starting data is shown in table 23 below, while the simulation model can be found in figure 44.

Table 23. *Cryogenic HP compressor and HP compressor gas feed system calculation input constants and variables.*

Calculation input constants		Calculation input variables	
Compressor adiabatic efficiency	80%	Gas injection pressure	300 bar

Table 23 continues. *Cryogenic HP compressor and HP compressor gas feed system calculation input constants and variables.*

Gas mass flow	100% CH_4 - 1815 kg/h		350 bar
	90% CH_4 / 10% N_2 - 2167 kg/h		400 bar
Temperature to engine	45°C		600 bar
		BOG Gas inlet temperature	-160°C
			-120°C
			-80°C
			-40°C

The compressor power requirements were calculated by evenly distributed pressure ratios over the compressor stages. The ideal pressure ratios are shown in table 24.

Table 24. *The evenly distributed pressure ratios for varying final pressures.*

Discharge pressure (bar)	**Stages**		
	4	5	6
300	4.06	3.07	2.55
350	4.22	3.17	2.61
400	4.37	3.25	2.67
600	4.83	3.53	2.86

The temperature and pressure changes for all the calculated cases can be seen in appendix 7. One example is picked here for reference in figure 56. From the figures the pressure and temperature variations over the compressor stages can be observed.

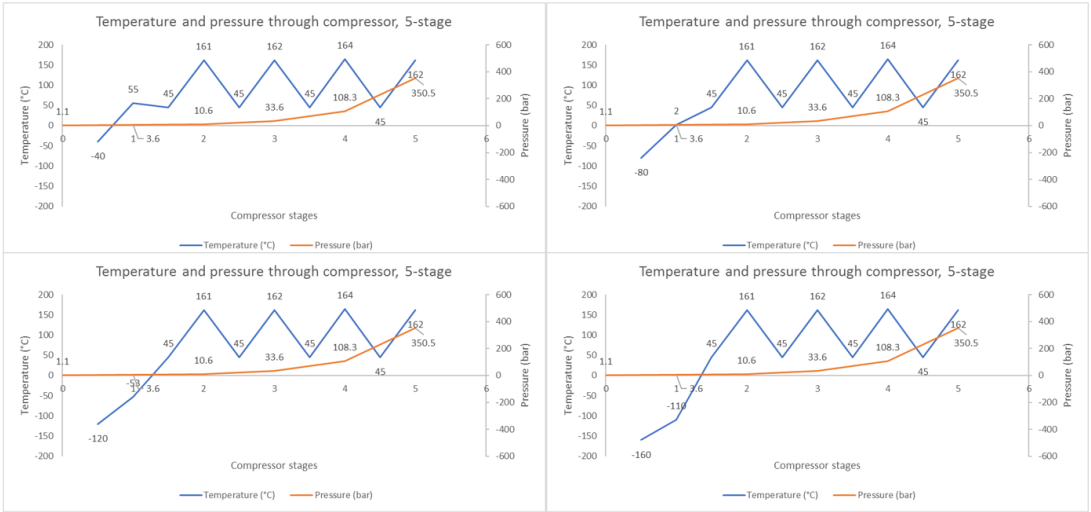

Figure 56. *Temperatures and pressures through the compressor with BOG temperature -40°C, -80°C, -120°C and -160°C at 350 bar.*

In figures 57 to 60 are shown the results for power consumption, required cooling power and compressor pressure ratios per stage, when a 90% CH_4 - 10% N_2 gas is compressed to varying final pressures. Finally, the FGSS power consumption is compared to the engine output in figure 60.

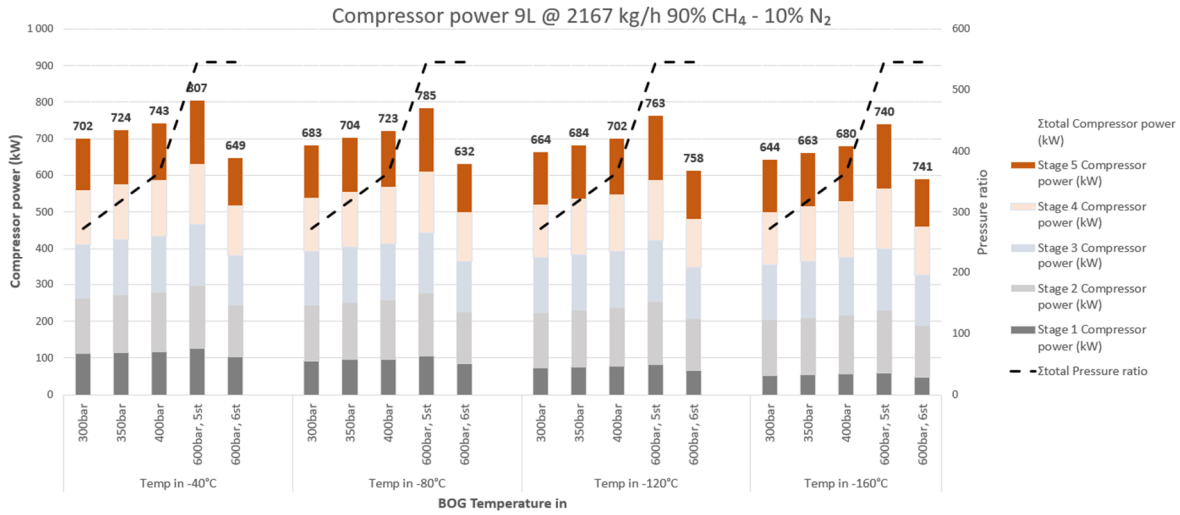

Figure 57. *Compressor power consumption for a 9L engine when running on a mixture of 90% CH_4 / 10% N_2 gas, with fuel gas outlet pressures from 300bar to 600bar and BOG inlet temperatures of -40°C, -80°C, -120°C and -160°C C.*

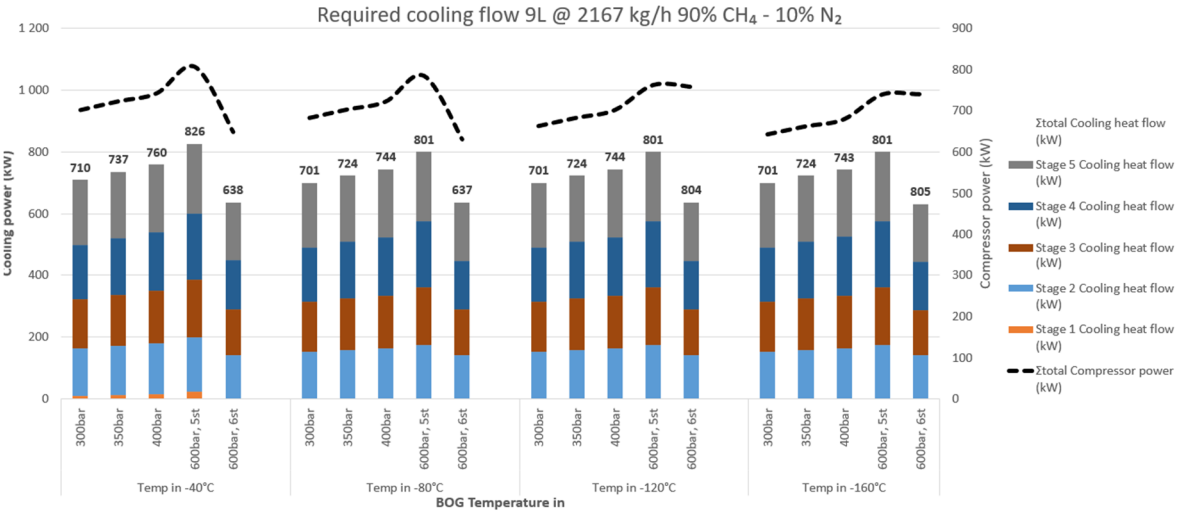

Figure 58. *Cooling power for 9L engine when running on a mixture of 90% CH4 / 10% N_2 fuel, with fuel gas outlet pressures from 300bar to 600bar and BOG inlet temperatures of -40°C, -80°C, -120°C and -160°C.*

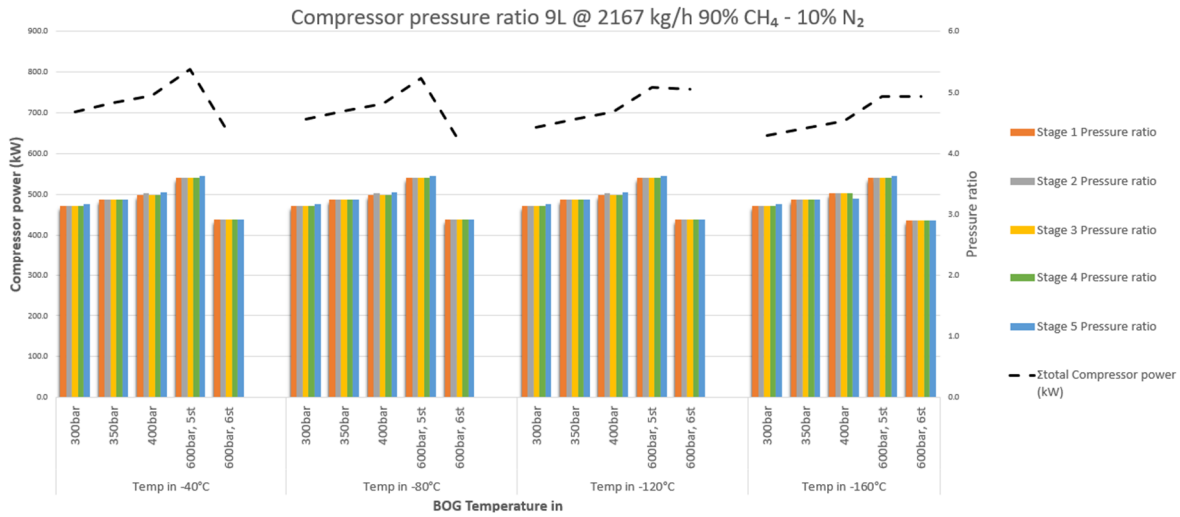

Figure 59. *Compressor pressure ratios per stage for 9L engine when running on a mixture of 90% CH4 / 10% N_2 fuel, with fuel gas outlet pressures from 300bar to 600bar and BOG inlet temperatures of -40°C, -80°C, -120°C and -160°C.*

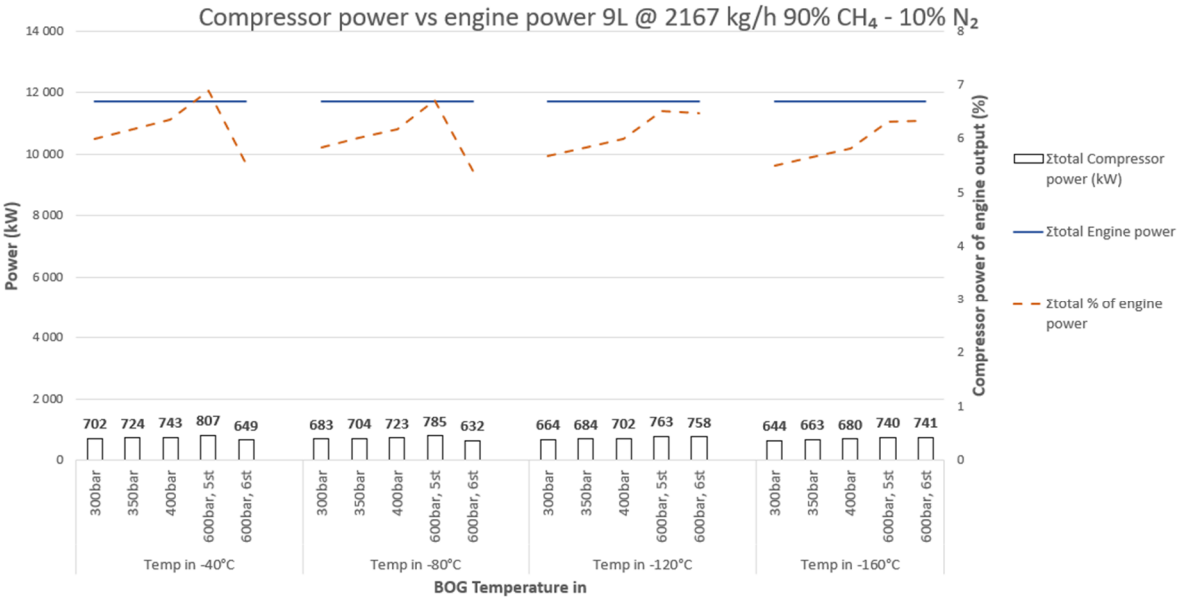

Figure 60. *Compressor power consumption versus 9L engine output when running on a mixture of 90% CH4 / 10% N_2 fuel, with fuel gas outlet pressures from 300bar to 600bar and BOG inlet temperatures of -40°C, -80°C, -120°C and -160°C.*

Similar figures for the power consumption, required cooling power and compressor pressure ratios per stage, when a 100% CH_4 gas is compressed to varying final pressures are shown in appendix 7. The FGSS power consumption for 100% CH_4 is compared to the engine output in figure 61.

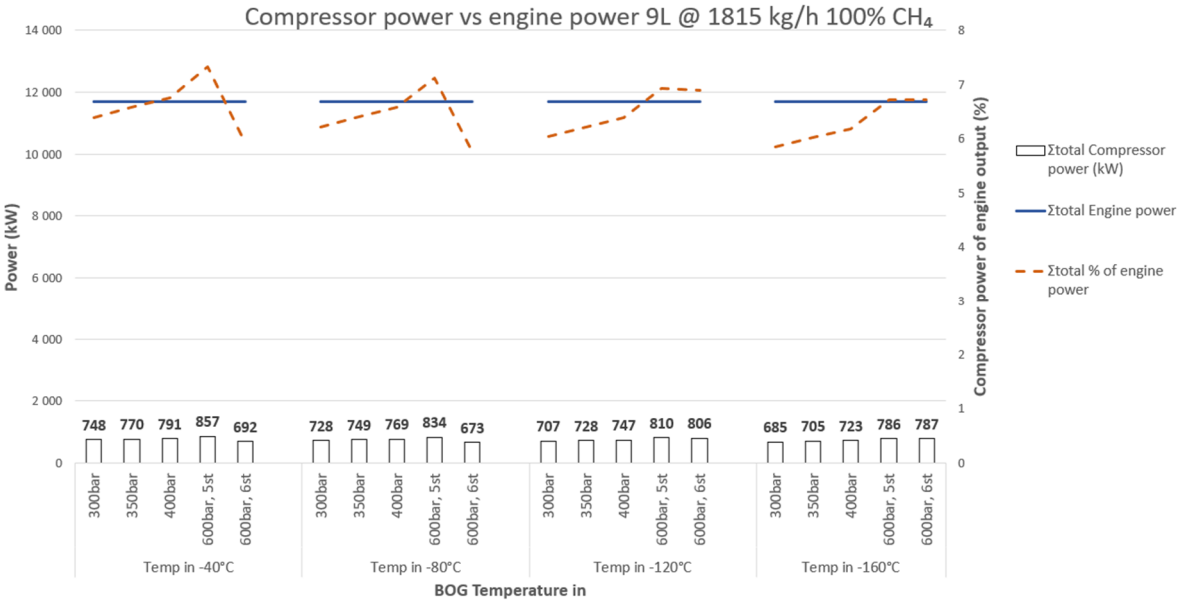

Figure 61. *Compressor power consumption versus 9L engine output when running on 100% CH4 fuel, with fuel gas outlet pressures from 300bar to 600bar and BOG inlet temperatures of -40°C, -80°C, -120°C and -160°C.*

In table 25 is shown the summary from the results of the HP compressor calculation.

Table 25. *Summary of the compressor calculation main results.*

Calculation results	100% CH_4	90% CH_4 - 10%N_2
Compressor power consumption (kW)	674 – 857 kW	632 - 807 kW
Compressor power consumption, percentage of engine output	5.8 – 7.3%	5.4 – 6.9%
Cooling need (kW)	690 - 889 kW	637 – 826 kW
Compressor pressure ratio	273 - 545	273 - 545

3.2 Cryogenic HP pump gas feed system

The fuel can be pressurized in its liquid state with a cryogenic HP pump and vaporized for the engine using a HP evaporator. The power consumption estimation of the system was done for the three specified LNG compositions as well as for a 100% methane gas composition. The inputs, along with the variables used in the calculation are shown below in table 26.

Table 26. *Cryogenic HP pump gas feed system calculation constants and variables.*

Calculation input constants		Calculation input variables	
Pump adiabatic efficiency	75%	Gas injection pressure	300 bar
Gas mass flow	LNG "Nigeria" - 1850 kg/h		350 bar
	LNG "Atlantic" - 1824 kg/h		400 bar
	LNG "Average" - 1842 kg/h		600 bar
	100% CH_4 - 1815 kg/h		
Temperature to engine	25°C		
LNG Inlet temperature	-161°C		
LNG Inlet pressure	1.1 bar		

During the fuel pressurizing process, the pressure as well as the temperature of the fuel changes somewhat. In figure 62 below is illustrated an example of the temperature and pressure changes, along with the temperature change that needs to be handled by the HP vaporizer. In the example the average LNG composition is pumped to pressures ranging from 300 to 600 bar. The temperature and pressure changes inside the system for all the cases can be found in appendix 8.

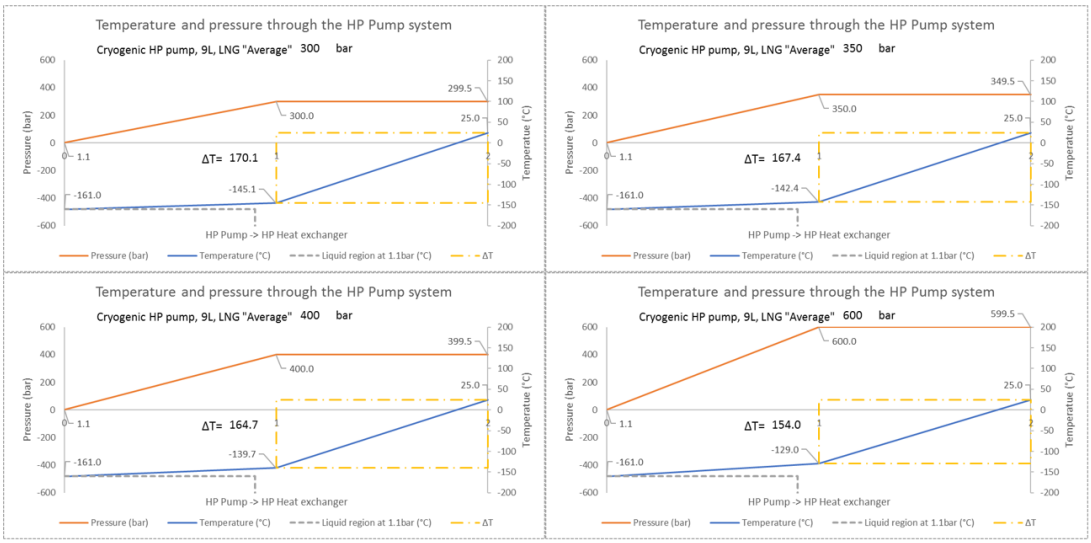

Figure 62. *Temperature and pressure through the HP pump system, LNG according to "average" composition at outlet pressures from 300 bar to 600 bar.*

The power consumption and required heating power results for the various LNG compositions considered are shown below in figures 63 to 65, along with a summary of the results in table 27.

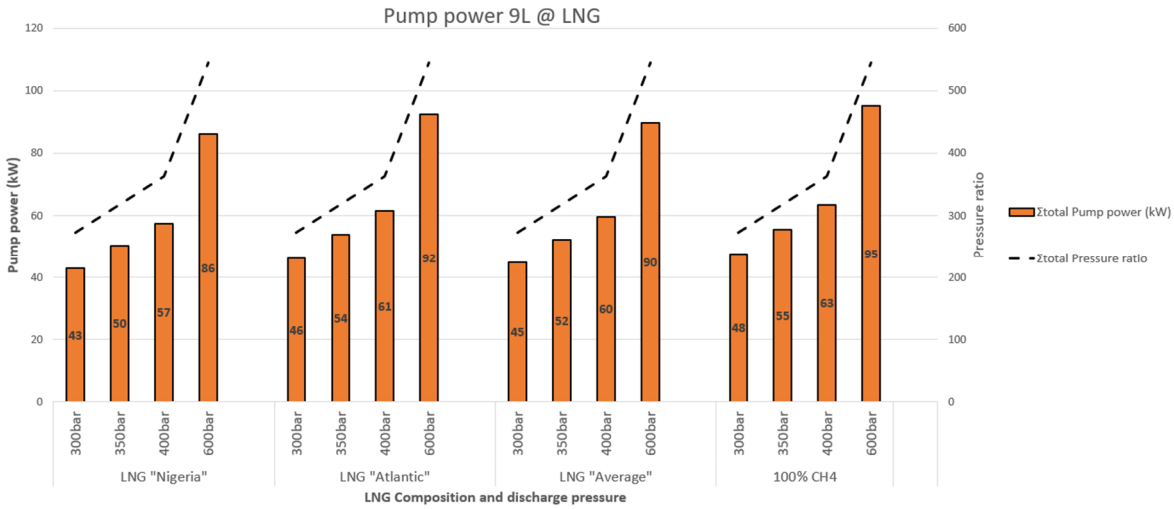

Figure 63. *HP pump power consumption for varying LNG compositions and varying end pressures.*

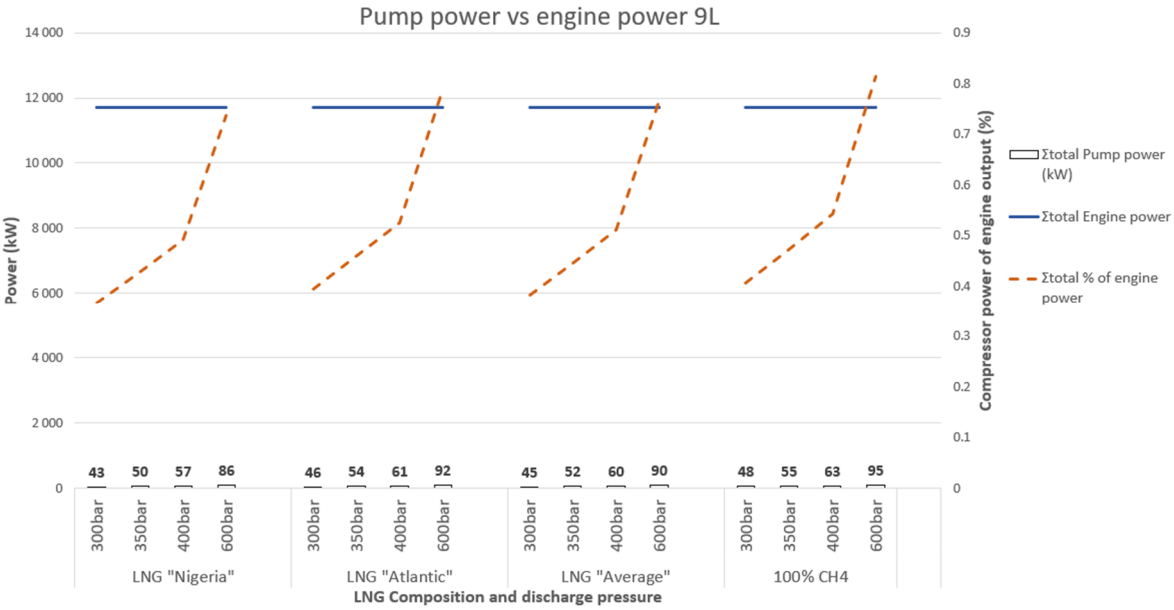

Figure 64. *HP pump power consumption for LNG pressurizing versus the engine output power.*

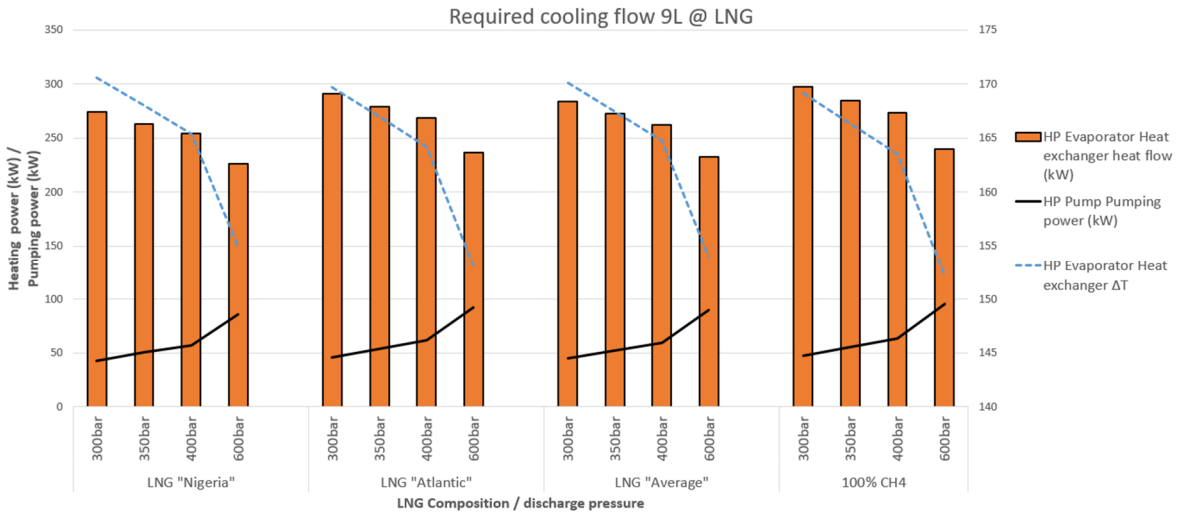

Figure 65. *The required heating power and the ΔT in the HP vaporizer, along with the HP pump power consumption for the LNG compositions and discharge pressures.*

Table 27. *Summary of the calculation results related to HP pumping.*

Calculation results	100% CH_4	LNG "Atlantic"	LNG "Nigeria"	LNG "Average"
Pump power consumption (kW)	47 – 95 kW	46 – 92 kW	43 – 86 kW	45 – 90 kW
Pump power consumption, percentage of engine output	0.4 – 0.8%	0.4 – 0.8%	0.4 – 0.7%	0.4 – 0.8%
HP Evaporator heating (kW)	240 – 297 kW	237 – 291 kW	227 – 274 kW	233 – 284 kW
HP Evaporator ΔT (°C)	152 – 169 °C	153 – 170 °C	155 - 171°C	154 - 170°C

3.3 LP-DF gas feed system

For comparing the HP-DF and LP-DF systems, an LP-DF gas feed system was also simulated. For comparability reasons, the LP fuel tank was kept at the same pressure as the HP fuel tank, namely 1.1 bar. A pump was used to raise the pressure to 12 bar, after which the gas fuel is vaporized in a heat exchanger resulting in a final pressure of 11.5 bar. The LP

pump simulation model is shown in figure 47 and appendix 9, along with the temperature and pressure changes in the system.

***Table 28**. The LP-DF gas feed system calculation constants.*

Calculation input constants	
Pump adiabatic efficiency	75%
Gas mass flow	LNG "Nigeria" - 1850 kg/h
	LNG "Atlantic" - 1824 kg/h
	LNG "Average" - 1842 kg/h
	100% CH_4 - 1815 kg/h
Temperature to engine	25°C
LNG Inlet temperature	-161°C
LNG Inlet pressure	1.1 bar
Gas injection pressure	11.5 bar

The results related to the LP gas feed system are shown in table 28 below.

***Table 29**. Summary of the calculation results related to LP pumping.*

Calculation results	100% CH_4	LNG "Atlantic"	LNG "Nigeria"	LNG "Average"
Pump power consumption (kW)	1.7 kW	1.7 kW	1.6 kW	1.7 kW
Pump power consumption, percentage of engine output	0.01%	0.01%	0.01%	0.01%
LP Evaporator heating (kW)	450 kW	447 kW	437 kW	443 kW
LP Evaporator ΔT (°C)	185 °C	185 °C	185°C	185°C

4 ANALYSIS

This section contains the analysis of the results from the calculation presented in chapter 3. In addition, the LP-DF and HP-DF systems are compared against each other. This includes the inspection of the emissions levels between the two different systems, as well as the equipment needs associated with the achievable emission levels. Also, some capex comparisons found from the literature are presented here. After the LP-DF and HP-DF comparison, the differing fuel pressurization methods related to HP-DF FGSS, namely pumping or compressing, are compared. This comparison includes the power consumption values as well as a rough review of the system layouts, needed equipment and possible equipment manufactures as well as rough estimations of prices. At the end a short sensitivity analysis related to the calculation results is presented.

4.1 Analysis of calculation results

For simpler comparability of the results from HP pumping and compression, the different mass flows and heating- and cooling powers for the differing fuel compositions were averaged for the varying pressures. The average values can be found in appendix 10. These average values are plotted in figure 66 below. In the figure is also shown the LP fuel feed system, where a relatively high injection pressure of 11.5 bar is assumed.

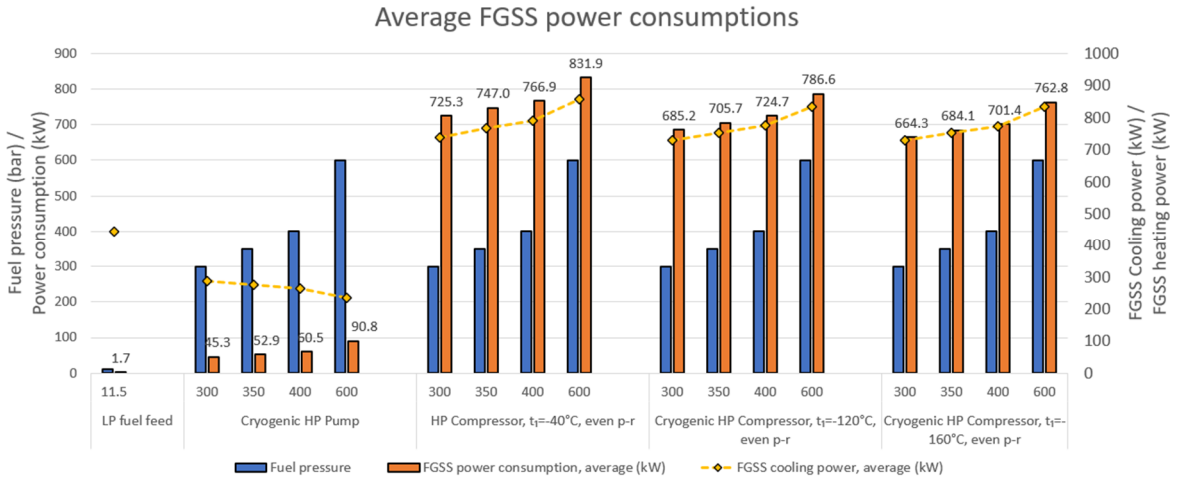

Figure 66. *The FGSS power consumption values calculated with Aspen HYSYS, averaged for all the fuel compositions calculated.*

From figure 66, it can be seen that the power consumption associated to compressing is significantly more than for pumping. The power consumption increases as the final pressure increases, but it is not a very significant increase. The pressure increase probably has a bigger

effect on the equipment side, where components are under more force. When comparing the power consumptions to the 9L engine output, the FGSS power consumption varies from values of under 1% to values of roughly 6%, as shown in figure 67.

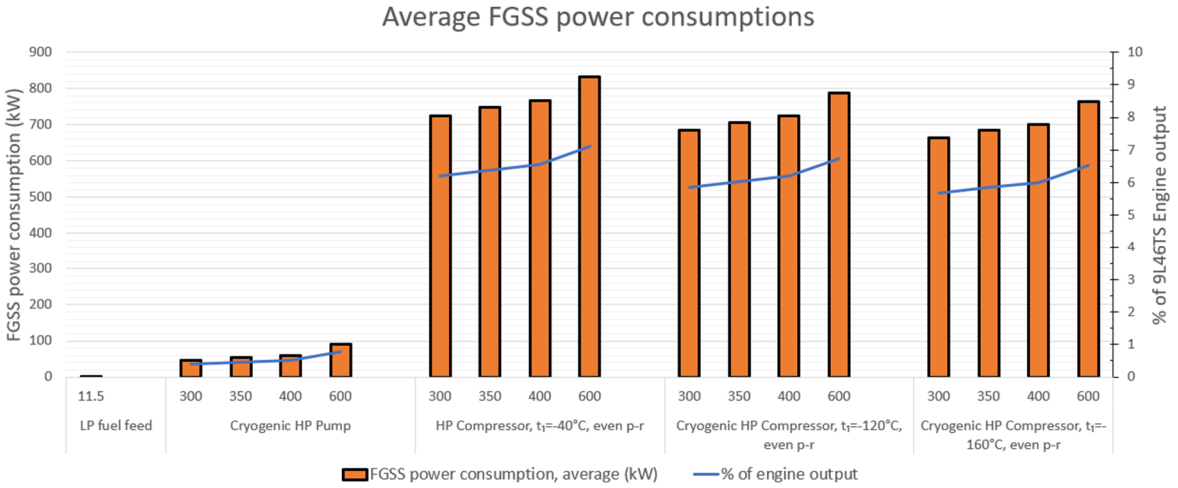

Figure 67. *The FGSS average power consumption as a percentage of the engine output achieved with the fuel feed.*

Both compression and pumping cases require external heating or cooling. With the pumping, the heating power is brought into the system in the HP evaporator. In the case of the compressors, the cooling power is needed in the intercoolers of the compressors. Heating energy needs are smaller for the pump, but the overall efficiency of the heating/cooling will depend on where the heating and the cooling can be taken from. If a side stream of something else can be used, the actual power need might not be as significant as stated here.

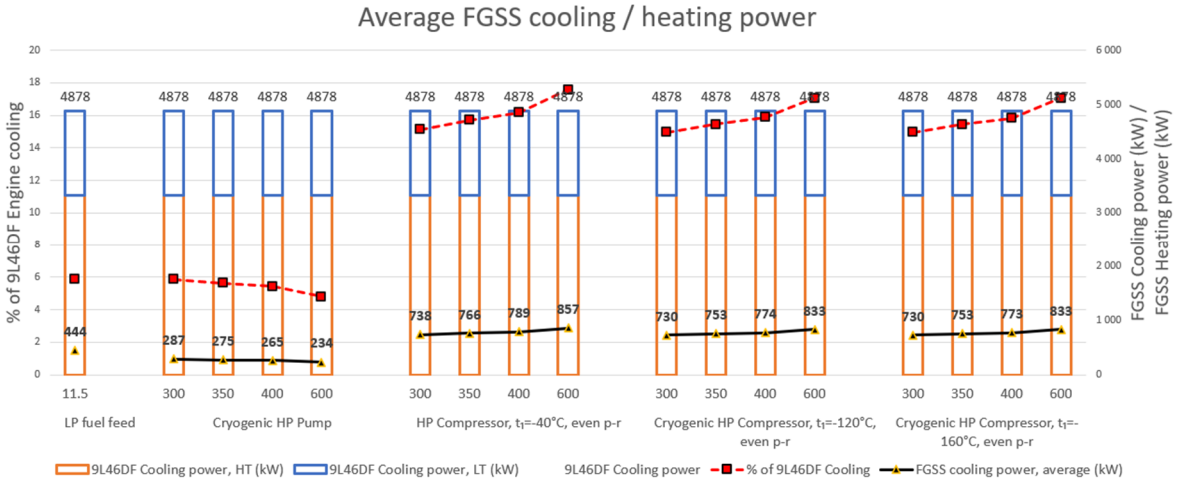

Figure 68. *The FGSS cooling power consumption values averaged for all the fuel compositions calculated, compared to 9L46DF cooling power.*

To get a view on the cooling flows required, the cooling can be compared to for example. a 46DF engine, where the amount of cooling per cylinder is 371 kW in the HT circuit and 174

kW in the low-temperature circuit when a 46DF diesel-electric main engine is operated on gas. So, in total the cooling circuits amount for 545 kW per cylinder. A concrete comparison of the cooling and heating needs is shown in figure 68. As can be seen, the values range roughly from the 5% of the total 9L46DF cooling related to the HP pump to values around 15% to 17% related to the compressors. (Wärtsilä 2019a, p.37)

To evaluate the credibility of the results, the results were compared to manufacturer estimations as well as to some values previously found from literature. A compressor manufacturer provided an estimation of 150 kW nominal shaft power for compressing 400kg/h of 100% CH_4 gas at a suction pressure of 1.1bar and a suction temperature of -40°C, while having a discharge pressure of 351 bar. Using these values in our 5-stage compressor model, we got a value of 142 kW, when the ideal pressure ratios were applied over 5-stages. Based on this, we can assume that we are close enough for rough estimation purposes.

From literature, a presumably somewhat rough estimation of the compressor power compared to the engine output of 46GD is available. From the "Survey of modern power plants driven by diesel and gas engines" by Seppo Niemi, the energy consumption for the compression of the fuel, for a V46GD gas engine, is 2.5% of the shaft output. The inlet gas pressure given for this value is 16 bar, while the closer gas composition or the inlet temperature is not known. (Niemi 1997, p.47)

4.2 "HP-DF" vs "LP-DF"

When comparing the HP-DF versus the LP-DF system, the main points of interests are in the emission levels achievable with both systems. Also, of some interest is the achievable gaseous fuel injection system efficiency as well as the overall engine performance along with the reliability. As a final comparison the capital expenditures (CAPEX) and operational expenditure differences between the two systems are looked at on a general level.

On a general scale the emissions between LP-DF and HP-DF systems have been predicted to be roughly as shown in figure 69, where the 4-stroke GD values are on the right with values picked from several studies also shown in the figure. These values are picked from a couple of different sources, where DF engine gas operation emissions have been compared with the emission levels, when distillate fuel is used in a marine diesel engine.

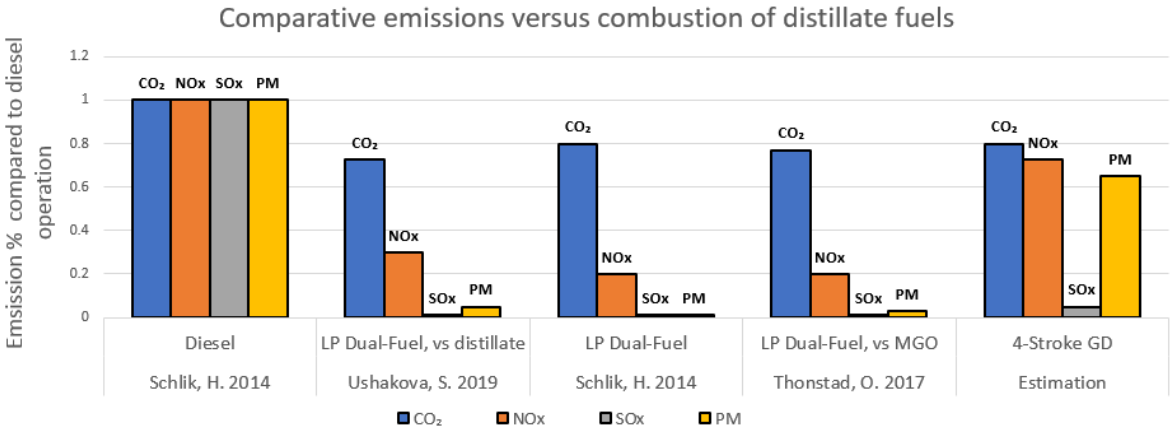

Figure 69. *Emission levels, on a general scale, of different fuel injection technologies compared to emission levels related to the combustion of distillate fuel. (Schlik 2014, p.5, Ushakov et al. 2019, p.1313, Stenersen et al. 2017, p.19)*

Both HP-DF and LP-DF CO_2 emissions are reduced when comparing to the usage of distillate fuels. The CO_2 emissions are mainly reduced because of the lower carbon-to-hydrogen ratio of the gaseous fuel, with the reduction being roughly 20% (Stenersen et al. 2017, p.12, Woodyard et al. 2009, p.41). CO_2 emissions can also be reduced with the aid of the higher thermal efficiency of DF engines compared to diesel engines (Woodyard et al. 2009, p.42). For the HP-DF CO_2 reduction estimates of 20-24% versus MGO (Stenersen et al. 2017, p.19) and 20-25% (Ushakov et al. 2019, p.1325) were used as the baselines.

Another consequence of the fuel choice is the low level of sulphur emissions from DF engines. As LNG does not contain sulphur, the sulphur emissions of DF engines consist entirely of the pilot fuel contribution. In figure 69 the SOx emissions have been estimated to be 95% lower than when using distillate fuels, based on estimations of a SOx reduction of 90-99% versus HFO (Balcombe et al. 2019, p.76), 95-98% versus diesel fuel (Krivopolianski et al. 2019, p.608) and a reduction of 95-97% versus MGO (Stenersen et al. 2017, p.19).

The HP-DF engines NOx emissions level will not meet IMO Tier III levels but can presumably be in the levels required for Tier II. The NOx emissions are larger than in the LP-DF engine for a couple of reasons. Firstly, the combustion temperature of the diesel process will be higher, as discussed in chapter 2.3.1. Secondly, LP-DF engines can be operated on leaner fuel-air mixtures, which also reduces the temperatures in the cylinder (Ushakov et al. 2019, p.1313). From the NOx emissions point-of-view, the amount of pilot fuel is desirable to be kept as little as possible (Ushakov et al. 2019, p.1313). Considered

HP-DF NOx emission reductions were 25-30% compared to distillate fuels (Ushakov et al. 2019. p.1313), 30-40% compared to HFO, and 25-30% compared to MGO (Stenersen et al. 2017, p.17,19). For LP-DF engines the NOx emission values considered were 75-90% reduction versus diesel (Ushakov et al. 2019, p.1313), 75-90% versus MGO (Stenersen et al. 2017, p.19) and 75-90% versus HFO (Balcombe et al. 2019, p.76)

The PM reduction estimations for LP-DF engines are along the lines of 95-98% (Stenersen et al. 2017, p.19, Krivopolianski et al. 2019, p.608, Schlik 2014, p.5). For the medium speed HP-DF engines the PM reduction estimations are however smaller, with Ushakov and Stenersen estimating an PM emission reduction of 30-40% versus MGO and Krivopolianski an similar figure versus diesel fuel (Ushakov et al. 2019, p.1314, Stenersen et al. 2017, p.19, Krivopolianski et al. 2019, p.608). In figure 69 an estimation of a 35% reduction was used.

A HP-DF engine can be run on higher compression ratios than the LP-DF engine. This will result in an increase in the engine efficiency, especially at lower loads. Another advantage of the HP-DF process is the removal of the knock limit, which for LP-DF engines is closely related to the methane number of the fuel. With a HP-DF engine lower quality gas can be used as a fuel. In figure 70 is an illustration of the methane number variation from various natural gas sources, as well as the global production capacity. The green rectangle shows the amount of gas that could be used as a fuel, if a methane number of 80 is required. The amount corresponds to roughly 40% of the production capacity, as a significant portion of the LNG produced has a low methane number. (MAN ES 2017a, p.6)

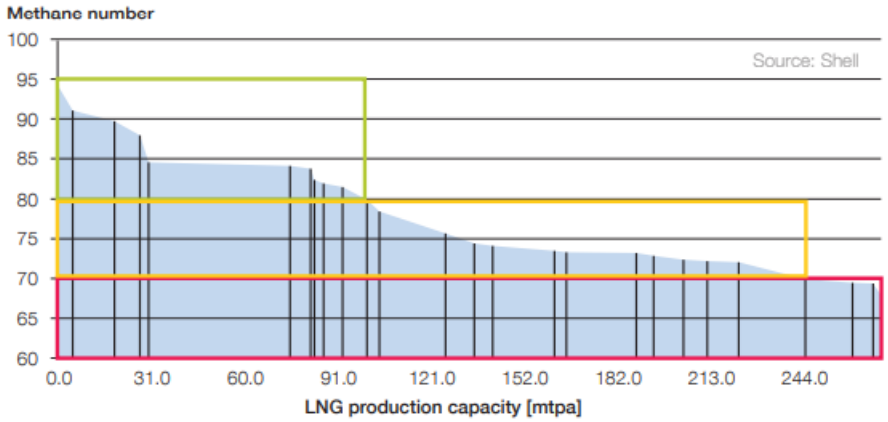

Figure 70. *LNG production capacity and the variation in the methane number. (MAN ES 2017a, p.6)*

The concrete consequence of the differences in the exhaust emissions is that the HP-DF engine will need an SCR reactor or EGR system to comply with IMO Tier III regulations. A Wärtsilä SCR reactor, for lowering the NOx exhaust emissions level from Tier II to Tier III is shown in figure 71 along with other typical exhaust line equipment, such as a boiler and silencer. For a HP-DF engine the standard reactor should be enough. The size of a standard reactor for the engine size considered in this work would be about 3 to 4m long and at the maximum 3 x 3 m in cross-sectional area, with the cross-sectional area depending on the placement of the catalyst layers. (Wärtsilä 2017, p.14-16)

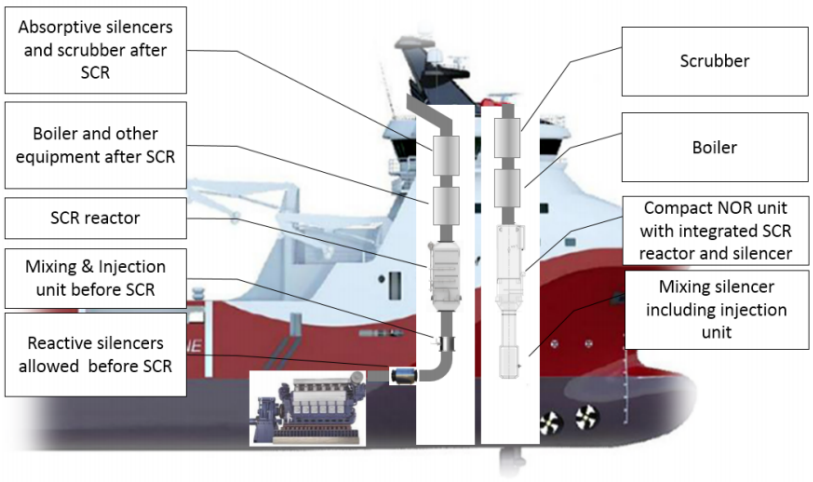

Figure 71. *Two different SCR units, along with typical exhaust line equipment, for reducing the NOx emissions from an engine. (Wärtsilä 2017, p.14)*

Other CAPEX differences between the HP- and LP-DF engines would be the gaseous fuel injection equipment, which can be predicted to be significantly lower for LP-DF engines. For an engine using two-stage turbocharging, the charge air pressure can be at levels of 8 bar. This means that even a LP-DF engine may need a pump or a compressor for pressurizing the gaseous fuel above the pressure in the charge air. The other option for pressurizing the BOG gas is to increase the pressure in the fuel tank, with for example nitrogen injection, to sufficient pressures. The downside of this is that the gas fuel tank construction becomes more complicated. The LP-DF injection pressures are however significantly lower, when compared against the HP-DF pressures required, and as such the prices are not in the same class.

To evaluate the prices, four price comparisons compiled by Win-GD, MAN and SEA-LNG, on the LP-DF and HP-DF CAPEX differences of 2-stroke engines in ships were inspected. The price comparison details can be seen in table 30. The comparisons have been made for

containerships, tankers and car carriers with both reciprocating HP compressors and HP cryogenic pumps represented.

Table 30. *Overview of the HP- and LP-DF cost comparisons. (MAN ES 2020i, p.11, SEA-LNG 2019, p.2,19-20, SEA-LNG 2020, p.2,13-14, Strödecke 2015, p.6,9, WinGD 2020f, p.9)*

	Vessel type	≈ Engine power, kW	DF Type	Engine	HP-DF FGSS	HP-DF Exhaust aftertreatment
WinGD, 2020	55 000 dwt tanker	7 800	HP-DF	6G50ME-C9.5-GI		
	55 000 dwt tanker	7 800	LP-DF	6X52DF	HP Compressor	EGR
	180 000 m^3 LNG carrier	25 000	HP-DF	2 x 5G70ME-C9.5-GI		
	180 000 m^3 LNG carrier	25 000	LP-DF	2 x 5X72DF	HP Compressor	EGR
MAN, 2018	14 000 TEU Containership	46 422	HP-DF	11G90ME-C10.5-GI	HP Pump	SCR-LP
	14 000 TEU Containership	46 422	LP-DF	11X92DF		
	21 000 TEU Containership	63 840	HP-DF	12G95ME-C9.6-GI	HP Pump	SCR-LP
	21 000 TEU Containership	63 840	LP-DF	12X92DF		
SEA-LNG, 2020	14 000 TEU Containership	47 000	HP-DF	ME-GI, Unspecified	HP Compressor	SCR
	14 000 TEU Containership	47 000	LP-DF	9X92DF		
SEA-LNG, 2019	6500 CEU Car carrier	16 660	HP-DF	7S60ME-C8.5-GI	Not stated	SCR/EGR
	6500 CEU Car carrier	16 695	LP-DF	7X62DF		
	8000 CEU Car carrier	19 040	HP-DF	8S60-ME-C8.5-GI	Not stated	SCR/EGR
	8000 CEU Car carrier	19 080	LP-DF	8X62DF		

Regarding the pricing, the major difference was that WinGD stated the gas system price as a whole package, while in the other comparisons the gas system is detailed into smaller pieces. An overview of the gas supply packages is shown in table 31. The LNG carrier cases were left out of the inspection, as the HP gas supply power specific prices were very high and not in-line with the other results. The prices associated to the HP- and LP-DF equipment as well as the power specific prices are shown in figures 72 and 73 below.

Table 31. *HP- and LP gas supply components included in the different comparisons. (MAN ES 2020i, p.11, SEA-LNG 2019, p.2,19-20, SEA-LNG 2020, p.2,13-14, Strödecke 2015, p.6,9, WinGD 2020f, p.9)*

	MAN	SEA-LNG	WinGD
HP Gas supply	PVU price	Total HP Gas supply value given	Total gas system (LP + HP) price given
LP Gas supply	Small LP compressor, booster pump, LP vaporizer, glycol water skid	Total LP Gas supply value given	Total gas system (LP) price given

From the comparisons an average $/kW price for the gas systems can be very roughly estimated. The average price associated to the HP gas system was 40 $/kW, while for the LP gas system an average price of 77 $/kW was calculated. From these values it is important to

note, that in these studies all the vessels with a HP gas system had also an LP gas system. As such, the HP gas system is "added" on top of the LP gas system price, when applicable.

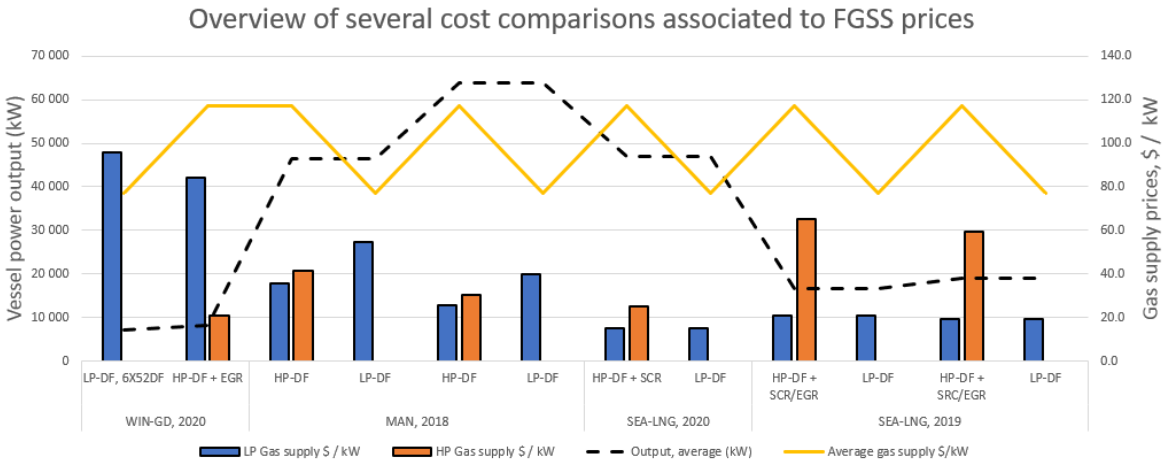

Figure 72.*The $/kW values from several price comparisons, showing the LP and HP gas system prices per kW along with the calculated average value from the studies. (MAN ES 2020i, p.13, SEA-LNG 2019, p.21-22, SEA-LNG 2020, p.2,15, Strödecke 2015, p.9-10, WinGD 2020f, p.9)*

There is some difference in the values of WinGD when compared to MAN and SEA-LNG values, even if the LNG carrier cases are neglected. WinGD average price for HP supply system is 22 $/kW while it is roughly 36 $/kW for MAN and 50 $/kW for SEA-LNG. If the LNG carrier cases were considered, the difference would be bigger, with WinGD average price for HP supply system raising to 145.6 $/kW. In figure 73 below is shown the direct comparison of the prices presented in the cost comparisons.

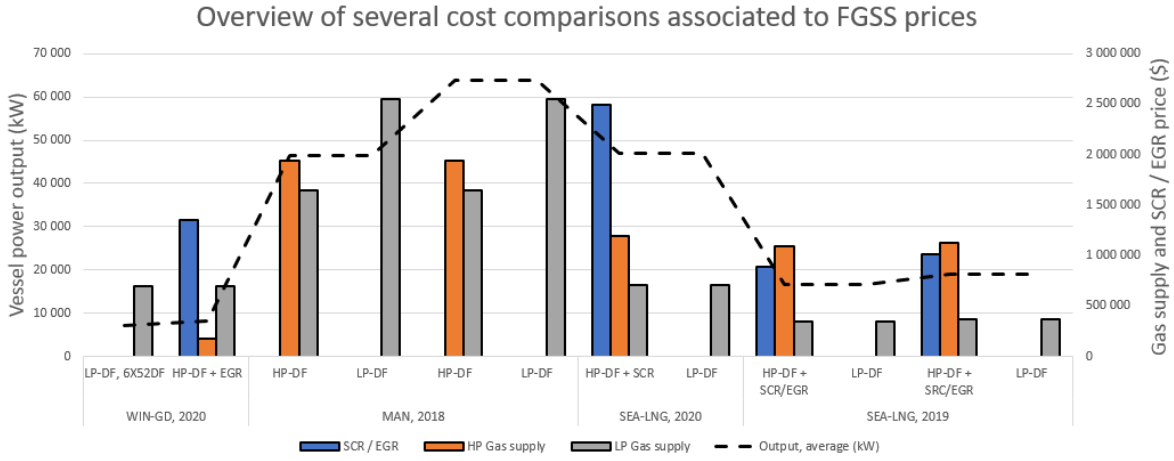

Figure 73. *The prices of HP and LP gas supply as well as of the potential SCR or EGR emission control system. (MAN. 2020i, p.13, SEA-LNG. 2019, p.21-22, SEA-LNG. 2020, p.2,15, Strödecke, D., 2015, p.9-10, WinGD, 2020f, p.9)*

The figures from the price comparisons are available in appendix 11. From the other associated costs, it can be stated that the fuel tank and yard work costs associated to LNG

are significant, with the power specific costs for LNG fuel tanks being 225 $/kW on average in the SEA-LNG and MAN study and 645 $/kW by WinGD. These are however costs independent of the choice of HP-DF or LP-DF engine. On the gas piping there might not be that much difference between HP and LP, as both are double-walled piping, but the HP piping is significantly smaller than the LP piping, perhaps evening out the price caused by the higher pressure. In the price comparison made by MAN, the HP-DF piping work of a containership is roughly 100 000$ more expensive than a similar LP-DF piping.

Operational expenditure (OPEX) differences between the HP- and LP-DF engines are mainly related to the exhaust aftertreatment system and the FGSS power consumption and maintenance, if the fuel costs are not included. The SCR unit needs to be fed with a reducing agent, normally a urea-water solution. This is a constant expenditure. The catalytic elements do not need maintenance, but they will have to be replaced somewhere in between every 4 to 6 years. The FGSS power consumption will be more for a HP-DF system, while the service costs associated with it will most probably also be more. (Wärtsilä 2017, p.11, 14-15)

With regards to reliability, the LP-DF system seems to be a winner with less equipment required than in the HP systems, while the operating pressures of the equipment are lower and at temperatures closer to ambient, which indicates that the equipment operation conditions are not as harsh as on a HP-DF system.

4.3 HP Compressor vs HP pumping

For comparing the three FGSS footprints and masses for the calculation example provided in chapter 3, some equipment estimation can be made. As shown in tables 23 and 25, the average mass flows needed will be in the region of 1 800 kg/h for the exemplary 9L engine. For the HP pump, for example ACD´s SGV 1.625x1.38, with a maximum output of 2565 kg/h, could be chosen. For the HP compressor, Burckhardt MHP compressors with an output of roughly 900 kg/h per unit could be chosen, but two would be needed to provide sufficient amounts of fuel. For cryogenic compressors the comparison is a bit unfair, as a cryogenic compressor could be used to feed two engines of this size. Nevertheless, for footprint comparison, a cryogenic compressor with an output of 5200 kg/h is plotted on the graph. The FGSS power consumptions are shown for the 9L engine output of 11 700 kW.

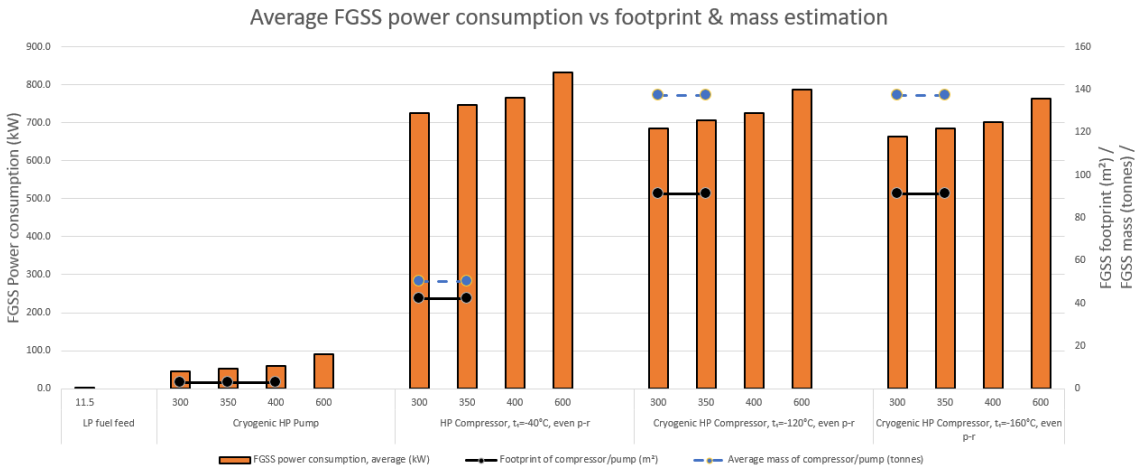

Figure 74. *The FGSS power consumption for the 11 700* kW *output versus roughly estimated compressor - and pump footprints and masses. Missing footprints/masses indicate that the product is not available at the pressure at the moment, based on the literature review.*

Even though the comparison of HP pumps is a bit unfair against compressors, the above figure shows that HP compressors tend to be quite big in size. From a dimensioning perspective, modular HP pumps are easier to fit for a specific fuel feed flow.

For the evaluation of costs associated with HP compression versus HP pumping there was not a lot of data available. Of the data available, the HP pumps seem to have a more favorable capex price per produced mass flow. In figure 75 can be seen a comparison of the prices for producing mass flow. For comparison purposes, the indicated volumetric flow of the HP pumps has been converted into a mass flow by using an average density of 450kg/m³ for LNG. For the cryogenic Laby-GI compressor, an estimation of 1.1 me is made based on the SEA-LNG estimation presented in the previous chapter, with dollars changed to euros.

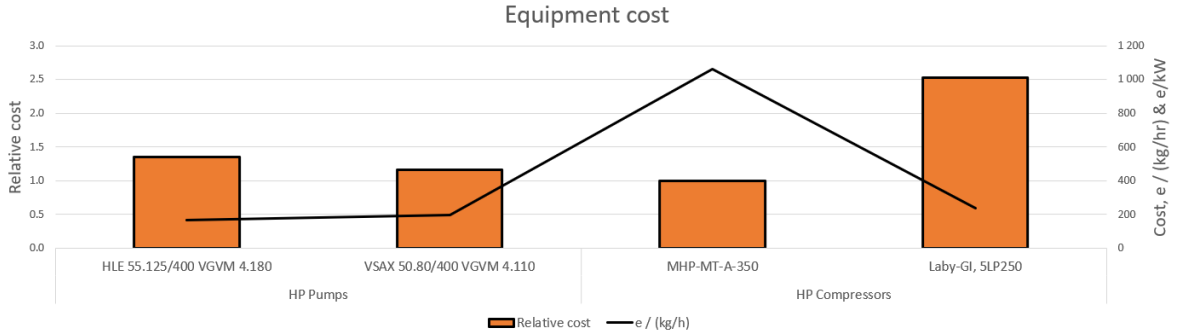

Figure 75. *Comparison of equipment cost, along with an estimated price of euros for kg/hour of mass flow capacity of the unit.*

Due to the different functioning philosophies of pumping and compressing, there are big differences in the footprint sizes and masses. In figure 76 is shown a comparison of the mass

flows produced along with the rough estimate of the equipment footprint as well as the mass. The compressor footprint is significantly larger than for pumps. On the mass side the difference is not that big. Also plotted in the figure is the 9L required mass flow.

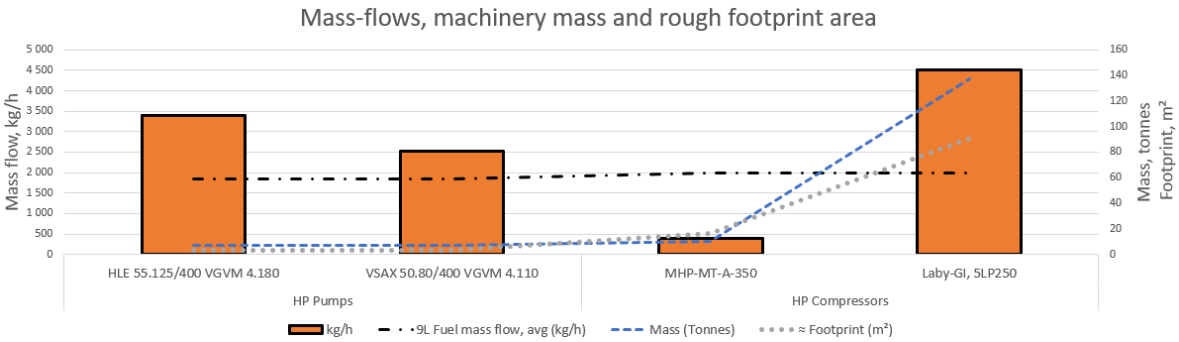

Figure 76. *Comparison of FGSS mass flows and the needed mass flow on the 9L engine, along with the equipment mass and - footprint.*

In addition to the fuel feed system main components, such as the pump and the compressor, also other components will be needed, such as heat exchangers and booster pumps. Naturally, this will increase the price of the package. From the available cost comparisons, the total add-on price of a HP-injection system was between 20 to 50 $/kW. The closer inspection of the price of the auxiliary equipment has been left out of the scope of this work, due to a lack of data. The needed equipment can be seen in table 32.

Table 32. *The additional equipment needed for HP compressors and cryogenic HP pumps.*

Additional equipment needed	
HP Compressor	**Cryogenic HP pump**
BOG pre-heater	Booster pump for HP pump or similar solution to increase NPSH
Possibly a gas fuel filter before engine	HP Vaporizer before engine

In table 33 are some maintenance outlines picked out from manufacturers. For an estimation of the operating costs for different HP-DF systems, the maintenance costs and the other running costs should be evaluated. In addition to the maintenance costs, there are costs associated to the possibly needed cooling or heating of the fuel. Also, nitrogen purging for the whole fuel system would most probably be needed.

Table 33. *The maintenance outlines related to HP compressors and cryogenic HP pumps. (ACD 2016a, p.10, Burckhardt 2019, p.21, Krytem 2018b, p.2)*

Compressor system	**Maintenance needs**			HP Pump system
Burckhardt – 8 000 hrs	Routine maintenance (inspection, checking)		HP pump, Cold end exchange	ACD – 3 000 to 5 000 hrs Krytem – 1 500 to 4 000 hrs or HC measurement
Burckhardt - 20 000 hrs	Overhaul maintenance		HP pump, warm end main service	ACD – 20 000 hrs Krytem – 40 000 hrs
			Lube oil filters	Yearly

Cryogenic compressors generally have a high availability. As the number of cryogenic compressors increase, also the operability and reliability has increased. For example, for the Laby-GI cryogenic compressors the overhaul of the main mechanical components, such as the main bearings, crosshead and pistons has increased from 16 000 hours in 2014 to 20 000 hours currently. For example, for the 5-stage compressor 5LP250-5B the reliability is calculated to be 98% with 300 000 accumulated operating hours. (Burckhardt 2019, p.21-22)

HP pump maintenance varies by manufacturer. For example, MSP pumps manufactured by ACD have an estimated cold end exchange interval between 3 000 to 5 000 hours. The HP pump cold end refurbishment typically includes the replacement of the cold end package as well as possibly the replacement of other wearing items, such as pistons and guide rings. In total the cold end refurbishment can be done typically in 2 to 8 hours. Other standard maintenance is for example the annual changing of the lube oil filters. The whole pump assembly, including drive end, the gear box and lube oil pumps, has an exchange interval defined to be about 20 000 hours. (ACD 2016a, p10)

4.4 Equipment and layout possibilities

In this chapter the FGSS fuel pressurizing equipment properties along with their volumetric sizes have been compared. For functionality details chapter 2.5 can be referred to. The FGSS flow schemes are according to figure 77. Along with the rough layouts, some of the equipment manufacturers that have been encountered during the writing process are stated. To limit the differing options, the BOG handling has not been illustrated here, even though it is an important part of the whole system. Also, other needed auxiliary equipment, such as nitrogen purging and have been left out to keep the systems relatively simple.

The fuel is pressurized in the FGSS, after which the gas is passed through a gas valve unit (GVU), before the engine. In the GVU the gas is filtered, and the pressure regulated by the engine control system for the required engine load. The different means of pressurizing the fuel gas are shown in the following chapters. (Wärtsilä 2019b, p.78)

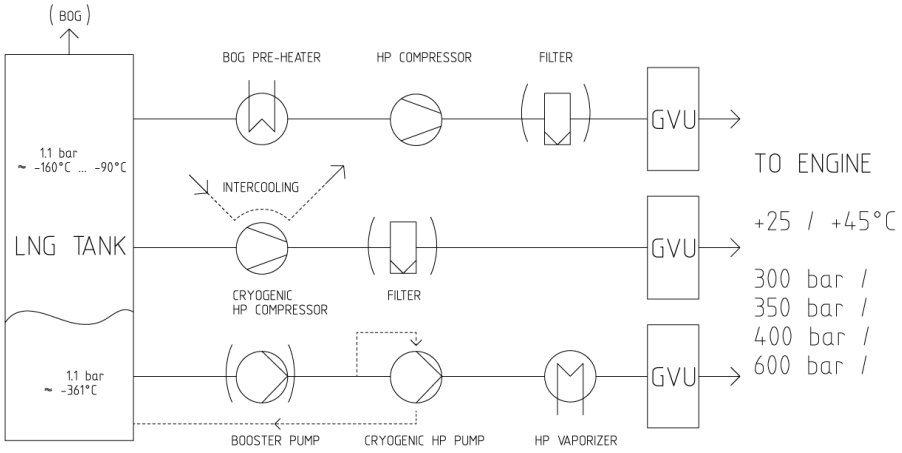

Figure 77. *The FGSS process flow diagrams.*

4.4.1 Cryogenic HP Compressors

In industrial use compressors are often horizontal compressors, mainly due to the fact that piston forces of horizonal compressors can be more easily balanced (Seyama et al. 2018, p.82). In marine applications vertical compressors are favored due to the significantly lower footprint required. The cryogenic compressor footprints are nevertheless quite large. In figure 78 below is shown in orange the volumetric proportions of a cryogenic compressor capable of injection pressures in the range of 350 bar when compared to the 9L engine.

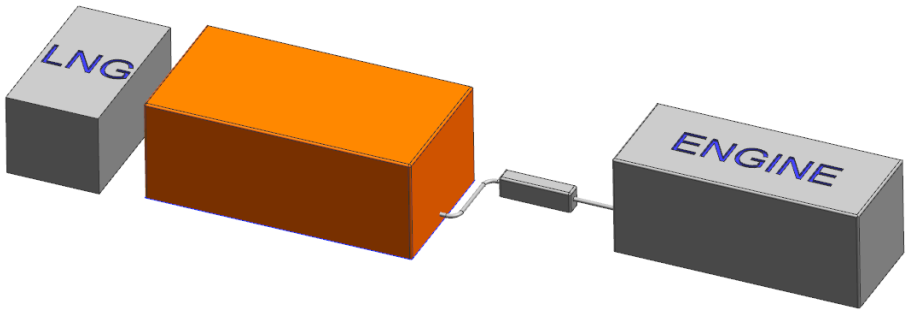

Figure 78. *Layout with a tank, cryogenic HP compressor, the GVU and the 9L engine.*

Cryogenic compressors are able to utilize the BOG directly from the storage tank without pre-heating or other measures. They are specially designed for large fuel tanks, where the amount of BOG can be used for the power consumption of the ship. Cryogenic HP compressors are manufactured at least by Burckhardt and Kobelco. Also, Neumann & Esser have an LNG fuel gas compressor, but not much data was found about the product. No other cryogenic compressor manufacturers, capable of suitable pressures for HP fuel injection, were found during the writing of this work. The most recognized cryogenic compressor is the Laby-GI by Burckhardt. It is available as a non-lubricated compressor to a pressure of 310 bar and to 500 bar, if lubrication is used. In figure 79 is shown a comparison of the flow ranges as well as the maximum pressures of cryogenic – and non-cryogenic HP compressors along with the required flow of the 9L engine.

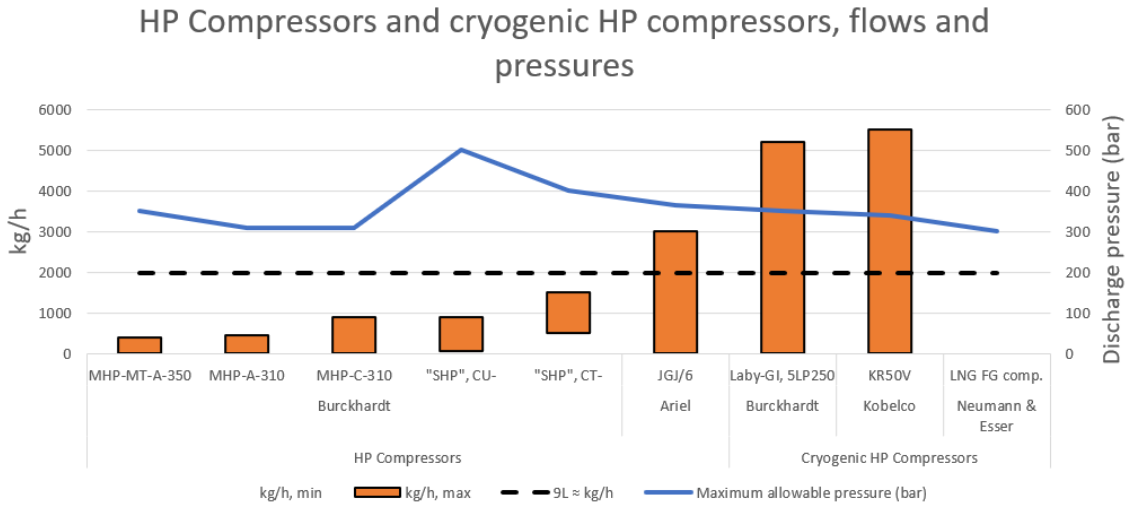

Figure 79. *Rough comparison of some HP compressor and cryogenic HP compressor mass flows and pressures. (Ariel Corporation 2018, p.1, Burkhardt 2017, p.8-9, Burckhardt 2020a, p.8, Burckhardt 2020b, Seyama et al. 2018, p.85)*

In figure 80 below are shown the masses, footprints and nominal shaft powers of the same compressors, for which data was found. The equipment mass and shaft powers should be taken as rough estimations. The final weight of compressors is heavily dependent on the

configuration of the compressor, while the shaft power is linked to the output pressure as well as the gas composition and suction conditions.

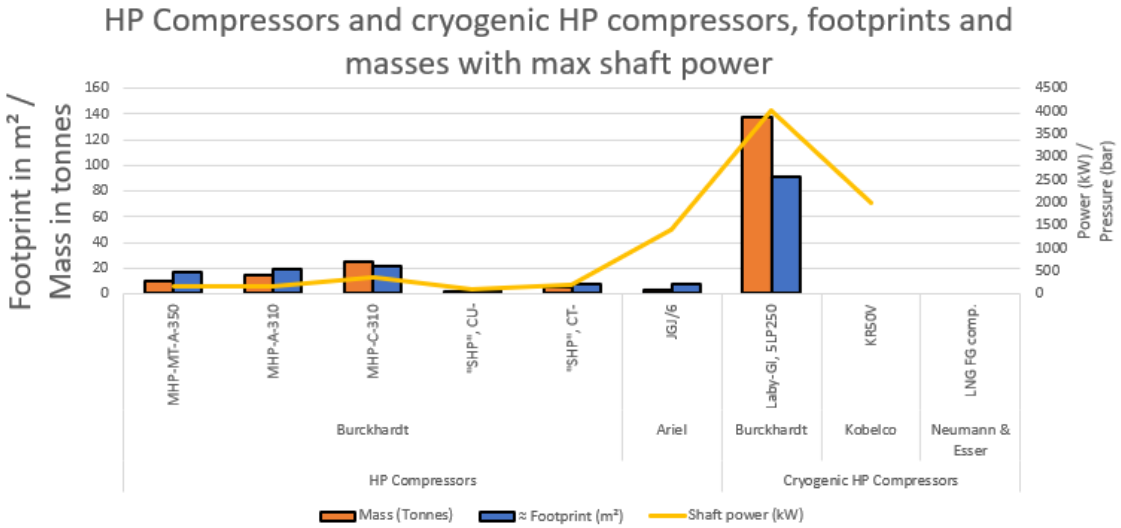

Figure 80. *Comparison of HP compressor and cryogenic HP compressor footprints, masses and maximum shaft powers. (Ariel Corporation 2018, p.1, Burkhardt 2017, p.8-9, Burckhardt 2020a, p.8, Burckhardt 2020b, Seyama et al. 2018, p.85)*

4.4.2 Cryogenic HP Pumps and HP vaporizers

Cryogenic HP pumps can be used to raise the pressure of the fuel with relatively low power consumption, when comparing to HP compressors. For the HP fuel to be usable on the engine, it must be heated to sufficient temperature and to a gaseous state. The general layout is shown in figure 81. There are many manufacturers of cryogenic HP pumps. During this work manufacturers such as ACD, Cryomec, Cryostar, Daewoo Shipbuilding & Marine engineering, Krytem, Mitsubishi Heavy Industries, IHI Rotating Machinery Engineering and Vanzetti have come across in the literature and various news articles.

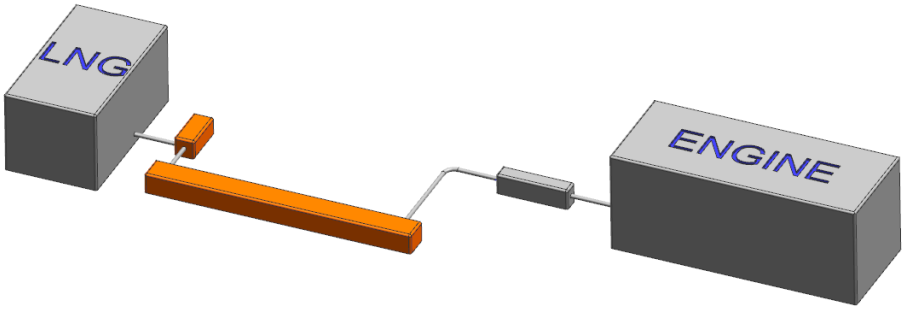

Figure 81. *Layout with cryogenic HP pumps, a HP vaporizer and the GVU.*

In figures 82 and 83 below are shown some of the products from these manufacturers that could be feasible for an LNG FGSS. When inspecting the data in these figures, it is good to note that the data is based mainly on commercial brochures, and as such should be treated

with a degree of reservation. Also, especially the powers will depend on the medium to be pumped as well as on the pressure and flow levels. For pump selection the most important criteria, other than reliability, is the achievable min and max pressures and flowrates.

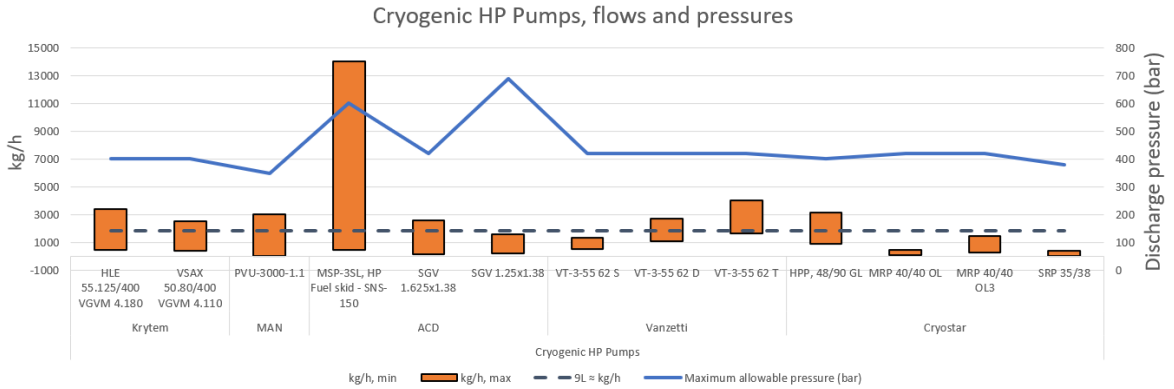

Figure 82. *Rough comparison of some cryogenic HP pump mass flows and pressures. Where applicable, volumetric flow has been turned into mass flow using an LNG density of 450kg/m³. (ACD 2016b, p.8, ACD 2017, p.1, Cryostar, p.7, Krytem 2018a, p.4, MAN ES 2019c, p.7, Vanzetti 2020, p.1)*

Of the cryogenic HP pump manufacturers at least some have experience from marine FGSS systems. For example, ACD has provided cryogenic HP pumps for LNG feeding into ME-GI engines for TOTE Marlin class containerships, with the first FAT being in 2014. The pumps provided have been MPS-3SLH pumps, with an output of 11 m³/h at a discharge pressure of 320 bar (LNG Industry, 2014). Also, Cryostar has a DNV-GL class approved FGSS system designed for LNG injection at roughly 300 bar for ME-GI engines, with a semi-open deck installation expected to function for the vessel lifetime of 40-years. The installation includes two MRP cryogenic HP pumps and a HP CWX vaporizer. Apparently, the operation has been quite smooth, as an availability rate of 95% has been reported. (LNG Industry, 2019)

In addition to the achievable discharge pressures and volumes, also the footprints and masses are of interest. Compared to HP compressors, the footprints and masses of HP pumps are quite small. Typically, the pumps are available in modules, where 1, 2 or 3 pumps are assembled to the same hot end, as discussed earlier in chapter 2.5.3. The footprint of these pumps is the same whether 1 or 3 pumps are used, as they are mounted on the same skid. In figure 83 are collected the footprints and masses of the pumps. As can be seen from the figure, the typical footprint of the pumps compared is roughly 3m². For some manufacturer's masses, footprints or shaft powers were not found.

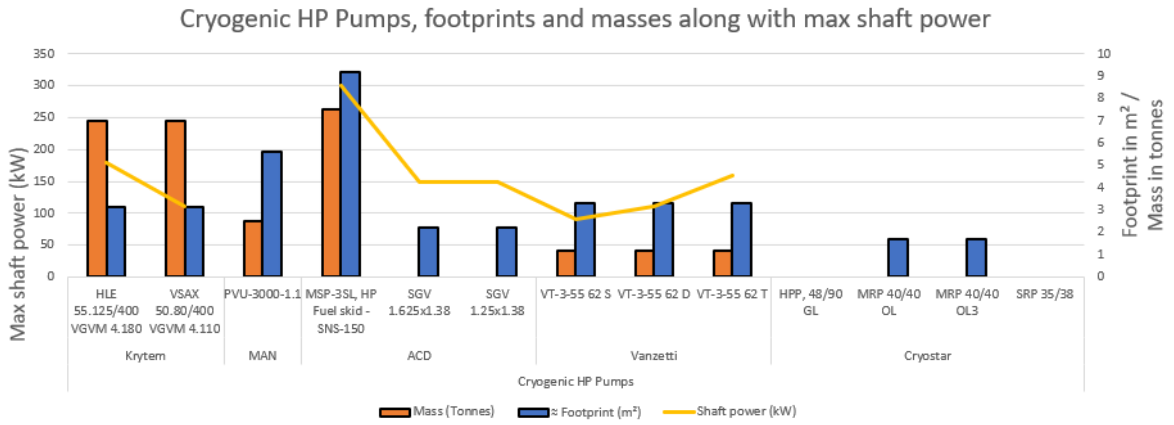

Figure 83. *Comparison of HP pump footprints, masses and maximum shaft powers. Weights are often average skid weights, with final weight dependent on the options chosen. (ACD 2016b, p.8, ACD 2017, p.1, Cryostar, p.7, Krytem 2018a, p.4, MAN ES 2019c, p.7, Vanzetti 2020, p.1)*

After LNG has been pressurized by the pump, it must be transferred to a gaseous phase and heated to such temperatures, that it can be fed into the engine. This can be accomplished with the use of HP vaporizers. HP vaporizers are manufactured at least by companies such as Alfa Laval, DongHwa Entec, Hyundai Heavy Industries, Krytem and Teyco.

4.4.3 HP Compressors

When using non-cryogenic HP compressors, the BOG must be preheated to a certain, manufacturer specific, temperature. These temperatures can be in the range of for example -40°C and higher. Non-cryogenic compressors for BOG handling are often smaller in output than their cryogenic counterparts. There are many manufacturers of non-cryogenic compressors for BOG handling, but when the pressure is raised to 300 bar, the amount starts to decrease. Some of the manufactures along with the rough mass flows and pressure ranges were presented in figure 79, chapter 4.4.1.

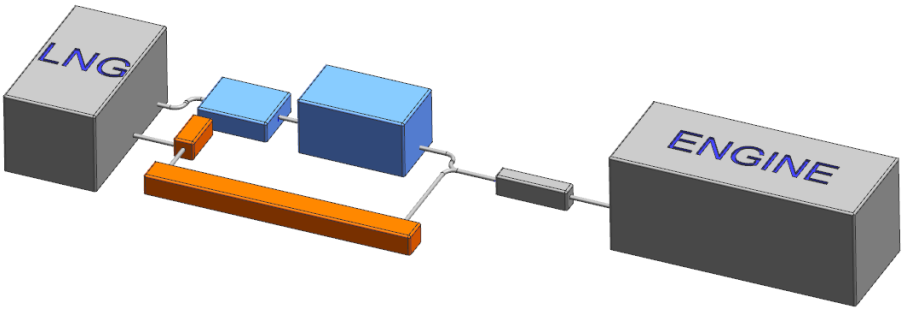

Figure 84. *Layout with a cryogenic HP pump and a vaporizer (orange), as well as a HP compressor with a BOG pre-heater (blue).*

The small output HP compressors are more “off the shelf”, while the higher output HP compressors are somewhat tailored case-by-case. As such there is not a lot of data about the high output HP compressors in figure 79. Some manufacturers of HP compressors include Ariel, GE, LMF, Kobelco and Mitsui Engineering & Shipbuilding. LMF has a wide offering for LNG compression, with maximum pressures in the range of 700 bar. Also Ariel has a couple of compressors, for example in the JGR and JGJ reciprocating gas compressor product family, that are capable of pressures up to at least 420 bar. At higher pressures the compressor cylinders are normally oil lubricated. For example, LMF offers compressors up to 250 bar with oil-free compression.

To be able to use simpler compressors, the FGSS compression system could also be built up of parallel compressors. For example, Burckhardt provides “standard” CC, CU and CT high-pressure compressors, which are available both as air and water cooled. The mass flows produced with these are relatively small, but with the application of four of the largest standard compressors, CT-compressors, in parallel, the output will be roughly equal to a large Laby-GI compressor output. (Burckhardt 2020a, p.8)

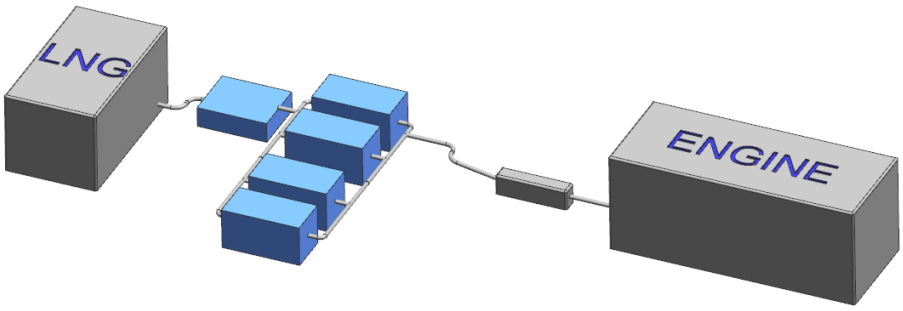

Figure 85. *Layout with four parallel HP compressors and a BOG pre-heater.*

The parallel compressing system is claimed to have a comparable, or even slightly lower power consumption when compared to the usage of a single cryogenic Laby-GI compressor (MAN-ES 2017a, p.11-12). Parallel compressors are advantageous from a redundancy point-of-view. With proper control, there could be good possibilities to improve the part load efficiency by running a fewer number of compressors at higher loads. Even with parallel operation, the compressors must have VFD controlled electric motors. But by having to buy for example 4 relatively small electric motors and VFD´s, the total price could still be lower than when having to buy a single large motor. As a downside the maintenance cycle of the CT-compressors are shorter. This combined with the fact that the number of compressors is

significantly more, means the amount of maintenance needed will also be large. (MAN-ES 2017a, p.11-12)

4.5 Sensitivity analysis

The calculation results sensitivity analysis can be separated to two different sets of results, namely the results related to the HP compressor - and the HP pump model. For both models the compression power requirements were inspected while fuel inlet temperatures and mass flows were varied.

For the HP compressor model, the power needed to compress the gas was inspected while the gas inlet temperature and mass flows were varied over a large range. The gas inlet temperature was varied from -170°C to -40°C, as shown in figure 86. As can be seen, the compression power rises as the BOG temperature raises, which can also be seen in the results section. In total the power consumption is raised from roughly 700 kW to 760 kW, so all in all not a very significant jump. At cold enough temperatures, where the medium to be compressed becomes liquid, the compressor will not work. In this inspection 100% methane was inspected, which liquefies at roughly -161°C. When inspecting the HP compressor power consumption as a function of the mass flow, the dependency can be seen to be linear, as is expected. In figure 86 mass flows from 1 000 to 5 000 kg/h are shown.

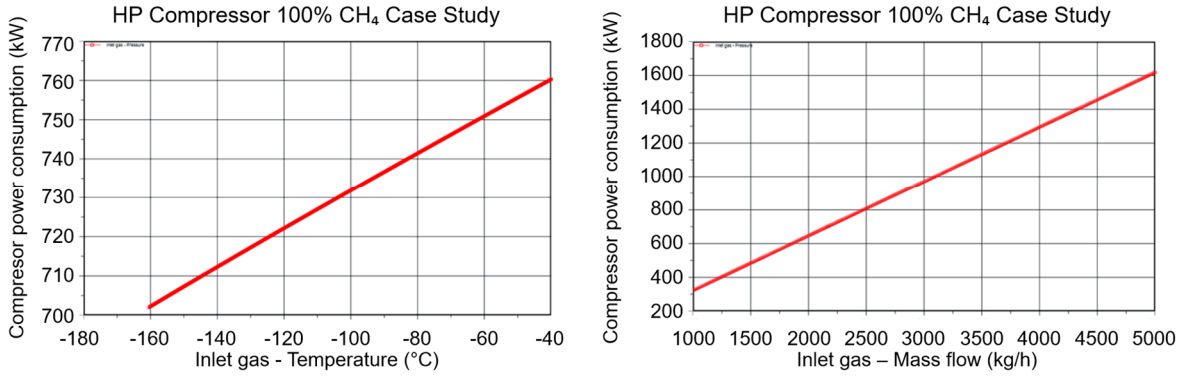

Figure 86. *Compressor power consumption versus the temperature of the BOG on the left side and the created mass flow on the right side.*

On the HP pump side, the power needed to pump the fuel was inspected while varying the fuel inlet temperatures and pressures. In figure 87 the LNG suction temperatures effect on the required pumping power is shown, in this case for the “average” composition. The required pumping power is almost constant, as long as the medium to be pumped remains in a liquid state. At a temperature of 160.5°C the required pumping power is 91.9kW while at

-170°C the corresponding power is 87.2kW, only a 5% difference. The noticeable jump in the required power happens after the medium to be pumped starts to turn into vapor and gas phase, with the critical temperature of the average composition being roughly -160.0°C.

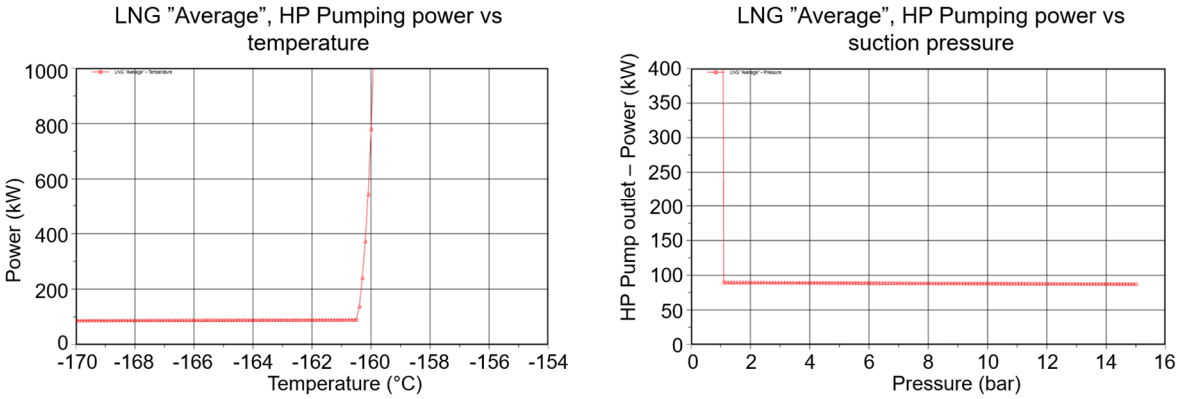

Figure 87. *Pumping power versus suction temperature on the left and suction pressure on the right, for LNG "average" composition.*

The effects of the pressure of the medium at the inlet of the pump can be seen in figure 87. Here also the critical point is clearly visible. With the suction temperature being constant at -161°C, resulting in a critical pressure of roughly 1.1 bar. As the pressure rises from this point, also the pumping power very slowly decreases from roughly 89kW at 1.101 bar to 87.4 kW at 15bar. From this it can be concluded that the inlet pressure does not have a significant effect on the required power as long as the pressure-temperature combination is such, that the medium remains in liquid state.

When inspecting the required pumping power versus the created mass flow, a linear curve from roughly 49 kW at 1000 kg/h to 243 kW at 5000kg/h can be observed, as would be anticipated.

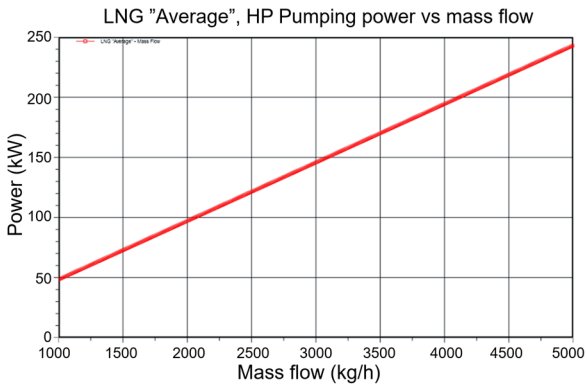

Figure 88. *Pumping power versus mass flow, for LNG "average"*

5 CONCLUSION

The aim of this thesis was to evaluate the technical and economical consequences related to the utilization of HP gas injection instead of LP gas injection, in a compression ignited 4-stroke DF engine. On the technical side both LP-DF and HP-DF engines have been proven to be technically feasible. The FGSS complexity is larger on the HP-DF engines, with the handling of high-pressure cryogenic fluids and gases causing their own challenges. For the HP-DF FGSS two alternative methods of fuel pressurization, namely compression or pumping were inspected. Both methods have been proven feasible on the field, but there are significant differences between them.

When comparing the pumping and compression pressurizing processes, several differences can be stated. The pressurizing of the fuel gas with a compressor is a reliable method, with availability values in the range of 98% reported in this work. Especially for the larger compressors, the maintenance schedule is favorable when comparing to cryogenic HP pumps. The cryogenic HP pumps consume less power during the fuel pressurization while having a superior footprint and mass compared to HP – and cryogenic HP compressors. The negative side of the cryogenic HP pumps is the maintenance schedule, with the cold end of the pumps having to be replaced roughly between 3 000 to 6 000 hours of operation, depending on the manufacturer. Due to pump design, the change is not very time consuming, but naturally it creates an additional operating effort and cost. Some pump manufacturers had operational agreements, where the pump manufacturer takes care of the cold-end replacement at given intervals. Both methods of producing HP fuel will have larger operating expenses when compared to the LP-DF process.

If inspecting only the equipment needed for fuel pressurization, the LP FGSS equipment will be cheaper. This was estimated by both HP-DF and LP-DF engine manufacturers. In the cost comparisons, the HP fuel supply system onboard a vessel generated additional cost between approximately 20 to 50 $/kW. However, the comparison becomes more complicated if the whole fuel system is included in the comparison. HP fuel supply can have a positive effect on the fuel tank price, if the fuel tank is not pressurized.

With HP-DF FGSS, the fuel storage can be kept pressureless, as the pumps are needed to pressurize the fuel gas anyhow. With an LP system, the choices are to increase the fuel tank pressure, to a level at which pumping of the fuel gas is not needed, or to use a pump to raise the fuel gas pressure to a sufficient level to allow fuel gas injection into the charge air. With traditional single-stage turbocharged engines, the required LP gas fuel pressure can be achieved with raising the fuel tank pressure, so only an evaporator is needed to gasify the fuel. With two-stage turbocharged engines, where a higher charge air pressure is present, the fuel tank pressure required will be more, if the pressurizing is handled with the fuel tank pressure. The fuel system pressure level will have an effect on the LNG storage system price and complexity, which can start to be significant after some point. For example in the CAPEX comparison of 14 000 TEU containership made by SEA-LNG, presented in chapter 4.2, the LNG fuel tank costs of a HP-DF system represented roughly 42% of the total costs while for the LP-DF case the similar figure was 55% (SEA-LNG 2020, p.15).

When comparing the FGSS efficiency of HP-DF and LP-DF engines, generally it can be stated that the LP-DF engine fuel system will have lower parasitic losses. The power required to pressurize the HP fuel gas ranged from 0.4 to 0.8 percent of the whole 9L engine output, if HP pumping was utilized. For the HP compressors, the corresponding values were between 5.4 and 7.3%. These values can be compared to the pressureless LP-DF FGSS, where the power consumption for the pressurizing of the fuel was in the range of 0.01% for similar output. The fuel pressurization losses of a HP-DF engine can at least partly be compensated with the anticipated higher engine efficiency, especially at lower loads.

In addition to the power consumption of the fuel pressurizing equipment, the FGSS will require external heating or cooling, depending on the pressurization method used. Heating is needed in the case of cryogenic HP pumps. As the fluid to be heated is at cryogenic temperatures, for the intermediate medium same streams could be utilized as are used for example for engine cooling. In average for the 9L engine, both the LP-DF and the HP-DF with HP pumps require heating flows of around 5 to 6% of a 9L engine cooling flow. A system with HP compressors will require intercooling of the compressors, with cooling flow values of around 15 to 18% of a 9L engine cooling flow.

On-engine equipment for the HP-DF engine would present some challenges, mainly related to the cylinder head area. The optimum solution would be to have separate gas – and liquid fuel injectors, but on the 4-stroke engines the space limitations might prevent this. Designing an injector, that could run on full output both in liquid and gas mode might at least require some compromises from both systems. As both the gas and the liquid fuel systems are essentially common rail systems, the placement of accumulator volumes at the injector will be problematic.

On the emission side the HP-DF and LP-DF systems have a trade-off, where LP-DF systems eliminate the NOx emissions to IMO Tier III levels and beyond, but a certain amount of methane slip is created. On the HP-DF side the methane slip is eliminated, but the NOx emissions only satisfy Tier II levels, meaning that additional exhaust aftertreatment systems will be needed with the usage of LNG to comply with Tier III regulations. The emission regulations will most likely have some changes forthcoming during the 2020´s, as the ambition of IMO is to reduce the annual GHG emissions by 50% by the year 2050. Ships built now will constitute to the GHG emissions still in 2050, making flexibility of the system most probably very important. In table 33 is a general level recap of the conclusions discussed above of the three different FGSS methods, with green cells representing the best feature of the three compared systems and red representing the least good.

Table 34. *Summary of the differences between the three considered fuel gas supply systems.*

	LP-DF	HP-DF, with HP Pump	HP-DF, with HP Compressor	note
Technical complexity				
Maintenance		4500 ± 1500hr, cold end	24 000 hr overhaul	
Footprint		2.2 - 3.2 m²	≈ 2 x 8 = 16 m²	of pump / compressor
Mass		7-8 ton	≈ 2 x 5 ton = 10 ton	For 9L46TS
Pressurization power consumption	0.01%	0.4-0.8%	5-7%	of 9L46TS output
FGSS heating/cooling	"Heating" 6%	"Heating" 5-6%	Cooling, 15-18%	of 9L46DF cooling
NOx emissions	Tier III	Tier II	Tier II	
CH_4 engine emissions				
Fuel requirements	min MN80	No MN requirement	No MN requirement	
Price of FGSS		+ 20...50 $/kW	+ 20...50 $/kW	Output of 8 000-64 000 kW
Relative price of pump/compressor		1.0	1.9	For 9L46TS
Relative price of mass flow		X e/(kg/h)	1.3X e/(kg/h)	For 9L46TS e/(kg/h)

To evaluate the possibility of using HP gas supply systems for larger outputs, the consumptions were estimated for three different power outputs. In figure 89 is illustrated the mechanical and cooling power consumptions as well as the pressurizing equipment footprint for outputs ranging from 21 MW to 163.8 MW. Footprints have been calculated for complete units, meaning that all values have been rounded up to the first whole number. The outputs correspond to cylinder amounts of 16, 36, 80 and 126 at an output power of 1300

kW/cylinder. The HP pump footprints and number of pressurization units is based on ACD´s SGV 1.625x1.38 data. For HP compressors, at compressor suction temperature -40°C, is based on both Burckhardt's SHP CT compressors and Ariel's JGJ/6-series data. For the cryogenic compressor, the compressor data is based on Burckhardt's Laby-GI 5LP250. It is worth noting that the usage of a cryogenic compressors for a large plant would not make sense unless LNG is used as the fuel instead of for example grid natural gas for some reason, but it is included in the comparison to illustrate the size difference.

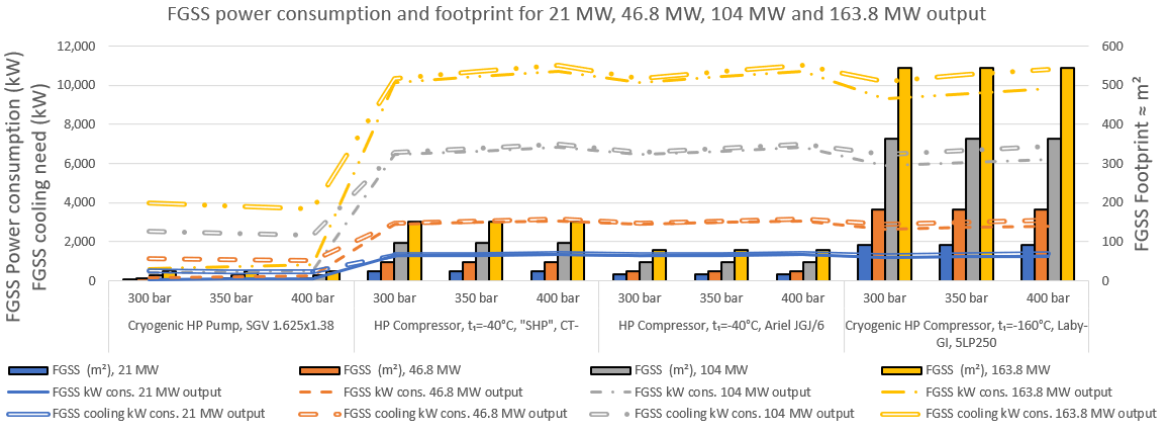

Figure 89. *Extrapolated FGSS power consumptions and footprints for four differing outputs ranging from 21 MW to 163.8 MW*

The number of pumps or compressors needed rises as the power output rises. In figure 90 are shown the number of pumps or compressors needed for the inspected outputs, along with the footprint. For example, for the 164 MW output the compressor footprints are roughly 2 to 3 times more than those of the HP pumps.

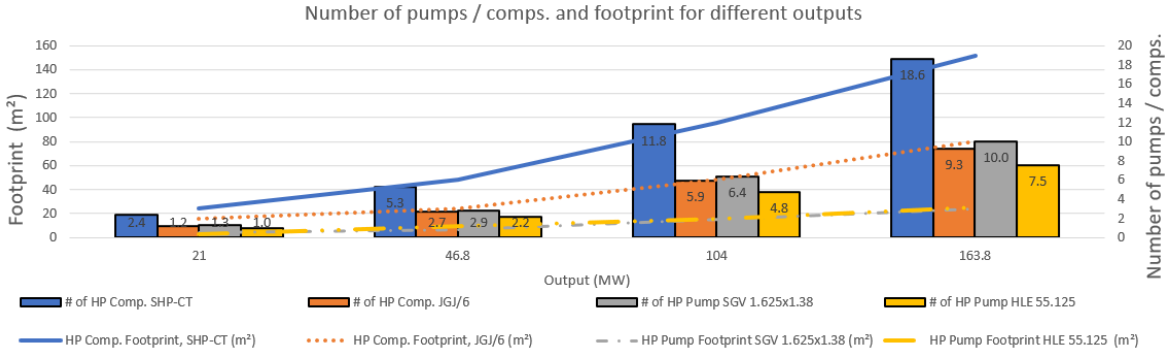

Figure 90. *The number of pumps or compressors needed for different outputs and their footprints.*

It would be important to inspect a plant or an installation from a system perspective. The emissions are a wide issue, resulting from upstream emissions as well as from the final combustion process. The upstream emissions from producing the fuel can be significant.

With the handling and compressing of natural gas, care should be taken to prevent methane from escaping at all processing steps. For example, in a study conducted in 2012 by Johnson et al (2012), the amount of gas turbine emissions from three NG compressor stations and two NG storage facilities in the US was 46% of the total methane emissions of the plants. It is worth noting that in the study 12% of all the methane emissions in the 5 sites measured were due to malfunctioning parts. (Johnson et al. 2012, p.8135)

If inspected the other way, methane should be used as much as possible from processes where it is a by-product or would go to waste otherwise. Examples of such processes are for example from landfills, where methane is created as a byproduct of decomposing. Especially the methane emissions are a popular subject at the moment as for example methane emissions are addressed by fuel manufacturers, such as Shell in their 2020 energy outlook (Shell 2020, p.12), by classification societies such as DNV-GL and Korean Register, and by research organizations and companies such ICCT, SINTEF and Thinkstep. The most efficient ways to cope with methane emissions on-engine are primarily related to combustion process selection. For example, with the application of HCCI or HP-DF the methane emissions could be significantly lowered. Other ways to reduce the methane emissions could be to employ skip-firing, as methane emissions are a problem mostly at low operating loads. An interesting alternative would also be to employ methane oxidizers in the exhaust system, but to date a functioning, commercially available methane oxidizer has not been produced, even though development work is ongoing, as was referenced in chapter 2.3.

Some of the methods foreseen by IMO to enable the reduction of the GHG emissions are for example the usage of wind, solar and even nuclear power. Also, the improvement in the efficiency of the ships has been predicted to constitute a large chunk of the reductions. The fuel selection is another topic which can help reduce GHG emissions. With the ambitious GHG emission reductions, the available fuels will most likely increase, both with biofuels but also other fossil-based fuels. Carbonless fuels, such as ammonia, have already been tested on engines, and expectations are that green ammonia could significantly reduce GHG emissions. Specific fuels maybe used in environments, where they are easily available, as can maybe be seen by the increasing number of engines running on various fuels, such as ethane and ammonia. This in addition to the fact, that the usage of renewable fuels will most likely rise, means that an engine might have to be able to use varying fuels during its lifetime.

An important point would be to create a widely accepted method of evaluating the GHG emissions of for example a specific power plant or ship, as at the moment there seems to be no clear or precise way to compare the effects that solutions have on the GHG emissions.

An advantage of the HP-DF process is that it is less sensitive to fuel variations and can utilize a wider amount of fuels, while being less sensitive to variations in fuel quality. From an engine manufacturer point-of-view the varying fuels should be utilized with as little changes as possible. The expanding fuel pallet might create a larger emphasis on the emissions of the fuel creation than what has been with the traditional fuels. This means that factors such as the conversion efficiency when manufacturing the fuel will start to play a bigger part. From the engine point of view, it is important to have an efficient and flexible method of utilizing the fuels available.

If biofuel availability and price will become competitive with the traditional fuels, there might come a situation where the engine emissions are not really dependent on the engine. If the emissions related to biofuels come almost mainly from the fuel production process, the role of the engine is to convert the fuel to energy efficiently while maybe creating sufficient conditions for the possible exhaust aftertreatment. Without considering the price, virtually zero emissions from the engine can be achieved already today with fuel choice and exhaust aftertreatment. For example, the usage of ammonia produced from renewable sources was in many reports mentioned as one of the most promising alternative fuels for CO_2 neutral shipping, while fuels such as methanol, if produced from renewable sources, would also significantly lower the CO_2 footprint.

Many subjects have been covered in this work starting from the fuel and ending in the emissions. Clearly HP-DF engines have caused interest on the market. This is shown by the number of HP-DF engines as well the number of manufacturers providing equipment to HP-DF FGSS. In addition to the interest on the market, there is also a lot of information and research around the HP-DF engines. As there was a lot of information available, the amount of information covered in this work is also quite large. There were many well written papers covering the subject of LNG usage and the utilization of LP- and HP-DF engines available. The problem in this work has been to summarize the findings from the literature review into a readable and understandable format, while trying to compress the data. As the final piece,

some of the areas that would need to be inspected more closely are gathered into the last chapter.

5.1 Future research

During this work many subjects have been touched upon lightly, and as such there is a decent amount of future research suggestions. On the engine the biggest problems seem to be at first glance at least the lack of space at the cylinder head for the accumulator volumes of both the liquid and the gaseous fuel feed system. A modular solution to this could help the changeover to other fuels as well. Another thing maybe worth thinking about, is if the liquid fuel mode is needed at full output, and if it is not could the common rail system be replaced with something simpler. From a space point-of-view the traditional jerk pump systems would free a lot of space up at the cylinder head. As the application of the HP-DF process would cause an need for exhaust aftertreatment in marine engines to satisfy the Tier III emission limits, the engine features, such as the liquid fuel injection and turbocharging equipment, should be evaluated with the view-point that a SCR unit must be deployed in the exhaust stack or an EGR system be put on the engine alternatively.

An interesting possibility could be if the HP-DF engine would be utilized for land power generation by compressing pipeline natural gas. The advantages would be lower GHG emissions, with the LNG liquefication stage removal decreasing the total CO_2 equivalent emissions. The total decrease would depend on the pipeline transportation distance. From the paper written by Verbeek et al, the removal of liquefication would decrease the CO_2 equivalent emissions by about 5 g CO_2-e/MJ, which is about 22% of the total WTT emissions of LNG produced in Qatar. If for example the worst case WTT value of 10.2 g/MJ from Verbeek et al. for gas transmission of a 7 000 km distance is taken, using the natural gas directly would increase the CO_2 equivalent emissions by 54% when compared to using LNG produced in Qatar. Assuming that the pipeline losses are linear, a transportation distance of 2 000 km would however reduce the well-to-tank emissions to roughly 5.7 g CO_2-e/MJ, which would be roughly 46% smaller than the value for LNG produced in Qatar. Also, the HP-DF engine would be more insensitive to the gas composition, so lower quality gas would also be applicable. Additionally, the HP-DF engine would seem to be well suited for combined heat and power production, as combustion temperatures are higher. The gas compression would consume less power, as pipeline gas is normally at elevated pressures.

Natural gas is not as “pure” as LNG, which could have some effect on the FGSS. Also, the effects of slightly higher NOx emission than LP-DF should be investigated. Here consideration should maybe given to the question, if liquid fuel output is needed at full load, or would a liquid pilot fuel be enough. (Verbeek et al. 2011, p.18-20)

Also, on the HP injection of the gas, alternative pressurization methods could be investigated. The pressurization of the fuel gas or liquid in the injector could prove to be space efficient. The downside to this approach is that the gas fuel must be delivered to the injector in liquid format, to enable pressurization by pumping. Also, here the space restrictions of a 4-stroke engine might become problematic. If both the liquid and gaseous fuels cannot be fitted onto the same injector, then alternative fuel injection positions should be inspected. One possibility could maybe be the feeding of the pilot fuel indirectly through a pre-chamber.

On the FGSS side the part load performance and the means of controlling the fuel pressurization equipment would need to be thoroughly checked. In this work VFD is assumed to be the solution to enable part load performance, with the performance limits coming from the pumps or compressors. From a part-load point-of-view the hydraulically driven HP pump solutions seem like the best choice, as all the pumps can be individually controlled. Other solutions could be larger accumulator volumes or the usage of multiple smaller pressurization units for example. Also, the alternative ways related to BOG handling should be studied in more detail. The most feasible way to deal with BOG seems to vary with the LNG storage tank solution as well as the LNG pressurization method. To get a good overview on the subject, different ship types and fuel storage solutions should be analyzed.

As a last subject the utilization of waste streams is raised. For this the whole ship or plant should be inspected for possibilities. Especially when LNG is used as a fuel, there is need for heating and cooling. This heating and cooling should be made with waste streams as much as possible, to increase the overall efficiency. Also, the cold LNG should be utilized as efficiently as possible. For example, utilization of the BOG for cooling the charge air or the circulation water could be investigated.

LIST OF REFERENCES

Aakko-Saksa, P., Cook, C., Kiviaho, J. Repo, T. 2018. Liquid organic hydrogen carriers for transportation and storing of renewable energy – Review and discussion. Journal of power sources. [Online] Vol. 396, p. 803–823. Available at: https://www-sciencedirect-com.ezproxy.cc.lut.fi/science/article/pii/S0378775318303483?via%3Dihub

Aakko-Saksa, P. & Lehtoranta, K. 2019. Ship emissions in the future - review. VTT Technical Research Centre of Finland. VTT Research Report, No. VTT-R-00335-19. [Online] Available at: https://cris.vtt.fi/en/publications/4e2a27e0-ee41-4bc9-bfe3-6214a3bf71bc

Abdul Karim, Z. & Sulaiman, S. 2018 Alternative Fuels for Compression Ignition Engines. [Online]. Singapore: Springer Singapore.

Abdullah, M., Zen, J., Yusof, M. 2011. Stress Corrosion Cracking, Crack Growth Prediction, and Risk-Based Inspection of Industrial Refrigerated Ammonia Tanks. Corrosion (Houston, Tex.). [Online] Vol. 67 (4), p. 46001–46001–12.

ACD. 2016a. Fuel Supply pumps -LNG, brochure. [online] Available at: https://www.acdllc.com/wp-content/uploads/2016/07/LNG_Bro_Part_3.pdf

ACD. 2016b. Fuel Supply pumps -LNG, brochure. [online] Available at: https://www.acdllc.com/wp-content/uploads/2016/07/LNG_Bro_Part_2.pdf

ACD. 2017 SGV Series. Cryogenic Pump, product brochure. [online] Available at: https://www.acdllc.com/wp-content/uploads/2017/10/SGV_Rev_2017Sep_CURRENT.pdf

Alfa Laval. 2020. Smaller footprint, bigger profit. Alfa Laval printed circuit heat exchanger, product brochure. [online] Available at: https://www.alfalaval.com/globalassets/documents/products/heat-transfer/plate-heat-exchangers/pche/printed-circuit-heat-exchangers-product-brochure.pdf

Agarwal, A., Gautam, A., Sharma, N., Singh, A. 2019. Methanol and the Alternate Fuel Economy. [Online] Singapore: Springer Singapore.

Agarwal, R., Rainey, T., Rahman, S., Steinberg, T., Perrons, R. & Brown, R. 2017. LNG Regasification Terminals: The Role of Geography and Meteorology on Technology Choices. Energies 2017 (ISSN 1996-1073). [online] Available at: https://www.mdpi.com/1996-1073/10/12/2152/pdf

Ahlvik, P. & Jääskeläinen, H. 2020. Natural gas. DieselNet Technology Guide. [online] Available at: https://dieselnet.com/tech/fuel_natural-gas.php

Andersson, K. Salazar, C. 2015. Methanol as a marine fuel report. Methanol Institute. [online] Available at: http://www.ourenergypolicy.org/wp-content/uploads/2015/12/8d318977-2811-4414-a5e1-9652c442c833_0815_MethanolMarineFuel_Report_V15_CM.pdf

Arcoumanis, C., Bae, C., Crookes, R., Kinoshita, E. 2008. The potential of di-methyl ether (DME) as an alternative fuel for compression-ignition engines: A review. Fuel (Guildford). [Online] Vol. 87 (7), p.1014–1030.

Ariel Corporation. 2018. JGR/JGJ. Product Brochure. [online] Available at: https://www.arielcorp.com/content/dam/ariel-corp/documents/product-spec-sheets/JGRJ_10.24.2018.pdf.coredownload.pdf

ASHRAE. 2013. ASHRAE handbook: fundamentals. I-P edition. Atlanta, Georgia: American Society of Heating, Refrigerating and Air-Conditioning Engineers, Incorporation.

Aspen HYSYS V11 Help Manual. 2019 a. [Online help manual]. Updated 27.1.2019. [Referred 21.11.2020]. HSYSY Properties Environment > Setting Up the Properties Environment > HYSYS Property Packages > EOS > Peng-Robinson > Peng-Robinson.

Aspen HYSYS V11 Help Manual. 2019 b. [Online help manual]. Updated 27.1.2019. [Referred 21.11.2020]. HYSYS Simulation Environment > Unit Operations > Rotating Equipment > Design Tab > Parameters Page > Specifying Compressor Parameters.

Bae, C. & Kim, J. 2017. Alternative fuels for internal combustion engines. Proceedings of the Combustion Institute. [Online]. Vol. 36 (3), p.3389–3413.

Bahadori, A. 2014. Natural Gas Processing: Technology and Engineering Design. Oxford: Elsevier Science & Technology.

Balcombe, P., Brierly, J., Lewis, C., Skatvedt, L., Speris, J., Hawkes, A., Staffell, I. 2019. How to decarbonise international shipping: Options for fuels, technologies and policies. Energy conversion and management. [Online] Vol.182, p.72–88.

Berstad, D. et al. 2010. Large-scale hydrogen liquefier utilising mixed-refrigerant pre-cooling. International journal of hydrogen energy. [Online] Vol. 35 (10), p. 4512–4523.

BP. 2020. Statistical Review of World Energy. [online] Available at: https://www.bp.com/content/dam/bp/business-sites/en/global/corporate/pdfs/energy-economics/statistical-review/bp-stats-review-2020-full-report.pdf

Brown, A., Waldheim, L., Landälv, I., Saddler, J., Ebadian, M., McMillan, J. D., Klein, B. 2020. Advanced biofuels – potential for cost reduction. (Task 41: 2020:01). [online] Available at: https://www.ieabioenergy.com/wp-content/uploads/2020/02/T41_CostReductionBiofuels-11_02_19-final.pdf

Burckhardt. 2017. Laby-GI Compressors. Fully balanced reciprocating compressors with highest operational flexibility, Product brochure. [online] Available at: https://www.burckhardtcompression.com/wp-content/uploads/2017/11/bc_bro_Laby-GI_171129_en.pdf

Burckhardt. 2019. New Developments in Piston Compressor Technology Applied to Gas-Fueled, 2-Stroke, ME-GI and X-DF Engines for LNG Carrier Propulsion. [online] Available

at: https://www.burckhardtcompression.com/wp-content/uploads/2019/09/Burckhardt-Compression_Paper_Gastech-2019.pdf

Burckhardt. 2020a. Standard High-Pressure Compressors, Product Brochure. [online] Available at: https://www.burckhardtcompression.com/wp-content/uploads/2020/03/Standard-High-Pressure-Compressors_Original_14759.pdf

Burckhardt. 2020b. MHP Compressor – Technical Data. [Burckhardt webpage]. [Referred 20.11.2020]. [online] Available at: https://www.burckhardtcompression.com/solution/compressor-technologies/marine-high-pressure-compressors/technical-data/

Bureika, M., Matijošius, J., Rimkus, A. 2020. 'Alternative Carbonless Fuels for Internal Combustion Engines of Vehicles', in Ecology in Transport: Problems and Solutions. [Online]. Cham: Springer International Publishing. pp. 1–49.

Campbell, J. 2014. Gas Conditioning and Processing, Volume 2: The Equipment Modules, 9th Edition. Campbell Petroleum Series. Norman, Oklahoma.

Carnival Corporation. 2019. Costa Smeralda: First Lng Refueling in Barcelona. [press release]. 18.12.2019. [online] Available at: https://www.carnivalcorporation.com/news-releases/news-release-details/costa-smeralda-first-lng-refueling-barcelona/

Christensen, P. 2017. Surveyor's day Gard / Norwegian Hull Club – Presentation on MAN ME-dual fuel engines. [online] Available at: http://www.gard.no/Content/24305569/Dual%20fuel%20engines.pdf

Chorowski, M., Deda, P. Polinski, J. Skrzypacz, J. 2015. LNG Systems for Natural Gas Propelled Ships. IOP Conf. Series: Materials Science and Engineering. [online] Available at: https://iopscience.iop.org/article/10.1088/1757-899X/101/1/012089/pdf

CIMAC. 2013. Information Concerning the Application of Gas Engines in the Marine Industry. CIMAC Working Group 17 "Gas Engines". [online] Available at:

https://www.cimac.com/cms/upload/workinggroups/WG17/WG17_Marine_Gas_information_document_FINAL.pdf

CMA CGM. 2020. The CMA CGM Jacques Saade joins the fleet: the first 23 000 TEU container vessel in the world to be powered by liquefied natural gas, news release, 2.9.2020. [online] Available at: https://cmacgm-group.com/en/news-media/The-CMA-CGM-JACQUES-SAADE-joins-the-fleet-the-first-23-000-TEU-container-vessel-in-the-world-to-be-powered-by-liquefied-natural-gas-Primary-tabs

Colson, S., Hayakawa, A., Kudo, T. and Kobayashi, H. 2016. Extinction characteristics of ammonia/air counterflow premixed flames at various pressures. Journal of Thermal Science and Technology. Vol.11 (3). [online] Available at: https://www.researchgate.net/profile/Sophie_Colson/publication/311878031_Extinction_characteristics_of_ammoniaair_counterflow_premixed_flames_at_various_pressures/links/5cdad270458515712ea9bc5d/Extinction-characteristics-of-ammonia-air-counterflow-premixed-flames-at-various-pressures.pdf

Commotti, M. 2015. Hydrogen generation system for ammonia–hydrogen fueled internal combustion engines. International journal of hydrogen energy. [Online] Vol. 40 (33), p.10673–10686.

Cox, G., DelVeccio, K., Hays, W., Hiltner, J. Nagaraj, R. & Emmer, C. 2000. Development of a Direct Injected Natural Gas Engine System for Heavy-Duty Vehicles. National Renewable Energy Laboratory. [online] Available at: https://www.nrel.gov/docs/fy00osti/27501.pdf

Cryostar. Equipment and Solutions, LNG Transportation, Cargo Handling and Fuelling Applications. [online] Available at: https://cryostar.com/datas-pdf/booklet/en/Equipment-and-Solutions-LNG-TRANSPORTATION,-CARGO-HANDLING-AND-FUELLING-APPLICATIONS.pdf

Cryostar. 2009. User´s Manual, Instructions for operation and maintenance of reciprocating pumps for liquefied gases for high pressures, SDPD 30/32-K.

Deb, M., Sastry, G., Bose, P. & Banerjee, R. 2015. An experimental study on combustion, performance and emission analysis of a single cylinder, 4-stroke DI-diesel engine using hydrogen in dual fuel mode of operation. International journal of hydrogen energy. [Online] Vol. 40 (27), p.8586–8598.

DieselNet. 2016. Conference report: 2016 CIMAC Congress. [online] Available at: https://www.cimaccongress.com/upload/program/press/diesel_net_2016_06_28_news__Conference_report__2016_CIMAC_Congress.pdf

DieselNet. 2020. IMO Marine Engine Regulations. [referred 10.9.2020] [online] Available at: https://dieselnet.com/standards/inter/imo.php

DNV-GL. 2019a. Assessment of selected alternative fuels and technologies in shipping, Høvik: DNV-GL.

DNV-GL. 2019b. Comparison of Alternative Marine Fuels. Rev. 3. [online]. Available at: https://safety4sea.com/wp-content/uploads/2019/09/SEA-LNG-DNV-GL-Comparison-of-Alternative-Marine-Fuels-2019_09.pdf

Duan, X., Liu, Y., Lai, M. Guo, G. Liu, J. Chen, Z. Deng, B. 2019. Effects of natural gas composition and compression ratio on the thermodynamic and combustion characteristics of a heavy-duty lean-burn SI engine fueled with liquefied natural gas. Fuel (Guildford). [Online] Vol.254, 115733.

Duebi, R. 2015. Unique reciprocating compressor solution for offshore applications. [online] Available at: https://www.burckhardtcompression.com/wp-content/uploads/2015/11/25_offshore_solutions_e.pdf

Eastop, T., Thomas D. & McConkey, A. 1993. Applied thermodynamics for engineering technologists. 5. ed. Harlow: Longman.

Ernst, P. 2015. High reliability of the Laby® LNG BOG compressor with the unique sealing system. [online] Available at: https://www.burckhardtcompression.com/wp-content/uploads/2015/11/21_lng_e.pdf

European commission. 2020. 2019 Annual Report on CO2 Emissions from Maritime Transport. [online] Available at: https://ec.europa.eu/clima/sites/clima/files/transport/shipping/docs/swd_2020_82_en.pdf

European Industrial Gases Association (EIGA). 2014. Reciprocating Cryogenic Pumps and Pump Installations. IGC Document 159/14/E. [online] Available at: https://www.eiga.eu/index.php?eID=dumpFile&t=f&f=2572&token=1e70b24b51ed7af93a8db24585278269c93a2baa

Fun-sang C., Pereira, N. Kahn, S., Caprace, J. 2019. A review of the use of LNG versus HFO in maritime industry. Marine systems & ocean technology: journal of SOBENA--Sociedade Brasileira de Engenharia Naval. [Online] Vol.14 (2-3), p.75–84.

Flach, B. Lieberz, S. Bolla, S. 2019. EU Biofuels Annual 2019. USDA. GAIN Report number NL9022. [online]. Available at: https://apps.fas.usda.gov/newgainapi/api/report/downloadreportbyfilename?filename=Biofuels%20Annual_The%20Hague_EU-28_7-15-2019.pdf

Flekiewicz, K. Gregorz, K., Pawel, F. 2020. 'The Gaseous Fuels Towards Contemporary Economic and Ecological Challenges', in Ecology in Transport: Problems and Solutions. [Online] Cham: Springer International Publishing. pp. 51–113.

Florentinus, A. Hamelinck, C. van den Bos, A. Winkel, R. Cuijpers, M. 2012 Potential of biofuels for shipping. Ecofys. [online] Available at: http://www.emsa.europa.eu/main/air-pollution/download/1626/1376/23.html

Fredriksen, A. 2019. Researchers investigate mew green fuel for ships. DTU Mechanical engineering. [online] Available at:

https://www.dtu.dk/english/news/Nyhed?id={7CCB5E33-F953-436E-B1A2-579886128C59}

Giampaolo, T. 2010. Compressor Handbook: Principles and Practice. Lilburn: The Fairmont Press, Inc.

GIIGNL. GIIGNL Annual Report 2020. [online] [Accessed 20.9.2020]. Available at: https://giignl.org/sites/default/files/PUBLIC_AREA/Publications/giignl_-_2020_annual_report_-_04082020.pdf

Gingell, L. 2019. MAN Energy Solutions Alternate Fuels for Large Engines, presentation. [online]. Available at: https://mtcclatinamerica.com/documents/cuarto-seminario-nacional/1-5-MTCC-March-2019--Alt-Fuels.pdf

Glassman, I. & Yetter, R. 2008. Combustion. San Diego: Elsevier Science & Technology.

Guo, B. & Ghalambor, A. 2012. Natural Gas Engineering Handbook (2nd Edition). Gulf Publishing Company.

Heywood, J. 1988. Internal combustion engine fundamentals. New York: McGraw-Hill.

Himsen. 2020 Hyundai Engine & Machinery Programme 2020. [online] Available at: http://www.hyundai-engine.com/about/images/EMD_programme.pdf

IEA. 2017. IEA – Biofuels for the marine shipping sector. [online] [Accessed 25 October 2020]. Available at: https://www.ieabioenergy.com/wp-content/uploads/2018/02/Marine-biofuel-report-final-Oct-2017.pdf

IEA. 2019. IEA - The future of Hydrogen. [online]. [Accessed 20 October 2020]. Available at: https://www.iea.org/reports/the-future-of-hydrogen

IGF. 2013. Draft International Code of Safety for Ships Using Gases or Other Low-Flashpoint Fuels.

IRENA. 2019. Hydrogen: A renewable energy perspective. [online] [Accessed 20 October 2020]. Available at: https://www.irena.org/-/media/Files/IRENA/Agency/Publication/2019/Sep/IRENA_Hydrogen_2019.pdf

IMO. 2018. INITIAL IMO STRATEGY ON REDUCTION OF GHG EMISSIONS FROM SHIPS - RESOLUTION MEPC.304 (72). [online] Available at: https://unfccc.int/sites/default/files/resource/250_IMO%20submission_Talanoa%20Dialogue_April%202018.pdf

IPCC. 2014. Climate Change 2014: Synthesis Report. Contribution of Working Groups I, II and III to the Fifth Assessment Report of the Intergovernmental Panel on Climate Change [Core Writing Team, Pachauri R. & Meyer, L. (eds.)]. IPCC, Geneva, Switzerland, 151 pp. [online]. Available at: https://www.ipcc.ch/site/assets/uploads/2018/02/SYR_AR5_FINAL_full.pdf

Jeppesen, M. 2020. MAN ES decarbonization options towards 2050. Prospects for energy and maritime transport in the Nordic Region, Malmø, 26-27.2.2020 [online]. Available at: https://www.itf-oecd.org/sites/default/files/docs/man-es-decarbonisation-options-towards_2050.pdf

Kass, M. et. al. 2018. Understanding the opportunities of biofuels for marine shipping. [online] Available at: https://info.ornl.gov/sites/publications/files/Pub120597.pdf

Kobayashi, H., Hayakawa A., Somarathane, K., Okafor, E. 2019. Science and technology of ammonia combustion. Proceedings of the Combustion Institute. [Online] Vol. 37 (1), p.109–133.

Korean register. 2020. Forecasting the Alternative Marine Fuel Ammonia. [online] Available at: http://www.krs.co.kr/TECHNICAL_FILE/KR_Forecasting%20the%20Alternative%20Marine%20Fuel_Ammonia.pdf

Kramer, U., Ferrera, M. Kunne, H., Moreira, D. Magnusson, I. 2015. Natural Gas / Methane Fuels: European Automotive Fuel Quality and Standardization Requirements.

Krivopolianski, V., Valberg, I., Stenersen, D., Ushakov, S. & Æsøy, V. 2018. Control of the combustion process and emission formation in marine gas engines. Journal of marine science and technology. [Online] Vol.24 (2), p.593–611.

Krytem. 2018a. HLEP / VSAX High Performance Cryogenic Reciprocating Pumps. Product brochure. [online] Available at: http://krytem.de/en/wp-content/uploads/sites/2/2018/08/KRYTEM-HLE-Pumps-R04.pdf

Krytem. 2018b. Low Temperature reciprocating pumps. [online] Available at: http://krytem.de/en/wp-content/uploads/sites/2/2018/08/KRYTEM-Cryogenic-Recip-Pumps-R04-08-18.pdf

Kutz, M. & Reed, R. 2015. Mechanical Engineers' Handbook, Volume 4: Energy and Power. Somerset: John Wiley & Sons, Incorporated.

Lapuerta, M., Agudelo, J. Porok, M. & Boehman, A. 2012. Bulk Modulus of Compressibility of Diesel/Biodiesel/HVO Blends. Energy & fuels. [Online] Vol.26 (2), p.1336–1343.

Laursen, R. 2018. Ship Operation Using LPG and Ammonia as Fuel on MAN B&W Dual Fuel ME-LGIP Engines. Presented 7.12.2018 at the 2018 NH3 Fuel conference. [online] Available at: https://www.ammoniaenergy.org/paper/ship-operation-using-lpg-and-ammonia-as-fuel-on-man-bw-dual-fuel-me-lgip-engines/

LeBlanc, Y., Yu, X. & Zheng, M. 2020. 'High Pressure DME Spray for Compression Ignition Engines', in Complementary Resources for Tomorrow. [Online] Cham: Springer International Publishing. p. 49–62.

Lee, J., Ray, R. Little, B., Duncan, K., Aktas, D., Aldham, A., Davidova, I. & Sulfita, J. 2014. Issues for storing plant-based alternative fuels in marine environments. Bioelectrochemistry (Amsterdam, Netherlands). [Online] Vol.97, p.145–153.

Lindstad, E. & Rialland, A. 2020. LNG and Cruise Ships, an Easy Way to Fulfil Regulations—Versus the Need for Reducing GHG Emissions. Sustainability, Vol.12(5), p.2080. Available at: http://dx.doi.org/10.3390/su12052080.

LNG Industry. 2014. ACD passes FAT for LNG fuel gas pump system. [online] Available at: https://www.lngindustry.com/small-scale-lng/04072014/acd_passes_first_article_test_for_lng_fuel_gas_pump_system_914/

Loyds Register. 2018. World's first LNG-fuelled bulk carrier delivered. [online] Available at: https://www.lr.org/en/latest-news/first-lng-fuelled-bulk-carrier/

Lowell, D. Wang, H. Lutsey, N. 2013. Assessment of the fuel cycle impact of liquefied natural gas as used in international shipping. The International Council on Clean Transportation. [online] Available at: https://theicct.org/sites/default/files/publications/ICCTwhitepaper_MarineLNG_130513.pdf

Lyons, W., Plisga, G. & Lorenz, M. 2017. Standard handbook of petroleum and natural gas engineering. Third edition. Amsterdam [Netherlands: Gulf Professional Publishing.

Martins, J. & Brito, F. 2020. Alternative Fuels for Internal Combustion Engines. Energies (Basel). [Online] Vol.13(16), p.4086–.

Majewski, W. 2012. What Are Diesel Emissions. Revision 2012.08b. DieselNet Technology Guide. [online]

Majewski, W. 2017. Dimethyl Ether. Revision 2017.09. DieselNet Technology Guide. [online]

MaK. 2015a. M46DF Project Guide / Propulsion. [online] Available at: https://s7d2.scene7.com/is/content/Caterpillar/C10859844

MaK. 2015b. M46DF Technical data. [online] Available at: https://s7d2.scene7.com/is/content/Caterpillar/C10752585

MaK. 2016. VM46DF Project Guide / Propulsion. [online] Available at: https://s7d2.scene7.com/is/content/Caterpillar/C10877915

MAN Energy Solutions. 2011. ME-GI/GIE pump vaporizer unit for LNG and ethane. [online] Available at: https://marine.man-es.com/docs/librariesprovider6/Misc/me-gi_low.pdf?sfvrsn=88a750a2_0

MAN Energy Solutions. 2017a. Cost-Optimised Designs of ME-GI Fuel Gas Supply Systems. [online] Available at: https://marine.man-es.com/docs/librariesprovider6/test/cost-optimised-designs-of-me-gi-fuel-gas-supply-systems.pdf?sfvrsn=72fbeca2_6

MAN Energy Solutions. 2017b. ME-GI Pump Vaporizer Unit Marine Systems. [online] Available at: https://primeserv.man-es.com/docs/librariesprovider5/primeserv-documents/me-gi-pump-vaporizer-unit.pdf?sfvrsn=db1afca2_6

MAN Energy Solutions. 2018a. MAN B&W ME-LGIP dual-fuel engines -Dual-fuel technology reshapes the future two-stroke engine operation. [online] Available at: https://www.man-es.com/docs/default-source/marine/5510-0210-00ppr-man-b-w-me-lgip-dual-fuel-engines-web.pdf?sfvrsn=eb5894b7_12

MAN Energy Solutions. 2018b. MAN 51/60DF Project Guide – Marine. Four-stroke dual fuel engine compliant with IMO tier III. [online] Available at https://marine.man-es.com/docs/librariesprovider6/4-stroke-project-guides/man-51-60df-imo-tier-iii-marine.pdf?sfvrsn=ea991bf3_6

MAN Energy Solutions. 2019a. The Flexible Dual-Fuel Solution. [online] Available at: https://www.man-es.com/docs/default-source/marine/me-gigie-pump-vaporizer-unit-for-lng-and-ethane-manpm-00-0580-preview.pdf?sfvrsn=de68c679_8

MAN Energy Solutions. 2019b. Press release. New ME-GA dual fuel gas engine [online] Available at: https://www.man-es.com/docs/default-source/marine/tools/new-me-ga-dual-fuel-gas-engine.pdf?sfvrsn=80aa9ad9_8

MAN Energy Solutions. 2019c. ME-GI/GIE Pump Vaporizer Unit for LNG and Ethane. [online] Available at: https://www.man-es.com/docs/default-source/marine/me-gigie-pump-vaporizer-unit-for-lng-and-ethane-manpm-00-0580-preview.pdf?sfvrsn=de68c679_8

MAN Energy Solutions. 2019d. 0.50% S fuel operation 2020. [online] Available at: https://marine.man-es.com/docs/librariesprovider6/test/0-50-s-fuel-operation.pdf

MAN Energy Solutions. 2019e. ME-GI/GIE pump vaporizer unit for LNG and ethane. [online] Available at: https://www.man-es.com/docs/default-source/marine/me-gigie-pump-vaporizer-unit-for-lng-and-ethane-manpm-00-0580-preview.pdf?sfvrsn=de68c679_8

MAN Energy Solutions. 2020a. Dual-Fuel ME-GI Engines to Power Newcastlemax Bulkers. [online] Available at: https://www.man-es.com/docs/default-source/press-releases-new/20201014_man_es_pr-me-gi-ep-newcastlemaxes_en.pdf?sfvrsn=705c2041_2

MAN Energy solutions. 2020b. MAN L35/44DF Project Guide – Marine. Four-stroke dual fuel engine compliant with IMO tier III. [online] Available at: https://marine.man-es.com/docs/librariesprovider6/4-stroke-project-guides/man-l35-44df-imo-tier-iii-marine.pdf?sfvrsn=ec24359a_8

MAN Energy Solutions. 2020c. Managing Methane Slip. White paper.

MAN Energy Solutions. 2020d. Emission Project Guide. [online] Available at: https://marine.man-es.com/applications/projectguides/2stroke/content/special_pg/PG_7020-0145.pdf

MAN Energy Solutions. 2020e. ME-GI Dual Fuel MAN B&W Engines 2020 [online] Available at:

https://www.corporate.man.eu/man/media/content_medien/doc/global_corporate_website_1/verantwortung_1/megatrends_2/klimawandel/me_gi_dual_fuel_en_01.pdf

MAN Energy Solutions. 2020f. At the Forefront of Green Engine Technology - The MAN B&W ME-GI and ME-LGI dual fuel concepts. [online] Available at: https://marine.man-es.com/docs/librariesprovider6/methanol-campaign/papers/5510-0178-00ppr-high-repro.pdf?sfvrsn=a77b02a2_8

MAN Energy Solutions. 2020g. Using Methanol Fuel in the MAN B&W ME-LGI Series. [online] Available at: https://marine.man-es.com/docs/librariesprovider6/methanol-campaign/papers/5510-0172-00ppr_low.pdf?sfvrsn=f37a02a2_4

MAN Energy Solutions. 2020h. MAN B&W G70ME-C9.5-GI – IMO Tier II Project Guide. [online] Available at: https://marine.man-es.com/applications/projectguides/2stroke/content/printed/G70ME-C9_5-GI.pdf

MAN Energy Solutions. 2020i. MAN B&W ME-GI installation in very large or ultra large container vessels. [online] Available at: https://www.man-es.com/docs/default-source/marine/man-es_b-w-me-gi---installation-in-very-large-or-ultra-large-container-vessels-manpm-00-0507-preview.pdf?sfvrsn=da22ed71_10

MAN Energy Solutions. 2020j. MAN B&W two-stroke engine operating on ammonia. [Online] Available at: https://marine.man-es.com/docs/librariesprovider6/test/man-b-w-two-stroke-engine-operating-on-ammonia_5510-0241-01_web.pdf?sfvrsn=6a88d2a2_6

MAN Energy Solutions. 2020k. MAN B&W G50ME-C9.6-GI-IMO Tier II Project guide. [Online] Available at: https://marine.man-es.com/applications/projectguides/2stroke/content/printed/G50ME-C9_6-GI.pdf

MAN Energy Solutions. 2020l. MAN B&W S70ME-C10.5-GI-IMO Tier II Project guide. [Online] Available at: https://marine.man-es.com/applications/projectguides/2stroke/content/printed/S70ME-C10_5-GI.pdf

MAN Energy Solutions. 2020m. MAN B&W S80ME-C9.5-GI-IMO Tier II Project guide. [Online] Available at: https://marine.man-es.com/applications/projectguides/2stroke/content/printed/S80ME-C9_5-GI.pdf

Maurya, R. 2018. Characteristics and Control of Low Temperature Combustion Engines Employing Gasoline, Ethanol and Methanol. [Online]. Cham: Springer International Publishing.

McAllister, S. Chen, J. & Fernanzed-Pello, C. 2011. Fundamentals of Combustion Processes. [Online]. New York, NY: Springer New York.

McKinlay, C., Turnock, S. & Hudson, D. 2020. A Comparison of hydrogen and ammonia for future long distance shipping fuels. LNG/LPG and Alternative Fuels Conference. London, UK. 29.1-30.1.2020.

Methanol institute. 2018. Renewable Methanol Report. [online] Available at: https://www.methanol.org/wp-content/uploads/2019/01/MethanolReport.pdf

Meriteollisuus. 2013. Shipbuilders describe the process of manufacturing the world's most environmentally friendly passenger ship. [online] Available at: https://meriteollisuus.teknologiateollisuus.fi/sites/meriteollisuus/files/file_attachments/Viking_Grace_ENG_web.pdf

Eriksson, T. & Mäkelä, J. / Meriteollisuus. 2020. Ways to decarbonize shipping. Meriteollisuus ry. [online] Available at: https://meriteollisuus.teknologiateollisuus.fi/sites/meriteollisuus/files/inline-files/Meriteollisuus%20Ry%20-%20Ways%20to%20decarbonize%20shipping.pdf

Michell Instruments. What is Hydrocarbon Dew Point. [online] Accessed 6.11.2020. Available at: http://www.michell.com/us/documents/whtpapers/What_is_Hydrocarbon_DewPoint.pdf

Mokhatab, S., Mak, J., Valappil, J. & Wood, D. 2014. Handbook of liquefied natural gas. Amsterdam: Elsevier/Gulf Professional Publishing.

Mokhatab, S., Poe, W. & Mak, J. 2019. Handbook of natural gas transmission and processing: principles and practices. Fourth edition. Cambridge, MA ;: Gulf Professional Publishing, An imprint of Elsevier.

Mollenhauer, K. & Tschöke, H. 2010. Handbook of Diesel Engines. Berlin, Heidelberg: Springer Berlin / Heidelberg.

The Motorship. 2019. MAN Energy Solutions to introduce PVU to ME-GI Engines. [online] Available at: https://www.motorship.com/news101/lng/man-energy-solutions-to-introduce-pvu-to-me-gi-engines

The Motorship. 2020. MAN Wins LGIP Engine Contract. [online] Available at: https://www.motorship.com/news101/engines-and-propulsion/man-wins-lgip-engine-contract

Myhre, G., D. Shindell, F.-M. Bréon, W. Collins, J. Fuglestvedt, J. Huang, D. Koch, J.-F. Lamarque, D. Lee, B. Mendoza, T. Nakajima, A. Robock, G. Stephens, T. Takemura and H. Zhang, 2013: Anthropogenic and Natural Radiative Forcing. In: Climate Change 2013: The Physical Science Basis. Contribution of Working Group I to the Fifth Assessment Report of the Intergovernmental Panel on Climate Change. Cambridge University Press, Cambridge, United Kingdom and New York, NY, USA. [online] Available at: https://www.ipcc.ch/site/assets/uploads/2018/02/WG1AR5_Chapter08_FINAL.pdf

Neste. 2016. Neste renewable diesel handbook. [online] Available at: https://www.neste.com/sites/default/files/attachments/neste_renewable_diesel_handbook.pdf

Nolan, D. 2015. Handbook of fire and explosion protection engineering principles. 3rd ed. Kidlington, England: William Andrew.

Okubo, M. & Kuwahara, T. 2019. New technologies for emission control in marine diesel engines. Oxford, United Kingdom: Butterworth-Heinemann, an imprint of Elsevier.

Ott, M. 2019. WinGD X-DF: the leading solution for LNG propulsion. CIMAC Cascades 2019. Wuxi, China. 10 – 11.9.2019. [online] Available at: https://www.cimac.com/cms/upload/events/cascades/CASCADES_2019_China/WINGD_SHANGHAI_Marcel_Ott.pdf

Owen, W. 2019. Cryostar develops new FGSS components. LNG Industry [online]. Available at: https://www.lngindustry.com/liquid-natural-gas/30092019/cryostar-develops-new-fgss-components/

Park, J., Choi, I., Oh, J. & Lee, C. 2020. Nitrogen Oxides and Particulate Matter from Marine Diesel Oil (MDO), Emulsified MDO, and Dimethyl Ether Fuels in Auxiliary Marine Engines. Journal of marine science and engineering. [Online] Vol.8 (5), p.322–.

Pinzi, S., Rounce, P., Herreros, J. Tsolakis, A. & Pilar Dorado, M. 2013. The effect of biodiesel fatty acid composition on combustion and diesel engine exhaust emissions. Fuel (Guildford). [Online] Vol.104, p.170–182.

Reference Fluid Thermodynamic and Transport Properties-REFPROP, Version 10.0. 2018. National Institute of Standards and Technology, Standard Reference Data Program. NIST Standard Reference Database 23.

Reiter, A. & Kong, S. 2010. Combustion and emissions characteristics of compression-ignition engine using dual ammonia-diesel fuel. Fuel (Guildford). [Online] Vol.90 (1), p.87–97.

Rolls-Royce. 2018. Bergen B gas engine. [online] Available at: https://bergen.rolls-royce.com/Portals/_default/assets/1/677/139_B35402018RevA.pdf

Rolls-Royce. 2020. Medium-speed generating sets portfolio. [online] Available at: https://bergen.rolls-royce.com/Portals/_default/assets/1/677/252_BookletEdition1-2020.pdf

Riviera Maritime Media. 2013. First order for Laby-GI LNG fuel gas compressor. [online] Available at: https://www.rivieramm.com/news-content-hub/news-content-hub/first-order-for-laby-gi-lng-fuel-gas-compressor-40149

Riviera Maritime Media. 2015. Introducing the world's first LNG-powered container ship. [online] Available at: https://www.rivieramm.com/opinion/opinion/introducing-the-worlds-first-lng-powered-container-ship-35923

Riviera Maritime Media. 2019. Ammonia emerges as clean fuel candidate. [online] Available at: https://www.rivieramm.com/opinion/opinion/ammonia-emerges-as-clean-fuel-candidate-21902

Rutar, T., Lee, J., Dagaut, P., Malte, P. & Byrne, A. 2007. NOx formation pathways in lean-premixed-prevapourized combustion of fuels with carbon-to-hydrogen ratio between 0.25 and 0.88. Proceedings of the Institution of Mechanical Engineers. Part A, Journal of power and energy. [Online] Vol.221 (3), p.387–398.

Sarvi, A., Lyyränen, J., Jokiniemi, J. & Zevenhoven, R. 2011. Particulate emissions from large-scale medium-speed diesel engines: 2. Chemical composition. Fuel processing technology. [Online] Vol.92 (10), p.2116–2122.

Schlapbach, L. & Züttel, A. 2001. Hydrogen-storage materials for mobile applications. Nature (London). [Online] Vol.414 (6861), p.353–358. Available at: https://www-nature-com.ezproxy.cc.lut.fi/articles/35104634#Tab1

Schlick, H. 2014. Potential and challenges of gas and dual-fuel engines for marine application. CIMAC Cascades 2014. Busan, South Korea. 2014. [online] Available at: https://www.cimac.com/cms/upload/events/cascades/cascades_2014_busan/presentations/Presentation_Session2_AVL_CASCADES_Busan_Oct2014_Harald_Schlick.pdf

SEA-LNG. 2019. LNG AS A MARINE FUEL – THE INVESTMENT OPPORTUNITY. SEA\LNG STUDY - NEWBUILD PURE CAR AND TRUCK CARRIER (PCTC) ON PACIFIC AND ATLANTIC TRADE LANES. [online] Available at: https://globalmaritimehub.com/wp-content/uploads/2019/09/SEALNGStudyFINAL2.pdf

SEA-LNG. 2020. LNG AS A MARINE FUEL – THE INVESTMENT OPPORTUNITY. SEA\LNG STUDY - NEWBUILD 14,000 TEU LINER VESSEL ON ASIA-USWC TRADE [online] Available at: https://sea-lng.org/wp-content/uploads/2020/04/190123_SEA-LNG_InvestmentCase_DESIGN_FINAL.pdf

Seyama, K., Tezuka, S., Okuno, T., Nagura, K. & Akamo, N. 2018. Vertical Type Reciprocating Compressor for LNG Boil Off Gas (BOG) Injection. Published in KOBELCO TECHNOLOGY REVIEW NO. 36 NOV. 2018. [online] Available at: https://www.kobelco.co.jp/english/ktr/pdf/ktr_36/081-086.pdf

Shell. 2020. Shell LNG Outlook 2020. [online] Available at: https://www.shell.com/promos/overview-shell-lng-2020/_jcr_content.stream/1584588383363/7dbc91b9f9734be8019c850f005542e00cf8ae1e/shell-lng-outlook-2020-march.pdf

Speight, J. G. 2007. Natural gas: a basic handbook. Houston, Texas: Gulf Pub. Co.

Speight, J. G. 2018. Rules of thumb for petroleum engineers. Beverly, Massachusetts: Scrivener Publishing.

Speight, J. 2018. Handbook of Natural Gas Analysis. Newark: John Wiley & Sons, Incorporated.

Srinivasan, K., Agarwal, A. Krishnan, S. & Mulone, V. 2019. Natural Gas Engines for Transportation and Power Generation. [Online]. Singapore: Springer Singapore.

Stenersen, D. & Thonstad, O. 2017. GHG and NOx emissions from gas fueled engines. SINTEF. [online] Available at: https://midc.be/wp-content/uploads/2018/06/methane-slip-from-gas-engines-mainreport-1492296.pdf

Stojcevski, T. Jay, D. & Vicenzi, L. 2016. Opeartion experience of world's first methanol engine in a ferry installation. CIMAC 2016. Helsinki, Finland. 6 – 10.6.2016.

Strödecke, D. 2015. Low- and high-pressure dual-fuel Technology Evaluation Process; Case Studies for LNG Carriers and Merchant Vessel. Licensees Conference. Interlaken, Switzeland. 6 - 9.9.2015. [online] Available at: https://www.wingd.com/en/documents/general/papers/dual-fuel-technology-selection-(d-stroedecke)/

Tagliaferri, C., Clift, R., Lettieri, P. & Chapman, C. 2017. Liquefied natural gas for the UK: a life cycle assessment. The international journal of life cycle assessment. [Online] Vol.22 (12), p.1944–1956.

Thiagarajan, S. & Seah, R. 2016. 'Liquefied Natural Gas Carriers', in Springer Handbook of Ocean Engineering. [Online]. Cham: Springer International Publishing. pp. 963–984.

Thinkstep. 2019. Life Cycle GHG Emissions Study on the Use of LNG as Marine Fuel. Report Version V1.1 [online]

Tilli, A., Larmi, M. & Kaario, O. 2009. BIOFUELS IN THE FUEL INJECTION SYSTEM OF A SINGLE CYLINDER MEDIUM-SPEED DIESEL ENGINE. [online] Available at: http://www.ffrc.fi/FlameDays_2009/1B/TilliPaper.pdf

Tripathi, G., Nag, S., Dhar, A. & Patil, D. 2017. 'Fuel Injection Equipment (FIE) Design for the New-Generation Alternative Fuel-Powered Diesel Engines', in Prospects of Alternative Transportation Fuels. [Online]. Singapore: Springer Singapore. pp. 387–405.

United Nations Economic Commission for Europe, UNECE, 2013a. Study on current status and perspective for LNG in the UNECE region. Introduction. [online] Available at:

https://www.unece.org/fileadmin/DAM/energy/se/pdfs/wpgas/session/1st_Session_Group_Experts_on_gas/0_-_LNG_Study__Introduction_and_Overview.pdf

United Nations Economic Commission for Europe, UNECE, 2013b. Study on current status and perspective for LNG in the UNECE region. Chapter 2. [online] Available at: https://www.unece.org/fileadmin/DAM/energy/se/pdfs/wpgas/session/1st_Session_Group_Experts_on_gas/2_-_Chapter_2_LNG_Study.pdf

Ushakov, S., Stenersen, D. & Einang, P. 2019. Methane slip from gas fueled ships: a comprehensive summary based on measurement data. Journal of marine science and technology. [Online] Vol.24 (4), p.1308–1325.

Valera, H. & Agarwal, K. 2019. 'Methanol as an Alternative Fuel for Diesel Engines', in Methanol and the Alternate Fuel Economy. [Online]. Singapore: Springer Singapore. pp. 9–33.

Vanzetti. 2020. Cryogenic Reciprocating Pumps for Marine Applications VT-3 Series for Liquefied Natural Gas (LNG). Product brochure. [online] Available at: https://www.vanzettiengineering.com/docs_uploaded/2575-vanzetti_vt3_marine_spec_sheet_en.pdf

Verbeek, R., Kadijk, G., van Mensch, P., Wulffers, C., can den Beemt, B. & Fraga, F. 2011. Environmental and Economic aspect of using LNG as a fuel for shipping in The Netherlands. [online] Available at: https://www.schonescheepvaart.nl/downloads/rapporten/doc_1370359071.pdf

Wik, C. & Niemi, S. 2016. Low emission engine technologies for future tier 3 legislations - options and case studies. Journal of shipping and trade. [Online] Vol.1 (1), p.1–22.

WinGD. 2019. X-DF by WinGD – Green propulsion. [online] Available at: https://www.wingd.com/en/documents/general/brochures/wingd-engine-booklet-2020.pdf/

WinGD. 2020a. Low-speed Engines 2020. [online] Available at: https://www.wingd.com/en/documents/general/brochures/x-df-engines-by-wingd.pdf/

WinGD. 2020b. Marine Installation Manual, X52DF – Issue 2020-07. [online] Available at: https://www.wingd.com/en/documents/x52df/engine-installation/mim/marine-installation-manual-(mim)/

WinGD. 2020c. Press release: WinGD drives sustainable dual-fuel engine performance with X-DF2.0 technology. [online] Available at: https://www.wingd.com/getattachment/2ae9feb2-8f08-45af-a97a-8ce11fb0a983/press-release

WinGD. 2020d. Next-generation technologies to safeguard LNG-fuelled engine investments. [online] Available at: https://www.wingd.com/en/documents/general/papers/next-generation-technologies-to-safeguard-lng-fuelled-engine-investments/

WinGD. 2020e. Flexible Injector to Advance Alternative Fuels Research. [online] Available at: https://www.wingd.com/en/documents/general/papers/fuel-flexible-injector-white-paper-single-pages-web/

WinGD. 2020f. Low-pressure X-DF Engines FAQ. [online] Available at: https://www.wingd.com/en/documents/general/brochures/x-df-faq-brochure/

Winterbone, T. 2015. Advanced Thermodynamics for Engineers. Second edition. Oxford: Elsevier Science & Technology.

Woodyard, D. & Latarche, M. 2009. Pounder's Marine Diesel Engines and Gas Turbines. Oxford: Elsevier Science & Technology.

Wärtsilä. 2009. Wärtsilä 50DF Engine Technology. [online] Available at: http://cdn.wartsila.com/docs/default-source/Power-Plants-documents/w%C3%A4rtsil%C3%A4-50df.pdf

Wärtsilä. 2011. Installation Manual for Wärtsilä 32GD-A.

Wärtsilä. 2015. Cargo handling systems for LPG, LNG, NH_3 & Ethylene. [online] Available at: https://cdn.wartsila.com/docs/default-source/product-files/ogi/gas-cargo/cargo-handling-systems-brochure.pdf

Wärtsilä. 2017. Environmental product guide. [online] Available at: https://cdn.wartsila.com/docs/default-source/product-files/egc/product-guide-o-env-environmental-solutions.pdf

Wärtsilä. 2019a. Wärtsilä 46DF Product Guide. [online] Available at: https://www.wartsila.com/docs/default-source/product-files/engines/df-engine/product-guide-o-e-w46df.pdf?utm_source=engines&utm_medium=dfengines&utm_term=w46df&utm_content=productguide&utm_campaign=msleadscoring

Wärtsilä. 2019b. 50DF Project guide. [online] Available at: https://cdn.wartsila.com/docs/default-source/product-files/engines/df-engine/product-guide-o-e-w50df.pdf?sfvrsn=9

Yang, L. 2015. Ethane as a Cleaner Transportation Fuel. Environmental science & technology. [Online] Vol.49 (6), p.3263–3264.

Zhou, Y., Pavlenko, N., Rutherford, D. Osispova, L. & Comer, B. 2020. The potential of liquid biofuels in reducing ship emissions. ICCT working paper. [Accessed 24 October 2020]. [online] Available at: https://theicct.org/sites/default/files/publications/Marine-biofuels-sept2020.pdf

In figures 91 is shown the price range of some of the alternative fuel production currently, as well as what the price is made up of. As a baseline reference to the figures below, the current fossil fuel price range can be though to be in the regions of 30 to 50 e/MWh. (Brown et al. 2020, p.55)

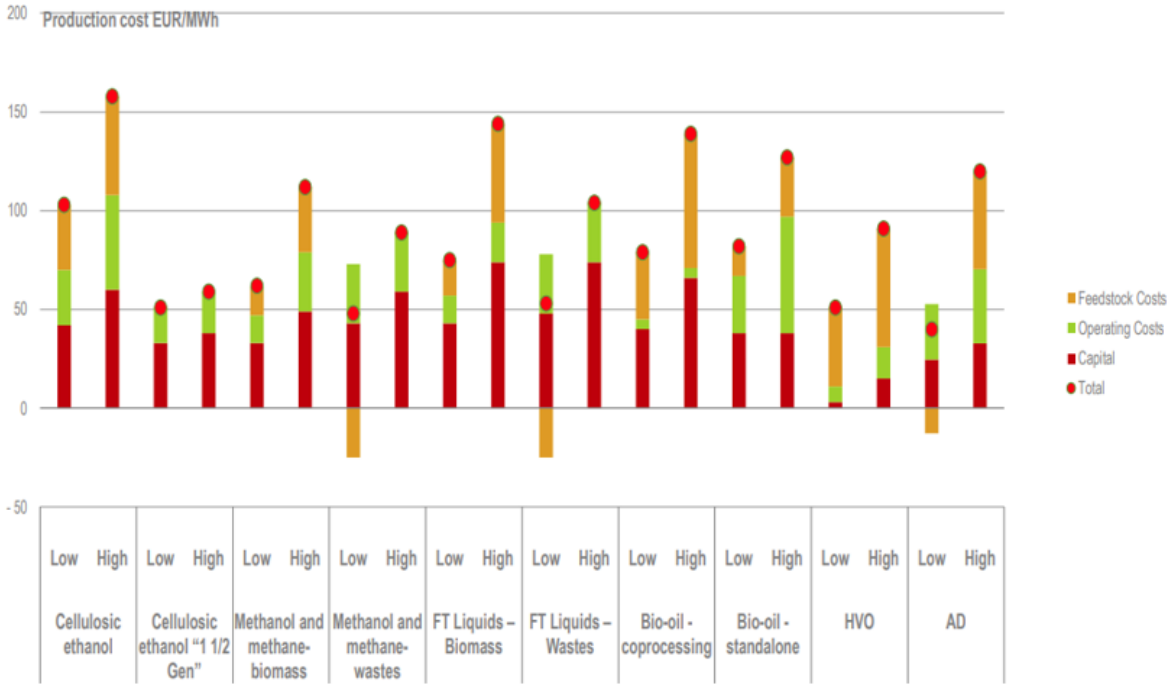

Figure 91. *Current price ranges of alternative fuel production. (Brown et al. 2020, p.34)*

With regards to the production directions, the production processes with the most signed contracts were synthetic fuels via gasification and lignocellulosic ethanol via fermentation. The number of contracts for synthetic fuels via gasification was 18, with the products being fuels such as biomethane, methanol ethanol and DME. Number of contracts for ethanol via fermentation was 14. The production prices are predicted to lower during the next 10 to 15-year period, as production is ramping up and economies of scale start to have an effect. One such prediction is shown in figure 92 below. As can be seen, the cost competitiveness with current fossil fuel prices is difficult. (Brown et al. 2020, p.14-15).

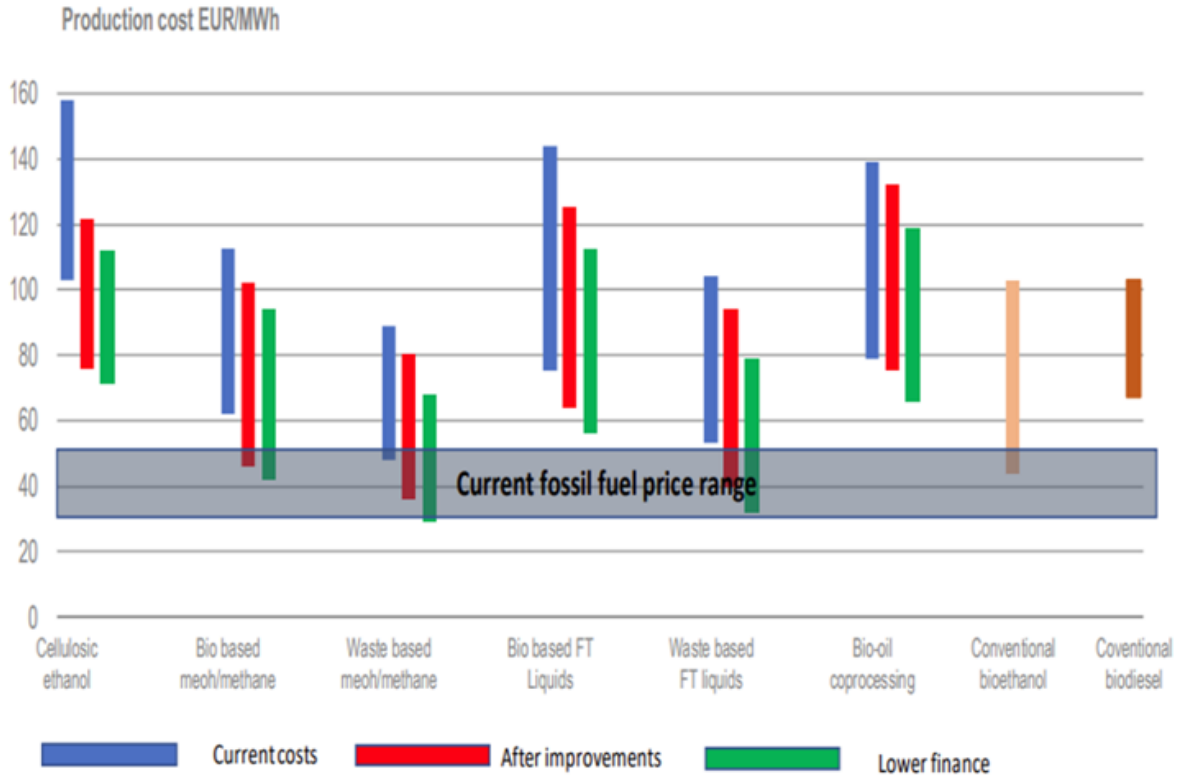

Figure 92. *Projected medium term (10 to 15 years) price ranges of alternative fuel production, with improvements in the range of 10-20% consisting of scale-up and efficiency improvements, excluding cellulosic ethanol with higher potential. (Brown et al. 2020, p.42)*

Hydrocarbons, which provide the heating value of natural gas, are classified by the number of carbon atoms they contain (Speight 2018, p.259). The range is from methane to heavier and longer carbon compositions ending in fuels such as gasoline and diesel. In figure 93 is shown the vapor density ratio and the specific gravity of hydrocarbons found in natural gas.

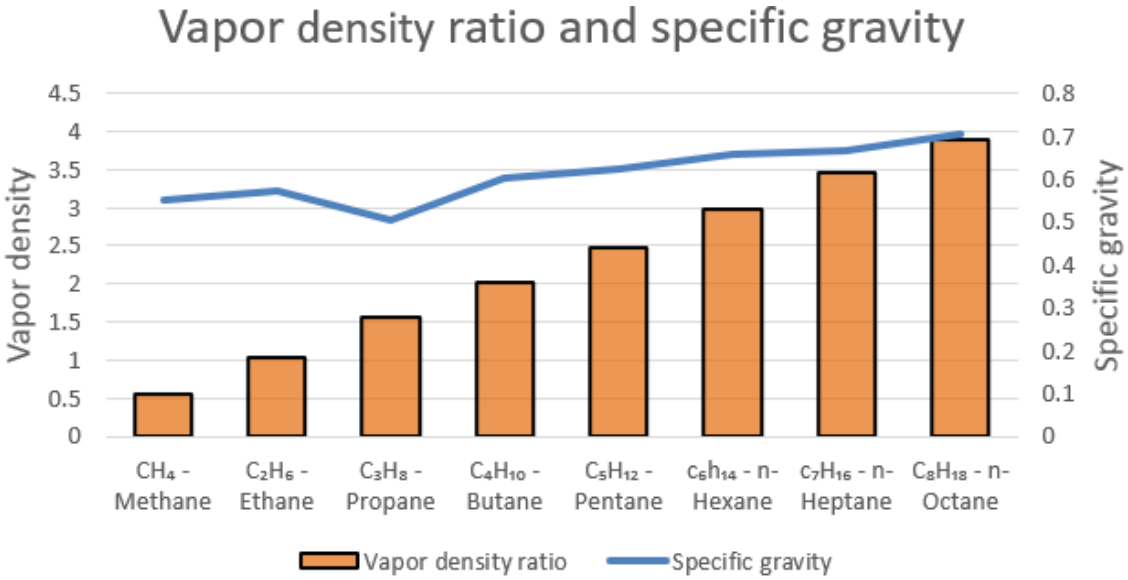

Figure 93. *Vapor density ratio (relative to air at 20°C, atm pressure) and specific gravity of hydrocarbons found in natural gas. (Speight, J. 2007. p.81)*

Other safety and combustion aspects of hydrocarbon include the flashpoint and the ignition temperature. Generally, the ignition temperature decreases as the amount of carbon atoms increases (Nolan, D. 2014, p.60-61).

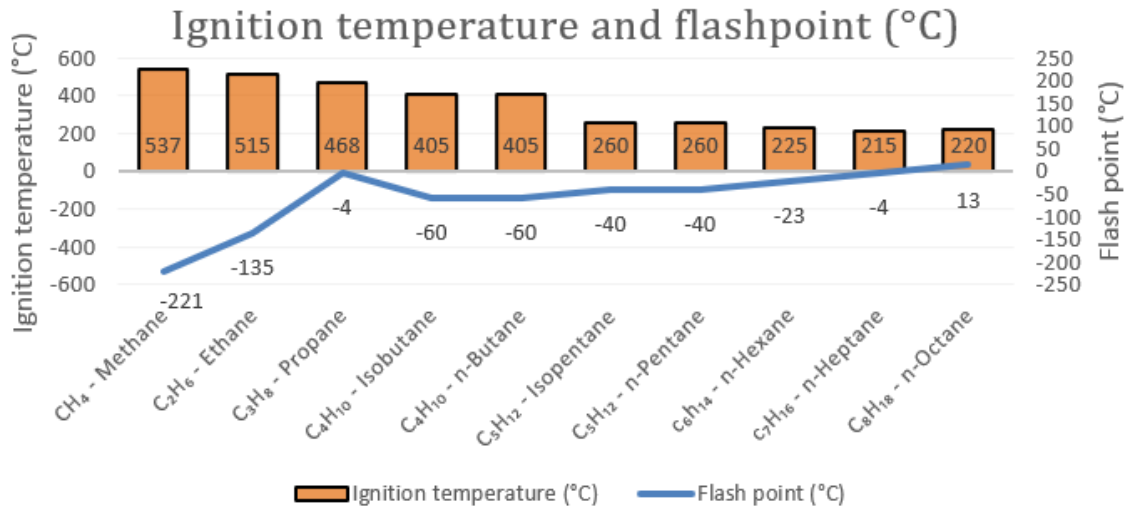

Figure 94. *Ignition temperatures and flash points of hydrocarbons found in natural gas. (Modified from, Speight, J. 2007, p.76,81)*

The LNG value chain can be thought to consist of three different streams, the upstream, midstream, and downstream value streams, as shown in figure 95.

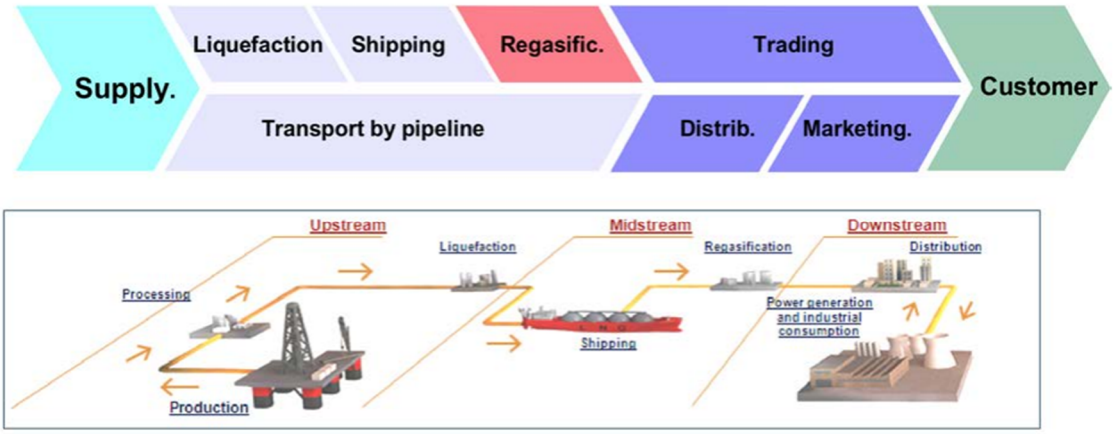

Figure 95. *Natural gas value chains (UNECE 2013b, p.2)*

LNG is primarily produced in huge base load liquefaction plants located near large gas reservoirs is Asia, Australia, the Middle East and West Africa. The base load plants typically have an output from 1.5 MTPA (million tonnes per annum) up to 7.8 MTPA. From the liquefaction plants LNG is shipped to customers, typically quite far away. LNG transportation is typically commercially viable if the transportation distance is over the range of 1 000 km. (Mokhatab et al. 2014, p.10-11)

The liquefication process is based on refrigeration cycles, whereby applying expansion and compression successively heat from the gas stream is removed with a refrigerant. Liquefication is an energy-intensive process, that consumes energy between 275-400 kWh/LNG ton (UNECE, 2013a, p.5). (Mokhatab et al. 2014, p.9, 31)

LNG is transported from the liquefication plants to receiving terminals. In figure 96 are shown the major LNG flows in 2019, as collected by GIIGNL. As can be seen, Qatar is by far the largest exporter of LNG. The four largest exporters, Qatar, Malaysia, Indonesia and Australia, account for 58% of global LNG exports.

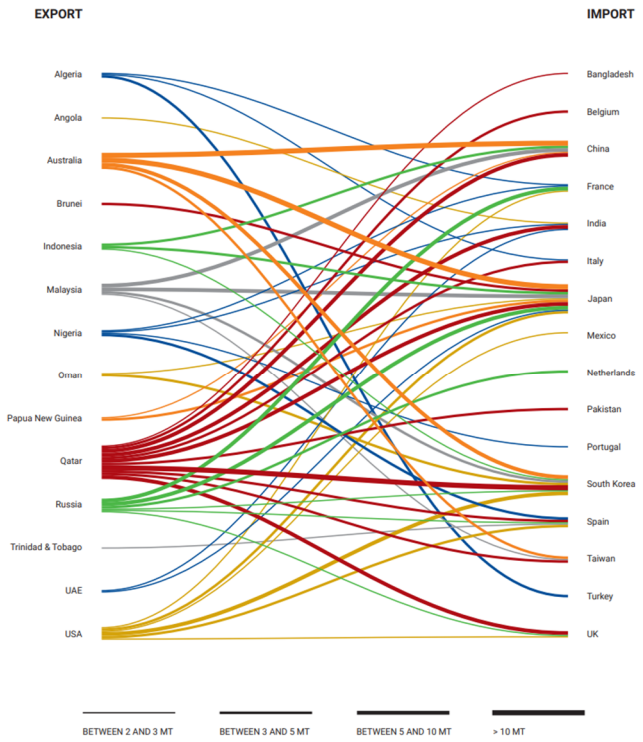

Figure 96. *The major LNG flows in 2019. (GIIGNL 2020, p.37)*

In the receiving terminal the LNG cargo is either put through a regasification process, where the LNG is vaporized to a gaseous state and after this transmitted to near-by customers via pipelines. Alternatively, LNG can also be stored at the receiving terminal before the eventual regasification for commercial use. LNG storage is based on the same insulation principles as the transportation. By using double-walled, insulated tanks the boil-off rate can be kept roughly at a level of 0.1 volume % per day. Normally the LNG storage tanks are sized by the LNG carrier capacity sizes, typically in the whereabouts of 160 000m³. The typical distribution of the capex related to an LNG supply chain is shown in figure X. As can be observed, the majority of the capex is related to the liquefaction of LNG, with shipping and regasification contributing under a quarter. (Mokhatab et al. 2014, p. 27)

Figure 97. *Distribution of Capex in an LNG chain (UNECE, 2013b, p.71)*

As LNG has become a choice of fuel also for vessels other than LNG carriers, also smaller LNG tanks have become prevalent, for example on cruise ships, containerships and bulk carriers. These vessels often use “type C” tanks, that are designed as pressure vessels, so BOG can be handled at least partially by allowing a pressure rise inside the tank, if wanted. (Mokhatab et al. 2014, p.19).

For example, the cruise ship Viking Grace has two 200m³ “type C” vacuum insulated fuel tanks mounted on the stern of the ship, as shown in figure 98 (Meriteollisuus 2013, p.2). Larger cruise ships tend to have larger fuel tanks. For example, the LNG powered cruise ship Costa Smeralda has three tanks with a total capacity of 3 200m³ (2 x 1 525m³ + 520m³), which is roughly enough for 2 weeks of operation (Carnival Corporation, 2019). Also, some bulk carriers have been delivered with LNG propulsion. For example, the 50 000 dwt bulk carrier Green Iris has a single “type C” tank with a capacity of 500m³ (Loyds Register, 2018) while larger containerships, such as the Isla Bella have larger, 2 x 900m³ tanks (Riviera MM 2015). Even though for “non-LNG-carrier” ships the “type C” tank is by far the most popular, not all LNG tanks of these ships are of the “type C”. For example, the 23 000 TEU CMA CGM Jacques Saade has a membrane LNG containment system, with a capacity of 18 600 m³ (CMA CGM, 2020).

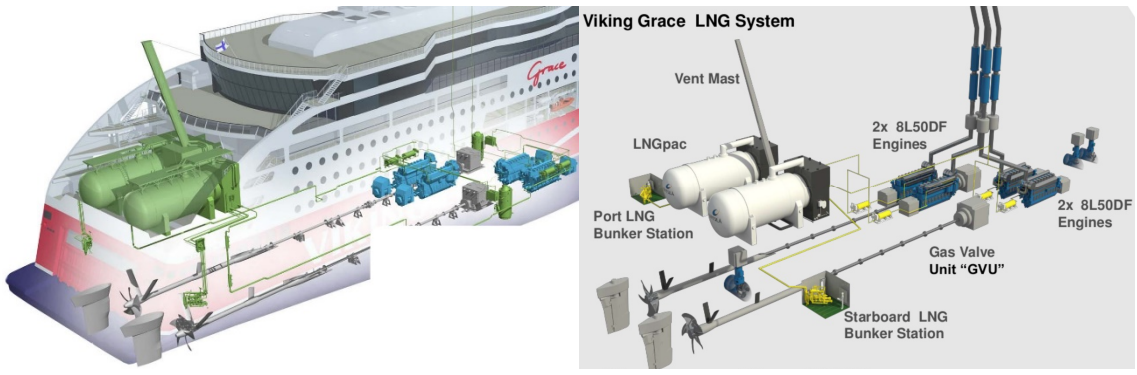

Figure 98. *The main engines and the LNG fuel system aboard Viking Grace (Meriteollisuus 2013, p.4)*

The details as well as the phase envelopes and the phase diagrams of the three LNG composition as well as pure methane:

Table 35. *Details of LNG according to the "Atlantic" specification.*

WÄRTSILÄ

NATURAL GAS CALCULATION **according to ISO 6976:2016**

Made by: rka027
Date and Time: 22-09-20 14:23
Comments: LNG-Atlantic

Project: 46TS GD Thesis
Number: number

ANALYSIS

at metering reference: 0 °C at 101.325 kPa

Substance	Formula	Vol-%	Mol-%	Mass-%
Methane	CH4	95.040	95.000	90.734
Ethane	C2H6	4.567	4.600	8.235
Propane	C3H8	0.373	0.380	0.998
i-Butane	i-C4H10	0	0	0
n-Butane	n-C4H10	0	0	0
i-Pentane	i-C5H12	0	0	0
n-Pentane	n-C5H12	0	0	0
n-Hexane	n-C6H14	0	0	0
n-Heptane	n-C7H16	0	0	0
n-Octanene	n-C8H18	0	0	0
n-Nonane	n-C9H20	0	0	0
n-Decane	n-C10H22	0	0	0
Hydrogen	H2	0	0	0
HydrogenSulfide	H2S	0	0	0
CarbonMonoxide	CO	0	0	0
Oxygen	O2	0	0	0
Nitrogen	N2	0.020	0.020	0.033
Carbon dioxide	CO2	0	0	0
Water	H2O	0	0	0
Helium	He	0	0	0
Argon	Ar	0	0	0
Ethene	C2H4	0	0	0
Propene	C3H6	0	0	0
neo-Pentane	neo-C5H12	0	0	0
Total		100	100	100

CALCULATION RESULTS

at metering reference: 0 °C at 101.325 kPa
and combustion reference: 15 °C at 101.325 kPa

Superior calorific value	molar basis	926.28 kJ/mol	equals	877.94	Btu/mol
Inferior calorific value	molar basis	835.91 kJ/mol	equals	792.29	Btu/mol
Superior calorific value	mass basis	55.146 MJ/kg	equals	23709	Btu/lb
Inferior calorific value	mass basis	49.766 MJ/kg	equals	21396	Btu/lb
Superior calorific value	volum.basis	41.436 MJ/m^3	equals	1112.1	Btu/ft^3
Inferior calorific value	volum.basis	37.393 MJ/m^3	equals	1003.6	Btu/ft^3
Molar mass		16.797 kg/kmol	equals	37.030	lb/kmol
Compression factor		0.9973			
Relative density		0.5811			
Density		0.7514 kg/m^3	equals	0.04691	lb/ft^3
Molar density		44.734 mol/m^3	equals	1.2667	mol/ft^3
Wobbe index		54.357 MJ/m^3	equals	1458.9	Btu/ft^3
Methane number (EN 16726)		87			

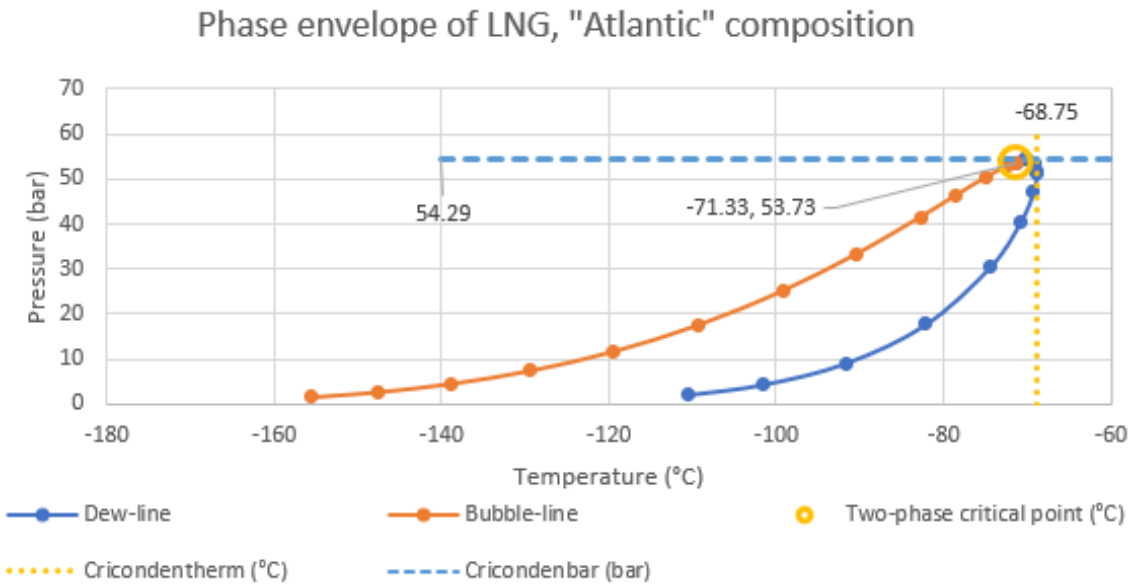

Figure 99. *Phase envelope (Peng-Robinson) of LNG according to "Atlantic" specification.*

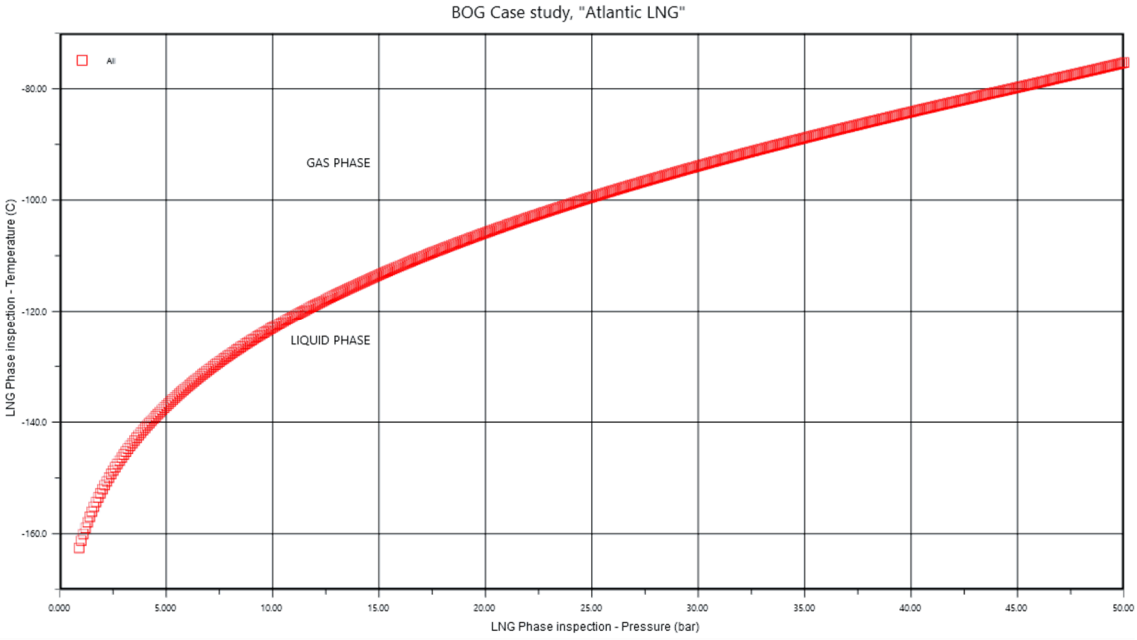

Figure 100. *Phase diagram (Peng-Robinson) of LNG according to "Atlantic" specification, critical point at roughly 54 bar, -71°C.*

Table 36. *Details of LNG according to the "Nigerian" specification.*

WÄRTSILÄ

NATURAL GAS CALCULATION according to ISO 6976:2016

Made by: rka027
Date and Time: 22-09-20 14:23
Comments: LNG-Nigeria

Project: 46TS GD Thesis
Number: number

ANALYSIS

at metering reference: 0 °C at 101.325 kPa

Substance	Formula	Vol-%	Mol-%	Mass-%
Methane	CH4	88.083	87.900	74.217
Ethane	C2H6	5.470	5.500	8.704
Propane	C3H8	3.932	4.000	9.283
i-Butane	i-C4H10	1.211	1.250	3.824
n-Butane	n-C4H10	1.204	1.250	3.824
i-Pentane	i-C5H12	0	0	0
n-Pentane	n-C5H12	0	0	0
n-Hexane	n-C6H14	0	0	0
n-Heptane	n-C7H16	0	0	0
n-Octanene	n-C8H18	0	0	0
n-Nonane	n-C9H20	0	0	0
n-Decane	n-C10H22	0	0	0
Hydrogen	H2	0	0	0
HydrogenSulfide	H2S	0	0	0
CarbonMonoxide	CO	0	0	0
Oxygen	O2	0	0	0
Nitrogen	N2	0.100	0.100	0.147
Carbon dioxide	CO2	0	0	0
Water	H2O	0	0	0
Helium	He	0	0	0
Argon	Ar	0	0	0
Ethene	C2H4	0	0	0
Propene	C3H6	0	0	0
neo-Pentane	neo-C5H12	0	0	0
Total		100	100	100

CALCULATION RESULTS

at metering reference: 0 °C at 101.325 kPa
and combustion reference: 15 °C at 101.325 kPa

Superior calorific value	molar basis	1029.24 kJ/mol	equals	975.54 Btu/mol
Inferior calorific value	molar basis	932.06 kJ/mol	equals	883.43 Btu/mol
Superior calorific value	mass basis	54.171 MJ/kg	equals	23289 Btu/lb
Inferior calorific value	mass basis	49.056 MJ/kg	equals	21090 Btu/lb
Superior calorific value	volum.basis	46.081 MJ/m^3	equals	1236.8 Btu/ft^3
Inferior calorific value	volum.basis	41.730 MJ/m^3	equals	1120.0 Btu/ft^3
Molar mass		19.000 kg/kmol	equals	41.888 lb/kmol
Compression factor		0.9965		
Relative density		0.6579		
Density		0.8507 kg/m^3	equals	0.05311 lb/ft^3
Molar density		44.772 mol/m^3	equals	1.2678 mol/ft^3
Wobbe index		56.814 MJ/m^3	equals	1524.8 Btu/ft^3
Methane number (EN 16726)		64		

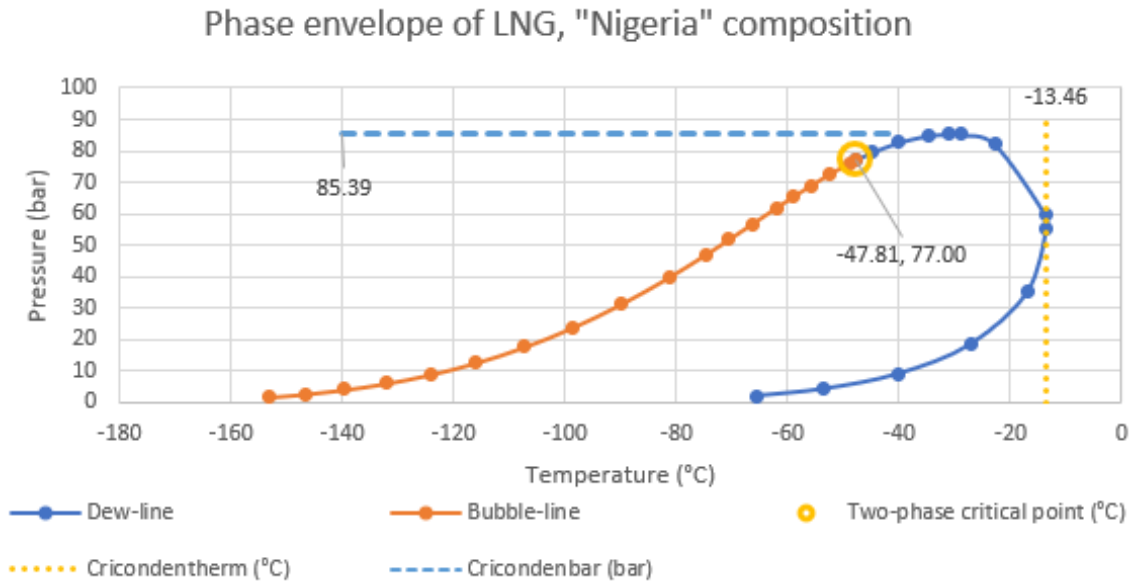

Figure 101. *Phase envelope (Peng-Robinson) of LNG according to "Nigerian" specification.*

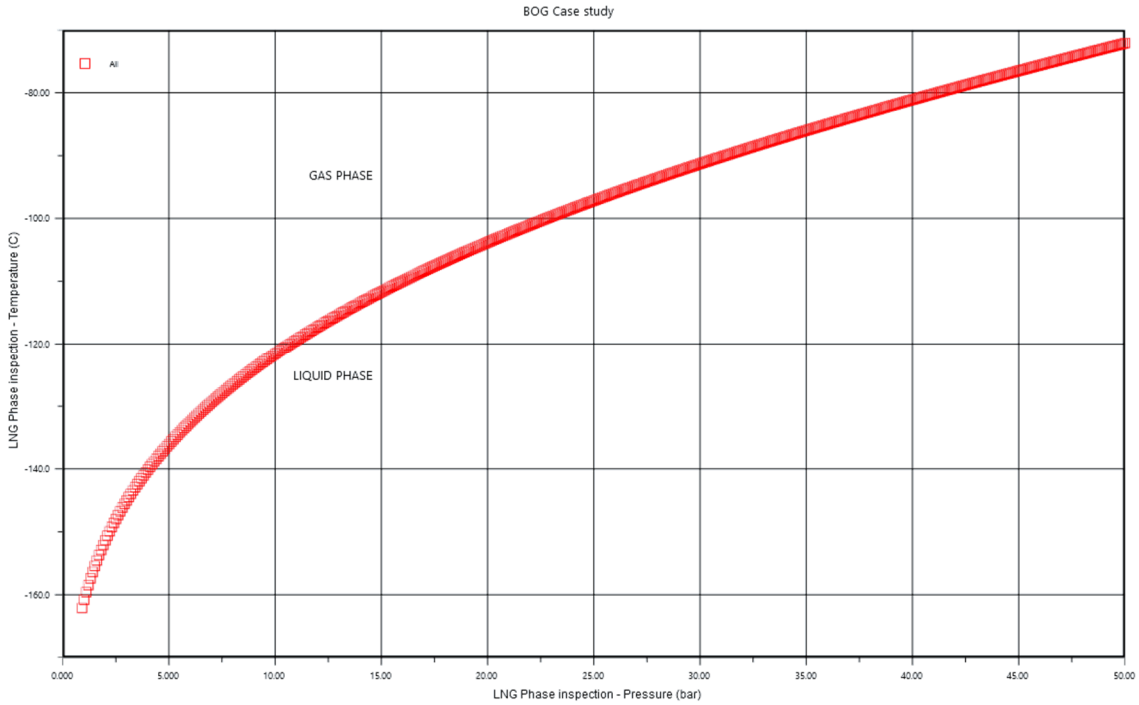

Figure 102. *Phase diagram of LNG according to "Nigerian" specification, critical point at roughly 77 bar, -48°C.*

***Table 37**. Details of LNG according to the "Average" specification.*

WÄRTSILÄ

NATURAL GAS CALCULATION **according to ISO 6976:2016**

Made by: rka027
Date and Time: 22-09-20 14:23
Comments: LNG-Average

Project: 46TS GD Thesis
Number: number

ANALYSIS

at metering reference: 0 °C at 101.325 kPa

Substance	Formula	Vol-%	Mol-%	Mass-%
Methane	CH4	91.865	91.760	82.834
Ethane	C2H6	5.167	5.200	8.798
Propane	C3H8	1.453	1.480	3.672
i-Butane	i-C4H10	0.639	0.660	2.159
n-Butane	n-C4H10	0.635	0.660	2.159
i-Pentane	i-C5H12	0	0	0
n-Pentane	n-C5H12	0	0	0
n-Hexane	n-C6H14	0	0	0
n-Heptane	n-C7H16	0	0	0
n-Octanene	n-C8H18	0	0	0
n-Nonane	n-C9H20	0	0	0
n-Decane	n-C10H22	0	0	0
Hydrogen	H2	0	0	0
HydrogenSulfide	H2S	0	0	0
CarbonMonoxide	CO	0	0	0
Oxygen	O2	0	0	0
Nitrogen	N2	0.241	0.240	0.378
Carbon dioxide	CO2	0	0	0
Water	H2O	0	0	0
Helium	He	0	0	0
Argon	Ar	0	0	0
Ethene	C2H4	0	0	0
Propene	C3H6	0	0	0
neo-Pentane	neo-C5H12	0	0	0
Total		100	100	100

CALCULATION RESULTS

at metering reference: 0 °C at 101.325 kPa
and combustion reference: 15 °C at 101.325 kPa

Superior calorific value	molar basis	969.12 kJ/mol	equals	918.55 Btu/mol
Inferior calorific value	molar basis	875.97 kJ/mol	equals	830.26 Btu/mol
Superior calorific value	mass basis	54.533 MJ/kg	equals	23445 Btu/lb
Inferior calorific value	mass basis	49.291 MJ/kg	equals	21191 Btu/lb
Superior calorific value	volum.basis	43.367 MJ/m^3	equals	1163.9 Btu/ft^3
Inferior calorific value	volum.basis	39.199 MJ/m^3	equals	1052.1 Btu/ft^3
Molar mass		17.771 kg/kmol	equals	39.179 lb/kmol
Compression factor		0.9970		
Relative density		0.6150		
Density		0.7953 kg/m^3	equals	0.04965 lb/ft^3
Molar density		44.750 mol/m^3	equals	1.2672 mol/ft^3
Wobbe index		55.299 MJ/m^3	equals	1484.2 Btu/ft^3
Methane number (EN 16726)		73		

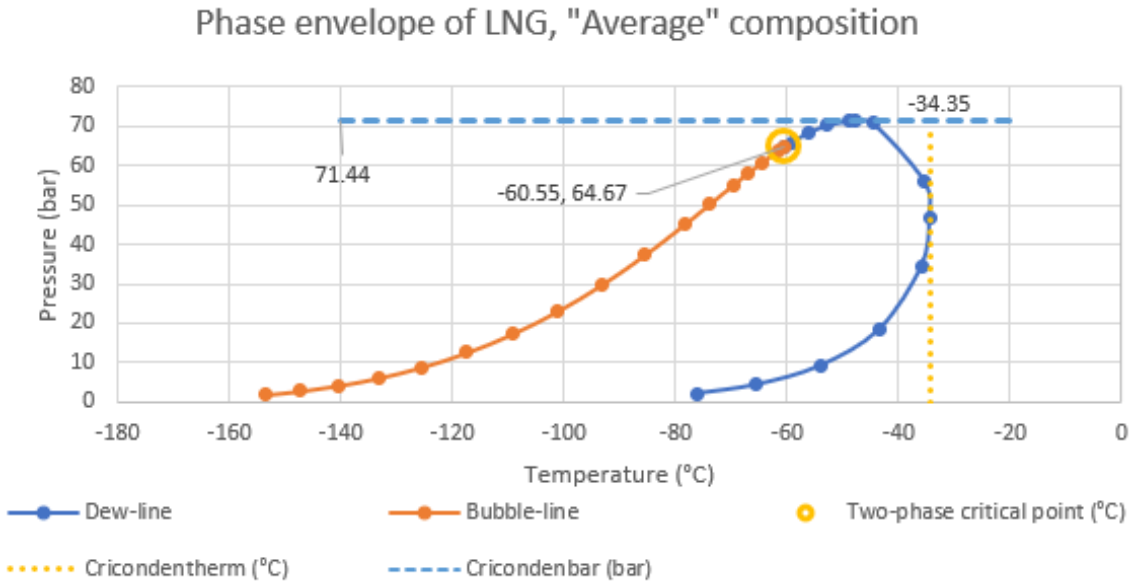

Figure 103. *Phase envelope (Peng-Robinson) of LNG according to "Average" specification.*

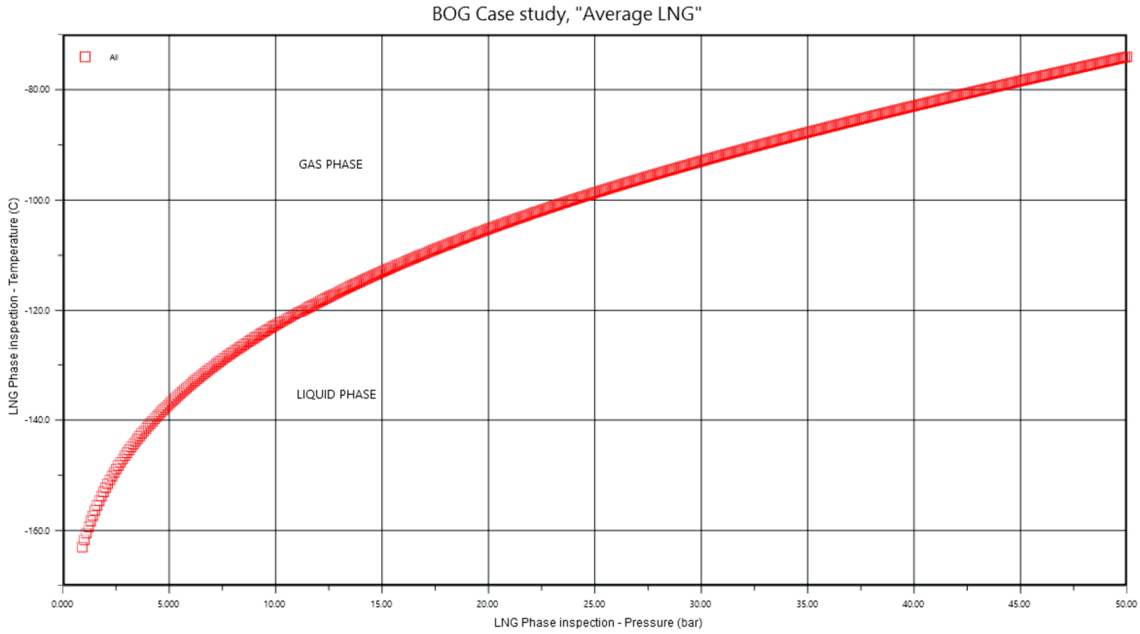

Figure 104. *Phase diagram of LNG according to "Average" specification, critical point at roughly 65 bar, -61°C.*

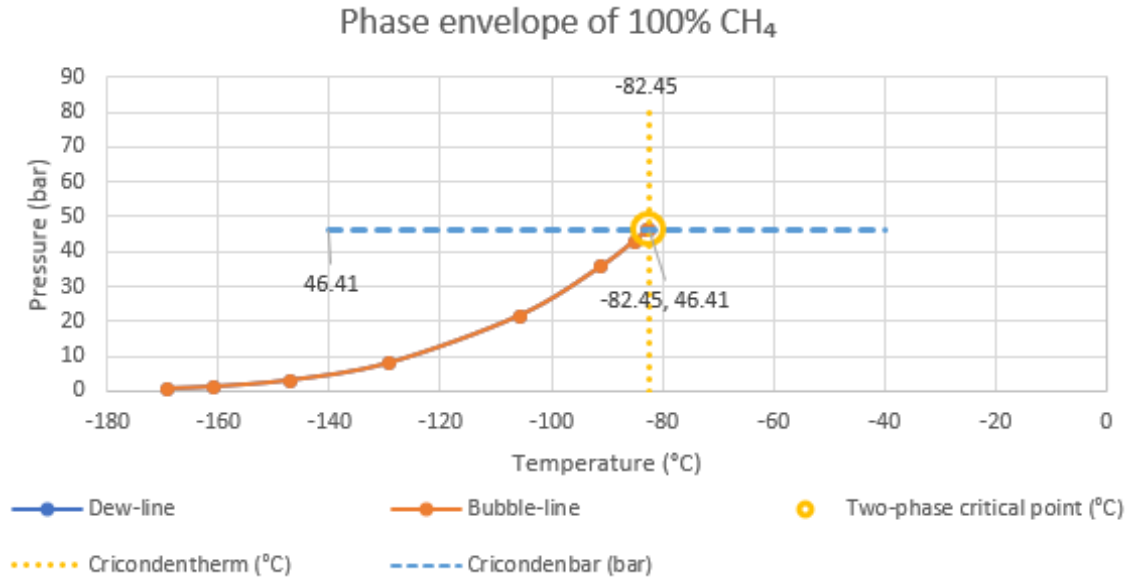

Figure 105. *Phase envelope (Peng-Robinson) of pure methane.*

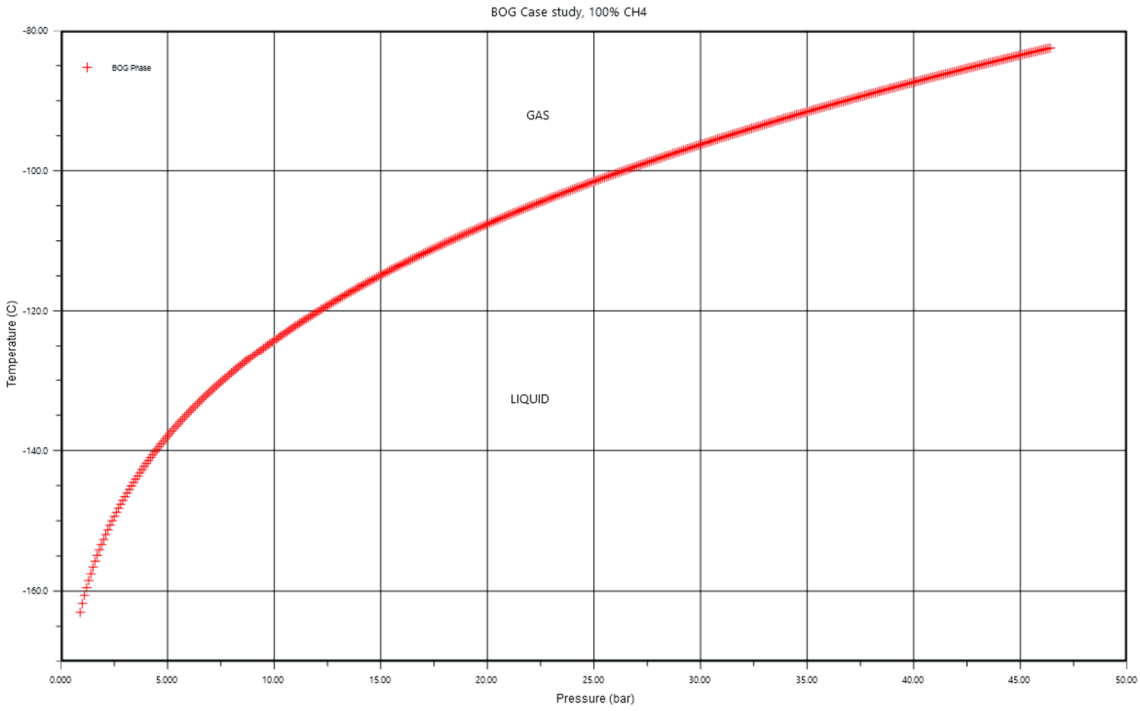

Figure 106. *Phase diagram of 100% CH_4, critical point at roughly 46 bar, -82°C.*

In addition to the HP gas injection engine ME-GI, MAN has developed engines for the usage of LPG and methanol. This engine type is referred to as ME-LGI, with most of the differences to ME-GI engines happening on the auxiliaries as well as to the fuel injection equipment. As LPG density is smaller than natural gas, the equipment size has been reduced. LPG atomization however requires higher injection pressures, with the pressure being in the range of 550 bar. Nevertheless, the fuel pressurizing power consumption is reported to correspond to a 0.5% reduction in the engine efficiency (MAN ES 2020e, p.27). In the LPG injection system, the fuel is fed onto the engine at a relatively low pressure of roughly 50bar. The LPG pressure is then raised for injection pressures inside the injection valve, with a hydraulically operated plunger. (MAN ES 2020e, p.26-28).

In addition to the ME-LGI, MAN is also developing other "add-ons" onto the ME engine for the utilization of different fuels. The LGIP engines are designed to be run on liquid propane, and potentially in the near future also on liquid ammonia. In addition, MAN has a LGIM "add-on", which allows the usage of methanol as the primary fuel. The basic idea behind ME-GI, ME-LGIP and ME-LGIM is to utilize mostly the same hardware, but then according to fuel need change gas control blocks, fuel injection piping and accumulators according to the needs of the fuel to be used.

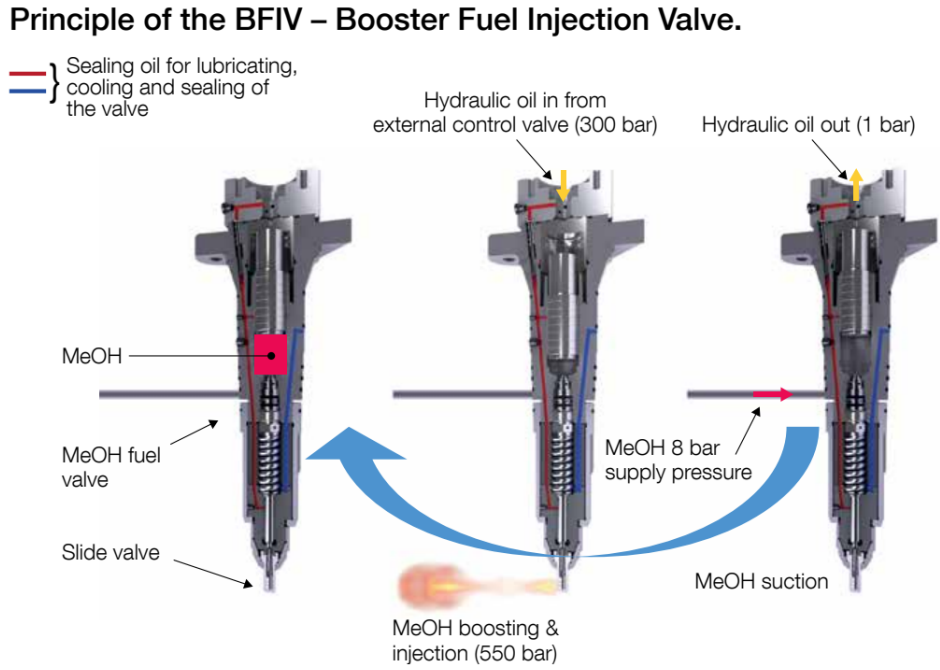

Figure 107. *The FBIV-P injection valve for LPG injection. (MAN e. 2020, p.7)*

The simulation model along with the temperature and pressure changes as well as the results of the calculated HP compressor cases:

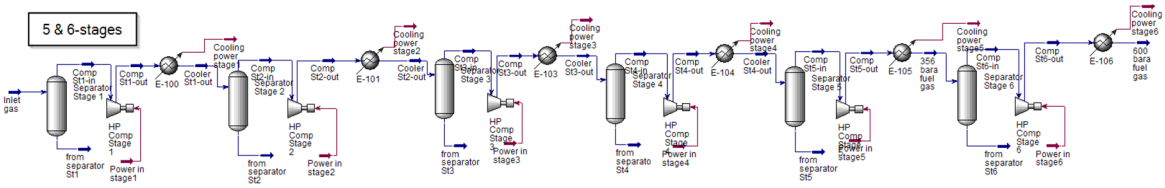

***Figure 108**. The HP compressor simulation model*

HP Compressor, compressing 100% CH_4 with a suction temperature of -40°C /-80°C / -120°C / -160°C with pre-defined pressure ratios and a pre-defined final pressure:

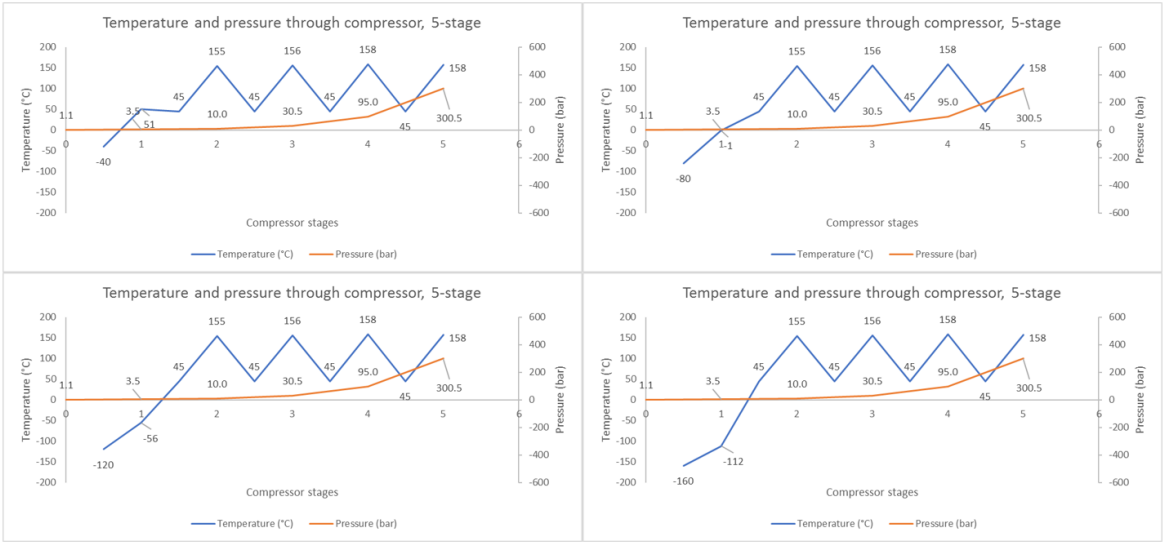

***Figure 109.** Temperatures and pressures through the compressor with BOG temperature -40°C, -80°C, -120°C and -160°C at 5 compressor stages, 100%CH_4 at 300 bar.*

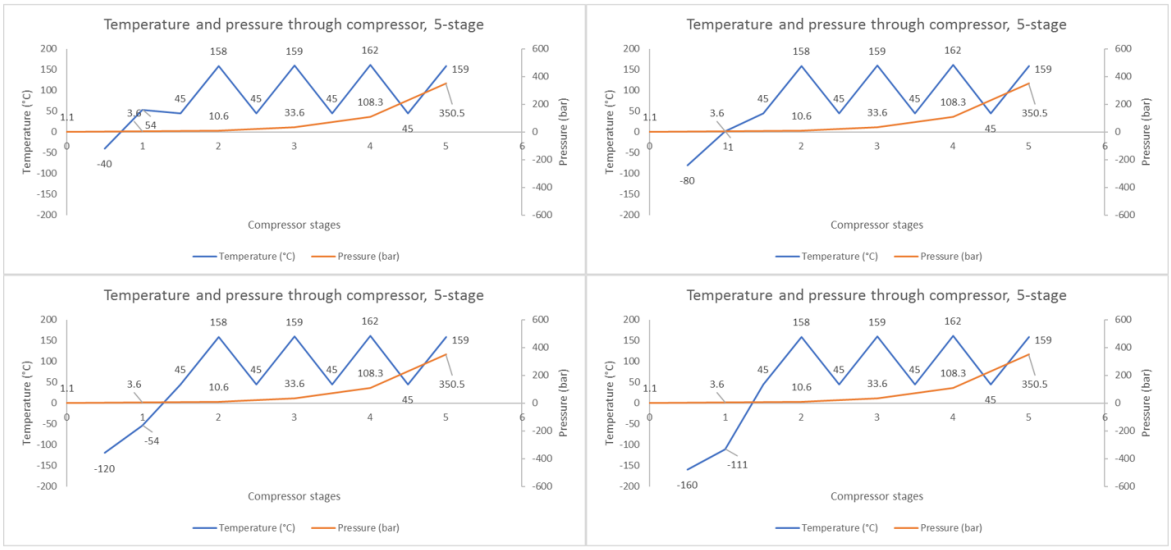

Figure 110. *Temperatures and pressures through the compressor with BOG temperature -40°C, -80°C, -120°C and -160°C at 5 compressor stages, 100%CH_4 at 350 bar.*

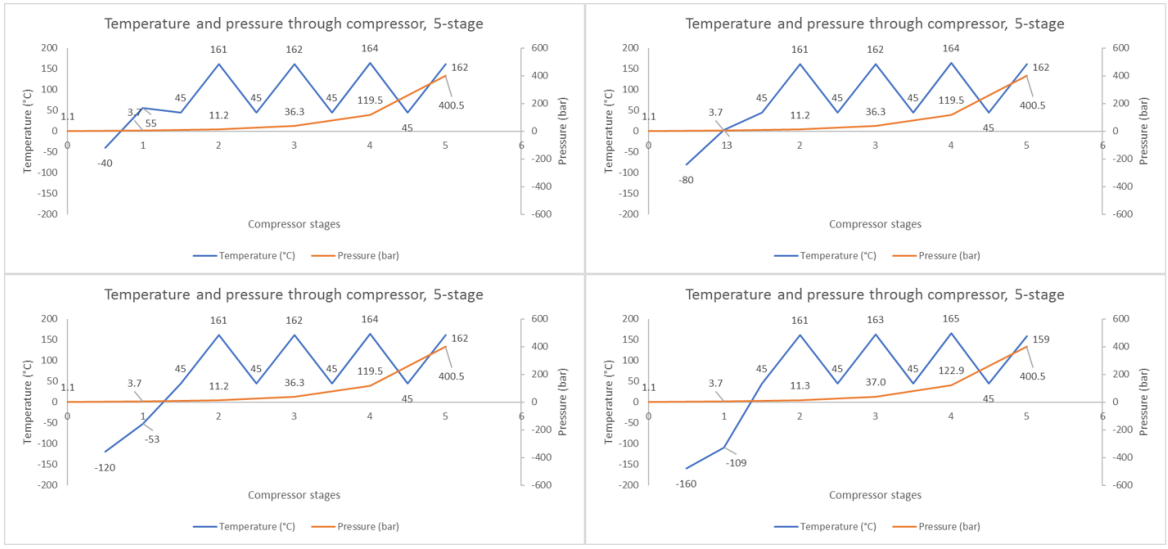

Figure 111. *Temperatures and pressures through the compressor with BOG temperature -40°C, -80°C, -120°C and -160°C at 5 compressor stages, 100%CH_4 at 400 bar.*

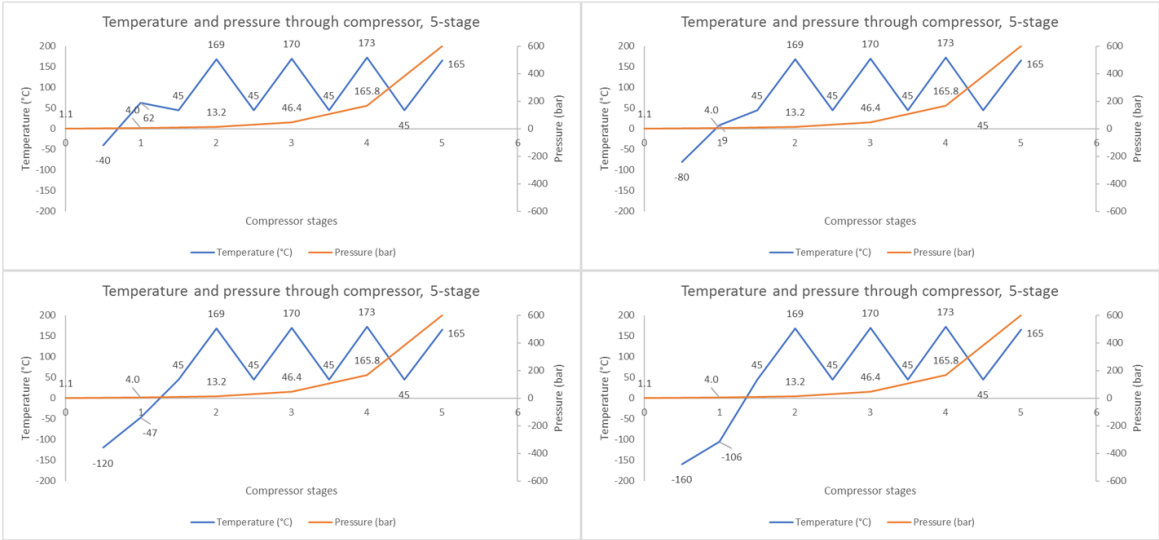

Figure 112. *Temperatures and pressures through the compressor with BOG temperature -40°C, -80°C, -120°C and -160°C at 5 compressor stages, 100%CH_4 at 600 bar.*

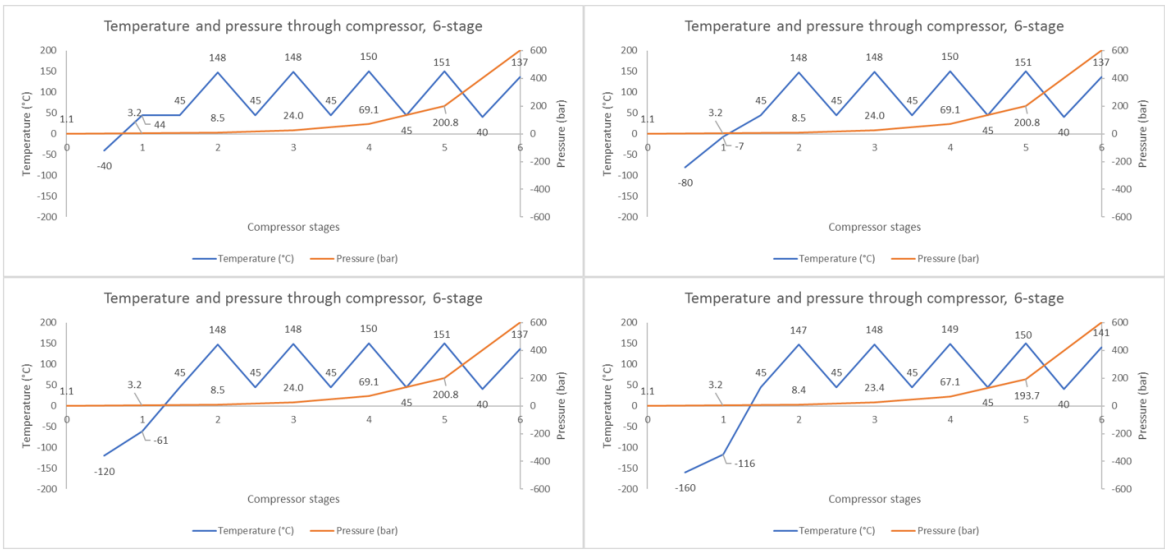

Figure 113. *Temperatures and pressures through the compressor with BOG temperature -40°C, -80°C, -120°C and -160°C at 6 compressor stages,100%CH_4 at 600 bar.*

Results for a gas with a composition of 100% CH_4:

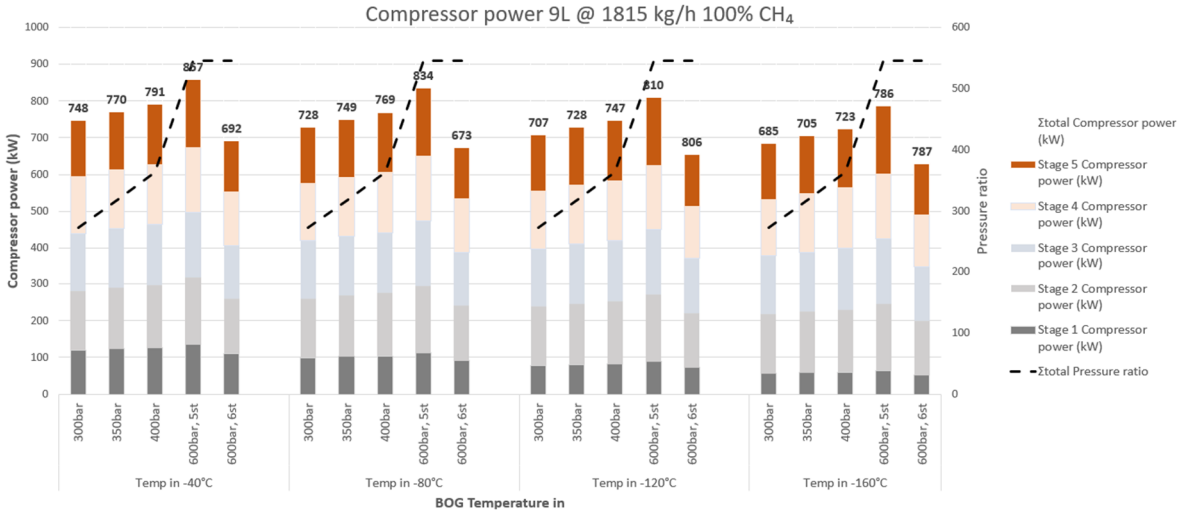

Figure 114. *Compressor power consumption for a 9L engine when running on 100% CH4 fuel, with fuel gas outlet pressures from 300bar to 600bar and BOG inlet temperatures of -40°C, -80°C, -120°C and -160°C.*

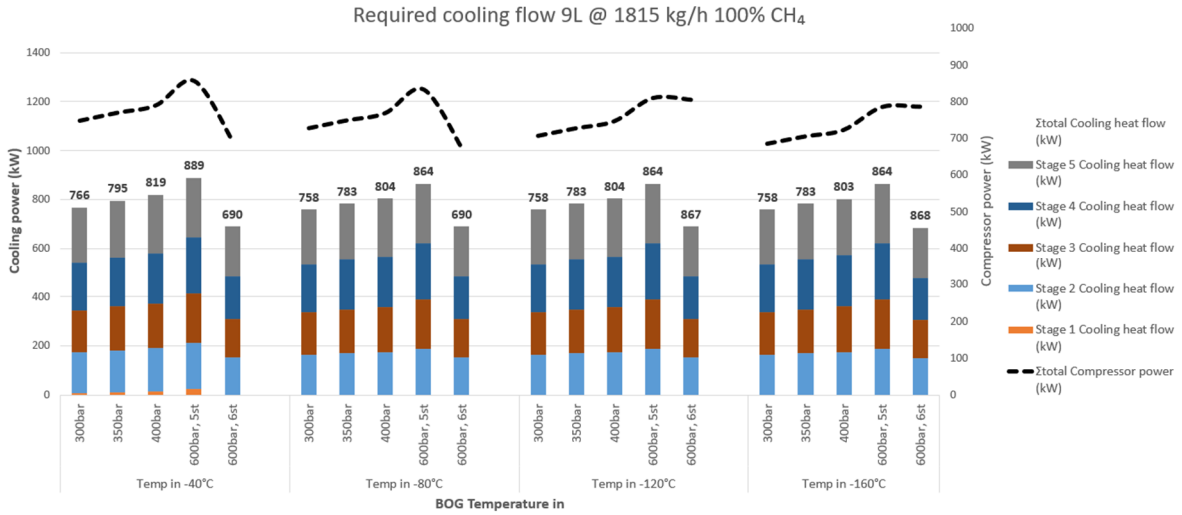

Figure 115. *Cooling power for 9L engine when running on 100% CH4 fuel, with fuel gas outlet pressures from 300bar to 600bar and BOG inlet temperatures of -40°C, -80°C, -120°C and -160°C.*

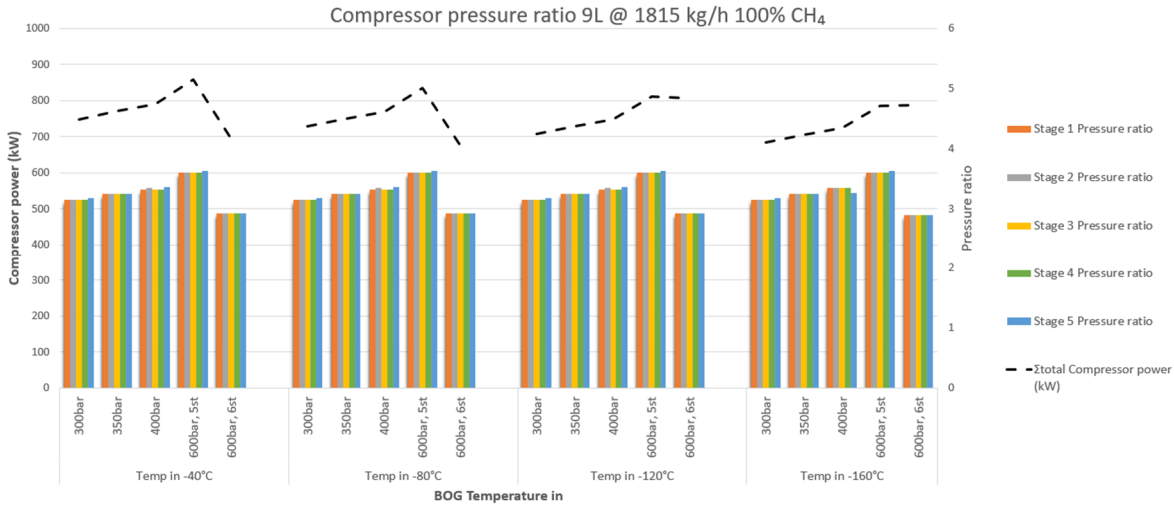

Figure 116. *Compressor pressure ratios per stage for 9L engine when running on 100% CH4 fuel, with fuel gas outlet pressures from 300bar to 600bar and BOG inlet temperatures of -40°C, -80°C, -120°C and -160°C.*

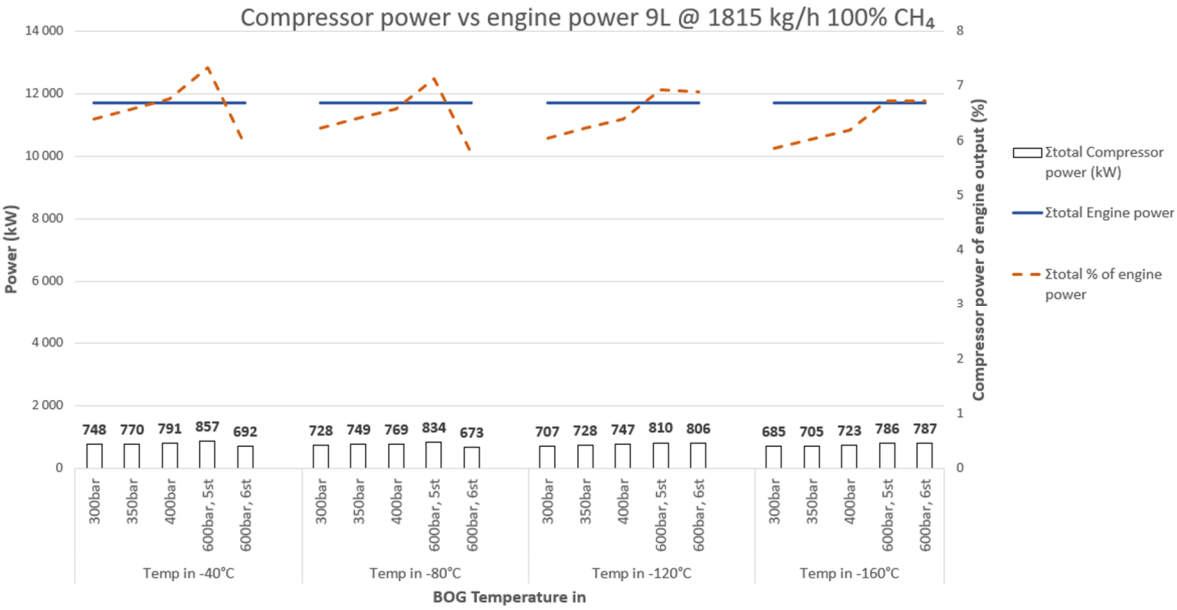

Figure 117. *Compressor power consumption versus 9L engine output when running on 100% CH4 fuel, with fuel gas outlet pressures from 300bar to 600bar and BOG inlet temperatures of -40°C, -80°C, -120°C and -160°C.*

HP Compressor, compressing 90% CH_4 - 10% N_2 with a suction temperature of -40°C /-80°C / -120°C / -160°C with pre-defined pressure ratios and a pre-defined final pressure:

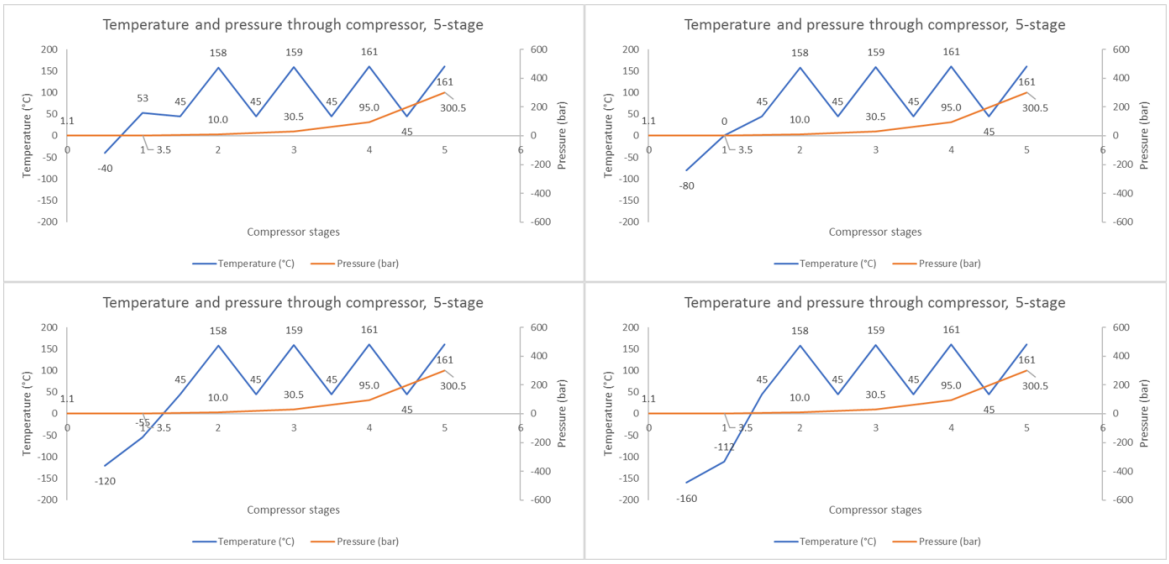

Figure 118. *Temperatures and pressures through the compressor with BOG temperature -40°C, -80°C, -120°C and -160°C at 5 compressor stages, 90%CH_4 -10%N_2 at 300 bar.*

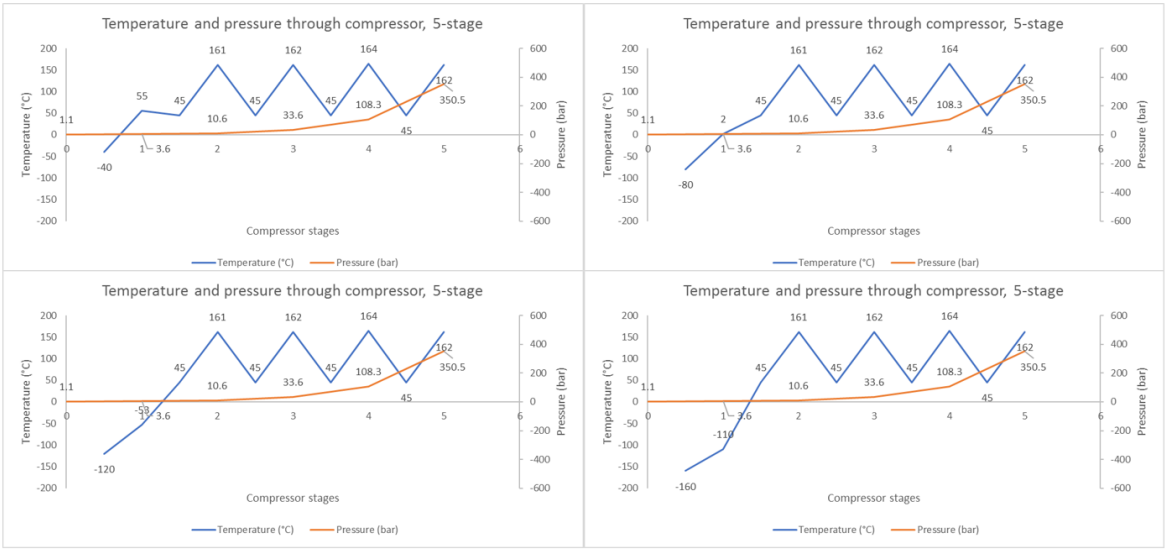

Figure 119. *Temperatures and pressures through the compressor with BOG temperature -40°C, -80°C, -120°C and -160°C at 5 compressor stages, 90%CH_4 -10%N_2 at 350 bar.*

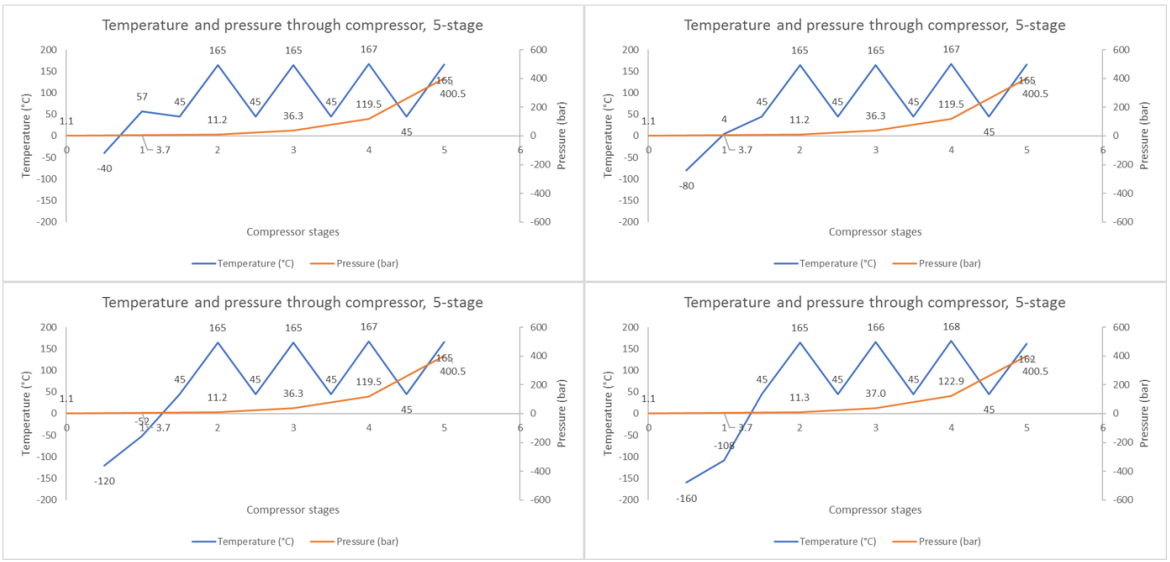

Figure 120. *Temperatures and pressures through the compressor with BOG temperature -40°C, -80°C, -120°C and -160°C at 5 compressor stages, 90%CH_4 -10%N_2 at 400 bar.*

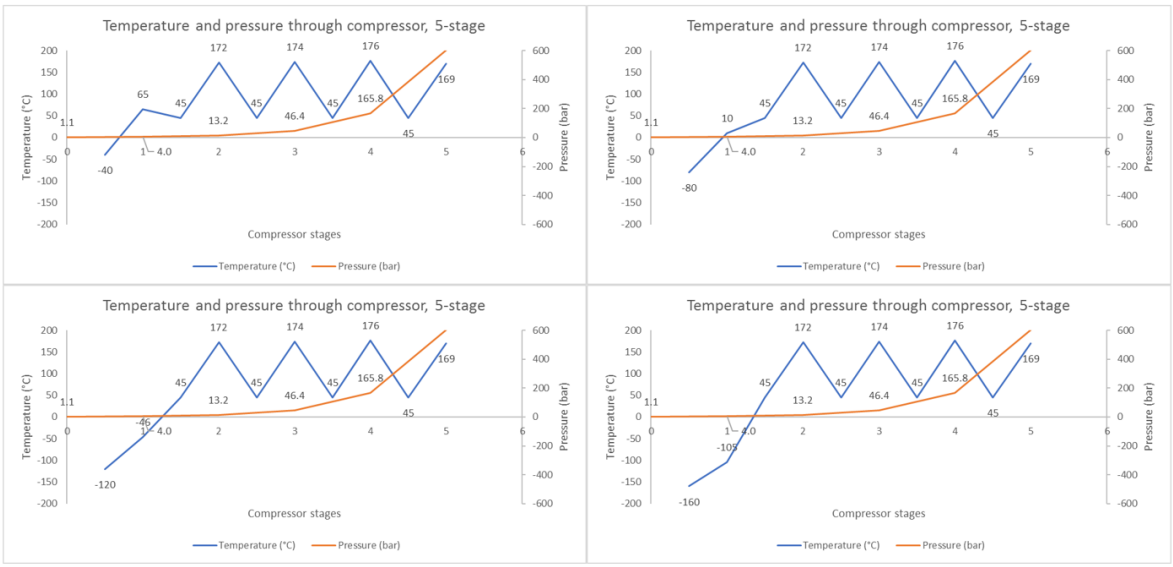

Figure 121. *Temperatures and pressures through the compressor with BOG temperature -40°C, -80°C, -120°C and -160°C at 5 compressor stages, 90%CH_4 -10%N_2 at 600 bar.*

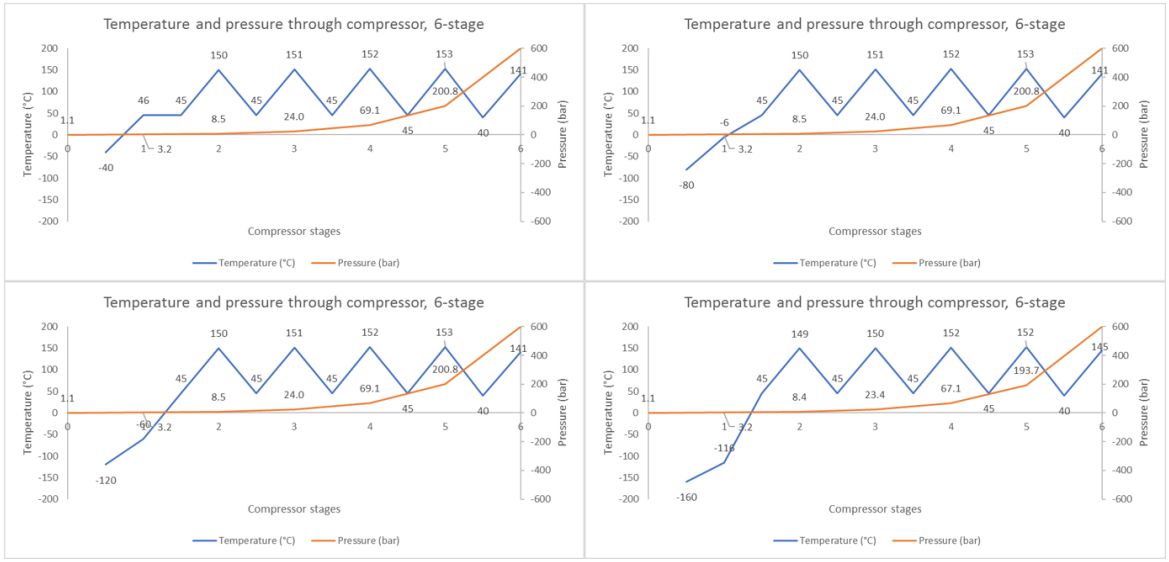

Figure 122. *Temperatures and pressures through the compressor with BOG temperature -40°C, -80°C, -120°C and -160°C at 6 compressor stages, 90%CH_4 -10%N_2 at 600 bar.*

Results for a gas with a composition of 90% CH_4 and 10% N_2:

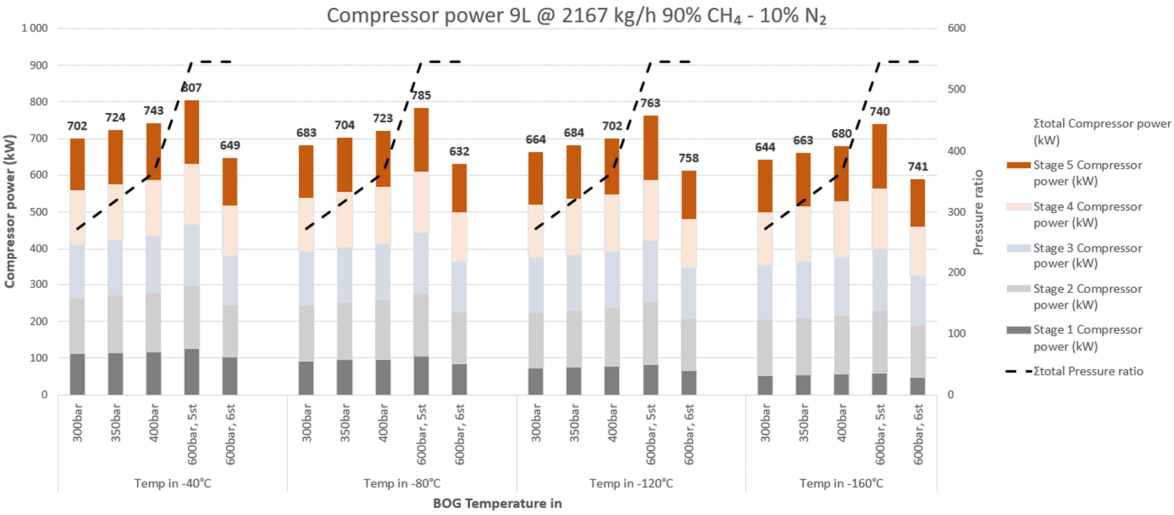

Figure 123. *Power consumption for HP compressor stages for differing suction temperatures, for a 90% CH_4 and 10% N_2 mixture.*

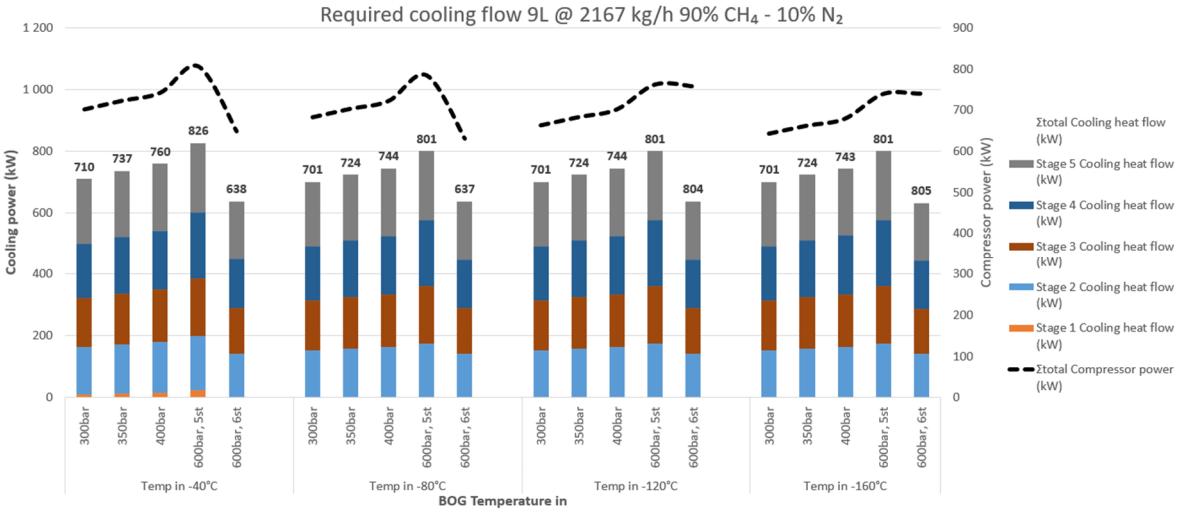

Figure 124. *Cooling power consumption for HP compressor stages for differing suction temperatures, for a 90% CH_4 and 10% N_2 mixture.*

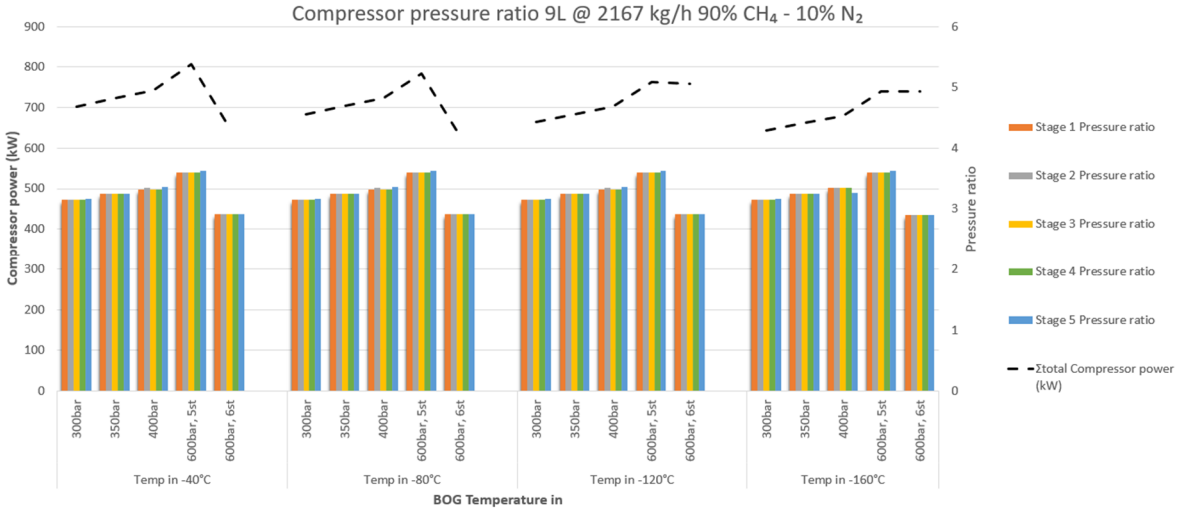

Figure 125. *HP Compressor pressure ratios per stages for differing suction temperatures, for a 90% CH_4 and 10% N_2 mixture.*

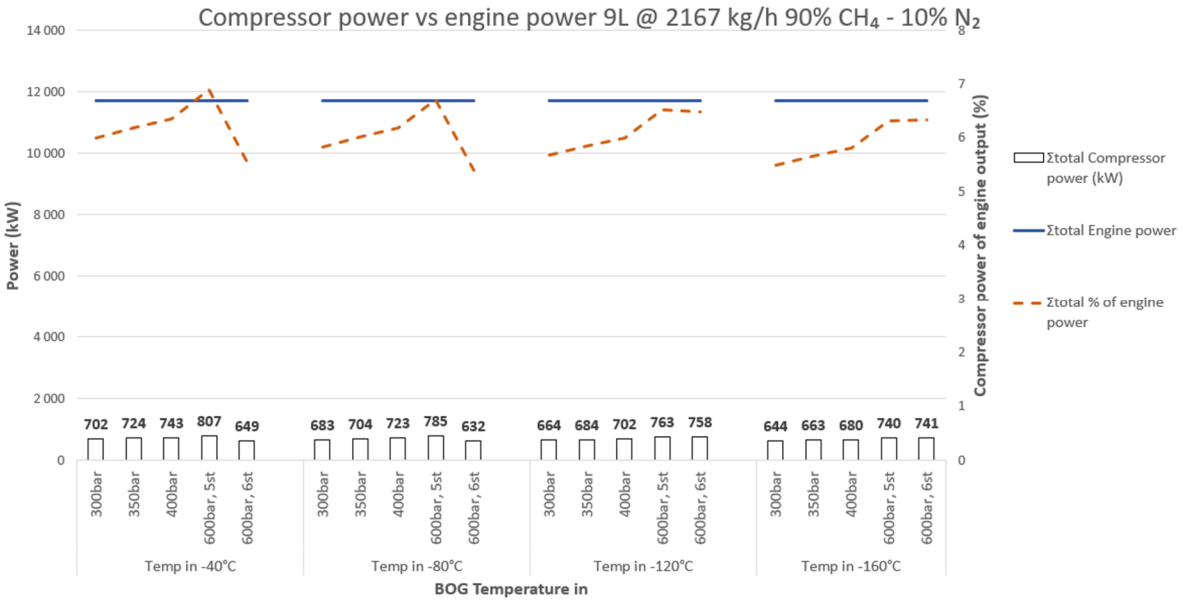

Figure 126. *HP Compressor power consumption versus engine output, for a 90% CH_4 and 10% N_2 mixture.*

The simulation model along with the results of the calculated HP pump cases:

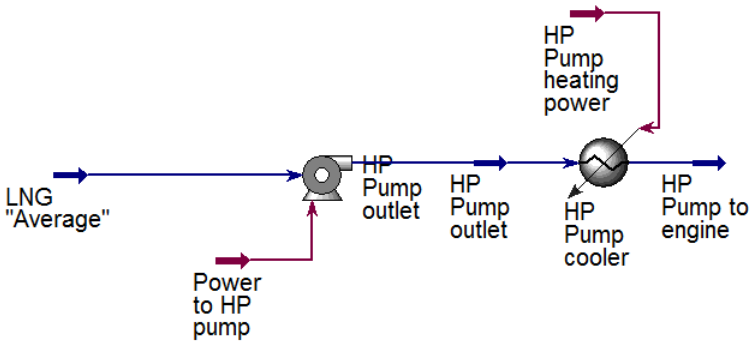

Figure 127. *The HP-DF FGSS simulation model with pumps.*

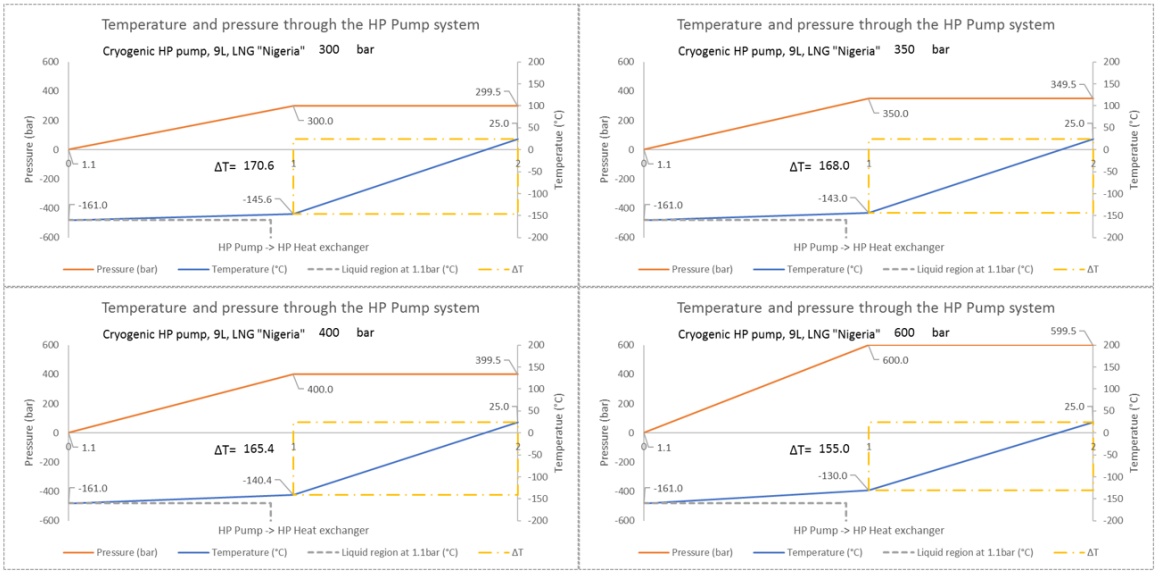

Figure 128. *Temperature and pressure through the HP pump system, LNG according to "Nigeria" composition at outlet pressure of 300 bar to 600 bar.*

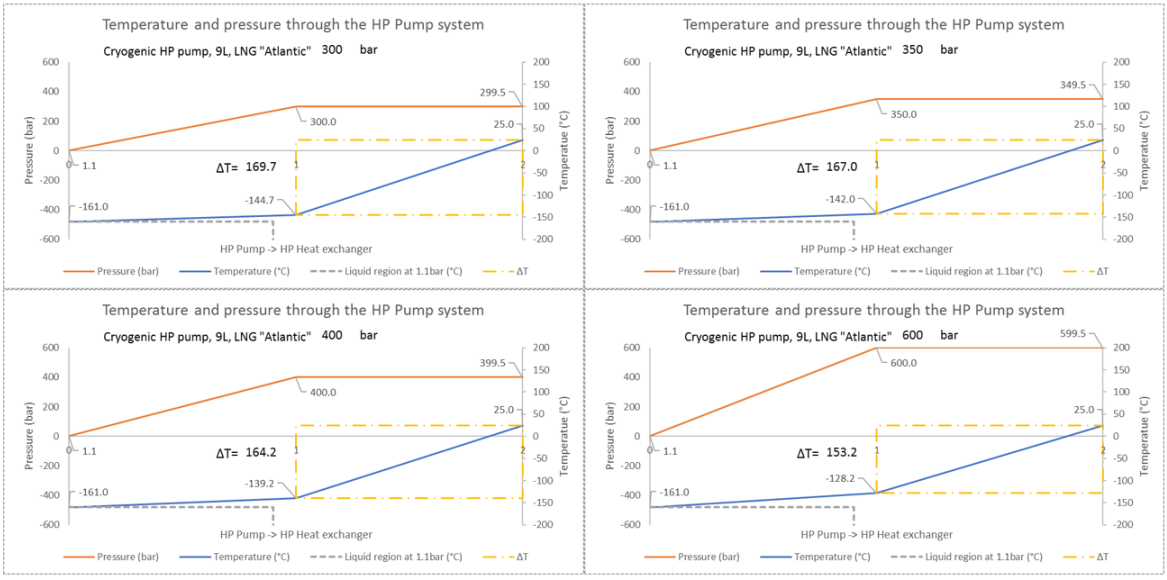

Figure 129. *Temperature and pressure through the HP pump system, LNG according to "atlantic" composition at outlet pressure of 300 bar to 600 bar.*

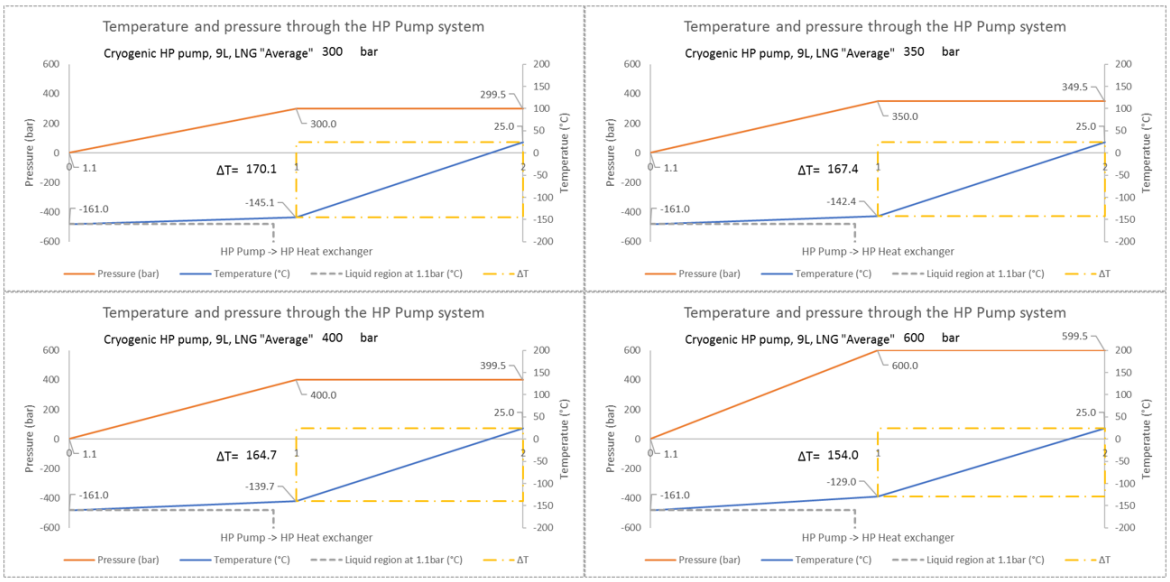

Figure 130. *Temperature and pressure through the HP pump system, LNG according to "average" composition at outlet pressure of 300 bar to 600 bar.*

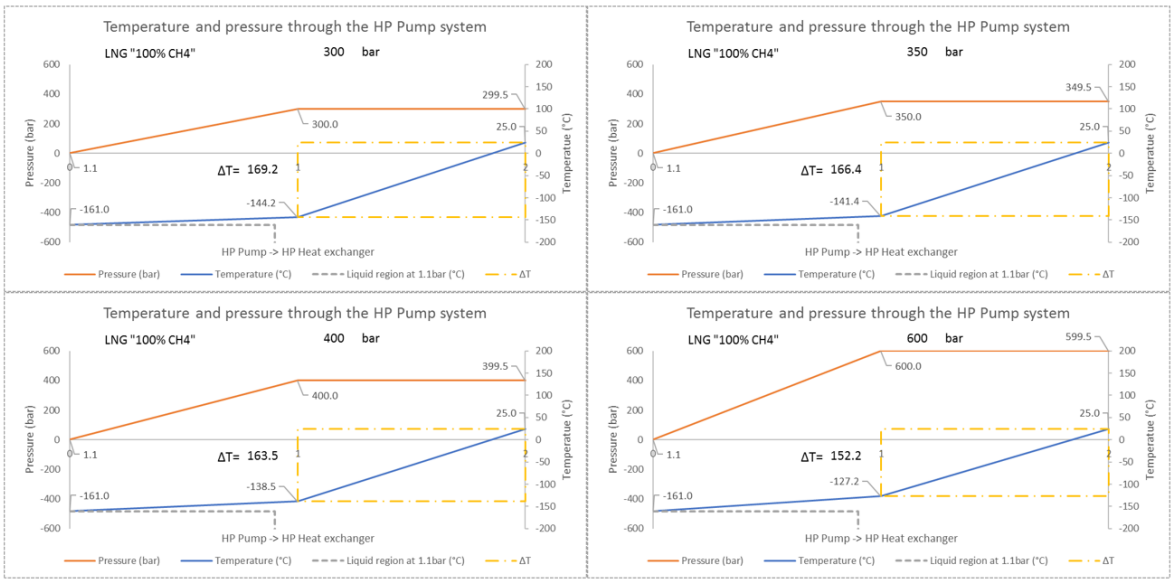

Figure 131. Temperature and pressure through the HP pump system, LNG according to "100% CH_4" composition at outlet pressure of 300 bar to 600 bar.

The simulation model along with the results of the calculated LP gas feed system.

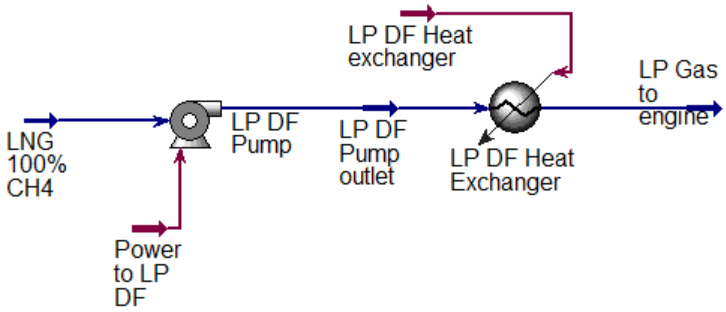

Figure 132. *The LP gas feed system simulation model.*

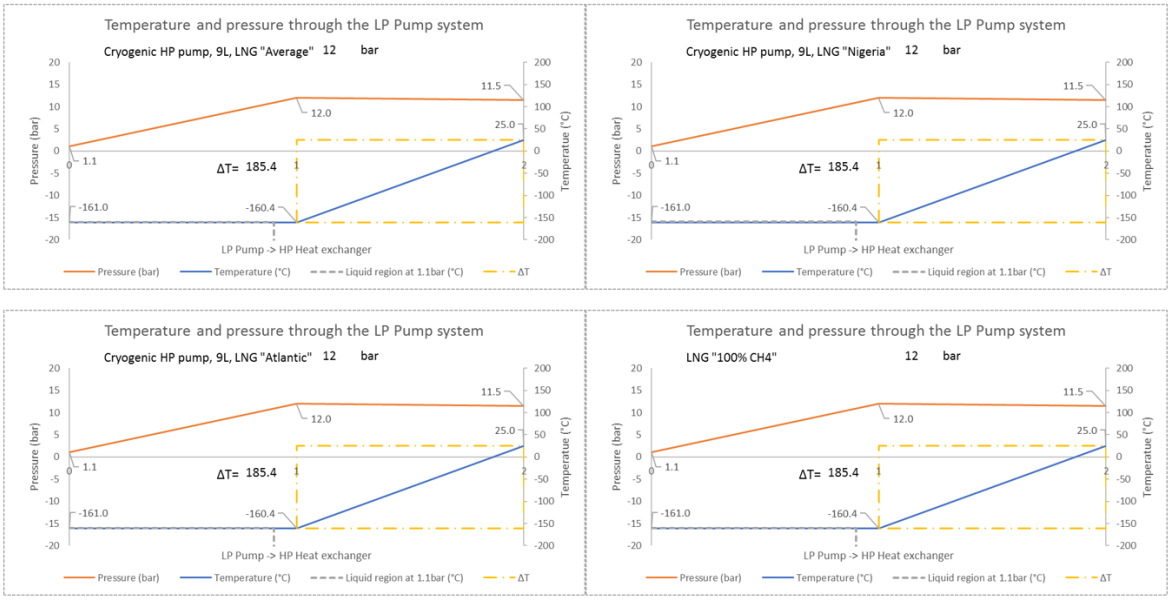

Figure 133. Temperature and pressure through the LP pump system, LNG according to all compositions and outlet pressure at 11.5 bar.

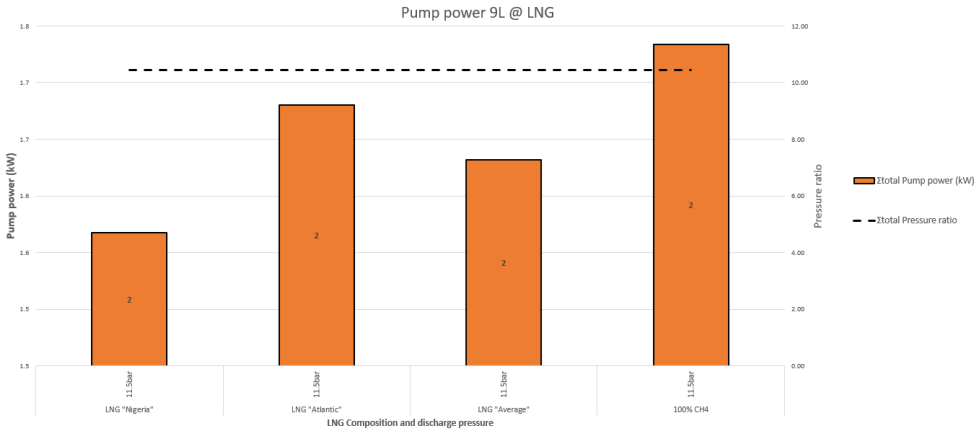

Figure 134. *Pump power of the LP-DF system, LNG according to all compositions and outlet pressure at 11.5 bar.*

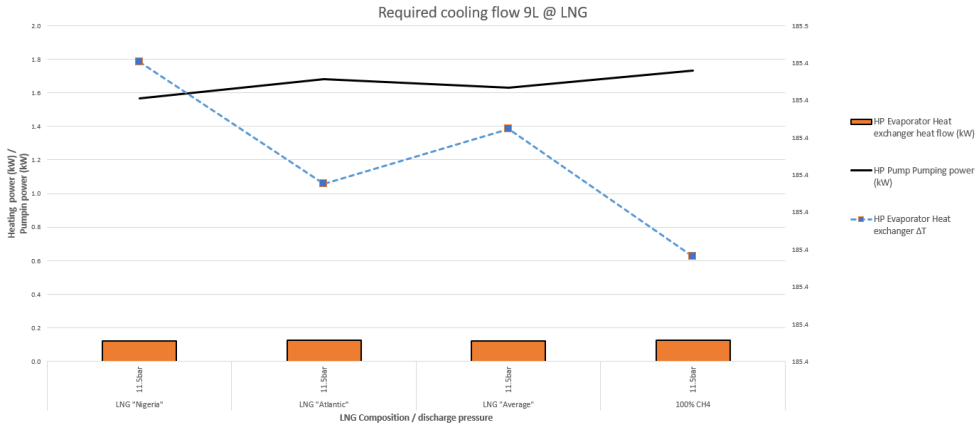

Figure 135. *Cooling power of the LP-DF system, LNG according to all compositions and outlet pressure at 11.5 bar.*

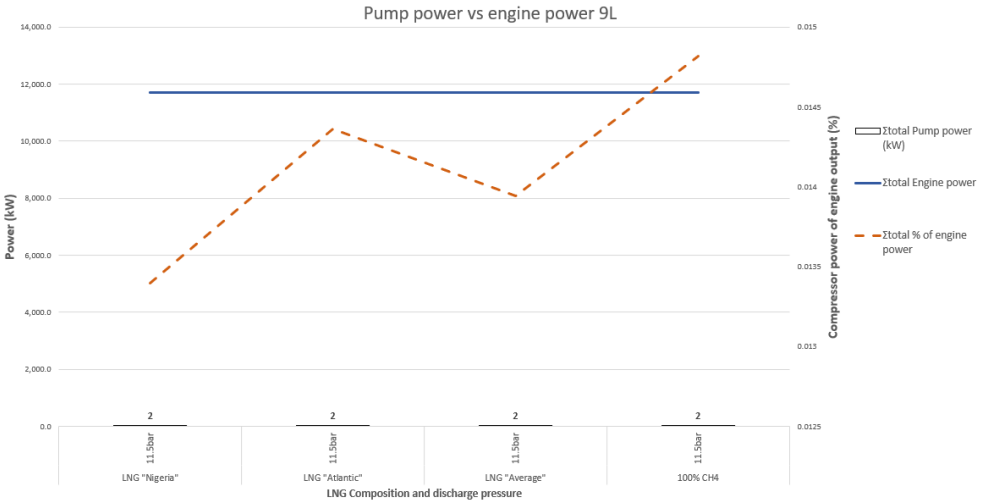

Figure 136. *Pump power of the LP-DF system versus the engine output, LNG according to all compositions and outlet pressure at 11.5 bar.*

Averaged mass -, heating – and cooling flows for different fuel compositions and inlet temperatures.

	Fuel pressure	FGSS power consumption, average (kW)	Power consumption, 100%CH_4 (kW)	Power consumption, LNG Atlantic (kW)	Power consumption, LNG Nigeria (kW)	Power consumption, LNG Average (kW)	FGSS cooling power, average (kW)	FGSS cooling power, 100%CH4 (kJ/H)	FGSS cooling power 90%CH4/10%N2 (kJ/h)	FGSS cooling power LNG Atlantic (kJ/h)	FGSS cooling power LNG Nigeria (kJ/h)	FGSS cooling power, LNG Average (kJ/h)
LP fuel feed	**11.5 bar**	**1.7**	1.7	1.7	1.6	1.6	**444.3**	449.6		447.3	437.1	443.2
Cryogenic HP Pump	**300 bar**	**45.3**	47.5	46.1	43.0	44.7	**286.6**	1069564.9		1048004.2	986615.5	1022269.0
	350 bar	**52.9**	55.5	53.8	50.2	52.2	**274.8**	1023869.4		1004015.6	948028.1	980523.8
	400 bar	**60.5**	63.4	61.5	57.4	59.7	**264.7**	984749.9		966550.5	915328.0	945082.8
	600 bar	**90.8**	95.3	92.3	86.1	89.6	**234.0**	864658.1		852052.9	815388.1	836912.5
HP Compressor, t_i=-40°C, even p-r	**300 bar**	**725.3**	748.1				**738.4**	2759028.3	2557572.463			
	350 bar	**747.0**	770.3				**765.7**	2860363.4	2652731.638			
	400 bar	**766.9**	790.6				**789.3**	2947597.1	2735037.53			
	600 bar	**831.9**	857.3				**857.3**	3198859.8	2973537.007			
Cryogenic HP Compressor, t_i=-120°C, even p-r	**300 bar**	**685.2**	706.6				**729.7**	2730440.1	2523390.3			
	350 bar	**705.7**	727.5				**753.3**	2818121.6	2605793.1			
	400 bar	**724.7**	747.0				**774.4**	2895985.9	2679344.6			
	600 bar	**786.6**	810.3				**832.7**	3111204.1	2884159.5			
Cryogenic HP Compressor, t_i=-160°C, even p-r	**300 bar**	**664.3**	685.0				**729.7**	2730440.1	2523390.2			
	350 bar	**684.1**	705.1				**753.3**	2818121.6	2605793.1			
	400 bar	**701.4**	722.8				**772.5**	2889252.6	2673090.1			
	600 bar	**762.8**	785.6				**832.7**	3111204.1	2884159.5			

Figure 137. *The averaged power and cooling power consumptions.*

In figure 142 is an indicative cost comparison, made by WinGD. of the capex costs related to a 2-stroke LP-DF engine versus a 2-stroke HP-DF engine for two different installations. The smaller engine, a 6X52DF with an output of about 8 000 kW, is fitted on a 55 000dwt tanker, so external LNG tanks must be supplied to the vessel. The larger engine, a 5X72DF with an output of between 19 000 and 13 000kW is installed onto a 180 000m³ LNG carrier, where the cargo BOG can directly be used as fuel. As can be seen, the additional LNG tank price is quite significant, but this is naturally needed for both HP- & LP-DF systems.

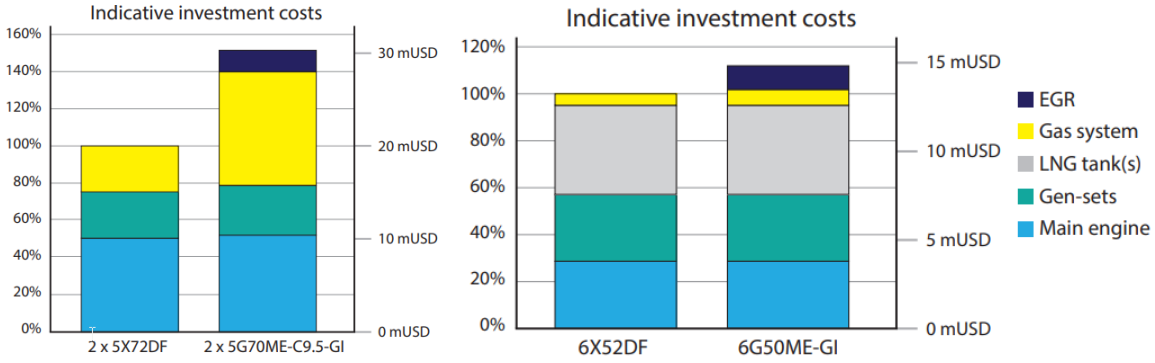

Figure 138. *2-stroke LP-DF and HP-DF capex comparison for a 180 000m³ LNG carrier on the left and a 55 000 dwt tanker on the right. (Strödecke 2015, p.9)*

Similar price comparisons have been presented by MAN, in which the products compared are 11- & 12X92DF engines along with MAN engines 11G90ME-C10.5GI and 12G95ME-C9.6-GI, as shown in figure X. The chosen engines are larger than in the case presented by WinGD, with the vessel size corresponding to a 14 000 TEU containership for the smaller engines and a 21 000 TEU containership for the larger. From the capex point of view the outcome is similar, with the HP equipment costing 0.6m$ more than the LP equipment, which totals 4.9m$ in this comparison. The HP FGSS equipment is priced into the PVU, which accounts for roughly 2m$ of the cost in both cases. (MAN ES 2020i, p.11-14)

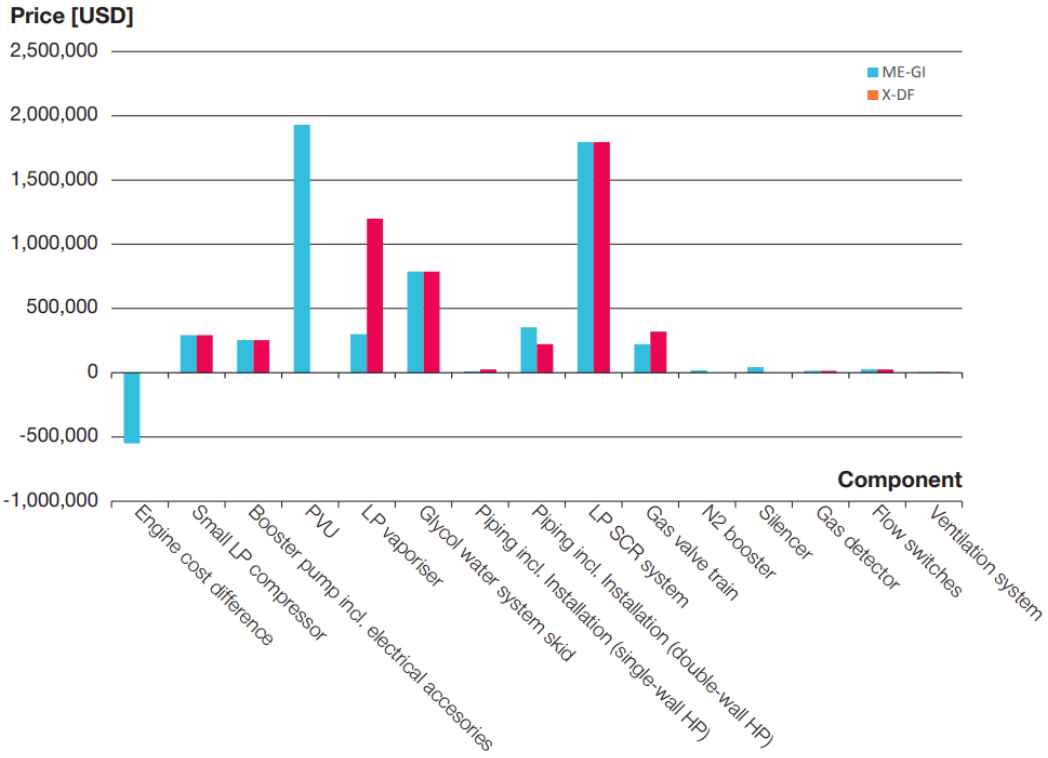

Figure 139. *stroke LP-DF and HP-DF capex comparison for a 21 000 TEU containership. (MAN ES 2020i, p.13)*

In figures 144 and 145 below are still the capex comparisons made by SEA-LNG.

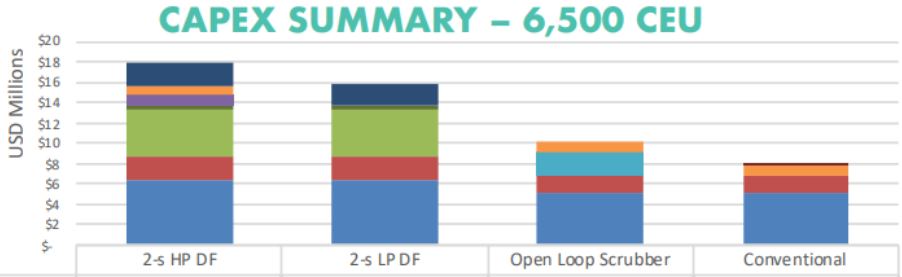

	2-s HP DF	2-s LP DF	Open Loop Scrubber	Conventional
Fuel Chiller				$118,000
LNG Yard Work	$2,110,000	$2,110,000		
SCR/EGR	$884,646		$1,040,229	$1,040,229
Scrubber (inc. yard work)			$2,292,030	
HP gas supply	$1,087,241			
LP gas supply	$349,138	$349,138		
LNG tanks	$4,712,734	$4,712,734		
Auxiliaries	$2,308,800	$2,308,800	$1,776,000	$1,776,000
Main Engine	$6,397,440	$6,397,440	$5,117,952	$5,117,952
Total	$17,850,000	$15,878,112	$10,226,211	$8,052,181
Delta (vs Conventional)	$9,797,819	$7,825,931	$2,174,030	$-

Figure 140. *Capex comparison of a 6 500 CEU car carriers propulsion alternatives. (SEA-LNG 2019, p.21)*

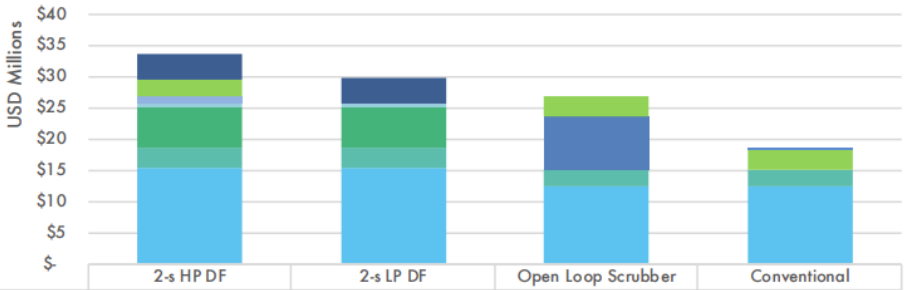

	2-s HP DF	2-s LP DF	Open Loop Scrubber	Conventional
Fuel Chiller	$-	$-	$-	$118,000
LNG Yard Work	$4,230,000	$4,230,000	$-	$-
SCR	$2,495,700	$-	$3,260,340	$3,260,340
Scrubber (inc. yard work)	$-	$-	$8,620,560	$-
HP gas supply	$1,190,621	$-	$-	$-
LP gas supply	$708,654	$708,654	$-	$-
LNG tanks	$6,382,837	$6,382,837	$-	$-
Auxiliaries	$3,327,600	$3,327,600	$2,662,080	$2,662,080
Main Engine	$15,396,552	$15,396,552	$12,317,241	$12,317,241
Total	$33,731,963	$30,045,642	$26,860,221	$18,357,661
Delta (vs Conventional)	$15,374,301	$11,687,981	$8,502,560	$-

Figure 141. *Capex comparison of a 14 000 TEU containership propulsion alternatives. (SEA-LNG 2020, p.15)*